Investigation of the effects of IGF-1 receptor blockade on chemoresistance of advanced melanoma

Roger Ramcharan (MBBS, MRCS)

Exeter College

Submission for the degree of Doctor of Philosophy (D.Phil)

Department of Medical Oncology

University of Oxford



Acknowledgements

I would like to thank my family for their support in pushing me forward to this point in my life and career. I am eternally grateful to my mother who has never stopped believing in me and has taught me to always strive for better. Without her struggle, thoughts and prayers I would not be where I am today. To my grandfather who passed away before I was born and my grandmother who passed away during my time in the lab, whose efforts decades ago still live and breathe in me today even if I couldn't be present near the end for them. To my four siblings, Sean, Barry, Rodney and Gail, from whom I stole a little bit of every one of their personalities and ways of thinking, I am also thankful for everything they said and did, and the things they never told me they did that helped me to be transformed from a small island boy to becoming a graduate student of the University of Oxford. Thanks to my big brother, Sean and his wife, Nisha, who made coming to the UK a reality in the many ways that they did and for supporting us while we were here.

To my two beautiful children, Chloe and Zachary, who teach me the real meaning of life every single day and remind me why I am here. They may never know how instrumental they were to my achieving this goal, but they most certainly were. To my lovely wife, Sairia, for all her love and support throughout this process. Unlike her own thesis, I cannot show her my gratitude by putting a picture of her heart in my thesis, but I am certain she knows that I am grateful.

I am extremely grateful to Val Macaulay for her guidance and supervision during my DPhil, and for being instrumental to developing my scientific mind. Thanks to Mark Middleton, for his supervision and support. It was easy to learn from Professor Middleton's example, which seems to be built around the philosophy that there are no problems, only solutions waiting to happen.

Thanks to all the present and past IGF lab members: Martin Kerr, Wang Yong, Mark Goodfellow, Meenali Chitnis, Kunal Lodhia, Tamara Aleksic, Megumi Takiguchi, Phil Earwaker, and most of all Gao Shan, whose advice and support made navigating my way through assays and lab life much easier being not just a great colleague but also a great friend.

I would like to extend my thanks to our collaborators, Geoff Margison, Mandy Watson and Gail Mcgown of the Carcinogenesis Group of the Paterson Institute for cancer research, Manchester who helped us with with base adduct quantification and repair assays and for supplying us with much needed temozolomide for both our *in vitro* and *in vivo* work as well as for their invaluable advice and guidance which were integral to carrying out this project. Professor Adrian Harris and Ji-Liang Li collaborated with us and guided us through preclinical studies under their project license. Jordan Tanner, Fred Dickinson, Esther Bridges and Alan McIntyre were all integral to planning, animal handling and interventions of these studies. Many thanks to Professors Colin Goding and Vincenzo Cerulendo for the help with assimilating the melanoma cell line panel used in this thesis. Thanks to Peter Thomas for confocal microscopy training, and along with Tamara Aleksic, for help with acquiring some of the immunofluorescence images in this thesis.

Thanks to Elena Favaro, Lonnie Swift, Andy Blackford and Annasurya Ramachandran, not only for their help with assays such as flow cytometry and chromatin isolation by small scale biochemical fractionation, but who so willingly lent their time to brain storm several aspects of this project and of course for being my very good friends at the institute.

AZ12253801 and olaparib were generously provided by AstraZeneca, and Liz Buck of Astellas Pharmaceuticals also generously provided OSI-906 for use in this study.

This project would not have been possible without the generous funding obtained from Professor Mark Middleton and the Oxford Biomedical Research Centre (BRC) as well as the Blonde McIndoe Fund of the Royal College of Surgeons Research Fellowship.

Table of Contents

ABSTRACT VIII

LIST OF FIGURES IX

LIST OF TABLES XIII

ABBREVIATIONS XV

CHAPTER 1 1

INTRODUCTION 1

1.1 Insulin-like growth factor (IGF) system 1

1.1.1 IGF axis components 2

1.1.1.1 Insulin-like growth factors 2

1.1.1.2 Insulin-like growth factor receptors (IGFRs) 3

1.1.1.3 Insulin-like growth factor binding proteins (IGFBPs) 4

1.1.2 IGF Signaling 5

1.1.2.1 PI3K/AKT pathway 6

1.1.2.2 RAS/RAF/MAPK pathway 9

1.1.3 IGF1R signaling and Cancer 11

1.1.4 IGF1R and Melanoma 12

1.2 Malignant Melanoma 13

1.2.1 Background 13

1.2.2 Malignant Melanoma Biology 14

1.2.3 Malignant Melanoma Treatment 20

1.2.3.1 Stage I and II Melanoma Treatment- Localized Disease 20

1.2.3.2 Stage III Melanoma Treatment – Regional Lymph Node Metastasis 21

1.2.3.3 Stage IV Melanoma – Distant Metastatic Spread 22

Immunotherapy 22

Targeted Therapy 24

Chemotherapy 25

1.2.4 Malignant melanoma resistance to treatment 26

1.2.4.1 Evasion of apoptosis 26
1.2.4.2 Drug Efflux Pumps or Detoxification enzymes 28
1.2.4.3 Intratumoral Heterogeneity 29
1.2.4.4 DNA repair mechanisms 30
1.2.5 Alkylating DNA damage and repair 31
1.2.5.1 Single Step Repair of alkylated DNA lesions 33
O^6-methylguanine-DNA methyltransferase 33
Human Alk B homologues 35
1.2.5.2 Multi-step repair of alkylated DNA lesions 36
1.2.5.3 Repair of secondary DNA damage 37
Homologous recombination in DSB repair and replication stress 38
Non-homologous recombination (NHEJ) in DSB repair 42

1.3 IGF1R signaling and the response to DNA damage 43

1.4 Aims of this project 44

CHAPTER 2 45

MATERIALS AND METHODS 45

2.1 Cell Lines and Cell Culture 45

2.2 Cytotoxic Agents and Other Treatments 47
2.2.1 Temozolomide (TMZ) 47
2.2.2 AZ12253801 47
2.2.3 Linsitinib (OSI-906) 48
2.2.4 Olaparib (AZD2281) 48
2.2.5 IGF-1 48
2.2.6 Doxycycline 48

2.3 Protein Analysis 49
2.3.1 Collection and lysis of adherent cells 49
2.3.2 Western Blotting 50
2.3.3 Chromatin isolation by small-scale biochemical fractionation 52

2.4 Gene silencing by RNA interference (RNAi) 53

2.5 RNA analysis 53

2.5.1 RNA Extraction 53
2.5.2 Reverse transcription 54
2.5.3 Quantitative real-time PCR (qRT-PCR) 54

2.6 Assays of alkylated base damage and repair 56
2.6.1 MGMT activity assay and O^6MeG quantification 56
2.6.2 AAG Activity Assay 57
2.6.3 N^7MeG Base Adduct Quantification 58

2.7 Cell-based assays 58
2.7.1 Cell cycle analysis by bromodeoxyuridine incorporation Method and PI staining 58
2.7.2 Clonogenic Assay 59
2.7.3 Apoptosis Assay 60
2.7.4 Cell viability assay: CellTiter-Glo (CTG) 61
2.7.5 Immunofluorescence microscopy 62
2.8 *In vivo* study 64
2.9 Statistical analysis 65

CHAPTER 3 66

INVESTIGATING IGF1R SIGNALING AND TMZ RESISTANCE IN A PANEL OF HUMAN MELANOMA CELL LINES 66

3.1 Introduction 66

3.2 Results and Discussion 67
3.2.1 Characterization of a panel of melanoma cell lines 67
3.2.2 Assessment of expression and activation of components of the IGF axis 68
3.2.3 Assessment of IGF1R nuclear localization in melanoma cells 70
Nuclear IGF1R immunostaining in full medium 71
3.2.4 Testing the sensitivity to TMZ in melanoma cells 74
3.2.5 Assessment of correlations with TMZ resistance in melanoma cells 76
3.2.6 Investigating the effects of IGF1R inhibition on TMZ resistance in melanoma cells 79

CHAPTER 4 84

INVESTIGATING MECHANISMS OF THE ENHANCEMENT OF TMZ SENSITIVITY BY IGF1R INHIBITION 84

Results and Discussion 84

4.1 Investigating the effects of IGF1R inhibition on TMZ-induced apoptosis 84

4.2 Effect of combining IGF1R inhibition with TMZ on cell cycle progression 87

4.3 Investigating Whether IGF1R Signaling Affects Repair of TMZ Induced DNA Damage 95

4.3.1 Investigating whether IGF1R Signaling affects repair of alkylated DNA bases 95

4.3.1.1 IGF1R Signaling and MGMT 96

4.3.1.2 Investigating the effect IGF1R signaling on Base Excision Repair 107

4.3.2 Investigating Whether IGF1R inhibition Affects TMZ induced Double Strand Break Formation 110

4.3.2.1 Investigating the effect of IGF1R Inhibition on TMZ induced Gamma-H2AX Focus formation 110

4.3.2.2 Investigating the effect of IGF1R Inhibition on TMZ induced 53BP1 Focus formation 114

4.3.2.3 Investigating the effect of IGF1R Inhibition on TMZ induced RPA Focus formation 118

4.3.2.4 Investigating the effect of IGF1R Inhibition on TMZ induced RAD51 Focus formation 122

4.3.2.5 Investigating the effect of IGF1R Inhibition on Chromatin bound DNA repair mediators 129

4.3.2.6 Testing the effect of IGF1R Inhibition on Sensitivity to PARP inhibition in Melanoma in vitro 134

CHAPTER 5 137

PRECLINICAL TESTING OF THE COMBINATION OF IGF1R INHIBITION TMZ IN MELANOMA 137

5.1 Introduction 137

5.2 Results and Discussion 139

5.2.1 Testing the effect of OSI-906 on IGF1R signaling in human melanoma in vitro 139

5.2.2 Testing the effect of OSI-906 on human melanoma cell viability *in vitro* 142
5.2.3 Investigating the effect of p53 status on OSI-906 sensitivity 146
5.2.4 Testing the effect of OSI-906 on TMZ sensitivity in melanoma 149
5.2.5 Preclinical Testing of the effect of OSI-906 on TMZ sensitivity in melanoma 152
5.2.5.1 Tumorigenicity study of A375M cells and TMZ tolerability in athymic nude mice 152
5.2.5.2 Testing the tolerability of OSI-906 in athymic nude mice 155
5.2.5.3 Initial *in vivo* test of the tolerability of combining OSI-906 with TMZ 159
5.2.5.4 Second *in vivo* test of the tolerability of combining OSI-906 with TMZ 161
5.2.5.4 Testing the effect of OSI-906 on TMZ sensitivity in human melanoma xenografts 164

CHAPTER 6 **171**

CONCLUSIONS AND FUTURE DIRECTIONS **171**

BIBLIOGRAPHY **178**

Abstract

Advanced melanoma poses a major therapeutic challenge, and despite the development of recent promising therapeutic agents, resistance to treatment remains a problem. Until recently, despite low response rates, alkylating agents dacarbazine and temozolomide (TMZ) were the standard of care for the treatment of advanced melanoma. The cytotoxic effects of these agents relies upon the formation of alkylated base lesions such as O^6-methylguanine (O^6MeG), which is repaired by a protein implicated in TMZ resistance called O^6-methylguanine-DNA methyltransferase (MGMT). Failure to resolve such alkylated bases results in DNA replication-associated double-strand breaks (DSBs). The type 1 insulin-like growth factor receptor (IGF-1R) mediates a number of characteristics common to cancers, including proliferation and survival, and evidence suggests it may also contribute to resistance to many anticancer agents. The aims of this study were to test whether melanoma cells could be sensitized to TMZ by small molecule IGF1R inhibitors, and to explore the mechanism of any chemosensitization. This study found an association between basal IGF1R phosphorylation and *in vitro* TMZ resistance in seven MGMT-proficient melanoma cell lines, suggesting that IGF1R activation may be linked with TMZ resistance. Furthermore, IGF1R inhibition caused dose-dependent sensitization of melanoma cells to TMZ, regardless of BRAF mutation status. This reduction in cell survival was not accompanied by an increase in apoptosis, but rather Chk2 activation and an accumulation of cells in the G2/M phase of the cell cycle, suggesting a possible effect of IGF1R inhibition on DNA repair. IGF1R depletion was found to increase MGMT protein levels and activity, but this effect was not seen in IGF1R inhibited cells. In addition, IGF1R inhibition was not epistatic with MGMT inhibition, and IGF1R inhibition reduced survival of TMZ treated MGMT-null cells. This suggested that TMZ sensitization by IGF1R inhibition was independent of MGMT. IGF1R inhibition did however cause an increase in the accumulation of TMZ-induced RPA foci, and delay in resolution of RAD51 foci. Together with the finding that IGF1R inhibition reduced survival in PARP inhibited melanoma cells, these results suggested that IGF1R inhibition influenced DSB repair by homologous recombination. Finally, the combination of IGF1R inhibition with TMZ was tested in a mouse model and was found to be tolerable. TMZ or IGF-1R inhibitor alone caused minor reduction in melanoma xenograft growth rates (rate reduction by 13% and 25% respectively), while combination treatment caused supra-additive growth delay (72%) that was significantly different from other treatment groups ($p<0.05$). The findings of this study suggest IGF1R inhibition as a possible option in overcoming alkylating drug resistance in melanoma.

List of Figures

Chapter 1

Figure 1.1	IGF1R signaling pathway	10
Figure 1.2	Biological events commonly associated with the formation of a melanoma	19
Figure 1.3	Methylated base lesions induced with TMZ treatment	32
Figure 1.4	Mechanism of repair and cytotoxicity of the O^6MeG lesion	35
Figure 1.5	Steps in homologous recombination (HR)	42

Chapter 2

Figure 2.1	Oligonucleotide-based MGMT activity assay principle.	58

Chapter 3

Figure 3.1	Expression of IGF1R signaling proteins in melanoma cell lines.	71

Figure 3.2	IGF1R expression and distribution in melanoma cell lines.	73-74
Figure 3.3	Effect of TMZ on melanoma cell viability	76
Figure 3.4	Correlation analysis between TMZ sensitivity and IGF1R levels or distribution in melanoma cells	79
Figure 3.5	AZ12253801 inhibits IGF1R signalling and survival	82
Figure 3.6	Combining IGF1R inhibition with TMZ reduces CHL-1 survival	84
Figure 3.7	AZ12253801 sensitizes to TMZ in A375M cells	85

Chapter 4

Figure 4.1	The effect of combining AZ12253801 with TMZ on Apoptosis in CHL1 cells	88
Figure 4.2	Testing AZ12253801 for induction of polyploidy	91
Figure 4.3	The effect of combining IGF1R Inhibition and TMZ on Cell Cycle Distribution by BrdU incorporation	93-94
Figure 4.4	The effect of IGF1R inhibition on cell cycle checkpoint mediators induced by TMZ	97
Figure 4.5	IGF1R Depletion increases level of MGMT protein in human melanoma cells	100
Figure 4.6	IGF1R Depletion leads to increased MGMT mRNA expression	101
Figure 4.7	MGMT levels increase with confluence and decrease with IGF-1 stimulation	103
Figure 4.8	Effect of IGF1R inhibition on MGMT levels	104

Figure 4.9 IGF1R depletion or inhibition does not alter MGMT function 106

Figure 4.10 IGF1R inhibition is not epistatic with MGMT inhibition 108

Figure 4.11 IGF1R inhibition does not affect AAG Activity 112

Figure 4.12 Effect of IGF1R inhibition on formation of TMZ induced γ-H2AX foci 115-116

Figure 4.13 Effect of IGF1R inhibition on formation of TMZ induced 53BP1 foci 118-119

Figure 4.14 IGF1R inhibition increased TMZ induced RPA foci 122-123

Figure 4.15 IGF1R inhibition causes persistence of TMZ induced RAD51 foci 127-128

Figure 4.16 The effect of IGF1R inhibition on DNA repair related proteins induced by TMZ 133

Figure 4.17 The effect of IGF1R inhibition on Chromatin binding of DNA repair mediators induced by TMZ 135

Figure 4.18 IGF1R inhibition enhanced melanoma sensitivity to PARP inhibition 137

Chapter 5

Figure 5.1 OSI-906 inhibited IGF1R receptor activation 143

Figure 5.2 The effect of OSI-906 on viability of melanoma cells 145-146

Figure 5.3 Sensitivity to OSI-906 is enhanced by functional p53 150

Figure 5.4 OSI-906 enhances melanoma sensitivity to TMZ in a schedule dependent manner 153

Figure 5.5 A375M cells form xenografts in nude mice and 156

TMZ inhibits xenograft growth

Figure 5.6 OSI-906 was tolerated and bioavailable in athymic nude mice 160

Figure 5.7 Testing the tolerability of combining OSI-906 with TMZ in athymic nude mice by two treatment schedules 162

Figure 5.8 Toxicity and pharmacokinetic study of alternative vehicles for TMZ and OSI-906 165

Figure 5.9 OSI-906 enhances the sensitivity of melanoma xenografts to TMZ 168-169

List of Tables

Chapter 2

Table 2.1	Cell lines used in this project	47
Table 2.2	Antibodies used for Western Blotting	52
Table 2.3	Primers and probes used for qRT-PCR	56
Table 2.4	Antibodies used for immunofluorescent staining	64

Chapter 3

Table 3.1	Genotypes of the melanoma cell line panel	68

Chapter 4

Table 4.1	Statistical analysis of caspase activation for TMZ and or AZ12253801 treatment	89
Table 4.2	Effect of O6BG on AZ12253801 induced TMZ sensitization	109

Chapter 5

Table 5.1 Summary of GI_{50} values for OSI-906 and mutation status of melanoma cells 146

Table 5.2 Comparison of 100mg/kg and 50mg/kg TMZ alone, and in combination with OSI-906 in vivo. 170

Abbreviations

AAG	Alkyladenine DNA glycosylase
ABC	ATP-binding cassette
ABH	Alk B homologue
AKT	'Ak' thymoma (also called protein kinase B or PKB)
ANOVA	Analysis of variance
CTLA-4	Cytotoxic T-lymphocyte antigen-4
APE 1	Apurinic/apyrimidic endonuclease 1
AP site	Apurininc/apyrimidic site
APNG	Alkylpurine DNA N-glycosylase
ARID	AT-rich interaction domain
ATCC	American Type Culture Collection
ATM	Ataxia telangiectasia mutated
ATP	Adenosine triphosphate
ATR	Ataxia telangiectasia and RAD3-related protein
ATRIP	ATR-interacting protein
BACT	β-Actin
BAD	Bcl-2-associated death promoter
Bak	Bcl-2 antagonist/killer
BCA	Bicinchoninic acid
Bcl-2	B cell lymphoma 2 protein
BER	Base excision repair
BRAF	Rapidly Accelerated Fibrosarcoma B
BrdU	5-bromo-2'-deoxyuridine
BRIM-8	BRAF inhibitor in Melanoma-8 trial
BSA	bovine serum albumin
cdc2	Cell division control 2 (also called cyclin-dependent kinase 1 or CDK-1)
CDKs	cell-cycle dependent kinases
cDNA	Complementary DNA
Chk	checkpoint kinase
CTG	CellTiter-Glo
DEPC	Diethylpyrocarbonate
DMEM	Dulbecco's Modified Eagle's Medium

DMSO	Dimethyl sulphoxide
DNA	Deoxyribonucleic acid
DNA-PK$_{cs}$	DNA-dependent protein kinase catalytic subunit
dNTPs	Deoxyribonucleotides
DSBs	Double strand breaks
DTIC	Dacarbazine
DTT	Dithiothreitol
4E-BP1	4E-binding protein 1
ECL+	Enhanced Chemiluminescence Plus Reagent
EDTA	Ethylenediaminetetraacetic acid
eIF4E	Eukaryotic translation initiation factor 4E
EGFR	Epidermal growth factor receptor
EGTA	Ethylene glycol tetraacetic acid
ERK1/2	Extracellular signal related kinase 1/2
eNOS	Endothelial nitric oxide
FBS	Fetal bovine serum
FDA	US Food and Drug Administration
FEN1	Flap endonuclease 1
FOXO	Forkhead box O
GADP	Glyceraldehyde-3-phosphate dehydrogenase
GI$_{50}$	Concentration of drug required to inhibit growth of cells to 50% of that in solvent treated cells
Grb2	Growth factor receptor-bound protein-2
GSK-3	Glycogen synthase kinase-3
GTP	Guanosine triphosphate
γ-H2AX	Phosphorylated histone H2A type X
HCl	Hydrochloric acid
HDI	High dose interferon
HDM2	Human homolog of MDM2
HIF1α	Hypoxia-inducing factor alpha
H_2O	Water
HR	Homologous recombination
HRP	Horse radish peroxidase
HRR	Homologous recombination repair
IGF	Insulin-like growth factor
IGFBPs	*Insulin-like growth factor binding proteins*
IGF1R	type 1 insulin-like growth factor receptor
IGF2R	type 2 insulin-like growth factor receptor

IL-2	Interleukin 2
ILP	Isolated limb perfusion
IP	Intraperitoneal
IR-A	Insulin receptor type A
IRS-1	Insulin receptor substrate-1
JARID	Jumonji/ AT-rich interaction domain
MAPK	Mitogen activated protein kinase
MAP2K	Mitogen activated protein kinase kinase
MAP3K	Mitogen activated kinase kinase kinase
MDC1	Mediator of DNA damage checkpoint protein 1
MDM2	Mouse double minute 2 homolog
MEK	MAPK/ERK kinase
$MgCl_2$	Magnesium chloride
MGMT	O^6-methylguanine-DNA methyltransferase
MITF	Microphthalmia-associated transcription factor
MMR	Mismatch repair
MMS	Methyl methanesulphonate
MPG	N-methylpurine-DNA glycosylase
MPP-2	Matrix metalloproteinase-2
mRNA	messenger RNA
MSH	Human MutS homolog
MTIC	Methyl-triazeno-imidazole-carboxamide
mTOR	Mammalian target of rapamycin
mTORC	Mammalian target of rapamycin complex
NaCl	Sodium chloride
NER	Nucleotide excision repair
NHEJ	non-homologous end joining
N^7MeG	N^7-methylguanine
N^3MeA	N^3-methlyadenine
O^6MeG	O^6-methylguanine
OS	Overall survival
PI3K	Phosphoinositide-3 kinase
p53	tumour protein 53
PARP	poly ADP-ribose polymerase
PBS	Phosphate buffered saline
PCNA	Proliferating cell nuclear antigen
PCR	Polymerase chain reaction

PD-1	Programmed death-1
PDGFR	Platelet-derived growth factor receptor
PDK1	PIP_3-dependent kinase-1
PD-L1	Programmed death ligand-1
PFA	Paraformaldehyde
PFS	Progression-free survival
PI	Propidium iodide
PIP_2	Phosphatidylinositol-4,5-bisphosphate
PIP_3	Phosphatidylinositol-3,4,5 triphosphate
PI3K	Phosphatidylinositol-3-kinase
PIPES	1,4-Piperazinediethanesulfonic acid
PK	Pharmacokinetic
PKB	Protein kinase B
Pol β	DNA polymerase β
Pol δ	DNA polymerase δ
PRAS40	proline-rich AKT substrate of 40kDa
PTEN	Phosphatase and tensin homolog
pTRE	Tet-responsive plasmid
qRT-PCR	quantitative real-time PCR
RAS	Rat sarcoma protein
RAF	rapidly Accelerated Fibrosarcoma kinases
Rb	retinoblastoma
RGP	radial growth phase
RFS	relapse-free survival
RL	Ringer's Lactate
RNA	Ribonucleic acid
RNAi	RNA interference
RPA	replication protein A
rpm	Revolutions per minute
RPMI	Roswell Park Memorial Institute Medium
RT	Room temperature
RTK	Receptor tyrosine kinases
SD	Standard deviation
SDS	Sodium dodecyl sulphate
SDS PAGE	SDS polyacrylamide gel electrophoresis
SEM	Standard error of the mean
SF_{50}	Concentration of drug required to inhibit cell survival to 50% of that in solvent treated cells

shRNA	Short hairpin RNA
SOS	Son of sevenless
SLNB	Sentinel lymph node biopsy
siRNA	small interfering RNA
SSB	Single strand break
ssDNA	Single-stranded DNA
TBS	Tris buffered saline
TBST	TBS with 0.1% Tween
TKI	tyrosine kinase inhibitor
TMZ	Temozolomide
TNF-α	Tumour necrosis factor -α
TSC1	Tuberous sclerosis complex 1
TSC2	Tuberous sclerosis complex 2
UV	Ultraviolet
VEGF	Vascular endothelial growth factor
WT	Wild type
XRCC1	X-ray repair cross-complementing protein 1

Chapter 1

Introduction

There is growing interest in the contribution of the type 1 insulin-like growth factor receptor (IGF1R to cancer biology) since it mediates many characteristics of the malignant phenotype including growth, proliferation, survival, motility and invasion. Evidence also suggests that IGF1R plays a role in mediating drug resistance, which is a serious ongoing problem encountered in treating malignant melanoma. Previous work from our group found that IGF1R depletion sensitized melanoma cells to an alkylating agent (Yeh et al., 2006). This project explored the role of IGF1R signaling in mediating alkylating drug resistance in malignant melanoma, and was carried out in collaboration with Geoff Margison of the Carcinogenesis group, Paterson Institute of Cancer Research, and Professor Adrian Harris of the Growth Factor Group, Weatherall Institute of Molecular Medicine, Oxford.

1.1 Insulin-like growth factor (IGF) system

The IGF system is important to both normal cell function and tumorigenesis since it regulates growth, development and metabolism both at a cellular level and in the organism as a whole. The IGF axis comprises two transmembrane

receptors, the type 1 insulin-like growth factor receptor (IGF1R) and the type 2 insulin-like growth factor receptor (IGF2R); two ligands, IGF-1 and IGF-2; and at least six high affinity insulin-like growth factor binding proteins or IGFBPs (Denley et al., 2005; Pollak, 2008; Werner, 2012)

1.1.1 IGF axis components

1.1.1.1 Insulin-like growth factors

IGF signaling is mediated through the action of the peptide hormones IGF-1 and IGF-2, which are structurally similar to each other and to insulin (Denley et al., 2005). The liver is the main source of circulating IGFs. In addition, somatic and neoplastic cells produce IGFs locally. Thus, these hormones execute their functions via endocrine, paracrine and autocrine processes (Gao et al., 2012). IGFs are important for normal cell growth, and IGF production has been found to be abnormally low in Laron dwarfism, which occurs in individuals with growth hormone receptor mutation (Baserga et al., 1997; Laron et al., 1989). A worldwide survey found that none of the 230 Laron syndrome patients studied developed malignancy up to an average age of 85, implicating an association between IGFs and tumour development (Steuerman et al., 2011). Postnatally, growth hormone stimulates IGF-1 production, which is the main regulator of normal growth and development at this stage. A number of murine models have investigated intrauterine growth regulation by IGFs. Mice that are homozygous for either IGF-1 or IGF-2 gene disruptions have similarly reduced birth weights, 60% below wild-type littermates (Liu et al., 1993). Further studies demonstrated differences in the roles of these two IGFs. IGF-2 was shown to coordinate early

embryonic growth, when IGF-1 levels appear to be lower. In late gestation however, IGF-1 is the main mediator of growth and development (Gluckman and Pinal, 2003). Also, mice with IGF-1 gene disruption are infertile while IGF-2 null mice are not, suggesting that IGF-1 is more important for reproductive development (Stratikopoulos et al., 2008). IGFs exert their effects by interacting with the type 1 insulin-like growth factor receptor (IGF1R) to initiate IGF signaling, IGF-1 binding to the IGF1R with greater affinity than IGF-2 (Clemmons, 2007).

1.1.1.2 Insulin-like growth factor receptors (IGFRs)

There are two IGFRs, type 1 and type 2, which are structurally and functionally different (Baserga et al., 1997; Clemmons, 2007). IGF1R is a cell surface receptor tyrosine kinase (RTK) that is expressed on most normal tissues, except for hepatocytes and T lymphocytes (Sachdev and Yee, 2001). Transcription of the *IGF1R* gene, located on chromosome 15, results in the formation of a single precursor polypeptide comprising an amino-terminal signal peptide, the α-subunit and the carboxy-treminal β-subunit (Ullrich et al., 1986). Cleavage of the signal polypeptide occurs on translocation to the endoplasmic reticulum, where dimerization of each of the α- and β-subunits results in IGF1R proreceptor-formation in the β-α-α-β arrangement (Denley et al., 2005). Glycosylation and further cleavage in the Golgi apparatus results in the formation of the mature hetero-tetrameric IGF1R, which comprises two α-subunits and two β-subunits linked by disulfide bonds (Adams et al., 2000).

The α-subunits are extra-cellular and perform the ligand-binding function of the receptor. The β-subunits are transmembrane and intracellular in location. The

β-subunit possesses the tyrosine kinase domain, which spans the region containing amino acids 973-1229 (Baserga et al., 1997; Denley et al., 2005; Larsson et al., 2005). Two important binding sites are also found on the β-subunit. One binding site for docking proteins, Shc and insulin receptor substrate-1 (IRS-1) is located at tyrosine-950 and another is the ATP binding site at lysine-1003 of the β-subunit (Baserga et al., 1997; O'Connor et al., 1997).

Unlike IGF1R, the type 2 insulin-like growth factor receptor (IGF2R) is monomeric, lacks tyrosine kinase activity and does not participate directly in signaling along the IGF axis (Larsson et al., 2005; Massoner et al., 2010). Instead, it binds to IGF-2 with high affinity, limiting its ability to interact with IGF1R. IGF-2/IGF2R binding results in IGF-2 internalization and degradation. IGF2R therefore acts as a negative regulator of the IGF axis (Denley et al., 2005; Ghosh et al., 2003; Massoner et al., 2010). In murine models, IGF2R null mice display excessive growth *in utero* and die soon after birth as a result of abnormal overgrowth of the skeleton, cardiac muscle and lungs (Wylie et al., 2003). IGF1R null mice on the other hand, are severely growth retarded and invariably die at birth from respiratory failure (Liu et al., 1993). This highlights the importance of regulated IGF signaling to growth and development.

1.1.1.3 Insulin-like growth factor binding proteins (IGFBPs)

IGFBPs are a family of at least six small proteins, most of which are key regulators of the activity of IGFs, although recent evidence suggests IGF-

independent functions. In the IGF system, IGFBPs bind to IGFs, preventing their degradation and limiting their availability to interact with the target receptor, IGF1R. Most of the circulating IGFs are bound to IGFBP3 in a trimeric complex along with another protein known as acid-labile subunit (ALS) (Hwa et al., 1999; Yu et al., 1999). The IGF/IGFBP complex can be cleaved by IGFBP-specific proteases, resulting in release of IGFs, which can bind to IGF1R, allowing IGF signaling to be initiated (Collett-Solberg and Cohen 1996).

1.1.2 IGF Signaling

The extracellular interaction of IGF ligand with the α-subunit of the IGF1R initiates IGF signal transduction by inducing autophosphorylation of tyrosine residues 1131, 1135 and 1136 within the kinase domain of the β-subunit (Baserga et al., 1997). This causes a conformational change of the β-subunit, which permits ATP binding, further enhancing intrinsic tyrosine kinase activity and the phosphorylation of juxtamembrane tyrosine residues of the IGF1R. Phosphorylation of tyrosine-950 allows docking of intracellular adaptor proteins, IRS-1 and Src homology and collagen domain protein (Shc) (Adams et al., 2000). The binding of these proteins activates signaling via two major pro-survival and pro-proliferative cell signaling pathways: the PI3K/AKT pathway and the RAS/RAF/MAPK pathway, as shown in Figure 1.1

1.1.2.1 PI3K/AKT pathway

IGF1R phosphorylates insulin receptor substrate-1 (IRS-1), allowing this adaptor protein to bind the p85 regulatory subunit of phosphatidylinositol-3-kinase (PI3K). This activates PI3K, which then phosphorylates phosphatidylinositol-4,5-bisphosphate (PIP_2) to form phosphatidylinositol-3,4,5-triphosphate (PIP_3) in a reaction that is reversed by phosphatase and tensin homolog (PTEN) (Vanhaesebroeck and Alessi, 2000). PTEN therefore acts as a tumour suppressor by negatively regulating PI3K/AKT signaling (Stambolic et al., 1998). PIP_3 formed on the plasma membrane binds to PIP_3-dependent kinase-1 (PDK1) and AKT (protein kinase B or PKB) so that PDK1 can then phosphorylate AKT on Threonine 308, which allows a second phosphorylation on Serine-473 of AKT by mammalian target of rapamycin complex 2 (mTORC2), which is activated by IGF1R via an unknown mechanism. AKT is a serine-threonine kinase which has multiple targets related to cell survival, proliferation, angiogenesis, invasion and metabolism (Chitnis et al., 2008; Manning and Cantley, 2007; Zha and Lackner, 2010).

PI3K/AKT signaling promotes cell survival by several pathways. AKT favours mitochondrial membrane stabilization by phosphorylating and inhibiting the pro-apoptotic factor, Bcl-2-associated death promoter (BAD). This prevents binding of BAD to Bcl-2, thus allowing Bcl-2 to exert its anti-apoptotic effect (Datta et al., 1997; Manning and Cantley, 2007). AKT also phosphorylates the FOXO (Forkhead box proteins subclass O) family of transcription factors, to inhibit FOXO mediated transcription of pro-apoptotic genes (Tran et al., 2003). In addition, AKT phosphorylates the ubiquitin-ligase, Mouse double minute-2

homolog (MDM2 or HDM2), promoting its nuclear translocation where it targets p53 for degradation as illustrated in Figure 1.1 (Franke et al., 2003).

AKT stimulates proliferation via a number of targets, which affect cell cycle regulation (Figure 1.1). For example, $p27^{Kip1}$ and $p21^{Waf1}$ inhibit cell-cycle dependent kinases (CDKs) responsible for G1-S progression (Figure 1.1). AKT directly phosphorylates $p27^{Kip1}$ and $p21^{Waf1}$, resulting in cytosolic sequestration, thus promoting cell cycle progression. The expression of $p27^{Kip1}$ is also reduced by AKT inhibitory phosphorylation of one of its transcription factors, FOXO (Medema et al., 2000). In addition, AKT activation leads to MDM2-mediated p53 degradation, reducing p53-mediated expression of $p21^{Waf1}$ (Murray-Zmijewski et al., 2008). AKT also induces inhibitory phosphorylation of glycogen synthase kinase-3 (GSK-3) blocking GSK-3-induced degradation of cyclin D and E, thereby promoting G1-S progression. In addition, GSK-3 phosphorylates and inhibits c-myc and c-jun, which are transcription factors of these cyclins (Manning and Cantley, 2007; Wisdom et al., 1999). AKT also causes inhibitory phosphorylation of FOXO transcription factors, preventing FOXO-induced $p27^{Kip1}$ expression and suppression of cyclin D expression, thereby promoting G1-S progression (Tran et al., 2003). AKT promotes G2-M transition by Serine 280 phosphorylation of cell cycle checkpoint kinase 1 (Chk1), resulting in its ubiquitination and degradation, thus preventing Chk1-induced G2 arrest (Donzelli and Draetta, 2003).

An important effector of AKT is the mammalian target of rapamycin complex 1 (mTORC1), which stimulates cell proliferation and growth via two mechanisms. Firstly, AKT phosphorylates tuberous sclerosis complex 2

(TSC2), to inhibit the GTPase activity of the TSC1/TSC2 complex. This allows GTP to accumulate and interact with RAS homologue enriched in brain (Rheb), facilitating binding with and activation of mTORC1 (Long et al., 2005). In parallel, AKT phosphorylates proline-rich AKT substrate of 40kDa (PRAS40), hindering its interaction with mTORC1, which it negatively regulates. Active mTORC1 phosphorylates eukaryotic translation initiation factor 4E-binding protein 1 (4E-BP1) allowing it to release eukaryotic translation initiation factor 4E (eIF4E), which is required to initiate protein synthesis necessary for growth and indirectly for proliferation by up regulating cyclins. The mTORC1 complex also phosphorylates and activates p70 S6 kinase, which activates ribosomal protein S6, enhancing translation (Ma and Blenis, 2009). In addition, mTORC1 and p70 S6 kinase directly phosphorylate IRS-1, allowing it to be targeted for degradation, thus serving as a negative regulator of PI3K/AKT signaling (Engelman et al., 2006).

AKT promotes angiogenesis by phosphorylating and activating endothelial nitric oxide synthase (eNOS) as well as increased expression of hypoxia-inducing factor alpha (HIF1α), a transcription factor for vascular endothelial growth factor or VEGF (Semenza, 2007; Zelzer et al., 1998). In addition, IGFs promote tumour cell invasion by increasing the expression of matrix metalloproteinase-2 (MMP-2), which breaks down the surrounding ECM. This effect was found in a lung cancer model to occur via the PI3K-AKT pathway (Zhang and Brodt, 2003; Zhang et al., 2003), however work in a prostate cancer model found this effect to be dependent on both PI3K/AKT and MAPK pathways (Saikali et al., 2008). Finally, AKT affects cellular metabolism by enhancing glucose uptake. AKT2 induces translocation to the plasma

membrane of the glucose transporter, GLUT4, in response to insulin receptor signaling (Kohn et al., 1996). Increased GLUT1 expression is also associated with AKT activation and appears to result from upregulation of HIF1α (Zelzer et al., 1998). HIF-1α may also regulate expression of IGF-2, IGF-2R and IGFBP-3 (Feldser et al., 1999).

1.1.2.2 RAS/RAF/MAPK pathway

IGF1R phosphorylation of Shc results in recruitment of growth factor receptor-bound protein-2 (Grb2) and mammalian homolog of son of sevenless (SOS). This initiates another signaling cascade known as the RAS-RAF-MAPK pathway (Figure 1.1). The Grb2-SOS complex causes activation of a small GTPase called rat sarcoma (RAS) (Egan et al., 1993). The RAS family of G-proteins consists of K-RAS, H-RAS and N-RAS. GTP binding to RAS activates Rapidly Accelerated Fibrosarcoma kinases (RAF kinase) of which there are three subtypes, ARAF, BRAF and CRAF (or RAF-1). Activitated RAF phosphorylates, and activates, mitogen activated protein kinase kinase (MAP2K) or MAPK/ERK kinase 1/2 (MEK1/2). MEK phosphorylates the downstream serine-threonine kinase, extracellular signal related kinase 1/2 (ERK1/2) (Crews et al., 1992), which regulates the expression of over 160 target genes responsible for cellular proliferation and differentiation (Adams et al., 2000; Chitnis et al., 2008; Inamdar et al., 2010). In addition, ERK1/2 increases HIF1α expression, which, as mentioned above, mediates angiogenesis via increased VEGF expression (Semenza, 2007; Zelzer et al., 1998).

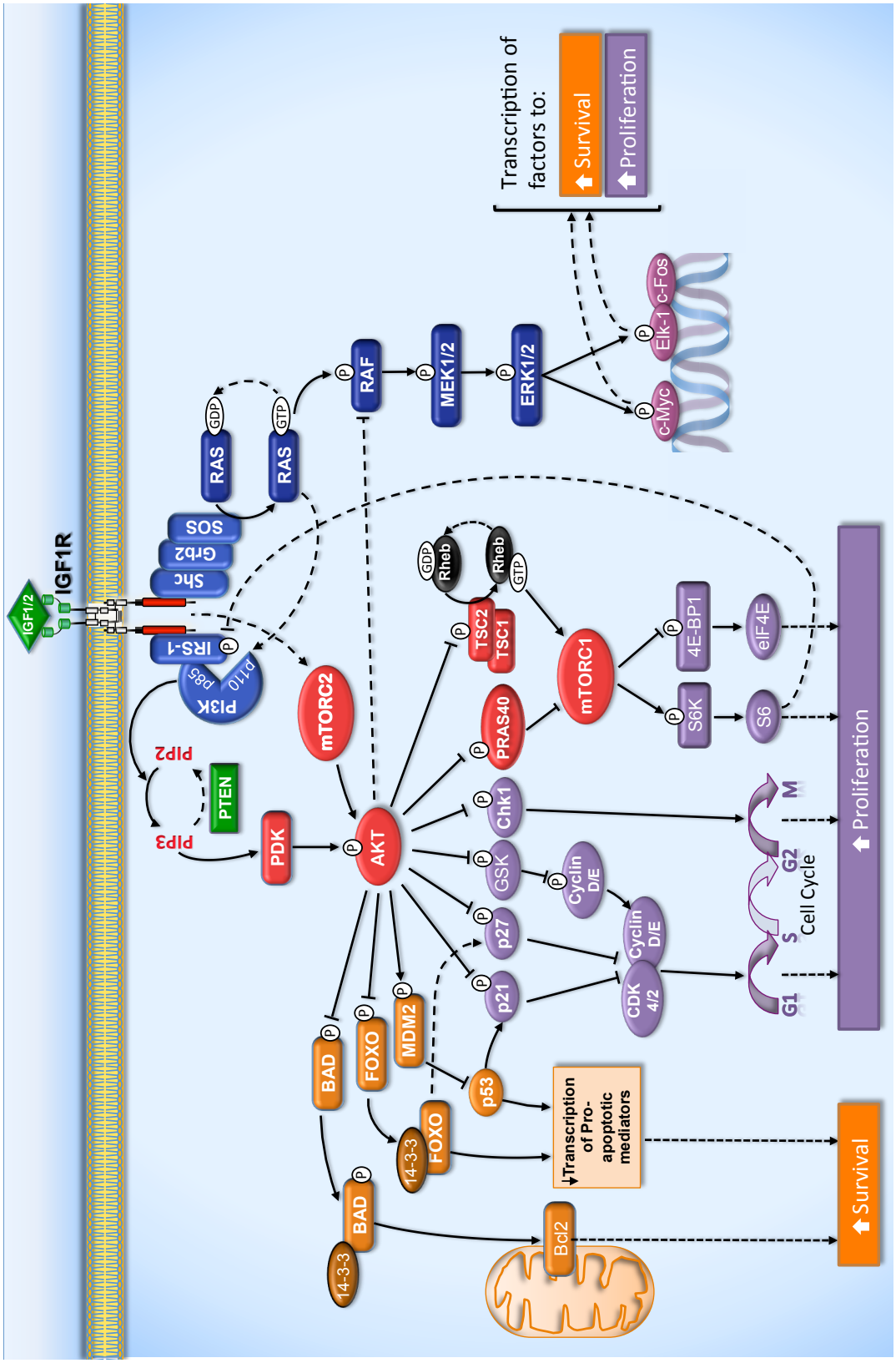


Figure 1.1 IGF1R signaling pathway. IGF1/2 ligand binding to IGF1R results in activation of PI3K/AKT and RAS/RAF/MAPK pathways, with enhanced effects on cellular survival, growth and proliferation. (Modified from Chitnis et al 2008, Zha and Lackner 2010)

1.1.3 IGF1R signaling and Cancer

Epidemiological and experimental evidence supports a link between IGF1R signaling and cancer risk. Initial studies demonstrated that serum IGF-1 levels in the upper limit of the normal range was associated with increased risk of prostate and premenopausal breast cancer (Chan et al., 2000; Hankinson et al., 1998), and a more recent metanalysis concluded that high IGF-1 ligand levels correlated with increased risk of these cancers (Renehan et al., 2004).

In addition, many established tumours frequently over-express IGF1R, particularly in prostate, renal, brain and haematologic malignancies (Hellawell et al., 2002; Werner, 2012). Experimentally, IGF1R null cells have been found to be refractory to transformation by known transforming oncogenes. Furthermore, the transformed phenotype can be reversed by reducing IGF1R signaling, using antisense mechanisms or blocking antibodies (Baserga et al., 1997; Sell et al., 1994). IGF1R expression determined by immunohistochemistry has also been associated with poorer prognosis in a number of cancer types, including renal, non-small cell lung cancer and squamous cell laryngeal cancer (Nakagawa et al., 2012; Parker et al., 2002). In addition, previous work from our lab showed that disease progression in prostate cancer has also been associated with increasing IGF1R expression (Turney et al., 2011).

1.1.4 IGF1R and Melanoma

A number of studies provide evidence for a role of IGF1R signaling in malignant melanoma biology. Progression from benign naevi to malignant melanoma is associated with increase in IGF1R expression determined by immunohistochemical staining of clinical samples (Kanter-Lewensohn et al., 2000). *In vitro,* experiments using RTK arrays found that IGF1R is commonly activated in a number of melanoma cell lines, even under serum-starved conditions, due to autocrine production of IGF-1 (Molhoek et al., 2011). Earlier work showed that blocking IGF1R signaling with an IGF1R antibody, IGF1R antisense oligonucleotide or short hairpin RNA (shRNA) caused growth inhibition of human melanoma cells *in vitro,* and *in vivo* in murine models (Furlanetto et al., 1993; Resnicoff et al., 1994; Tworkoski et al., 2011). As mentioned above, IGF1R promotes growth and survival via RAS/RAF/MAPK and PI3K/AKT signaling. Activating mutations in these pathways are common in melanoma (Gray-Schopfer et al., 2007), suggesting that IGF1R signaling blockade may be less effective in mutant BRAF melanoma cells. However, previous work from our group showed that IGF1R depletion with small interfering RNA (siRNA) was shown to reduce survival and increase apoptosis in melanoma cells *in vitro* regardless of BRAF mutation status (Yeh et al., 2006). IGF1R signaling has also been shown to promote migration of melanoma cells *in vitro*, suggesting that the IGF1R may also contribute to the invasiveness or progression of melanoma (Neudauer and McCarthy, 2003).

1.2 Malignant Melanoma

1.2.1 Background

Melanoma is a malignant tumour that arises from pigment producing cells called melanocytes. Such cells are most abundant in the skin, but are also found in other parts of the body of similar embryological origin. Hence, cutaneous melanoma is the most prevalent type of melanoma, but this malignancy can also affect other non-cutaneous sites, including the eye and the mucosa of the head and neck, gastrointestinal or urogenital tracts (Tas et al., 2011). This project focuses on the common, cutaneous form of melanoma.

Melanoma is a growing public health problem with an estimated 160,000 new cases diagnosed worldwide in 2008 (GLOBOCAN 2008 v1.2. Cancer Incidence and Mortality Worldwide: IARC Cancerbase). Individuals who are fair skinned, have had a significant history of UV sun exposure, have multiple atypical or dysplastic naevi or have a family history of melanoma are particularly at risk (Gandini et al., 2005a; Gandini et al., 2005b; Gandini et al., 2005c). In the UK, it is the fifth most common cancer, with 12,818 new cases diagnosed in 2010. Its incidence is rising faster than any other cancer. (http://info.cancerresearchuk.org/cancerstats). Even though it is not the most common form of skin cancer, it is the most lethal, accounting for 80% of skin cancer related deaths. Eighty percent of melanomas can be cured by simple surgical excision, however this is dependent upon early detection. In the

remainder of cases in which melanoma has spread, the prognosis is extremely poor. Five-year survival rates in the presence of regional nodal metastases range from 20 to 70% depending on the nodal burden, and this rate falls to less than 10% in patients with distant metastases (Coit et al., 2012). Moreover, the median survival from the development of distant metastases is only 6 to 10 months (Tsao et al., 2004a). A significant problem with this aggressive disease has been its resistance to conventional therapy and more recently to newer agents. A number of inherent biological mechanisms have been identified that may explain the resilience and aggressiveness of this disease.

1.2.2 Malignant Melanoma Biology

Melanoma is able to escape the normal mechanisms that regulate cellular proliferation and survival, via altered intracellular signaling (Gray-Schopfer et al., 2007). This enables melanoma to progress through the classical histological stages first described by Clark (Miller and Mihm, 2006), where normal melanocytes undergo stepwise changes toward becoming the eventual malignant entity. Enhanced proliferative and survival capacity also contribute to resistance to therapy. Key biological events, that appear to contribute to the development of melanoma, are summarized as follows:

Melanocyte hyperplasia and benign naevus formation: The earliest stage in melanocyte transformation involves hyperplasia and benign naevus formation, which is a consequence of enhanced proliferative signaling. A critical advancement was the recognition of the importance of the RAS-RAF-MAPK pathway, which is often constitutively activated as a result of NRAS or

BRAF mutations. Hyperactivation of ERK, a downstream effector of this pathway, is found in up to 90% of human melanomas, due to a high rate of such gain of function mutations along this pathway. The most common of these is the V600E BRAF mutation occurring in approximately 40-60% of melanomas (Davies et al., 2002; Long et al., 2011; Uribe et al., 2003), followed by NRAS mutation in 15-30% of cases (Colombino et al., 2012; Davies et al., 2002). The finding that greater than 80% of benign naevi possess an activating BRAF mutation is interesting, given that the vast majority of these naevi will not progress to become malignant melanomas (Gray-Schopfer et al., 2007; Pollock et al., 2003; Tsao et al., 2012). It is paradoxical therefore, that the product of mutant BRAF-related hyperproliferation is the formation of a benign naevus, which essentially is a cluster of senescent melanocytes. The reason rests on the function of intact cell cycle regulators, tumour protein 53 (p53) or Retinoblastoma (Rb) proteins, which keep hyper-proliferating mutant BRAF melanocytes in check by mediating cell cycle arrest, exit from cell cycle and replicative senescence (Ha et al., 2008; Patton et al., 2005). Even though evidence suggests that activation of MAPK signaling is often necessary for melanoma cell viability, it appears that the activating BRAF mutation alone is insufficient to cause malignant transformation of melanocytes (Tsao et al., 2012), and further events are necessary to produce this change toward the malignant phenotype.

Dysplastic naevus Formation: Senescence is a major obstacle to the malignant transformation and loss of cell cycle regulation allows melanocytes to escape senescence, forming atypical cells which grow aberrantly to form

dysplastic naevi (Ha et al., 2008; Miller and Mihm, 2006). As mentioned above, p53 or Rb pathways play an important role in mediating senescence. Mutations of p53 are relatively uncommon, occurring in 9% of melanomas (Bennett, 2008; Hocker and Tsao, 2007). On the other hand, 78% of melanomas have a defect in a gene closely related to these pathways, namely *CDKN2a (Bennett, 2008)*. This locus encodes for both $p16^{INK4a}$ and $p14^{ARF}$. The protein $p16^{INK4a}$ acts as a tumor suppressor in the Rb pathway by binding and inhibiting cyclin dependent kinase 4 and 6 (CDK4 and CDK6). These kinases phosphorylate Rb in G1, blocking the inhibitory interaction of Rb with E2F, a transcription factor required for expression of S phase genes that enable G1-S transition (Coqueret, 2002). Defective $p16^{INK4a}$ inhibits melanocyte senescence allowing mutant BRAF or NRAS mediated proliferation to continue unchecked, leading to dysplastic naevus formation (Gray-Schopfer et al., 2007) . It is therefore not unexpected that defective $p16^{INK4a}$ is encountered in dysplastic naevi but not benign ones (Tsao et al., 2012).

The protein $p14^{ARF}$ also acts as a tumour suppressor, but in the p53 pathway. MDM2 binding to p53 results in proteasomal degradation of p53 and $p14^{ARF}$ binds to MDM2 thus allowing accumulation of p53 (Coqueret, 2002). *CDKN2a* deletions result in loss of both $p16^{INK4a}$ and $p14^{ARF}$, whereas other *CDKN2a* mutations can produce defects in function of $p16^{INK4a}$ alone or with $p14^{ARF}$, but rarely is $p14^{ARF}$ alone affected (Gray-Schopfer et al., 2007). *CDKN2a* mutations are also present in 20-40% of familial melanomas (Bishop et al., 2002; Soufir et al., 1998), further highlighting the importance of this mutation in malignant transformation of melanocytes.

Radial Growth Phase of Melanoma: Dysplastic naevi may undergo further changes to form radial growth phase (RGP) melanoma. These comprise neoplastic melanocytes, which grow horizontally but these remain confined to the epidermis (Elder, 2006). These lesions can therefore be cured by simple surgical excision. Melanocytes of dysplastic naevi have higher levels of telomerase activity compared to benign naevi (Rudolph et al., 2000) and it has been proposed that RGP melanoma may represent immortalization of melanocytes of dysplastic naevi due to telomerase activation in the presence of $p16^{INK4a}$-Rb pathway dysfunction (Bennett, 2003).

Vertical Growth Phase of Melanoma: The next stage in melanoma development is the vertical growth phase, in which the tumour becomes invasive (Elder, 2006), and is postulated to be keratinocyte-independent, due to acquisition of anti-apoptotic signaling (Bennett, 2003). While activating BRAF and NRAS mutations promote proliferation and cell survival, deregulation of additional survival pathways in melanoma is thought to be required for invasive growth.

The PI3K pathway is commonly implicated in melanoma, and has potent survival and proliferative effects. Although mutations of PI3K itself are rare, AKT activation is found in 34-67% of melanoma, (Ibrahim and Haluska, 2009). This may be secondary to mutation in PTEN, a major regulator of the PI3K/AKT pathway, which is mutated or deleted in 20-40% of melanomas (Celebi et al., 2000; Pollock et al., 2002; Tsao et al., 2012), and occurring simultaneously with V600E BRAF mutations in 20% of melanomas (Tsao et al., 2004b). On the other hand, NRAS mutations are virtually mutually

exclusive of either PTEN or BRAF mutations, possibly because PI3K and BRAF are activated downstream of RAS. Additional activation of these mediators would therefore be redundant. PTEN and BRAF, however, act in parallel and therefore may provide greater proliferative and survival advantage in combination, to cooperate in melanoma development (Bis and Tsao, 2013; Gray-Schopfer et al., 2007; Tsao et al., 2012).

Another key regulator of apoptosis, B cell lymphoma 2 protein (Bcl-2) is over-expressed in 90% of melanomas (Ibrahim and Haluska, 2009). Bcl-2 is an anti-apoptotic mediator and is up-regulated in response to NRAS activation (Tsao et al., 2012). In the PI3K pathway, AKT activation results in BAD phosphorylation, which blocks its inhibitory effect on Bcl-2, allowing Bcl-2 to inhibit the pro-apoptotic proteins Bcl-2 associated x (Bax) and Bcl-2 antagonist/killer (Bak) protein, leading to pro-survival effects (Chipuk et al., 2010).

An important transcription factor called Microphthalmia-associated transcription factor (MITF), increases Bcl-2 expression and is amplified in 10-15% of melanomas (Gray-Schopfer et al., 2007; McGill et al., 2002). In addition, constitutive BRAF activation causes ERK-induced MITF phosphorylation, which further enhances survival via Bcl-2 expression (Sekulic et al., 2008). Although MITF has been implicated in melanocyte transformation, it is generally accepted that it cannot achieve this alone and often requires a co-existing activating BRAF mutation (Garraway et al., 2005).

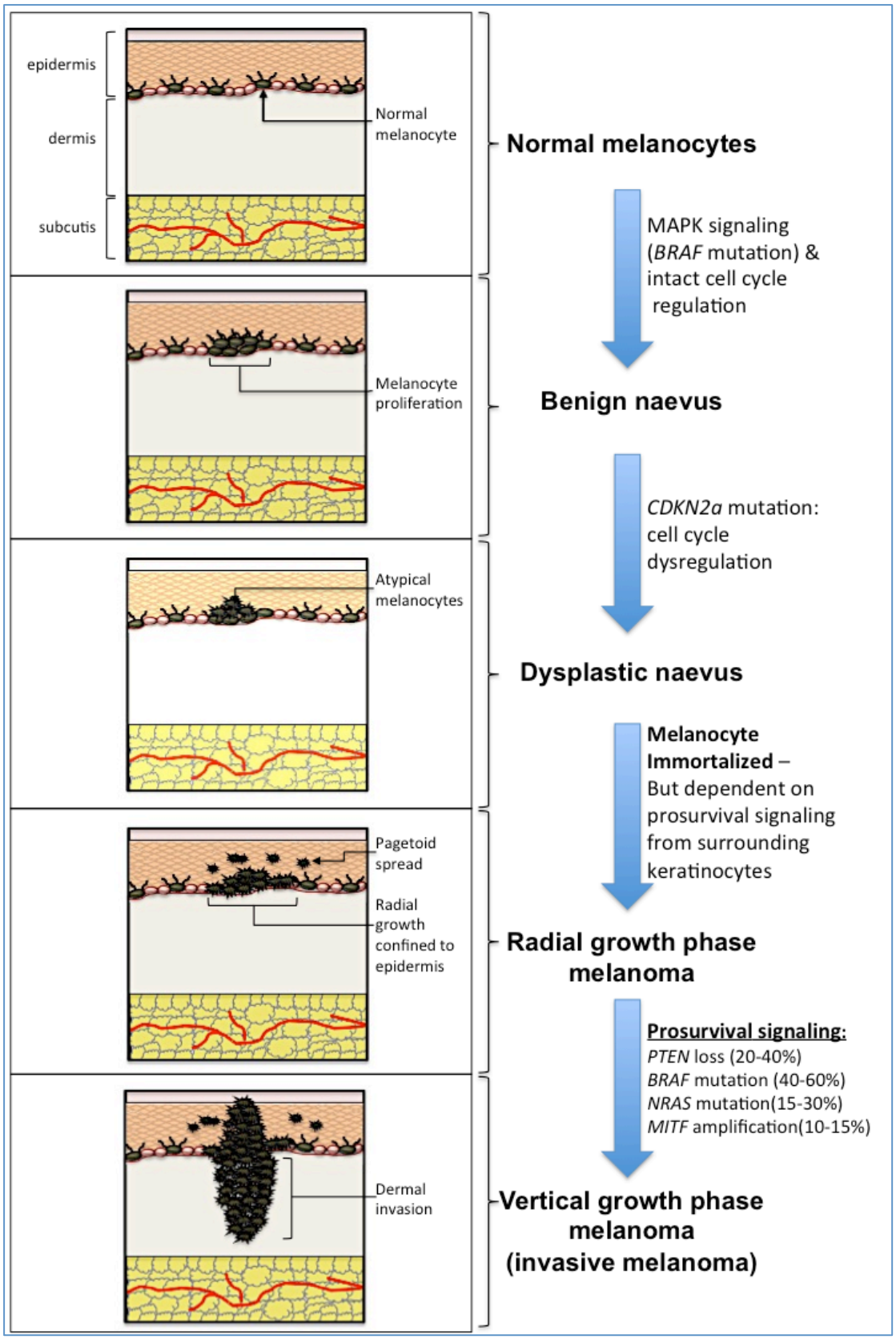


Figure 1.2 Biological events commonly associated with the formation of a malignant melanoma. Histological changes appear to be associated with intracellular signaling changes. Three of the four mutations encountered in invasive melanoma are downstream of the IGF1R. (Modified from Gray-Schopfer et al., 2007).

1.2.3 Malignant Melanoma Treatment

Treatment of malignant melanoma depends upon the stage of the disease, classified by the TNM system. This system uses the depth of invasion or Breslow thickness, presence of ulceration or mitoses, in-transit spread and regional lymph node metastasis or distant metastasis to determine the stage of the disease.

1.2.3.1 Stage I and II Melanoma Treatment- Localized Disease

Early stage melanomas, which are localized to the primary site, can be cured by surgery alone. The 20-year survival for stage I (<1mm thick) and stage II (1-4mm thick) melanomas is 90% and 80% respectively (Bis and Tsao, 2013).

Patients with intermediate thickness melanomas (>1mm thick) may be offered lymphatic mapping and sentinel node biopsy (SLNB) as a staging procedure, although this has no proven survival benefit (BAD guidelines 2010). Using this procedure, patients without clinically evident lymph nodes may be upstaged if histopathological examination confirms microscopic nodal involvement (Coit et al., 2012). The clinical relevance of the presence of nodal micrometastases is yet to be defined and many centers offer completion lymphadenectomy, though others may opt for surveillance (Morton, 2012).

1.2.3.2 Stage III Melanoma Treatment – Regional Lymph Node Metastasis

Stage III resectable disease can be managed with wide excision of the primary lesion with regional lymphadenectomy. For patients who are at high risk of relapse, that is with melanomas >4mm thickness or lymph node metastasis, adjuvant treatment with high-dose (HDI) or pegylated alpha-2b Interferon may be an option (Morton, 2012). The mode of action of interferon alpha-2b remains to be confirmed, although evidence suggests immunomodulatory effects including recruitment of macrophages and natural killer cell which may improve antigen presentation to lymphocytes. In addition, interferon therapy has also been associated with a reduction in growth and angiogenic factors such as VEGF and EGF (Ascierto and Kirkwood, 2008; Okuyama et al., 2010). Regardless of the mechanism, the FDA approved High-dose and pegylated interferon therapy in 1995 and 2011 respectively, as adjuvant treatment following complete resection of high risk melanoma based on clinical trials which demonstrated improved relapse-free survival (RFS) but no overall survival (OS) benefit (Eggermont et al., 2008; Kirkwood et al., 2000; Kirkwood et al., 1996).

Patients with unresectable stage III disease can be offered systemic treatments such as ipilimumab or vemurafenib, as used in stage IV disease (see below). For patients with unresectable in-transit and or satellite lesions, hyperthermic isolated limb perfusion (ILP) with melphalan, with or without TNF-α may be offered, since such regional therapy has been associated with improved tumour response rates and palliative benefit, though no overall survival benefit has been demonstrated (Lens and Dawes, 2003).

Currently, several trials are testing the effects of signalling inhibitors as adjuvant treatment for patients with high-risk melanoma, including the BRAF inhibitor, vemurafenib, in Melanoma-8 (BRIM-8) trial, and the COMBI-AD trial of dabrafenib with trametinib (Ascierto et al., 2012; Menzies and Long, 2013).

1.2.3.3 Stage IV Melanoma – Distant Metastatic Spread

The prognosis for metastatic melanoma is poor. The management is dependent on the extent of metastasis and whether the disease is resectable.

For decades alkylating agents were the mainstay of systemic treatment and this class of chemotherapeutic agents remained the standard of care for treating metastatic melanoma until recently (Marsden et al., 2010a). Immunotherapy and targeted therapy are now at the forefront of metastatic melanoma therapy.

Immunotherapy

Immunotherapy with Interleukin 2 (IL-2) gained FDA approval for the treatment of metastatic melanoma in 1998. Approximately 16% of patients respond to IL-2 monotherapy and 4-6% of patients may benefit from durable complete remission (Atkins et al., 1999). Its use however, can be limited by significant toxicity (Chapman et al., 2011; Kushnir and Merimsky, 2013). One trial demonstrated that high-dose IL-2 combined with with gp100 vaccine could improve response rates and progression-free survival over IL-2 alone, with a similar IL-2 related side effect profile (Schwartzentruber et al., 2011).

The use of IL-2 has now largely been superseded by recent developments in immunotherapy.

The first of the modern era of immunotherapies is ipilimumab, a fully humanized monoclonal antibody (IgG1) against cytotoxic T-lymphocyte antigen (anti-CTLA-4), which increases antitumour immunity by blocking the suppressive effects of this antigen on T cell activation (Hodi et al., 2010). In 2011, the FDA approved its use for the treatment of unresectable or metastatic melanoma, since it was shown to improve overall survival (OS) in a phase III international, multicenter, double-blind study compared with gp100 vaccine with a median OS of 10 months in patients treated with ipilimumab compared with 6.4 months with gp100 vaccine (Hodi et al., 2010). This agent is not without significant side effects, with immune-mediated toxicity affecting the skin, gastrointestinal or endocrine systems (Maio et al., 2013).

Newer immunotherapy agents directed against the programmed death-1 (PD-1) receptor have shown promise in treating advanced melanoma. The programmed death ligand-1 (PD-L1) is expressed by many cancer tissues, and upon binding with PD-1, reduces T cell activation, thereby inhibiting self-directed immune recognition (Okazaki and Honjo, 2007). Nivolumab, a monoclonal antibody directed against PD-1, has shown objective responses in early phase trials in 28% of patients with advanced melanoma, with median overall survival of 16 months (Topalian et al., 2012). This and other PD-1 antibodies appear to be better tolerated than ipilimumab, show more durable responses, and are presently under further clinical evaluation (Homet and Ribas, 2013)

Targeted Therapy

Targeted therapy in melanoma has focused initially on the development of inhibitors of mutant BRAF. The FDA approved Vemurafenib, a selective, small molecule mutant V600E BRAF inhibitor, in 2011 for the treatment of unresectable or metastatic melanoma that tested positive for the V600E BRAF mutation. This was based on results of the BRIM-3 multicenter, randomized control trial, which demonstrated superior response rates with vemurafenib (48%) compared with the standard of care, dacarbazine (DTIC) chemotherapy (5%). Vemurafenib also produced superior median progression-free survival (PFS) of 5.3 months, compared with 1.6 months with DTIC treatment (Chapman et al., 2011). However, vemurafenib causes significant toxicity, with nonmelanoma skin cancers and keratoacanthomas occurring in up to 30%, and the early development of resistance is problematic (Ascierto et al., 2012). Dabrafenib, another mutant V600E BRAF inhibitor, has recently gained FDA approval for the treatment of unresectable or metastatic melanoma. This agent has shown similar clinical efficacy to vemurafenib but with improved toxicity profile (Cheng et al., 2013; Salama, 2013). Neither of these agents is used in WT BRAF melanomas due to preclinical evidence suggesting that these agents paradoxically induce enhanced MAPK signaling (Solit and Rosen, 2011).

The selective MEK inhibitor, trametinib, was recently approved for the treatment of unresectable or metastatic melanoma harbouring V600E or K BRAF mutation. This was based on phase III trial data, which demonstrated improved overall survival (81% vs 76%) and median progression free survival

(4.8 vs 1.5 months) over chemotherapy with DTIC or paclitaxel (Flaherty et al., 2012).

Chemotherapy

A number of chemotherapeutic agents have been tested over the years, but only dacarbazine (DTIC), an alkylating agent received FDA approval in 1976 for the treatment of metastatic melanoma (Lee et al., 2013) . Response rates with DTIC are in the range of 10-20%, and are often transient, with a median duration of response of 3-6 months, although 1-2% may benefit from durable responses (Chapman et al., 1999; Rughani et al., 2013). Temozolomide (TMZ) is a derivative of DTIC, which has shown similar response rates but no difference in overall survival compared with DTIC. TMZ has advantages over DTIC in that it is orally bioavailable and penetrates the CNS (Middleton et al., 2000a), however is not licensed for melanoma treatment since it was not thought to be superior to DTIC (Patel et al., 2011).

Other chemotherapeutic agents trialed in advanced melanoma include vinca alkaloids, taxanes and platinum analogues. Response rates and OS were no better than that achieved with DTIC (Bhatia et al., 2009).

Immunotherapy and targeted therapy have overtaken alkylating agents in treating metastatic melanoma. Alkylating agents, however, are not obsolete and remain an option in treatment. Many of the newer agents can induce significant toxicity, and the use of vemurafenib, dabrafenib and trametinib is limited to mutant BRAF melanomas, while 40-60% of melanomas carry a wild-type BRAF genotype (Davies et al., 2002; Long et al., 2011; Uribe et al., 2003), Furthermore, development of early resistance to mutant BRAF

inhibition (Solit and Rosen, 2011) and prolonged responses to ipilimumab occurring in only a minority of cases (Hodi et al., 2010), highlights the resistant nature of this cancer to treatment.

1.2.4 Malignant melanoma resistance to treatment

A number of characteristics have been suggested to explain the resistance of melanomas to systemic treatment. Some factors are intrinsic and have been necessary for the development of the malignant disease. These are therefore present at the time of treatment. Other mediators of resistance develop in response to treatment and are therefore acquired (Bagrodia et al., 2012).

Intrinsic resistance to chemotherapy may be related to enhanced pro-survival or anti-apoptotic signaling, DNA repair mechanisms, failure of intracellular drug accumulation or intratumoral heterogeneity.

1.2.4.1 Evasion of apoptosis

Intrinsic resistance in melanoma may be related to the innate ability of these cells to survive, driven by derangements in normal apoptotic pathways and pro-survival cell signaling pathways (described in section 1.1.2). Many chemotherapeutic agents ultimately depend on apoptosis to produce cell death in response to their cytotoxic effects (Soengas and Lowe, 2003).

The anti-apoptotic mediator, Bcl-2, is overexpressed in most melanomas and its blockade enhances chemosensitivity via increased apoptosis (Jansen et

al., 2000; Wacheck et al., 2003). In addition, PTEN loss, and deranged MAPK signalling, via activated BRAF or NRAS mutations, may further contribute prosurvival effects which may interfere with the efficacy of cytotoxic therapy (Soengas and Lowe, 2003). This was previously investigated as a means of improving cytotoxic agent sensitivity. For example, one of the first BRAF inhibitors developed, sorafenib, enhanced temozolomide sensitivity in preclinical melanoma studies (Augustine et al., 2010). However, sorafenib combined with chemotherapy by way of carboplatin and paclitaxel in phase II trial failed to demonstrate any survival benefit over chemotherapy alone (Flaherty et al., 2013). This agent was subsequently found to be a poor BRAF inhibitor with activity towards alternative kinases (McDermott et al., 2008). Similarly, targeting the PI3K-AKT-mTOR pathway with an mTOR inhibitor enhanced chemosensitivity to TMZ preclinically (Thallinger et al., 2007), but clinical trials failed to show benefit of this combination over single agent TMZ chemotherapy (Dronca et al., 2013).

The rapid development of resistance to mutant BRAF inhibitors highlights the adaptability of this aggressive cancer. Many patients on vemurafenib relapse within 6-12 months of treatment (Bagrodia et al., 2012). A number of mechanisms have been identified to explain this, some related to activation of the ERK pathway which my be attributed to the acquisition of NRAS point mutations (Nazarian et al., 2010) or alternative signaling via increased expression of CRAF also known as RAF1 (Solit and Rosen, 2011). MEK or ERK activation associated with BRAF inhibitor resistance has also been linked with overexpression of mitogen activated kinase kinase kinase 8 (MAP3K8) also known as cancer Osaka thyroid oncogene or COT (Solit and

Rosen, 2011). Increased expression of receptor tyrosine kinases (RTKs) including platelet-derived growth factor receptor (PDGFR) and IGF1R has also been associated with resistance not only to BRAF inhibition but also to inhibitors of other signaling pathways such as AKT (Bagrodia et al., 2012; Chandarlapaty et al., 2011; Solit and Rosen, 2011; Villanueva et al., 2010).

1.2.4.2 Drug Efflux Pumps or Detoxification enzymes

Multidrug resistance may be attributed to the presence of P-glycoprotein which acts as a transmembrane drug transporter in a number of cancers, however, it is infrequently expressed in melanoma cells (Wu and Singh, 2011). Another family of transmembrane transporters, the ATP-binding cassette (ABC) proteins, has also been implicated in multidrug resistance. Members of this group expressed in melanoma include ABCA9, ABCB1, ABCB5, ABCB8, ABCC1, ABCC2 and ABCD1 (Chen et al., 2009), but thus far, only ABCB5 has been shown to cause drug resistance in melanoma cells, being associated with reduced intracellular accumulation of doxorubicin and resistance to this agent (Frank et al., 2005). ABCB5 expression in melanoma cells has also been associated with resistance to DTIC and vemurafenib, although intracellular accumulation of these agents was not quantified in this study (Chartrain et al., 2012). Another member of the ABC family, ABCG2, mediates vemurafenib resistance when ectopically expressed in A375 melanoma cells, however the significance of this result is debatable given that this ABC subtype is not commonly expressed in melanoma (Wu et al., 2013).

1.2.4.3 Intratumoral Heterogeneity

Melanoma is known to be a heterogenous tumour, and has been shown to contain subpopulations that are resistant to many forms of treatment.

One such feature that varies is the rate of division within the same tumour. A small subpopulation of cells, approximately 5-10% of the tumour mass, has been shown to express a histone 3 K4 demethylase known as jumonji/ARID (AT-rich interaction domain) or JARID1B. These cells are also negative for the proliferation marker, Ki-67, suggesting they are a slowly proliferating or slow-cycling subpopulation of melanoma cells (Roesch et al., 2010). Such slowly proliferating cells are more resistant to chemotherapy (Somasundaram et al., 2012). This is supported by the finding that chemotherapy results in an increase in the proportion of JARID1B positive melanoma cells which are capable of producing both JARID1B positive and negative progeny (Roesch et al., 2010).

Some subpopulations within melanomas have been found to display stem-like characteristics. These cells are relatively quiescent, and have been found to be highly resistant to treatment (Schatton and Frank, 2008). One study found that resistant non-small cell lung cancer cells express another histone 3 K4 demethylase known as JARID1A as well as IGFBP3, resulting in activation of IGF1R signaling. Such cells survive treatment and can expand or reform a heterogenous cell population. This study did not test for JARID1A expression in melanoma cells, but showed that histone deacetylase inhibition could restore BRAF inhibitor sensitivity in a resistant subpopulation of melanoma cells (Sharma et al., 2010).

Another potential mechanism related to tumour heterogeneity is the phenotype-switching model, in which cells reversibly switch from highly proliferative to slowly proliferative phenotypes. The reversibility of phenotype is in contrast to the stem cell model (Bell and Levy, 2011; Hoek and Goding, 2010). MITF (microphthalmia-associated transcription factor), frequently described as the master controller of melanocyte differentiation, has been implicated in phenotype switching, is upregulated in 20% of melanomas and is activated by MAPK signaling (Bell and Levy, 2011).

1.2.4.4 DNA repair mechanisms

Genomic integrity is essential for the survival of a cell and it is estimated that each cell of the human body must cope with tens of thousands of DNA lesions per day (Krejci et al., 2012). The assault on the genome may originate exogenously, such as from food, ultraviolet radiation, or combustion byproducts of tobacco or fuel. Endogenous sources of DNA damage include oxidant byproducts or molecules involved in intracellular metabolic pathways (Fu et al., 2012; Shrivastav et al., 2010). In order to deal with the resultant harmful DNA damage, organisms have evolved complex DNA repair mechanisms in order to preserve normal cellular integrity. This advantage unfortunately plays a significant role in mediating resistance chemotherapeutic resistance in cancer cells. Of relevance to melanoma are the processes involved in the repair of alkylating DNA damage, which are discussed further in the next section.

1.2.5 Alkylating DNA damage and repair

TMZ and DTIC are methylating agents, which are pro-drugs of the active metabolite methyl-triazeno-imidazole-carboxamide (MTIC). Formation of MTIC from DTIC requires metabolism by the liver whereas TMZ, which is orally bioavailable, becomes spontaneously hydrolyzed in solution at physiological pH to form this active metabolite (Stevens et al., 1987). MTIC methylates DNA bases on N- and O-atoms producing approximately a dozen types of alkylated base lesions or base adducts (as shown in Figure 1.2) (Fu et al., 2012).

DNA repair systems either deal with the primary alkylated base lesion itself or the secondary lesions formed as a result of processing of the primary lesions, such as double strand breaks (DSBs). As described in the following section, DSBs arise when replication forks stall at alkylated lesions or intermediates of base lesion repair. The ability of a cell to deal with DSBs is essential for cell survival, since this is the most toxic and lethal type of DNA damage (Kaina et al., 2007; Krejci et al., 2012).

Repair of a primary alkylated base adduct occurs by single step repair or multi-step repair depending on the type of base lesion.

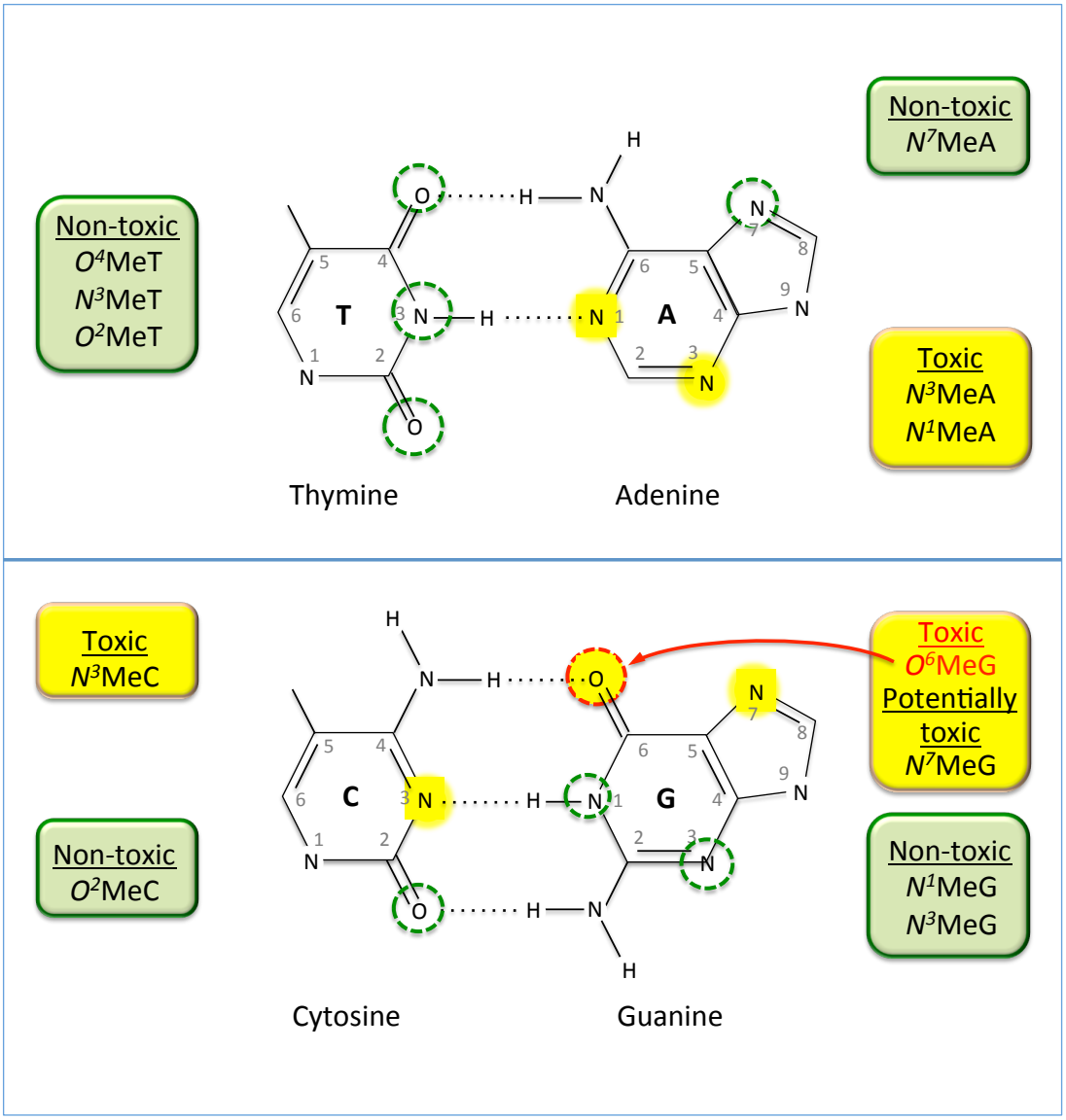


Figure 1.3 Methylated base lesions induced with TMZ treatment. The four DNA bases are shown with the possible alkylation sites from TMZ treatment. Toxic lesions cause replication block and are highlighted in yellow. O^6MeG is particularly toxic and is also circled in red. N^7MeG is non-toxic on its own, however may be potentially toxic if it undergoes depurination (Modified from Fu et al., 2012).

1.2.5.1 Single Step Repair of alkylated DNA lesions

O^6-methylguanine-DNA methyltransferase

Alkylation of the oxygen atom at position-6 of the guanine base forms the lesion O^6-methylguanine or O^6MeG. This is by no means the commonest alkylated base lesion, accounting for only 0.6-8% of all methyl adducts. It is however, the most toxic alkyl adduct and therefore the most important alkylated base lesion formed from TMZ treatment (Shrivastav et al., 2010). Its repair is therefore essential to understanding TMZ resistance. O^6MeG lesions persist indefinitely, unless they are removed by the protein, O^6-methylguanine-DNA methyltransferase (MGMT or alkyltransferase or ATase) (Klapacz et al., 2009). Upon formation of O^6MeG, MGMT translocates from the cytosol to the nucleus where it covalently accepts the methyl group from O^6MeG onto the cysteine-145 residue within its active site. In doing so, MGMT becomes inactivated, after which it undergoes ubiquitination and proteasomal degradation (Kaina et al., 2007; Pegg, 2000). If MGMT levels are inadequate, O^6MeG persists, pre-replicatively resulting in the disruption of hydrogen bonds between the methylated guanine and cytosine (ie O^6MeG:C pairing). This event on its own does not significantly distort the DNA double helix. Paradoxically, it is the intervention of another DNA repair pathway that makes O^6MeG such a toxic lesion (Figure 1.4).

During replication, O^6MeG may be paired with cytosine or mispaired with thymine. The MutSα complex, which is a heterodimer of human MutS homologs 2 and 6 (hMSH2 and hMSH6), recognizes this mispairing and initiates mismatch repair or MMR (Kondo et al., 2010). Post-replicatively the O^6MeG base adduct post-replicatively is in the template strand, and the MMR

machinery acts on the synthesized strand, thus DNA polymerase δ (Pol δ) resynthesizes cytosine or thymine so that the O^6MeG:C pair or O^6MeG:T mispair persists, triggering the MMR machinery to repeatedly and unsuccessfully attempt to resolve the mispair. This process is known as "futile MMR cycling" (Karran and Marinus, 1982). The repeated MMR processing induces DNA nicks or gaps, causing replication fork collapse, which ultimately leads to toxic DSB formation (Ochs and Kaina, 2000). In addition MMR complexes are said to interact directly with ATM or ATR, which initiate cell cycle arrest via activation of checkpoint kinases as well as p53-mediated apoptosis signaling (Jiricny, 2006; Kaina et al., 2007).

In vitro experimental resistance to methylating agents has been linked to high levels of expression of MGMT, which is related to reduced MGMT promoter methylation (Esteller and Herman, 2004; Margison et al., 2003; Middleton et al., 1998). This link has clearly been demonstrated in clinical studies of malignant gliomas (Esteller et al., 2000; Gorlia et al., 2008; Hegi et al., 2005). In melanoma however, the relationship between MGMT expression and alkylating drug sensitivity is less clear. In a study of melanoma biopsies, Middleton et al found that pretreatment MGMT levels were not predictive of clinical response to TMZ using an MGMT activity assay as the quantification technique (Lee et al., 1991; Middleton et al., 1998). In contrast, Ma et al found that clinical response to DTIC was inversely related to MGMT expression determined by immunohistochemistry (Ma et al., 2003). As stated above, alkylating agent cytotoxicity from O^6MeG is not solely dependent on MGMT status, and MMR function must also be considered (Kawate et al., 2000).

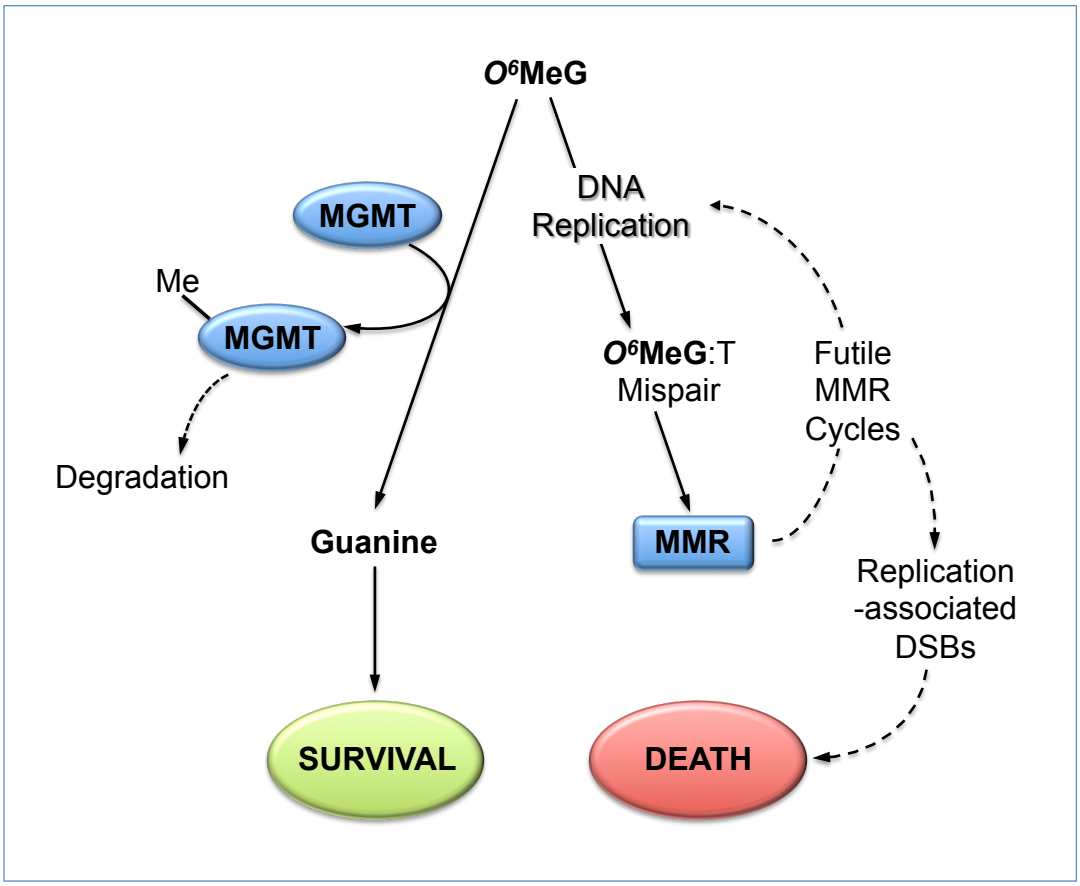


Figure 1.4 Mechanism of repair and cytotoxicity of the *O*^{6}MeG lesion. *O*^{6}MeG lesions are repaired by single step demethylation by MGMT, which results in proteasomal degradation of MGMT. If MGMT is absent or present in insufficient amounts, *O*^{6}MeG persists and post replicatively becomes mispaired with thymine. The MMR system recognizes but fails to correct this *O*^{6}MeG:T mispair, resulting in futile MMR cycles and, after at least two rounds of replication, in replication associated DSBs.

Human Alk B homologues

DTIC and TMZ treatment also leads to the formation of other alkylation lesions such as *N*^{1}MeA and *N*^{3}MeC, which are toxic since they cause replication block. Human Alk B homologues 2 and 3 (ABH2 and ABH3) repair these and other less toxic lesions including, *N*^{3}MeT and *N*^{1}MeG. ABH2 and ABH3 belong to the family of α-ketoglutarate- and Fe(II)-dependent dioxygenases, capable of repairing these alkyl adducts in a single step reaction which involves oxidative deamination of the alkyl group (Duncan et al., 2002). Experimental evidence has shown that ABH2 null cells and mice

are more sensitive to the alkylating agent methyl methanesulphonate (MMS) suggesting that these repair enzymes also contribute to alkylating agent sensitivity (Ringvoll et al., 2006).

1.2.5.2 Multi-step repair of alkylated DNA lesions

The most common methylation adduct is N^7-methylguanine (N^7MeG) accounting for 60-80% of all methylated DNA lesions produced from exposure to methylating agents. On its own however, N^7MeG is non-toxic unless it undergoes spontaneous depurination (Fu et al., 2012). N^3-methlyadenine (N^3MeA), accounts for 10-20% of methyl adducts formed from methylating agent treatment. This lesion is more toxic than N^7MeG since it sterically interferes with DNA-binding by DNA polymerases, thereby blocking replication (Fu et al., 2012; Shrivastav et al., 2010). The base excision repair (BER) pathway resolves both these lesions. This is a multistep pathway beginning with recognition and excision of the altered base by a DNA glycosylase that hydrolyzes N-glycosidic bonds (Kaina et al., 2007). Approximately 11 types of DNA glycosylases have been identified, these alkyl adducts are excised by N-methylpurine-DNA glycosylase (MPG), otherwise known as 3-Alkyladenine DNA glycosylase (AAG) or alkylpurine DNA N-glycosylase (APNG) (Singer et al., 1992). The resulting abasic or apurininc/apyrimidic site (AP site) is then recognized by a second enzyme called apurinic/apyrimidic endonuclease 1 (APE1) that cleaves the phosphodiester bond just 5' of the AP site forming a single strand break (SSB). This can be repaired by a complex comprising DNA polymerase β (Pol β), XRCC1 and DNA ligase III (Lig III) (Matsumoto and Kim, 1995). Pol β possesses AP lyase activity and removes the sugar-phosphate moiety as well as filling the single nucleotide gap which is sealed

by Lig III (Kubota et al., 1996). This type of BER is called short patch repair (Robertson et al., 2009). Alternatively, if Pol β is unable to excise the sugar-phosphate moiety, Pol δ/ε adds up to 10 nucleotides to repair the gap, causing the formation of a flap. This is removed by flap endonuclease 1 (FEN1) in the presence of proliferating cell nuclear antigen (PCNA) and ligation is performed by DNA ligase I (Lig I) (Kaina et al., 2007; Kondo et al., 2010). Poly (ADP-ribose) polymerase 1 (PARP-1) is another important cofactor of the BER pathway. It binds to SSBs and becomes auto-poly-(ADP)-ribosylated thereby promoting XRCC1 recruitment and nucleotide synthesis by Pol β (Fu et al., 2012; Kaina et al., 2007).

The role of BER in mediating alkylating drug resistance is complex, and any imbalance in the pathway can affect cellular sensitivity to alkylating agents. For example, overexpression of the BER initiator, AAG, results in accumulation of toxic BER intermediates and results in increased alkylating agent sensitivity (Posnick and Samson, 1999), whereas reduced AAG expression confers resistance (Roth and Samson, 2002). In addition, there is evidence that PARP-1 inhibition improves alkylating agent sensitivity (de Murcia et al., 1997; Miknyoczki et al., 2003), but PARP inhibition in Polβ null cells results in resistance to alkylating agents (Jelezcova et al., 2010)

1.2.5.3 Repair of secondary DNA damage

As mentioned above, the replication machinery may be obstructed by alkyl adducts, mispairing, or the products of MMR processing such as single-

stranded DNA (ssDNA) gaps. The result is replication fork stalling and collapse, which leads to the formation of replication-associated DSBs. In order to survive these events, cells possess mechanisms to resolve stalled replication forks and to repair DSBs, and it appears that there is some degree of overlap between these mechanisms (Jones and Petermann, 2012). DSB repair occurs via two main pathways, homologous recombination (HR) and non-homologous end joining (NHEJ). HR also plays a major role in stabilizing replication forks and repairing replication associated DSBs (Liu et al., 1999), and HR-deficient cells are more sensitive to alkylating agents (Kaina et al., 1991; Tsaryk et al., 2006).

Homologous recombination in DSB repair and replication stress

Homologous recombination (HR) plays an important role in DSB repair. Unlike the NHEJ pathway, HR utilizes a homologous template, usually a sister chromatid, to perform error-free DSB repair. Hence, HR is restricted to the late S and G2 phases of the cell cycle via regulation by cyclin-dependent kinases (CDKs). In addition to DSB repair, HR also repairs single-strand-gaps and damaged replication forks, both of which may result from alkylating agent treatment (Pascucci et al., 2005).

The process of HR in dealing with stalled replication forks is similar to its DNA DSB repair activity; however, the initial DNA lesions are dealt with differently. The response to DSBs is initiated when the Mre11-RAD50-NBS1 (MRN) complex detects the DSB and begins DNA end processing via its exonuclease activity, to generate exposed 3’ ssDNA ends. On the other hand, when the replication machinery encounters an obstacle, it is postulated that helicases

become uncoupled from the rest of the replicative machinery and may continue to unwind the helix, exposing ssDNA (Costanzo, 2011). Hence, stalled or collapsed replication forks, or DSB processing can expose regions of ssDNA, known to be the initial substrate of HR in late S/G2. Replication protein A (RPA) coats these ssDNA regions, activating ataxia telangiectasia mutated (ATM) or ataxia telangiectasia and RAD3-related protein (ATR). Both of these serine-threonine kinases have numerous phosphorylation targets that influence a variety of cellular processes including DSB repair, but ATR appears to be more important for replication stress (Carr and Lambert, 2013; Lavin et al., 2006).

Upon activation, ATM and ATR phosphorylate histone H2A, resulting in the formation of γ-H2AX spreading from the DNA damage site serving to facilitate DNA repair (Bonner et al., 2008). ATM and ATR also further regulate cell cycle progression and activate apoptotic signaling via activation of p53 (Meek, 2009).

ATR and ATM also mediate cell cycle arrest via activation of downstream checkpoint kinases, Chk1 and Chk2 respectively. Chk1 and Chk2 in turn phosphorylate and inhibit the cell cycle regulator, Cdc25c. Inhibition of this phosphatase results in the accumulation of phosphorylated CDK1, which hinders its interaction with cyclin B. This CDK1-cyclin B interaction is necessary for G2-M transition; hence Chk1/2 activation results in G2-M arrest. The resultant slowing of S phase and reduced mitotic entry gives the cell time to repair the DNA damage so that altered genetic material is not passed on to daughter cells (Boutros et al., 2007; Wang et al., 2009). HR mediators,

RAD51 and BRCA2 are phosphorylated and activated by Chk1, while Chk2 phosphorylates BRCA1 (Sorensen et al., 2005; Zhang et al., 2004).

BRCA1 and 2 aid RPA dissociation and RAD51 loading onto ssDNA and promote RAD51 filament formation (Esashi et al., 2007; Moynahan et al., 1999), marking the onset of HR, which occurs in 3 phases called presynapsis, synapsis and postsynapsis. Presynapsis involves RAD51 loading on ssDNA forming the presynaptic filament, consisting of six RAD51 molecules per helical turn of eighteen nucleotides (Chen et al., 2008; Ogawa et al., 1993). RAD51 then performs a homology search for a region of DNA complementary to the exposed ssDNA region of the damaged DNA (San Filippo et al., 2008). Synapsis is the formation of a D-loop heteroduplex comprising the original exposed ssDNA region invading toward a homologous region of dsDNA from elsewhere in the genome. RAD51 facilitates the interaction of these regions of DNA. Postsynapsis occurs when Rad51 dissociates, allowing DNA synthesis to occur using the invaded homologous DNA as a template (Yata and Esashi, 2009). This step ends with D-loop resolution, and DNA ligases catalyze the covalent joining of newly synthesized regions of DNA to the native regions, which originally flanked the DNA damage site (Krejci et al., 2012; Sung and Klein, 2006).

Of note, gene expression profiling of clinical melanomas has shown that metastatic progression is associated with increased expression of a number of DNA repair genes. Of these, two thirds represent pathways that deal with replicative stress and included core HR proteins such as RAD51 and BRCA1 (Kauffmann et al., 2008). This highlights the importance of DNA repair mechanisms, including the HR pathway in advanced melanoma.

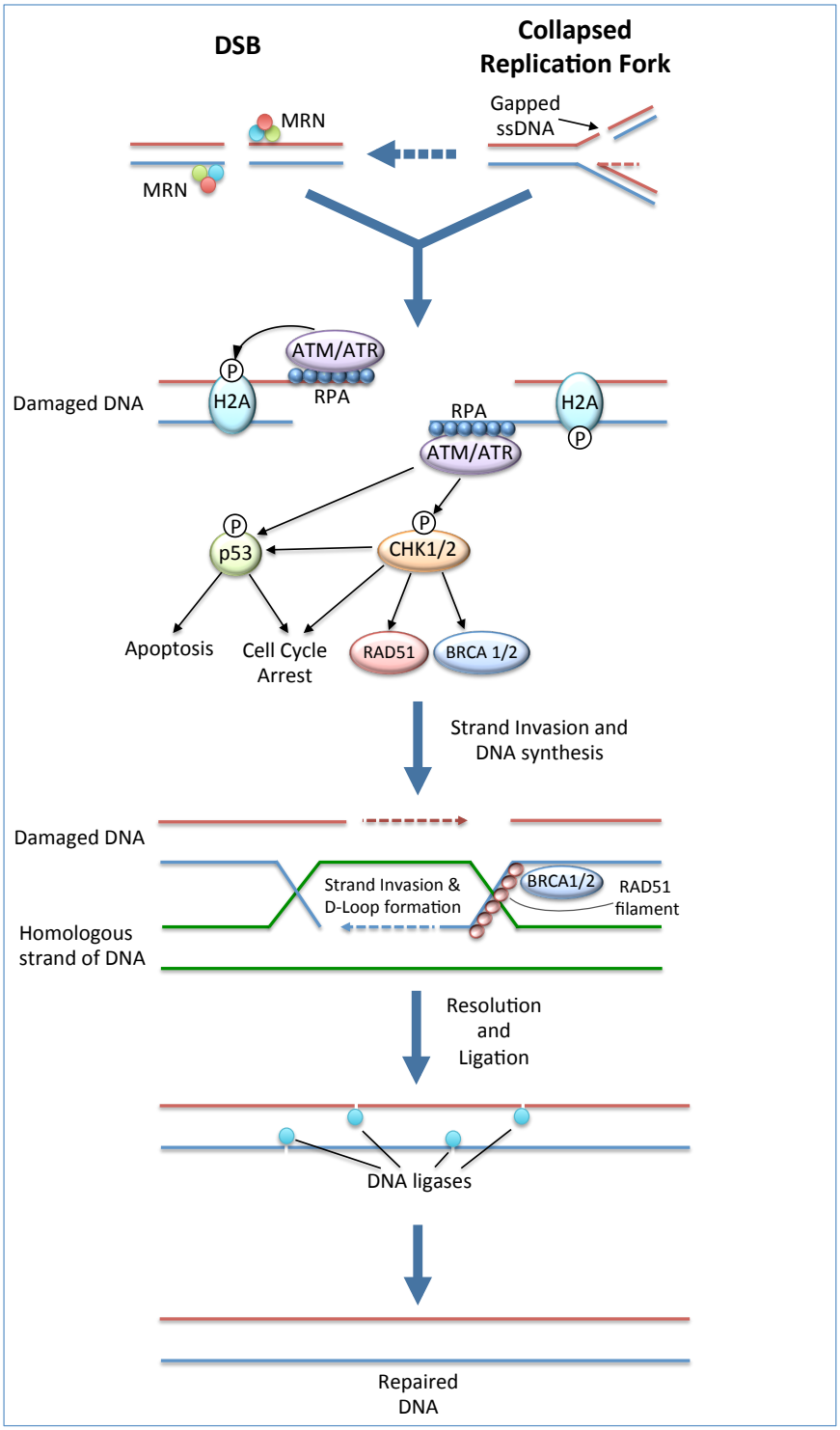


Figure 1.5 Steps in homologous recombination (HR). HR may deal with DSBs or stalled collapsed replication forks which occur secondary to alkylated base lesions formed following TMZ treatment. (Modified from Sung and Klein, 2008; Costanzo, 2011; San Filippo et al, 2008)

Non-homologous recombination (NHEJ) in DSB repair

Unlike HR, NHEJ repairs DSBs by simple end ligation without a homologous region of DNA to act as a template, and is therefore the more rapid and error-prone form of DSB repair. In addition, unlike HR which only occurs in S and G2 phases of the cell cycle, NHEJ can occur in any phase, but is particularly important in G0, G1 and early S (Polo and Jackson, 2011).

NHEJ begins with binding of the Ku70-Ku80 heterodimer to DNA ends. Binding of the MRN complex may tether the DNA end, facilitating Ku recruitment (Gottlieb and Jackson, 1993). The interaction of the Ku complex with DNA allows the recruitment of the DNA-dependent protein kinase catalytic subunit (DNA-PK_{cs}), activating this protein's serine/threonine kinase activity. DNA-PK_{cs} is then able to phosphorylate DNA repair targets such as H2AX, RPA and Artemis (Collis et al., 2005; Ma et al., 2002; Park et al., 2003), and cell cycle target p53 indirectly by inhibitory phosphorylation of MDM2 (Mayo et al., 1997). DNA ends are processed to ensure that 5' phosphate and 3'-hydroxyl ends are present so that ligation can occur. Such end-processing is achieved via a balance between removal of damaged nucleotides by nucleases such as Artemis, which is activated when it interacts with DNA-PK_{cs}, and resynthesis by DNA polymerases (Goodarzi et al., 2006). Finally, ligation of DNA ends is then performed by DNA ligase IV complex or the X4-L4 complex, which comprises DNA ligase IV, XRCC4 and XRCC4-like factor (XLF), thus completing the process of DSB repair (Ahnesorg et al., 2006; Hartlerode and Scully, 2009; Helleday et al., 2007).

1.3 IGF1R signaling and the response to DNA damage

Several studies have suggested that IGF1R signaling could alter the sensitivity of a number of cancer types to various forms of DNA damage. The first of these found that IGF1R overexpression induced radioresistance in fibroblast cell lines, and showed that higher IGF1R expression assessed by immunohistochemical staining of clinical breast cancer samples correlated with recurrence following radiotherapy (Turner et al., 1997). IGF1R depletion with small interfering RNA was shown to enhance the sensitivity of prostate cancer cells to ionizing radiation and to DNA damaging cytotoxic agents, but not to non-DNA damaging cytotoxic agents (Rochester et al., 2005). In a non-small cell lung cancer model, IGF1R signaling blockade using an anti-IGF1R monoclonal antibody caused radiosensitization *in vitro* and *in vivo* and delayed DSB resolution measured by immunocytochemical staining for γH2AX focus formation (Allen et al., 2007; Iwasa et al., 2009). Light was shed on the possible mechanism of this effect when it was reported that IGF signaling affected the HR pathway of DNA repair, via an interaction between IRS-1 and RAD51 (Trojanek et al., 2003). A previous study from our group confirmed that IGF1R depletion led to a delay in DSB repair, and found that this was related to impaired HR function, although an interaction between IRS-1 and RAD51 could not be detected in prostate cancer cells (Turney et al., 2012).

Studies in melanoma models from our group have also implicated an effect of IGF1R signaling on the DNA damage response. In a murine model, IGF1R depletion using stable antisense RNA expression, caused radiosensitisation

that was found to be related to impaired ATM activity (Macaulay et al., 2001). IGF1R gene silencing with siRNA was shown to sensitize human melanoma cells to cisplatin and TMZ *in vitro*, regardless of BRAF mutation status (Yeh et al., 2006), however the mechanism of this effect was not explored.

1.4 Aims of this project

Prior reports suggest that IGF1R signaling may influence the DNA damage response in a number of cancer models, with evidence that IGF1R gene silencing is capable of chemosensitizing melanoma to TMZ. The molecular basis for this effect is unclear, and it is not certain whether this finding can be translated to a clinically meaningful setting. The specific aims of this project were:

1. To assemble and characterize a panel of human melanoma cell lines with respect to IGF1R signaling and TMZ sensitivity, and to determine whether any of these features is related to the response to TMZ.
2. To determine whether IGF1R blockade using a clinically relevant small molecule inhibitor, can sensitize human melanoma cells to TMZ.
3. To investigate the mechanistic basis for effects of IGF1R inhibition on TMZ sensitivity in melanoma cells *in vitro.*
4. To assess the tolerability of combining TMZ with IGF1R inhibition *in vivo,* and to determine whether this IGF1R inhibition is capable of influencing the efficacy of TMZ in this model.

Chapter 2

Materials and methods

2.1 Cell Lines and Cell Culture

All melanoma cell lines were adherent and were cultured in medium supplemented with 10% fetal bovine serum (FBS), 100U/ml penicillin and 0.1mg/ml streptomycin. Table 2.1 shows the derivation of each cell line used in this project and the medium used for culturing each cell line. The B231 subline of H1299 cells were cultured in tetracycline free DMEM supplemented with 10% FCS, penicillin/streptomycin and 2mM glutamine. All cell lines were negative on mycoplasma testing (MycoAlert kit, Lonza Rockland Inc, Rockland US).

For routine passage, cells were disaggregated using 3mM EDTA in phosphate buffered saline (PBS) or Trypsin. Cells were washed in complete medium and reseeded into new flasks or plates. For cryopreservation, cells were resuspended in a freezing medium comprising 10% dimethyl sulphoxide (DMSO), 50% FBS in the appropriate medium, aliquoted into sterile Nunc vials and stored in the short term at -80^{o}C or in liquid nitrogen for long term storage. To recover frozen stocks, the frozen cell suspension was thawed rapidly to 37^{o}C and transferred to flasks with complete medium for culturing.

Table 2.1 Cell lines used in this project

Cell line	Cancer type	History	Medium
CHL-1	Melanoma	Derivative of RPMI-7932, from pleural effusion of 36 year old female with malignant melanoma (Sigma website)	DMEM
A375	Melanoma	Derived from a 54 year old female with malignant melanoma (Sigma website)	DMEM
A375M	Melanoma	Pulmonary metastasis in mice injected with A375 cells intravenously (Kozlowski et al., 1984)	DMEM
A2058	Melanoma	Lymph node metastasis from 53 year old male with melanoma	DMEM
SK-MEL-2	Melanoma	Cutaneous metastasis from 60 year old male with melanoma (ATCC website)	RPMI
SK-MEL-23	Melanoma	Unknown patient details	RPMI
SK-MEL-28	Melanoma	Primary tumour of cutaneous melanoma of a 51 year old male (ATCC website)	DMEM
HMCB	Melanoma	Unknown patient details	DMEM
COLO858	Melanoma	Right axillary lymph node metastasis from 43 year old male with malignant melanoma (Sigma website)	RPMI
501mel	Melanoma	Unknown patient details	DMEM
B231	Non-small cell lung cancer	Derived from the p53-null H1299 cell line with a wild type-p53 containing Tet-responsive plasmid (pTRE) stably expressed. (Fogal et al., 2005)	DMEM (tet free)

A375, A357M, 501mel and COLO858 were obtained from Professor Colin Goding, Ludwig Institute for Cancer Research, Oxford; and SK-mel-23 was obtained from Professor V Cerundolo, Weatherall Institute of Molecular Medicine, Oxford. CHL1, SK-MEL-2 and HMCB were purchased from American Type Culture Collection (ATCC) and SK-MEL-28 and A2058 were obtained from Cancer Research UK Cell Services, London. Cell lines used were readily available from collaborators within the university and to include

commonly encountered mutations in melanoma. The B231 cell line was obtained from Professor Xin Lu, Ludwig Institute for Cancer Research, Oxford.

2.2 Cytotoxic Agents and Other Treatments

2.2.1 Temozolomide (TMZ)

TMZ was kindly provided by our collaborator, Dr Geoff Margison (Paterson Institute of Cancer Research PICR, Manchester) and was stored at +4^{o}C protected from light. For *in vitro* experiments, a working stock of 100mM concentration was made up in anhydrous DMSO (Sigma). This was then diluted to the required concentrations in DMEM with 10% FBS.

2.2.2 AZ12253801

This agent is an ATP-competitive inhibitor of the IGF1R tyrosine kinase domain, which has about 10-fold selectivity over the insulin receptor and 25-fold selectivity over EGFR. Information from a large screen of related kinases performed by AstraZeneca indicated that AZ12253801 inhibited other kinases at concentrations at least ten times that used in this project (Aleksic et al., 2010). AZ12253801 was provided as a dry powder by AstraZeneca and a 10mM stock solution was made by dissolving in DMSO. This was then aliquoted and stored at -20^{o}C. Further dilutions were made in DMEM with 10% FBS to obtain the required final concentrations.

2.2.3 Linsitinib (OSI-906)

The selective IGF1R/IR TKI, OSI-906, was provided as a dry powder by Dr Elizabeth Buck, OSI Pharmaceuticals (Pitts et al., 2010), and was stored protected from light at room temperature in a dessicator. For *in vitro* use, a stock solution of 10mM OSI-906 was prepared in sterile DMSO forming a transparent yellow solution and was aliquoted and stored at -20^{o}C. To treat cell cultures, OSI-906 was further diluted in DMSO and then in pre-warmed culture medium containing 10% FBS and 5% DMSO to produce 10x OSI-906 solutions that were added to cultures to produce the correct final concentration.

2.2.4 Olaparib (AZD2281)

This selective PARP inhibitor was provided by AstraZeneca as a powder and was dissolved in DMSO to make a stock solution of 10mM. Further dilutions were made in DMEM with 10% FBS to obtain the required final concentrations, thus keeping the final DMSO concentration below 0.1%.

2.2.5 IGF-1

The IGF-1 ligand was used primarily to test the ability of IGF1R inhibitors to inhibit IGF-1 induced IGF1R activation or phospho-IGF1R levels. Long-R3 IGF-1 (Sigma) was dissolved in 10mM HCL, aliquoted and stored at -80^{o}C.

2.2.6 Doxycycline

Doxycycline (Sigma) was obtained as a dry powder, dissolved in sterile distilled water to a concentration of 1mg/ml, aliquoted and stored at -20^{o}C.

2.3 Protein Analysis

2.3.1 Collection and lysis of adherent cells

After treatment with chemical inhibitors and/or cytotoxic drugs, adherent cells were gently washed twice with ice cold PBS and disaggregated by scraping into ice cold PBS. The cell suspension was centrifuged at 5,000rpm for 5 minutes at 4°C, PBS removed and cell pellets frozen in liquid nitrogen and stored at -80°C. Cell pellets were thawed on ice and lysed for 30 minutes in IGF-1R lysis buffer (50mM Hepes, 100mM sodium chloride, 10mM EDTA, 4mM sodium pyrophosphate, 2mM sodium orthovanadate, 10mM sodium fluoride and 1% Triton-X-100, EDTA-free protease inhibitor cocktail, and 1.5mM Pefabloc SC Plus® (Roche)). Some cultures were lysed directly into Laemmli sample buffer. Whole cell lysis was achieved using a buffer similar to IGF1R lysis buffer in which Triton was replaced with 1% sodium dodecyl sulfate (SDS). Phosphatase inhibitors (I and II, Sigma) were added to lysis buffers if phosphorylated proteins were being investigated. Cell lysates were centrifuged at 13,000 rpm for 10 minutes at 4°C and supernatants were collected. The protein concentrations of these lysates were determined by Bicinchoninic acid or BCA™ Protein Assay (Thermo Scientific) in parallel with bovine serum albumin (BSA) standards and analysed on a plate reader at 562nm (μQuant Universal Microplate Spectrophotometer, NorthStar Scientific). Protein concentrations could not be determined following direct lysis in

Laemmli sample buffer but western blotting for actin or β-Tubulin assessed protein loading.

2.3.2 Western Blotting

Proteins (50μg per sample, unless stated) were denatured at 95°C for 5 minutes in Laemmli buffer and were separated according to molecular weight by SDS polyacrylamide gel electrophoresis (SDS PAGE) on 5 to 15% polyacrylamide gels. Proteins were transferred to Hybond-C extra nitrocellulose membrane (Amersham Pharmacia Biotech) in semi-dry transfer buffer (48mM Tris-Cl, 39mM glycine, 20% methanol, 1.3mM SDS (final pH 9.2) at a constant current of 35mA per 8x10cm gel for 3 hours using a semi-dry transfer pack (Hoefer Semiphor Transfer Unit, Amersham Biosciences). Following this, the membrane was blocked for 1 hour at room temperature using 5% non-fat milk or 5% BSA in TBS with 0.1% Tween (TBST). This was also used to dilute the primary antibody for incubation at 4°C overnight (see Table 2.2). Primary antibody was removed and the membrane washed with TBST and incubated for 1 hour at room temperature with anti-rabbit or anti-mouse secondary antibody conjugated to HRP, diluted in blocking buffer. Thereafter the nitrocellulose membrane was washed again with TBST and proteins detected on radiological film using Enhanced Chemiluminescence Plus Reagent (ECL+, Amersham Corporation,UK).

Table 2.2. Antibodies used for Western Blotting

Antibody	Source (catalogue number)	Primary Antibody	Blocking Buffer	Secondary Antibody
IGF1R β -subunit	Cell Signaling (3027)	1:1000	5% Skim Milk	Rabbit 1:5000
phospho-IGF1R β (Tyr1135/1136)/IR β (Tyr1150/1151)	Cell Signaling (3024)	1:1000	5% (BSA)	Rabbit 1:5000
phospho-Akt (Ser473)	Cell Signaling (4051)	1:1000	5% BSA	Rabbit 1:5000
Total Akt	Cell Signaling (9272)	1:1000	5% Skim Milk	Rabbit 1:5000
phospho-Thr202/Tyr204 ERK 1/2	Cell Signaling (4377)	1:1000	5% BSA	Rabbit 1:5000
total ERK 1/2	Cell Signaling (4695)	1:1000	5% Skim Milk	Mouse 1:5000
p53	Cell Signaling (9282)	1:1000	5% Skim Milk	Rabbit 1:5000
phospho-Chk1 (Ser345)	Cell Signaling (2341)	1:1000	5% BSA	Rabbit 1:5000
phospho-Chk2 (Thr68)	Cell Signaling (2661)	1:1000	5% BSA	Rabbit 1:5000
Phospho-ATM (Ser1981)	Rockland (200-301-400)	1:500	5% BSA	Mouse 1:5000
ATM	Cell Signaling (2873)	1:1000	5% Skim Milk	Rabbit 1:5000
Cyclin B1	Cell Signaling (4138)	1:1000	5% Skim Milk	Rabbit 1:5000
phospho-cdc2 (Thr15)	Cell Signaling (9111)	1:1000	5% BSA	Rabbit 1:5000
γ-H2AX (Ser139)	Upstate/Millipore (05-636)	1:1000	5% BSA	Mouse 1:5000
53BP1	Novus (NB100-305)	1:1000	5% BSA	Rabbit 1:5000
RAD51	Abcam (ab213)	1:1000	5% Skim Milk	Mouse 1:5000
RPA 32/2	Abcam (ab10359)	1:1000	5% Skim Milk	Rabbit 1:5000
BRCA2	Millipore/Calbiochem (OP95)	1:1000	5% Skim Milk	Mouse 1:5000
RAD52	Abcam (ab61211)	1:1000	5% Skim Milk	Rabbit 1:5000
RAD54	SantaCruz (sc-5849)	1:1000	5% Skim Milk	Goat 1:5000
PARP	Cell Signaling (9542)	1:1000	5% Skim Milk	Rabbit 1:5000
MGMT	BD Pharmingen (557045)	1:1000	5% Skim Milk	Mouse 1:5000
Histone H3	Cell Signaling (9715)	1:5000	5% Skim Milk	Rabbit 1:5000
actin	Abcam (ab8227, Rabbit; ab8224, Mouse)	1:5000	5% Skim Milk	1:10000
β-Tubulin	Sigma (5168)	1:5000	5% Skim Milk	Mouse 1:10000

2.3.3 Chromatin isolation by small-scale biochemical fractionation

Chromatin fractionation was performed according to the method of Mendez and Stillman (2000). Adherent cells (1-2x10 ^{7}) were washed twice and scraped in ice cold PBS. Cell suspension was centrifuged at 1,300xg for 5 min at 4^{o}C, and the cell pellet was resuspended and lysed for 5 minutes on ice in 200µl buffer A (0.1% Triton X-100, 10 mM HEPES pH 7.9, 10 mM KCl, 1.5 mM $MgCl_2$, 340 mM sucrose, 10% glycerol, 1mM dithiothreitol (DTT), EDTA-free protease inhibitor cocktail, and 1.5mM Pefabloc SC Plus® (Roche)). After centrifugation at 1,300xg for 5 min at 4^{o}C, the supernatant, representing the cytosolic fraction was collected. The resulting nuclear pellet was washed by resuspending in 200µl buffer A and centrifuged at 1,300xg for 5 min at 4^{o}C. The nuclear pellet was then lysed on ice for 30 minutes in 100µl buffer B (3mM EDTA, 0.2mM EGTA, 1mM DTT, EDTA-free protease inhibitor cocktail, and 1.5mM Pefabloc SC Plus®). The lysate was centrifuged at 1,700xg for 5 minutes and the nuclear lysate (supernatant) was collected and stored at -20 ^{o}C. The resulting chromatin pellet was washed and centrifuged in 100µl buffer B, resuspended in 200µl Urea/Tris buffer (50mM Tris-HCl ph 7.5, 8.5M urea and 150mM β-mercaptoethanol) and sonicated intermittently for three 10-second cycles, each separated by cooling on ice, to achieved DNA disruption. The protein concentrations of these lysates were determined by Bradford Bio-Rad Protein Assay, in parallel with bovine serum albumin (BSA) standards and analysed on a plate reader at 595nm (µQuant Universal Microplate Spectrophotometer, NorthStar Scientific). Lysates were then western blotted as described above.

2.4 Gene silencing by RNA interference (RNAi)

RNA interference experiments focused on targeting the IGF1R. Experiments used non-silencing control siRNA (Qiagen) as a control for non-specific effects of siRNA treatment. Two siRNAs directed against the IGF1R were employed: R4 duplex previously designed in our lab (Bohula, et al, 2003) and a validated human IGF1R siRNA (Qiagen, S100017521). The siRNA transfections were performed using a reverse transfection protocol with HiPerFect reagent (Qiagen) and IGF1R depletion was assessed by western blotting.

2.5 RNA analysis

2.5.1 RNA Extraction

The RNeasy kit (Qiagen) was used according to manufacturer's recommended protocol. Cultured cells were harvested, washed once with cold PBS and cell pellets (10^6-10^7 cells) were lysed and homogenized in Buffer RLT containing β-mercaptoethanol (Sigma, St. Louis, MO, USA) by passage through a 20-gauge needle at least 5 times. An equal volume of 70% ethanol was added to the lysate before applying the lysate to a silica-membrane column. After centrifugation at 10000 rpm for 1 minute, the silica-bound RNA was washed once with Buffer RW1 and twice with Buffer RPE. Total cellular RNA was eluted from the column with RNase-free water. The concentration and purity was assessed using the Nanodrop

spectrophotometer (Nanodrop Technologies). DNA removal was performed by treating samples with DNA-*free* (Applied Biosystems) and RNAs were stored at –80°C or directly reverse transcribed to cDNA.

2.5.2 Reverse transcription

cDNA was synthesized by reverse transcribing total RNA using the High Capacity cDNA Archive® Kit (Applied Biosystems) according to the manufacturer's instructions. Briefly, 5µg of RNA was diluted with diethylpyrocarbonate (DPEC)-treated water in PCR reaction tubes to a volume of volume of 25µl. A reaction mastermix was prepared, comprised of 5µl of 10x RT Buffer, 5µl of 10x Random Primers, 2µl of 25x dNTPs, 10.5µl of DEPC water, and 2.5µl of reverse-transcriptase per reaction. Twenty-five microliters of the reverse-transcriptase mastermix was added to each PCR reaction tubeand placed in a Peltier Thermo Cyler (MJ Research, Waltham, MA, USA) and incubated at 25°C for 10 minutes, 37°C for 2 hours and 4°C for 10 minutes. The cDNA produced was either stored at -20°C or subjected to quantitative real-time PCR for genes of interest.

2.5.3 Quantitative real-time PCR (qRT-PCR)

Quantative RT-PCR was performed using primers designed using the web-based Universal ProbeLibrary Assay Design Center (Roche Applied Science, www.roche-applied-science.com). The primers were synthesised by Operon

Biotechnologies and the probes were purchased from Exiqon Universal Probe Library (Roche), as listed below in Table 2.3.

Table 2.3 Primers and probes used for qRT-PCR

Gene	Probe	Forward Primer	Reverse Primer
MGMT	52	GCGTTTCGGATATGTTGGGATAGT	AACGACCCAAACACTCACCAAA
GAPD	60	AGCCACATCGCTCAGACAC	GCCCAATACGACCAAATCC
BACT	63	CCAGAGGGGTACAGGGATAG	CCAACCGGAGAAGATGA

The PCR reaction consisted of 12.5µl of the QPCR Master Mix, 10pmoles of forward and reverse primers, 25ng template cDNA and 0.25µl PCR probe in a total volume of 25µl. Conditions for the PCR reaction were 2 minutes at 50°C, 10 minutes at 95°C and then 40 cycles, each consisting of 15 seconds at 95°C, and 1 minute at 60°C. Analysis was performed using the Corbett Research Rotor Gene 3000 qPCR system, and the conditions for the PCR were: 2 min at 50 ^{o}C, 10 min at 95 ^{o}C and then 40 cycles, each consisting of 15 seconds at 95 ^{o}C and 1 minute at 60 ^{o}C. Relative quantification of expression of the gene of interest was compared against the geometric mean of the mRNA expression of housekeeping genes, β-Actin (*BACT)* and glyceraldehyde-3-phosphate dehydrogenase (*GAPD)*.

2.6 Assays of alkylated base damage and repair

2.6.1 MGMT activity assay and O^6MeG quantification

MGMT activity was quantified using an oligonucleotide-based assay kindly performed by our collaborator, Dr A Watson in the Dr G Margison Carcinogenesis group, PICR, Manchester. This assay utilized ^{32}P labelled 23bp oligonucleotides streptavidin-biotin fixed to 96 well plates (Morten and Margison, 1988). These oligonucleotides were designed to possess a Pst restriction site containing an O^6MeG residue. Whole cell lysates (containing MGMT of unknown activity) were applied to the wells in triplicate. Incubation with Pst I endonuclease resulted in cleavage of only the oligonucleotides in which the restriction site O^6MeG residues had been demethylated by MGMT. Such cleavage reveals the ^{32}P-labelled fragment, which was quantified by scintillation counting. The MGMT activity of the unknowns was extrapolated from a standard curve (Morten and Margison, 1988). In addition, the O^6MeG content of DNA was quantified by measuring the residual MGMT activity in a sample with or without alkylating agent treatment. This was based on the principle that O^6MeG inactivates MGMT and results in MGMT degradation. Hence the amount of unrepaired O^6MeG could be extrapolated by the amount of residual MGMT activity relative to controls (Jackson et al., 2000; Watson and Margison, 1999).

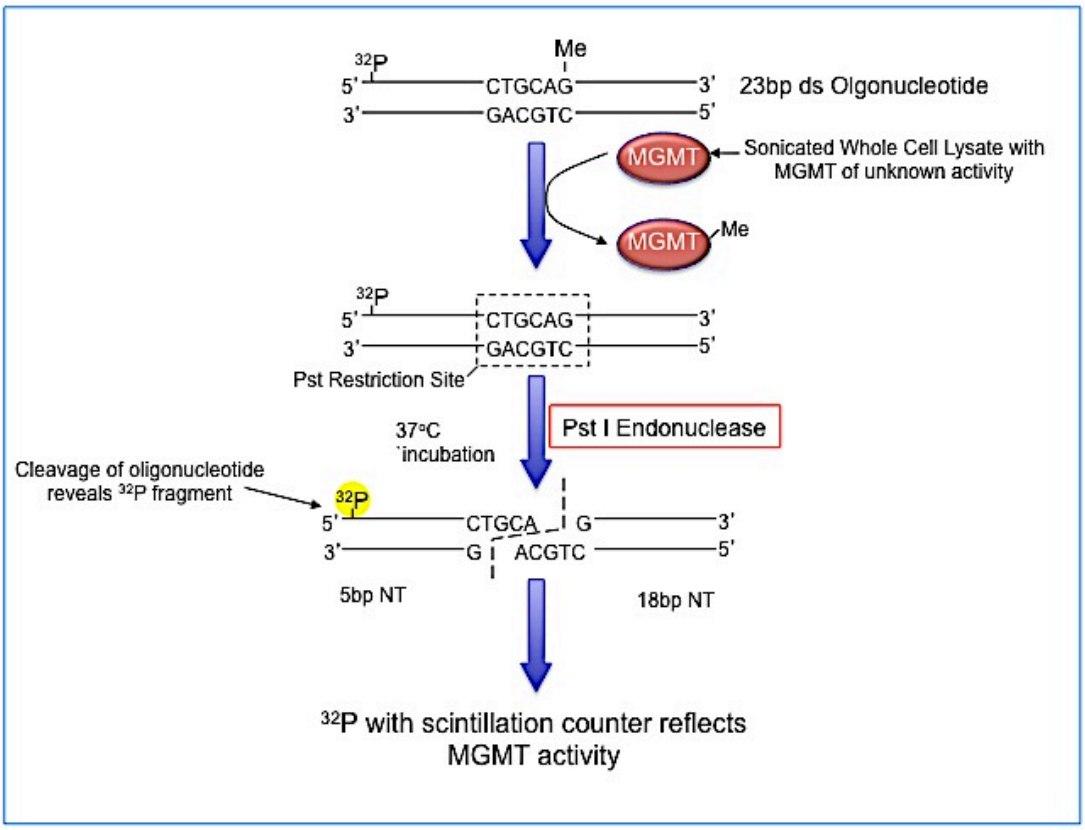


Figure 2.1 Principle of oligonucleotide-based MGMT activity assay.

2.6.2 AAG Activity Assay

Following treatment, adherent cells were collected, snap frozen in liquid nitrogen and assayed for AAG activity by our collaborator Geoff Margison, PICR, Manchester according to the method described by Elder et al (1998). In brief, lysates were incubated in ^{3}H-labelled DNA substrate. DNA and protein were precipitated out using absolute ethanol, allowed to dry, and dissolved in buffer containing known concentrations of N^{3}MeA and N^{7}MeG, the major substrates for AAG. Samples were analysed by high-performance liquid chromatography, and N^{3}MeA and N^{7}MeG peaks allowed samples containing these bases to be collected. Scintillation measurements of these samples

reflected the free ^{3}H-labelled purines released as a result of AAG processing and such activity was quantified against controls (Elder et al., 1998).

2.6.3 *N*^{7}MeG Base Adduct Quantification

This assay was performed by Amanda Watson and Geoff Margison, PICR, Manchester, using an immunoslot blot technique. Snap frozen cell pellets (collected as described in 2.3.1) were used for genomic DNA extraction using the Qiagen Blood and Cell culture DNA midi prep kit. Genomic DNA was transferred onto a nitrocellulose membrane and probed with a polyclonal antibody to *N*^{7}MeG. Detection of bound antibody was via a horse-radish peroxidase (HRP)-conjugated anti-rabbit secondary antibody and ECL detection. Image quantification allowed measurement of *N*^{7}MeG levels (Harrison et al., 2001).

2.7 Cell-based assays

2.7.1 Cell cycle analysis by bromodeoxyuridine incorporation Method and PI staining

Propidium iodide (PI) is a fluorescent dye that stoichiometrically binds to the DNA. Quantification of PI staining therefore identifies the proportion of cells present in each phase of the cell cycle by estimating cellular DNA content. This assay does not allow accurate discrimination of cells in early S from G1 cells with similar DNA content, and likewise late S from G2/M cells. Detection of replicating cells would therefore identify S phase cells. BrdU (5-bromo-2'-

deoxyuridine) is a thymidine analogue that becomes incorporated into newly synthesized DNA during S phase. This assay was performed by pulsing 10^6 cells with 10μM BrdU (Sigma-Aldrich) for 30 minutes in cell culture prior to harvest. Cells were harvested, centrifuged at 2000rpm for 5 minutes at room temperature and fixed in cold 70% ethanol for 30 minutes and centrifugation repeated. The cell pellet was acid permeabilised in 3ml of a 2M HCl, 0.5% Triton X 100 for 30 minutes at room temperature, centrifuged at 2000rpm and supernatant aspirated. Samples were then neutralised with 3ml of 0.1 M $Na_2B_4O_7 \cdot 10\ H_2O$ for 5 minutes on ice and then centrifuged again**.** The cell pellet was resuspended in 0.6ml blocking solution (0.5% Tween/ 1% BSA/PBS) with 15μl of 20μg/ml anti-BrdU primary antibody (Abcam, catalog #6326) and incubated for 30 minutes at room temperature. After centrifugation at 5000 rpm for 2 minutes and discarding the supernatant, cells were incubated for 30 minutes at room temperature with 1:250 dilution of Alexa Fluor 488 goat anti-rat secondary antibody (Life technologies, A-11006). Following removal of secondary antibody, cells were resuspended in 1.5 mL PBS containing 40 μg/mL PI and DNase-free RNase (12 μg/ml, Sigma). After 30 minutes incubation at room temperature, each sample was analysed using the Cyan ADP Color FACS analyser and FloJo v 8.8.7 software.

2.7.2 Clonogenic Assay

The growth and survival of tumours depends on the ability of its cells to form clones. The effects of anti-cancer therapy can be assessed using a cell culture-based assay that measures the effect of such agents on the ability of single tumour cells to form clones or colonies. This is known as colony

formation or clonogenic assay (Franken et al., 2006; Munshi et al., 2005). To perform the assay, cells were disaggregated and seeded in 10cm dishes in triplicate at 2000 cells per dish. The following day drug treatment or solvent control of equivalent concentration was applied and dishes were incubated for 7 to 14 days at 37 ^{o}C until visible colonies developed. Colonies were then fixed and stained for 30-60 minutes in a solution comprising 0.1% Coomassie brilliant blue (Sigma Aldrich), 7% acetic acid and 50% methanol. Colonies were counted using the Colcount® automated colony counter (Oxford Optronix) and colony numbers were normalized to the solvent-treated cells (designated 100% survival). Curves were fitted to the data points using GraphPad Prism v5, and the SF_{50} values were calculated from these curves.

2.7.3 Apoptosis Assay

Caspase activation is central to apoptotic cell death. This was quantified using the Apo-ONE® Homogenous Caspase 3/7 Assay. Ten thousand cells were seeded in 100μl medium per well of a 96 well plate and the following day treated with drug or solvent. After 24 to 48 hours of treatment, 100μl of Apo-ONE reagent was added to each well, including blank wells (medium only) and incubated for 4 hours at room temperature. The Apo-ONE reagent lyses cells and also contains a profluorescent rhodamine-110 molecule bound to the amino acid sequence, DEVD (Asp-Glu-Val-Asp). Active caspase 3-like proteases are known to cleave the C-terminal side of aspartate residues of this sequence (Nicholson et al., 1995) and therefore cleave the Apo-ONE reagent, releasing active rhodamine-110. The quantification of fluorescence reflects the amount of caspase activation and therefore apoptosis.

Fluorescence following addition of Apo-ONE reagent was measured at an excitation wavelength of 485±20nm and an emission wavelength of 530±25nm on the FluorScan Universal Microplate Spectrophotometer (NorthStar Scientific).

2.7.4 Cell viability assay: CellTiter-Glo (CTG)

The ability of a cell to produce ATP is essential to its growth and survival. ATP produced by metabolically active cells was measured by the CTG assay. This assay is able to lyse cells and uses a buffer containing luciferin and recombinant luciferase, which, in the presence of oxygen and ATP, produces oxyluciferin in an electrically excited state, resulting in the emission of light. Thus the quantity of light emitted reflects the amount of ATP produced by metabolically active or viable cells. To assess cell viability with this assay, 1000 cells were seeded per well into opaque side-walled, clear bottom 96 well plates (Grenier Bio-one). After two days, cells were treated in triplicate with drug or equivalent concentration of solvent. When solvent-control cells approached confluence 3-5 days later, depending on the cell line, an equivalent volume of CTG assay reagent was added directly to each well and the plate was shaken for 5-10 minutes. ATP-induced luminescence was measured with a plate-reading luminometer (Fluorstar Optima, BMG Labtech). Individual luminescence values were normalized to solvent (DMSO)-treated cells (designated 100% growth), the data were graphed and curve-fitted using GraphPad Prism v5 software, and GI_{50} values were extrapolated.

When the CTG cell viability assay was used to determine the effect of p53 induction on OSI-906 sensitivity, B231 cells were treated with 2μg/ml doxycycline or solvent for 24 hours. Cells were then disaggregated and reseeded at 1000 cells per well in 96 well plates for CTG and the remaining cells analysed by western blot to determine p53 expression. Cells that were seeded into 96 well plates, were treated with solvent or OSI-906, and the cell viability was measured by CTG assay after 5 days as above.

2.7.5 Immunofluorescence microscopy

Cells cultured on coverslips were washed twice with ice-cold PBS, fixed with 4% paraformaldehyde (PFA) in PBS for 10-20 minutes, and permeabilized in 0.5% Triton-X-100. Following three washes with PBS 0.1% Tween (PBST), each of 5 minutes duration, cells were blocked with 5% BSA (Sigma) in PBST for 30 minutes at room temperature. Cells were then incubated in primary antibodies diluted in blocking solution overnight at 4°C. After three washes with PBST, cells were incubated with secondary antibody conjugated to Alexa Fluor 488 or 594 for one hour in the dark. After three PBST washes, coverslips were mounted with Fluoromount G reagent with DAPI (Southern Biotech). Images were acquired on a LSM 510 confocal microscope (Zeiss) at x63 magnification to obtain at least 30-50 cells per treatment condition. Projection images of z-stacks were made using the LSM software and these images were viewed with ImageJ software to manually quantify DNA damage foci. GraphPad Prism v5 was used to perform statistical analyses. This was the method used for detection of γ-H2AX and 53BP1 foci, however for RAD51 detection, permeabilisation was performed with methanol at -20^{o}C for 30

minutes, instead of 0.5% Triton-X-100, and blocking used 10% FCS at RT, as guided by the datasheet for this primary antibody (http://www.abcam.com/rad51-antibody-14b4-ab213). In addition, because RPA is quite abundant, its response to DNA damage would not be discernable unless the non-chromatin bound fraction was removed. Hence cells for RPA staining were incubated for 5 minutes on ice with a pre-extraction buffer (10mM PIPES, 300mM Sucrose, 20mM NaCl, 3mM MgCl2, 0.5% Triton X-100, pH 6.8) (Kaidi et al., 2010; Weston et al., 2012) prior to fixation with 4% PFA 0.5% Triton-X-100 permeabilisation and immunofluorescent staining as above.

Table 2.4 Antibodies used for immunofluorescent staining

Antibody	Primary Antibody		Secondary Antibody from Molecular Probes
	Source (catalogue number)	Dilution	
γ-H2AX (Ser139)	Upstate/Millipore (05-636)	1:500	Mouse 1:2000
53BP1	Novus (NB100-305)	1:500	Rabbit 1:2000
RAD51	Abcam (ab213)	1:500	Mouse 1:2000
RPA 32/2	Merck Biosciences (NA-18)	1:500	Mouse 1:2000

2.8 *In vivo* study

In vivo work was carried out under the Home Office approved Project Licence of our collaborators, JiLiang Li and Professor Adrian Harris (project license number PPL30/2771). All procedures were performed by Jordan Tanner, Biomedical Services, John Racliffe Hospital, Oxford. Six to seven-week old female BALB/c NuNu mice (Harlan Sprague Dawley, Inc.) were injected subcutaneously in the lower flank with 100µl of Matrigel (BD Bioscience) mixed with $1x10^7$ cells suspended in 100µl of serum-free medium. Tumour growth was monitored and measured three times per week using calipers. Tumour volume was calculated using the formula $V = L \times W \times H \times \pi/6$ (L=length, W=width and H=height).

When tumour volumes reached 100-200mm^3, mice were randomly allocated to treatment groups. Treatments were prepared fresh each day and treatment volumes were adjusted based on daily weights. For pharmacokinetic (PK) testing, 4 hours after OSI-906 dosing, whole blood was obtained under anaesthetic by cardiac puncture and stored in EDTA tubes, and mice were sacrificed by cervical dislocation. Plasma was stored at -80^oC, and tumour samples were snap frozen in liquid nitrogen and stored at -80^oC. OSI-906 levels were analyzed by Andy Cooke and Mark Bittner (OSI Pharmaceuticals, Boulder, CO, USA). Mice were sacrificed when tumours reached project licence limits or based on welfare grounds or for weight loss of ≥20% of baseline.

2.9 Statistical analysis

The graphing and statistical analysis software GraphPad Prism v.5.0 (GraphPad) and Excel (Microsoft) were used to plot and analyze data. Graphs were plotted to show mean values, and error bars. Error bars were standard deviation (SD) or the standard error of the mean (SEM). The student's t-test and analysis of variance (ANOVA) were used for the comparison of mean values between two and multiple (>2) data sets, respectively. Xenograft growth rates were compared by linear regression using GraphPad Prism v5. A minimum of 95% level of significance ($p<0.05$) was used to define statistical significance

Chapter 3

Investigating IGF1R signaling and TMZ resistance in a panel of human melanoma cell lines

3.1 Introduction

Alkylating drugs have long been the standard of care for treatment of advanced melanoma (Marsden et al., 2010b). Dacarbazine (DTIC) and the orally bioavailable derivative, Temozolomide (TMZ), produce responses in fewer than 20% of patients (Middleton et al., 2000a) and DTIC is the only form of chemotherapy licensed for advanced melanoma. The IGF1R is well recognized as an important mediator of cell survival, and has been implicated in mediating chemoresistance (Chitnis et al., 2008; Sharma et al., 2010). Previous work from our group indicated that IGF1R depletion using siRNA enhanced sensitivity of melanoma cells to TMZ *in* vitro (Yeh et al., 2006).

The initial aim of this project was to characterize a panel of melanoma cell lines for expression and activation of IGF1R axis components, to determine their sensitivity to TMZ and to determine whether IGF1R inhibition could influence TMZ sensitivity.

3.2 Results and Discussion

3.2.1 Characterization of a panel of melanoma cell lines

The initial approach was to assimilate a panel of ten melanoma cell lines from Professor Colin Goding's group at the Ludwig Institute for Cancer Research, Oxford, Professor Cerundolo (Tumour Immunology Group, Weatherall Institute of Molecular Medicine, Oxford), American Type Culture Collection (ATCC) and Cancer Research UK Cell Services, London. Table 3.1 summarizes the mutations present in this melanoma cell line panel.

Table 3.1 **Genotypes of the melanoma cell line panel**

	GENOTYPE					
CELL LINE	BRAF	NRAS	CDKN2a	PTEN	TP53	Other Mutations
CHL-1	WT	WT	*Mut*	WT	Mut	
A375	*Mut*	WT	*Mut*	WT	WT	
A375M	*Mut*	WT	*Mut*	WT	WT	
A2058	*Mut*	WT	*Mut*	*Mut*	*Mut*	
SK-MEL-2	WT	*Mut*	WT	WT	*Mut*	
SK-MEL-23	WT	WT	WT	*Mut*	WT	
SK-MEL-28	*Mut*	WT	*Mut*	*Mut*	*Mut*	*EGFR*
HMCB	WT	*Mut*	WT	WT	WT	
501Mel	*Mut*	WT	WT	*Mut*	WT	*CTNNB1*
COLO858	*Mut*	WT	WT	WT	WT	

Information on the mutation status of these cell lines was obtained from the Catalogue Of Somatic Mutations In Cancer (COSMIC-www.sanger.ac.uk/genetics/CGP/CellLines) website, the International Agency for Research on Cancer TP53 Database http://p53.iarc.fr/CellLineCriteria.aspx) and individual publications (Ducker et al., 2013; Greshock et al., 2010; Lu et al., 2013; McDermott et al., 2007; Tsao et al., 2004b), since this could also impact on chemoresistance (Cully et al., 2006; Goh et al., 2011).

3.2.2 Assessment of expression and activation of components of the IGF axis

To characterize the cell line panel, western blot analysis was performed to assess total IGF1R and phospho IGF1R levels together with levels and activation of the downstream mediators, ERK1/2 and AKT. ImageJ software was used to quantify protein in the western blot shown in Figure 3.1. Western blotting was also performed for MGMT, which is known to be associated with alkylating drug resistance (Esteller and Herman, 2004; Margison et al., 2003; Middleton et al., 1998).

Figure 3.1 shows that all ten melanoma cell lines expressed IGF1R, at varying levels. Of all the cell lines, CHL-1 cells expressed the lowest levels of total IGF1R, but its presence was confirmed on a longer exposure of this western blot shown. IGF1R expression is reportedly regulated by p53 as well as PTEN (Nahor et al., 2005; Werner et al., 1996; Zhao et al., 2004); however there was no apparent association between p53 or PTEN mutation status and IGF1R levels in this melanoma cell line panel. It was also noted that the

electrophoretic mobility of the IGF1R beta subunit varied between cell lines. This may reflect differences in posttranslational modification of the IGF1R, although there did not appear to be a correlation between electrophoretic mobility of total IGF1R and IGF1R phosphorylation levels. Alternative forms of posttranslational modification include ubiquitination and SUMOylation of the IGF1R, implicated respectively in degradation and nuclear transport of this receptor (Sehat et al., 2010; Vecchione et al., 2003). These modifications generally cause more substantial mobility shift. The extent of variability in IGF1R mobility observed would be more in keeping with glycosylation of the IGF1R, which has recently been implicated in its 'non-membrane localization' (Kim et al., 2012).

Basal levels of phosphorylated AKT were observed to be low, with the highest levels of AKT activation in SK-MEL-23, SK-MEL-28 and A2058, in keeping with the loss of functional PTEN in these cell lines (Table 3.1).

Most of the cell lines showed detectable ERK1/2 phosphorylation consistent with the frequency of gain of function mutations in the RAS-RAF pathway in melanoma (Davies et al., 2002). The exception was CHL-1, which expresses wild-type (WT) NRAS and BRAF. All cell lines expressed detectable levels of the DNA repair protein, MGMT, except SK-MEL-23, HMCB and A2058.

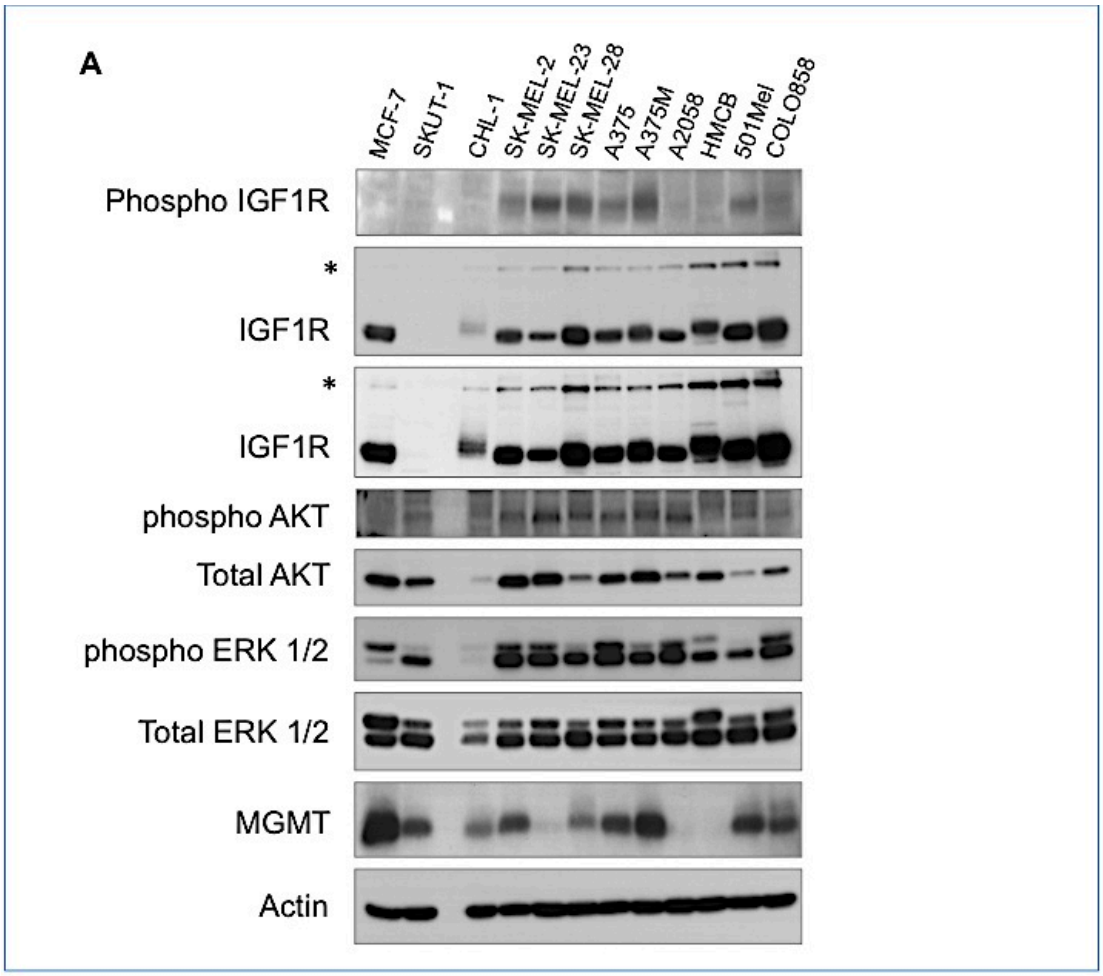


Figure 3.1 Expression of IGF1R signaling proteins in melanoma cell lines.
Whole cell lysates of ten melanoma cell lines grown in full media (with 10% FBS) were analyzed by western blot. Two additional cell lines were included as controls: MCF-7 breast cancer cells, which are known to express physiological levels of IGF1R, and SKUT-1 leimyosarcoma cells which are IGF1R deficient. IGF1R proreceptor is labelled *.

3.2.3 Assessment of IGF1R nuclear localization in melanoma cells

Our group was one of the first to report IGF1R translocation to the nucleus in human tumour cells. The association of nuclear IGF1R with adverse prognosis in renal cancer suggests that nuclear IGF1R may promote an aggressive phenotype (Aleksic et al., 2010). Early evidence suggests a transcriptional role (Sehat et al., 2010) and there has been a report of nuclear

IGF1R being associated with gefitinib resistance (Bodzin et al., 2012). Nuclear IGF1R was also detected by others in melanoma cell lines and a few samples of clinical tissues (Sehat et al., 2010) though no clinical associations were reported in this study. As such immunocytochemistry was used to determine if nuclear staining of IGF1R could be detected in our melanoma cell line panel.

Nuclear IGF1R immunostaining in full medium

All ten melanoma cell lines were grown on cover slips in complete medium and fixed and stained for IGF1R using the protocol previously published by our group (Aleksic et al., 2010). IGF1R was detected in all of the cell lines (Figure 3.3) with relatively intense membrane and cytoplasmic signal in COLO858, 501Mel, A2058, SK-MEL-2 and SK-MEL-23, not entirely reflecting the relative levels of IGF1R detected on western blot (Figure 3.1). Most of the cells had a bright focus of perinuclear signal, which was likely to be due to the presence of IGF1R in the endoplasmic reticulum and Golgi apparatus. Nuclear IGF1R staining was observed in cells cultured in complete medium in CHL-1, A375M, A2058, SK-MEL-2, SK-MEL-23, 501Mel and COLO858.

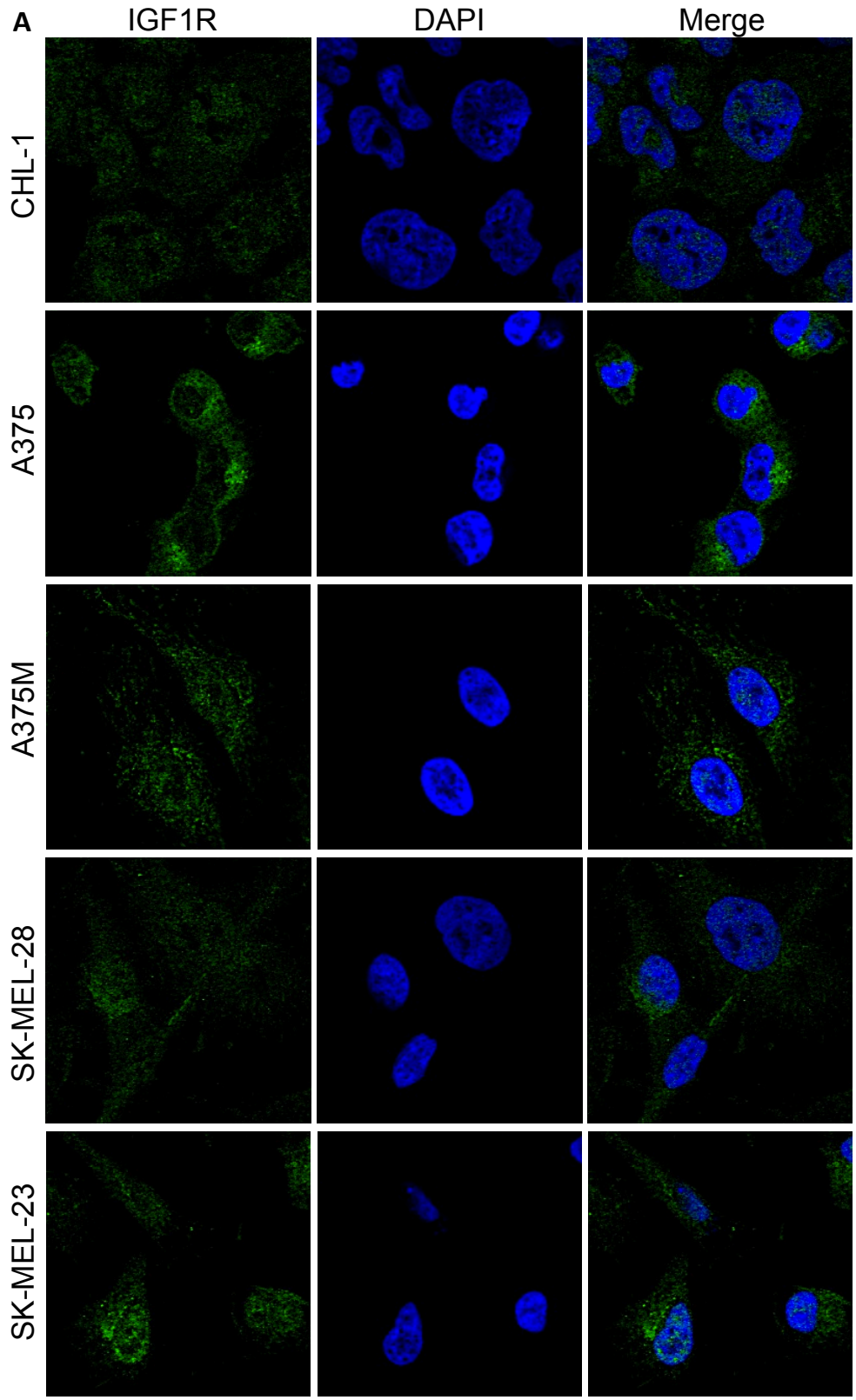


Figure 3.2 (A) IGF1R expression and distribution in melanoma cell lines. Melanoma cell lines (CHL-1, A375, A375M, SK-MEL-28 & SK-MEL-23) were cultured in complete medium with 10% FBS on coverslips and fixed and immunostained for IGF1R (green) and for DAPI for nuclear staining (blue). Images were obtained on confocal microscopy by Tamara Aleksic.

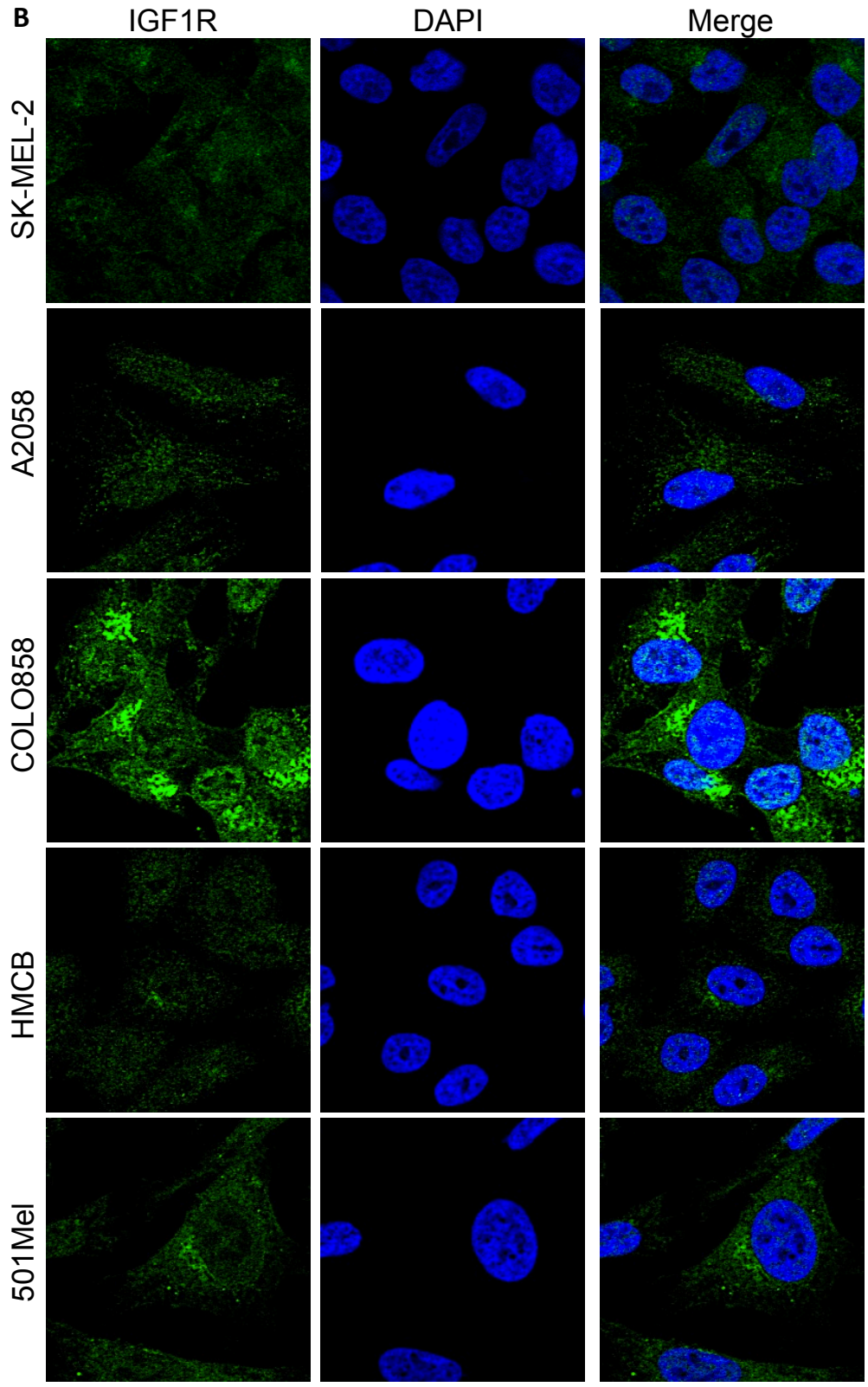


Figure 3.2 (B) IGF1R expression and distribution in melanoma cell lines. Melanoma cell lines (SK-MEL-2, A2058, COLO858, HMCB & 501Mel) were cultured in complete medium with 10% FBS on coverslips and fixed and immunostained for IGF1R (green) and for DAPI for nuclear staining (blue). Images were obtained on confocal microscopy by Tamara Aleksic.

3.2.4 Testing the sensitivity to TMZ in melanoma cells

The CellTiter-Glo® Luminescent Cell Viability (CTG) assay was utilized to assess the effects of the alkylating agent, temozolomide (TMZ) on melanoma cell sensitivity (Figure 3.3). In the literature, other cell line panels including the NCI60 and other melanoma cell lines have been tested in a similar manner (Augustine et al., 2009; Boeckmann et al., 2011).

The concentration of TMZ required to inhibit growth of cells to 50% of that in solvent treated cells (GI_{50} for TMZ) ranged between 150μM and 950μM (Figure 3.1). This is above the maximum clinically achievable serum concentration of TMZ, which is 60-75μM (Middleton et al., 2000a; Sankar et al., 1999).

Having characterized the degree of TMZ resistance, it was therefore of interest to determine whether any factors may be associated with this chemo resistance in the melanoma cell line panel, since any such findings could potentially be exploited to overcome alkylating drug resistance in melanoma.

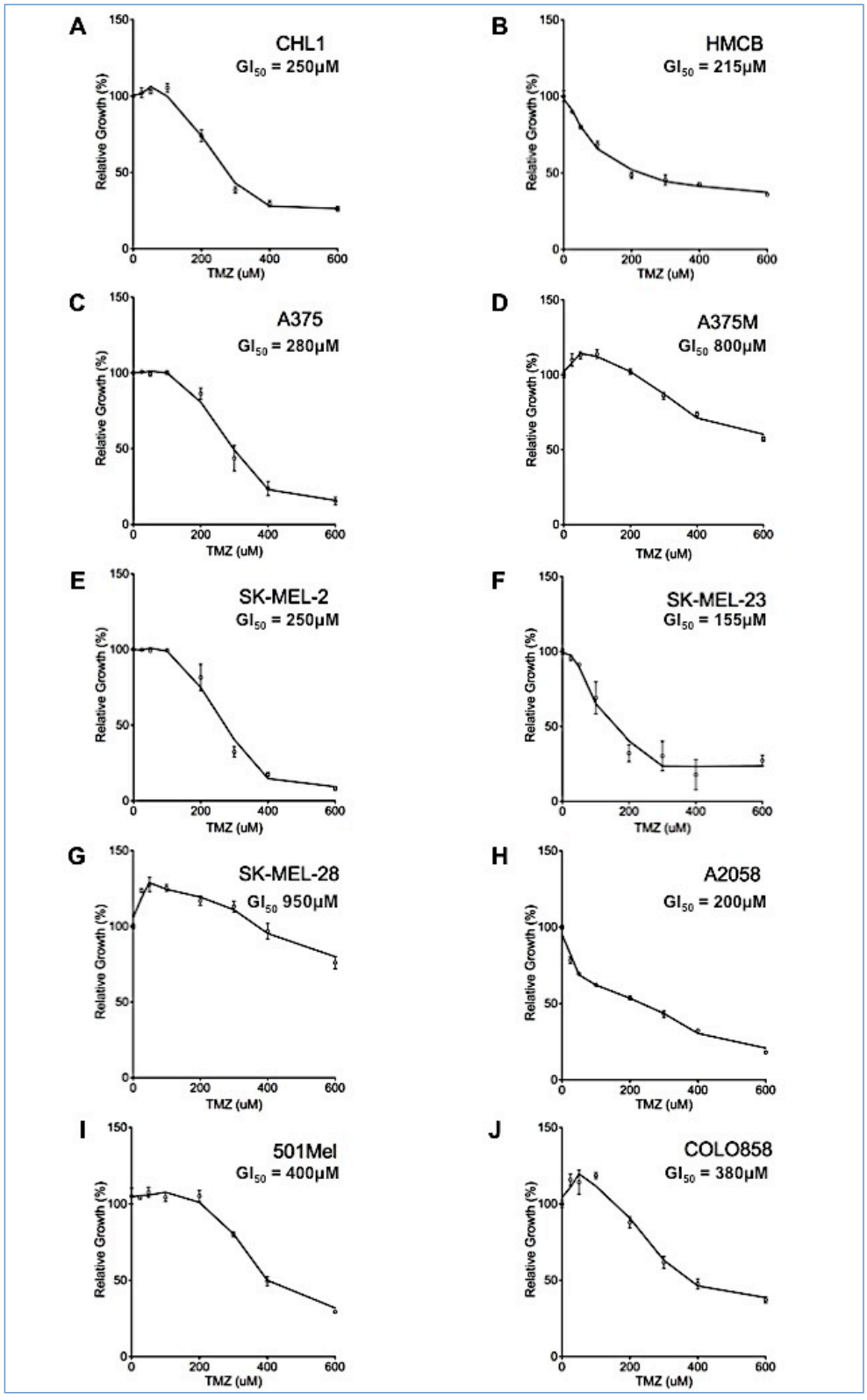


Figure 3.3 Effect of TMZ on melanoma cell viability. (A) CHL-1, (B) HMCB, (C) A375, (D) A375M, (E) SK-MEL-2, (F) SK-MEL-23, (G) SK-MEL-28, (H) A2058, (I) 501Mel and (J) COLO858 melanoma cells were seeded at 1000 per well and treated the following day with TMZ (50-600µM) or solvent (DMSO<0.1%). After 5 days, cell viability was quantified using the CTG assay. Graphs show mean viability from two independent experiments, each with triplicate points, expressed as a fraction of viability in solvent-treated cells. Error bars (SEM). The data were curve fitted and GI_{50} values were calculated using GraphPad Prism software, which was also used to extrapolate GI_{50}'s above 600µM.

3.2.5 Assessment of correlations with TMZ resistance in melanoma cells

To assess whether IGF1R expression showed any association with response to TMZ, ImageJ software was used to quantify protein levels in the western blot shown in Figure 3.1. Correlation analysis between protein expression and GI_{50} for TMZ treatments was performed using GraphPad Prism software. MGMT protein expression positively correlated with GI_{50} for TMZ (Spearman's rank correlation coefficient r = 0.79, p = 0.009 in Figure 3.4 A), suggesting that increasing MGMT expression conferred greater TMZ resistance in these melanoma cell lines. This relationship has previously been described *in vitro* (Esteller and Herman, 2004; Margison et al., 2003) and also clinically in malignant gliomas (Esteller et al., 2000; Gorlia et al., 2008; Hegi et al., 2005), although any association in clinical melanomas is controversial (Lee et al., 1991; Ma et al., 2003; Middleton et al., 1998).

Examining all ten cell lines together, total IGF1R expression did not correlate with GI_{50} for TMZ (Spearman's rank correlation coefficient r = 0.577, p=0.085, data not shown). This association was greater in the MGMT-proficient cells, although this did not reach statistical significance (r = 0.64, p=0.052, in Figure 3.4 B). There was, however a significant correlation between phospho-IGF1R expression and TMZ GI_{50} in the MGMT proficient melanoma cell lines (r=0.81, p=0.038, Figure 3.4 B)), suggesting a link between IGF-1R activation and intrinsic TMZ resistance. The expression of mediators downstream of IGF1R such as AKT and ERK1/2 did not correlate with GI_{50} for TMZ (r = -0.072,

p=0.857 and r = 0.414, p=0.356 respectively, data not shown). Phospho-ERK1/2 levels did not correlate with TMZ GI_{50} (r = -0.108, p=0.792) whereas phospho-AKT levels showed a trend to correlation, although this was not statistically significant (r = 0.774, p = 0.051). This may suggest that the PI3K pathway may play a greater role in TMZ resistance than RAS/RAF/MAPK signaling and may further justify IGF1R blockade as a therapeutic option in overcoming chemoresistance by utilizing its ability to diminish signaling along both these pathways.

Immunocytochemistry images were quantified using ImageJ software. The relative nuclear IGF1R expression was calculated by expressing the integrated density of nuclear IGF1R staining as a percentage of the integrated density of IGF1R staining of the whole cell (Figure 3.2). The integrated density of a selected area on ImageJ measures the sum of the intensity values of the pixels in the area of interest. This analysis revealed that the mean intensity of nuclear staining and relative nuclear IGF1R expression did not correlate with GI_{50} of TMZ in MGMT-proficient cell lines (r = 0.339, p=0.309 and r = -0.595, p=0.155 respectively).

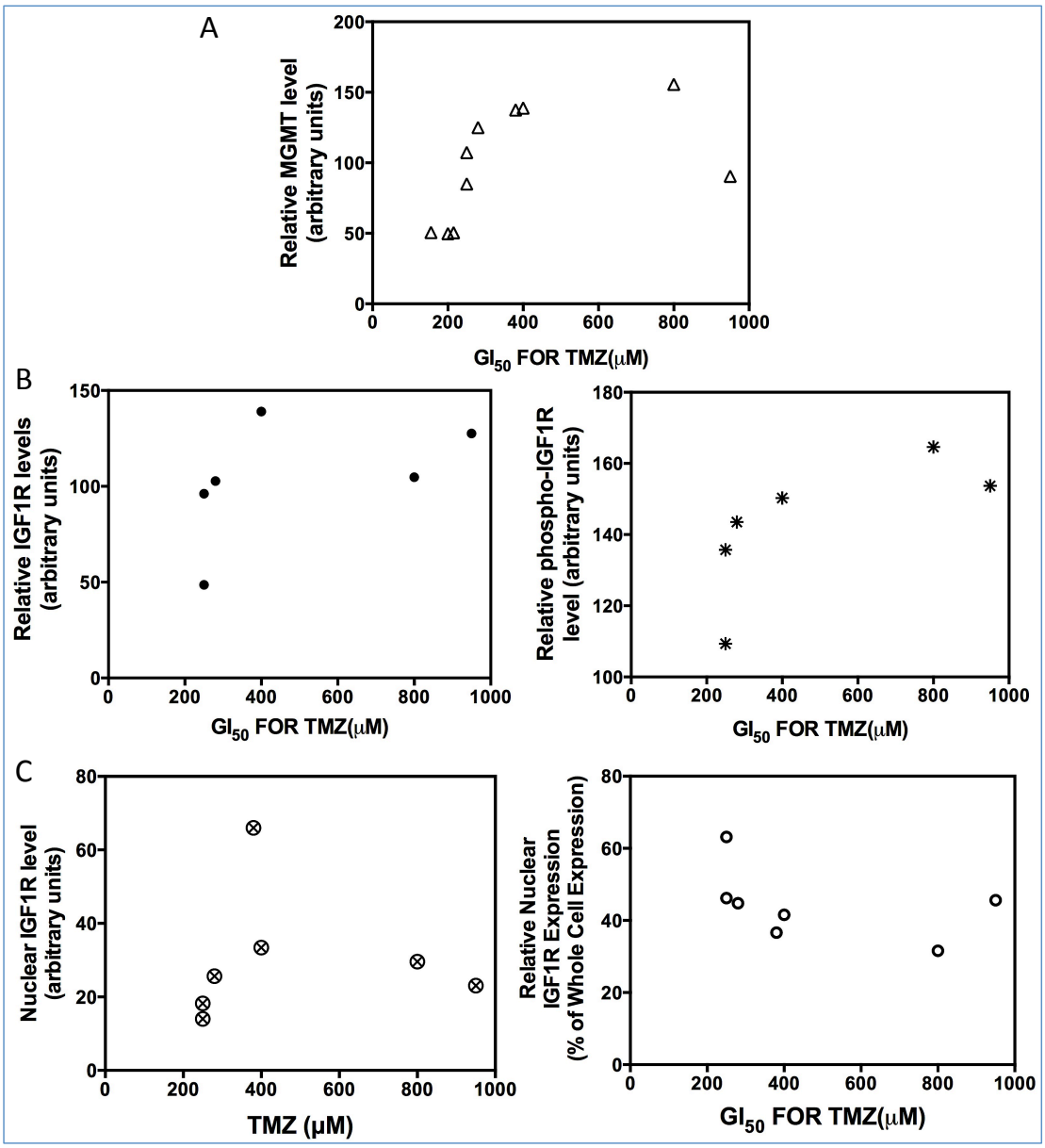


Figure 3.4 Correlation analysis between TMZ sensitivity and IGF1R levels or distribution in melanoma cells. Levels of IGF1R, phospho IGF1R and MGMT were quantified in the western blot of this cell line panel from Figure 3.1, using ImageJ software. **(A)** Correlation analysis revealed a significant association between MGMT level and GI_{50} for TMZ (Spearman's rank coefficient, r = 0.79, p = 0.009). **(B)** MGMT proficient cells showed no significant relationship between GI_{50} for TMZ and IGF1R (left) (r = 0.64, p=0.052) and a significant relationship between GI_{50} for TMZ and phospho IGF1R level (r=0.81, p=0.038). **(C)** From the immunofluorescence staining performed in Figure 3.2, ImageJ software was used to quantify nuclear IGF1R intensity (or level) in at least 20-30 cells. Correlation analysis revealed no significant relationship between GI_{50} for TMZ and either absolute nuclear IGF1R level (left) or relative nuclear IGF1R expression (ie a percentage of whole cell IGF1R level) (right) (r = 0.487, p=0.27; and r = -0.595, p=0.15 respectively).

3.2.6 Investigating the effects of IGF1R inhibition on TMZ resistance in melanoma cells

Previous work in our group demonstrated that IGF1R depletion caused two-fold sensitization of melanoma cells to TMZ, as judged by changes in GI_{50} values, and this effect occurred regardless of BRAF mutation status (Yeh et al., 2006). This technique of manipulating IGF1R expression has limited applications clinically. Exploring whether a similar effect could be demonstrated using an IGF1R inhibitor would therefore have potential clinical relevance. Notably, TMZ has recently been combined with an IGF1R inhibitor antibody in a neuroblastoma model, with beneficial effects both *in vitro* and *in vivo* (Geoerger et al., 2010), further supporting the evaluation of this combination in malignant melanoma. The present study used the compound AZ12253801, developed and supplied by AstraZeneca. This small molecule tyrosine kinase inhibitor selectively inhibits IGF1R and the closely related insulin receptor by competing for ATP-binding in the kinase domain of the β-subunit of the receptor. It is ten times more selective for the IGF1R than the insulin receptor and the GI_{50} for IGF1R-driven proliferation in mouse fibroblasts was found to be 20 times greater than EGFR-driven proliferation according to AstraZeneca in-house data (Aleksic et al., 2010).

In the first instance, the ability to inhibit the IGF1R was tested in CHL-1 human melanoma cells, the same cell line used in the *IGF1R* silencing experiments performed by Yeh et al (2006). Figure 3.5 A shows that concentrations of AZ12253801 greater than 10nM caused inhibition of IGF1R phosphorylation in CHL-1 melanoma cells. To test the duration of action of AZ12253801 *in vitro*, serum-starved CHL-1 cells were treated with 30nM

AZ12253801 for up to 72 hours, with 50nM IGF-1 stimulation in the final 15 minutes. The results suggested that the inhibitory effect of AZ12253801 was maintained for 48 hours (Figure 3.5 B).

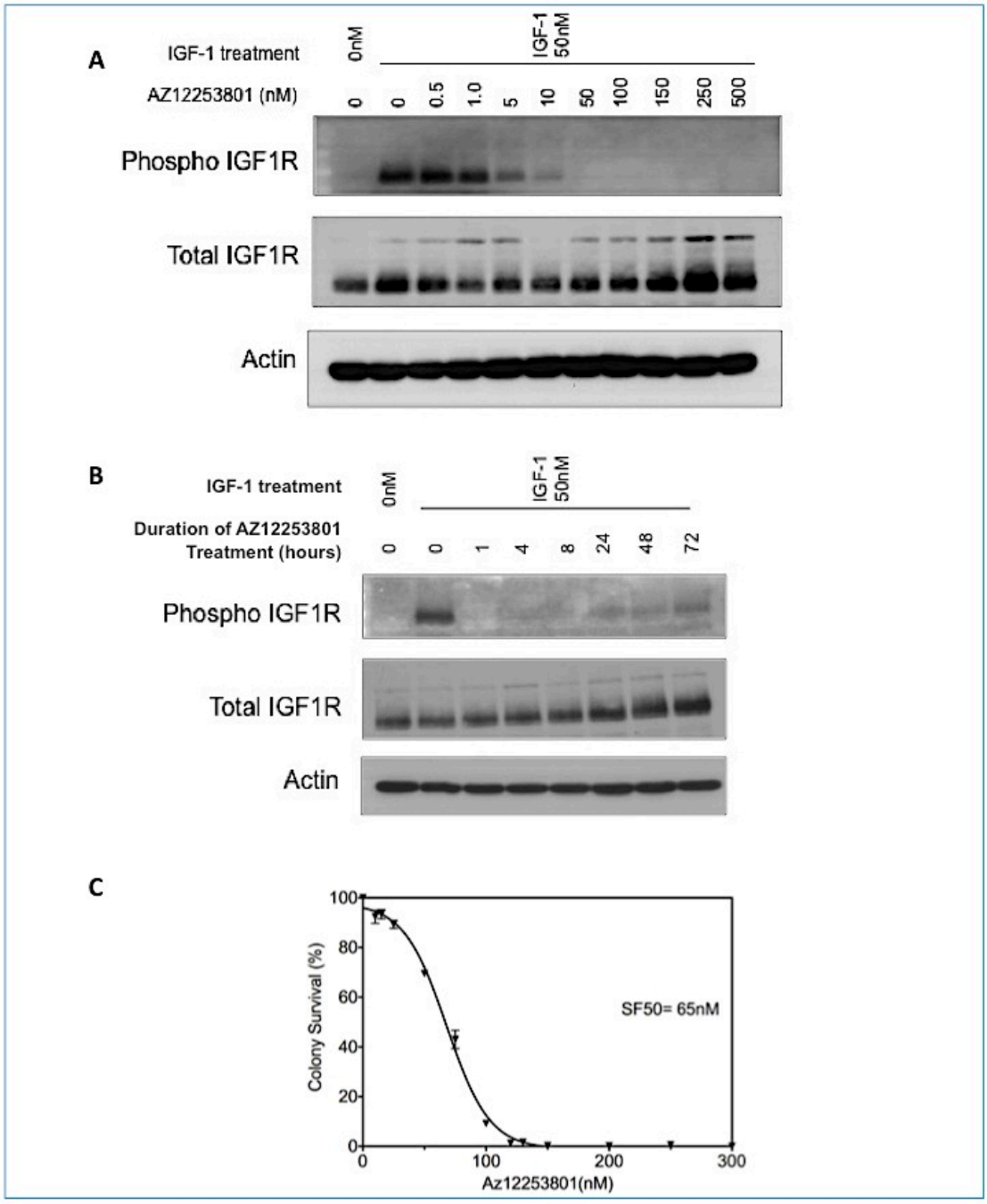


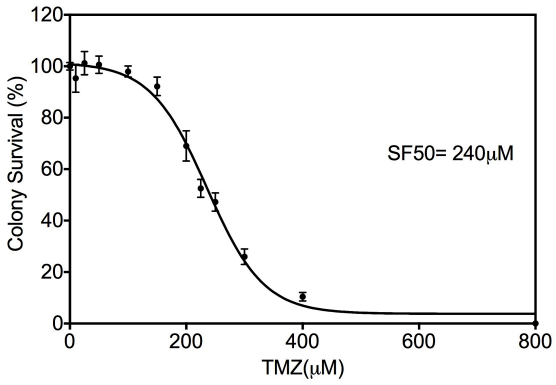
Figure 3.5 AZ12253801 inhibits IGF1R signalling and survival. **A,** CHL-1 cells were serum starved, treated with AZ12253801 and in the final 30 minutes with 50nM IGF-1. Lysates were analyzed by western blot. **B**, Time course of treatment with 30nM AZ12253801 under the same conditions as A. **C** CHL1 cells were seeded in 10cm dishes in complete medium and treated12 hours later with increasing concentrations of IGF1R inhibitor AZ12253801 for continuous until fixing and staining 7-10 days later. Results are expressed as percentage of the colony count of the solvent (DMSO<0.1%) treated dishes. SF_{50} refers to the concentration of drug required to produce 50% survival (survival fraction).

To determine whether the IGF1R inhibitor affected melanoma cell survival, clonogenic assay was performed in CHL-1 cells (Figure 3.5C), since our group previously demonstrated that IGF1R silencing with siRNA sensitized CHL-1 cells to TMZ (Yeh et al., 2006). This demonstrated that AZ12253801 used as a single agent could inhibit survival of CHL-1 melanoma cells, with a SF_{50} of 65nM, where SF_{50} refers to the concentration of drug required to reduce survival to 50% compared with the solvent treated control. The effect of TMZ on CHL-1 survival was assessed in a similar way and the SF_{50} value for TMZ in CHL-1 cells was found to be 240μM (Figure 3.6 A). This is comparable to the GI_{50} value of 250μM obtained by CTG assays (Figure 3.3)

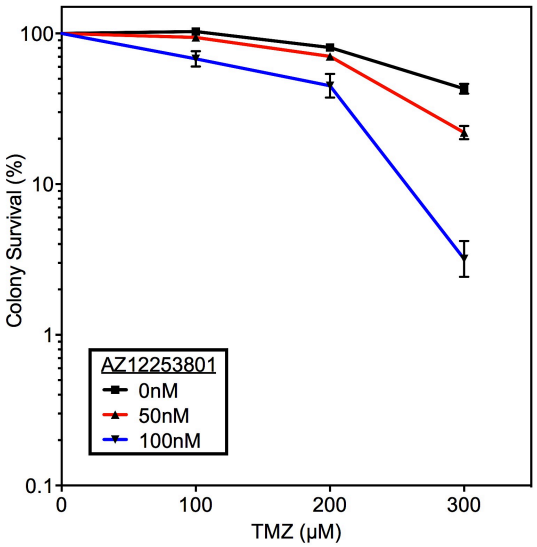
Colony formation assay was also used to further assess the combination of AZ12253801 with TMZ, using increasing concentrations of both agents, applied simultaneously to CHL-1 cells (Figure 3.6 B). This demonstrated that AZ12253801 induced statistically significant dose dependent TMZ sensitization, particularly at the higher concentrations of the combination treatment (Figure 3.6 B and C). As stated above, the SF_{50} of TMZ in the CHL1 cell line was found to be 240μM (Figure 3.6 A), which is above the clinically achievable concentration 75μM (Middleton et al., 2000a; Sankar et al., 1999). Figure 3.6 B shows that 100nM AZ12253801 induces 43% reduction in the survival of cells treated with 100μM TMZ. This is closer to the clinically achievable concentration for TMZ and is potentially encouraging. In addition, AZ12253801 was capable of enhancing the effect of TMZ in the A375M cell line (Figure 3.7). This cell line was used since it is known to carry the V600E BRAF mutation (Table 3.1), common to this cancer type (Davies et al., 2002). These results confirm the findings of a previous study from our group, which

indicated that IGF1R depletion reduced TMZ sensitization in cells harbouring either WT or mutant BRAF (Yeh et al., 2006).

A



B



C

Comparison of Treatments (ANOVA)		p value	Summary
AZ 0nM vs AZ 50nM	+ TMZ 100μM	0.708	ns
	+ TMZ 200μM	0.067	ns
	+ TMZ 300μM	0.001	**
AZ 0nM vs AZ 100nM	+ TMZ 100μM	<0.0001	****
	+ TMZ 200μM	<0.0001	****
	+ TMZ 300μM	<0.0001	****
AZ 50nM vs AZ 100nM	+ TMZ 100μM	<0.0001	****
	+ TMZ 200μM	<0.0001	****
	+ TMZ 300μM	0.002	**

Figure 3.6 Combining IGF1R inhibition with TMZ reduces CHL-1 survival. **(A)** CHL1 cells were seeded in 10cm dishes in complete medium and treated 12 hours later with TMZ (0-800μM) for continuous exposure until fixing and staining 7-10 days. SF_{50} for TMZ treatment was determined as in Figure 3.4 C. **(B)** CHL-1 cells were seeded for clonogenic assay as in A and tretated with TMZ alone or with AZ12253801 (50 or 100nM). After fixation and staining at 7-10 days, colonies were counted and expressed as a precent survival in solvent treated controls (DMSO<0.1%). Data were analyzed by one-way ANOVA and are shown in **C**.

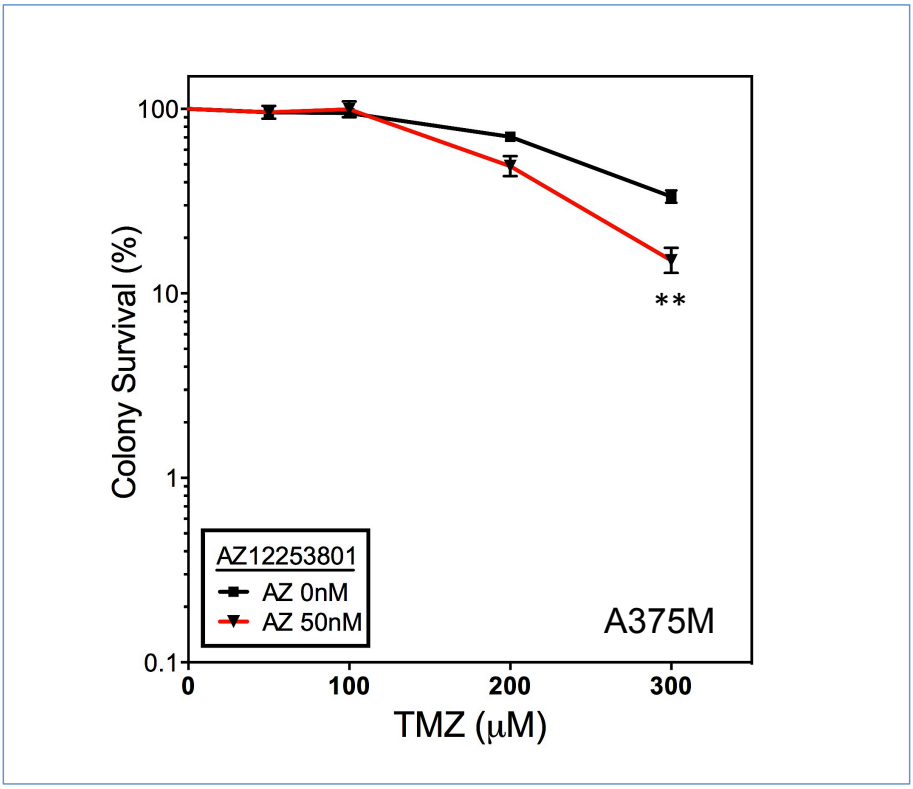


Figure 3.7 AZ12253801 sensitizes to TMZ in A375M cells. A375M melanoma cells were seeded in 10cm dishes in complete medium and treated 12 hours later with increasing doses of TMZ and either solvent (DMSO<0.1%) or 50nM AZ12253801. Colonies were fixed and stained 10-14 days later and survival fraction expressed as a percentage of solvent treated dishes. 50nM AZ12253801 significantly reduced colony survival in response to 300μM TMZ treatment (p=0.006, student's t test).

These initial studies suggest that IGF1R inhibition may be a viable approach to increase the response of human melanoma cells to TMZ. It will be informative to understand the mechanism of interaction between IGF1R signalling and alkylating DNA damage, given the chemoresistant nature of malignant melanoma, and this is explored in Chapter 4. Chapter 5 then uses an alternative IGF1R inhibitor that is currently undergoing early phase clinical testing, to perform preclinical studies in melanoma xenografts *in vivo.*

Chapter 4

Investigating mechanisms of the enhancement of TMZ sensitivity by IGF1R inhibition

Having found evidence that IGF1R inhibition contributed to sensitization of melanoma cells to TMZ, demonstrated in Chapter 3, the next step was to investigate the molecular basis of TMZ sensitization. The initial experiments attempted to assess whether the influence of IGF1R on the response to TMZ was linked to its well-recognized ability to regulate cell survival and cell cycle distribution.

Results and Discussion

4.1 Investigating the effects of IGF1R inhibition on TMZ-induced apoptosis

IGF1R is known to contribute to cell survival, protecting from apoptosis via PI3K/AKT and MAPK signaling (Peruzzi et al., 1999). Consistent with this, IGF1R depletion with siRNA was shown by our group to induce apoptosis in melanoma cells (Yeh et al., 2006) and similarly IGF1R inhibitors have also

been shown to induce apoptosis (Karasic et al., 2010). In addition, alkylating DNA damage indirectly induces apoptosis, via MMR and via DSB formation (Fu et al., 2012). With apoptosis being a common feature of both IGF1R inhibition and TMZ induced cytotoxicity, the initial investigation into the mechanism of a possible interaction between these two agents sought to quantify this.

Figure 4.1 (A) and (B) shows the effect of combining AZ12253801 with TMZ for 24 and 48 hours respectively on apoptosis induction in CHL-1 cells. TMZ treatment for 24 and 48 hours did not produce a significant increase in caspase activation (Figure 4.1 A). IGF1R inhibition with AZ12253801 for 24 and 48 hours produced a significant dose dependent increase in caspase activation (see table 4.1), which was not significantly altered by the addition of TMZ treatment.

Another marker of apoptosis is Poly (ADP-ribose) polymerase (PARP) cleavage. This was measured by western blot of whole cell lysates for CHL-1 cells treated with TMZ (0-300μM) and/or AZ12253801 (0-150nM). Treatment with either TMZ or AZ12253801 caused dose-dependent increase in PARP cleavage, however combining these two agents produced no further PARP cleavage, which was in agreement with the findings of the caspase activation assay in Figure 4.1 A. Thus, although apoptosis induction with either AZ12253801 or TMZ alone was demonstrated, the combination of these agents did not increase this effect and therefore would be unlikely to account entirely for the chemosensitization demonstrated in Figure 3.6 B.

Both agents affect cellular proliferation and cell cycle progression, and therefore, cell cycle analysis was next performed to determine the effects of AZ12253801 treatment TMZ-induced cell cycle distribution.

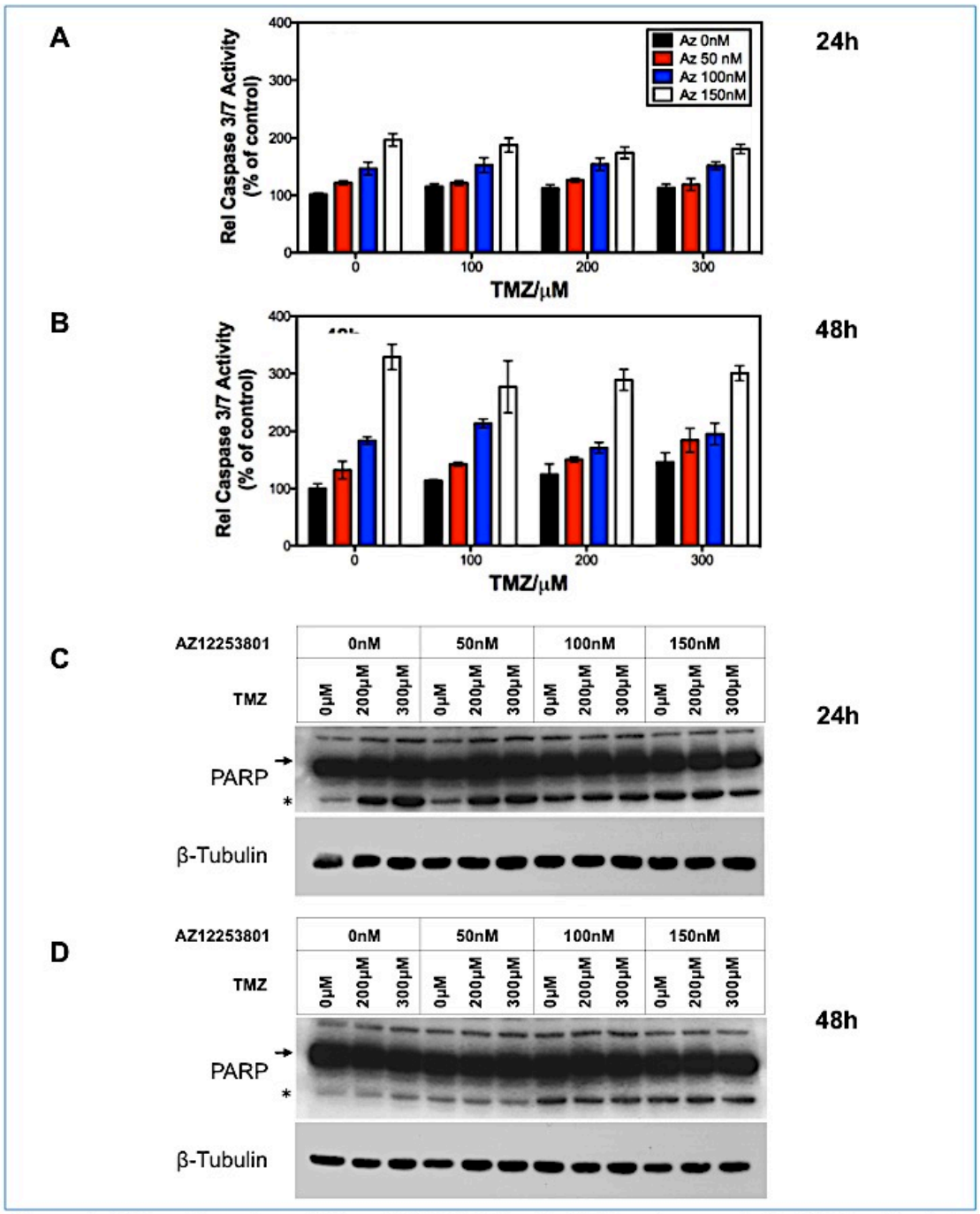


Figure 4.1 The effect of combining AZ12253801 with TMZ on Apoptosis in CHL1 cells. Cells were seeded in triplicate at 5,000 (in 100μl medium) per well in 96 well plates on the first day and combination treatment applied simultaneously on the following day. Apo-ONE® Homogenous Caspase 3/7 Assay kit was used to determine caspase activation after 24 hours **(A)** and 48 hours **(B)**. Graphs of results from two independent experiments show relative caspase activity expressed as a percentage of signal in control (less than 0.1% DMSO) treated cels. Western blot of whole cell lysates for PARP cleavage was also performed for 24 hour **(C)** and 48 hour **(D)** combination treatments of AZ12253801 and TMZ. Arrowhead, full length PARP; asterisk, cleaved PARP.

Table 4.1 A - Statistical analysis of caspase activation in response to 24 hour treatment with TMZ and/or AZ12253801 shown in Figure 4.1 A (using one-way ANOVA)

Treatment comparison		p value	Statistical significance
Solvent treated vs	TMZ 100 μM	0.999	ns
	TMZ 200 μM	0.999	ns
	TMZ 300 μM	0.999	ns
	AZ 50nM	0.960	ns
	AZ 100nM	0.038	*
	AZ 150nM	<0.0001	****
AZ vs	AZ+TMZ	≥ 0.90	ns

Table 4.1 B - Statistical analysis of caspase activation in response to 48 hour treatment with TMZ and/or AZ12253801 shown in Figure 4.1 A B (using one-way ANOVA)

Treatment comparison		p value	Statistical significance
Solvent treated vs	TMZ 100 μM	0.999	ns
	TMZ 200 μM	0.999	ns
	TMZ 300 μM	0.905	ns
	AZ 50nM	0.996	ns
	AZ 100nM	0.100	ns
	AZ 150nM	<0.0001	****
AZ vs	AZ+TMZ	≥ 0.78	ns

4.2 Effect of combining IGF1R inhibition with TMZ on cell cycle progression

Cellular proliferation depends on cell cycle progression, which is regulated by a complex system of mediators and any threat to cellular integrity can trigger cell cycle arrest. IGF1R signaling can affect the G1 or G2M checkpoints (Chitnis et al., 2008; Shaw and Cantley, 2006). DNA damage is another important trigger of many forms of cell cycle arrest, which ultimately functions to prevent transmission of defective DNA to daughter cells (Iliakis et al.,

2003). Since both IGF1R inhibition and TMZ-induced DNA damage could affect cell cycle progression, it was therefore important to quantify this to determine whether altered cell cycle progression could contribute to the increased cytotoxicity observed by combining these two agents.

At this point in the project, unpublished data provided by AstraZeneca suggested that IGF1R inhibitor, AZ12253801, could also cause polyploidy, particularly in murine cells due to aurora B kinase inhibition. Such activity could confound the interpretation of the results of this project. Therefore, initial tests of cell cycle distribution were undertaken to determine whether AZ12253801 was inducing polyploidy in CHL1 melanoma cells.

Figure 4.2 shows the effect of increasing AZ12253801 concentration on DNA content. The x-axis acquisition settings were chosen to detect polyploid cells, but limited the interpretation of the cell cycle distribution. In cells treated with AZ12253801 at concentrations of up to 100nM, fewer than 2% of cells had DNA content greater than 4N. However, treatment with 150nM AZ12253801 resulted in the emergence of polyploid cells, increasing from 3-4% at 24 hours to 20% at 48 hours. This suggested that this concentration of AZ12253801 might have been inducing aurora B kinase inhibition. This might also explain the apparent increase in caspase activation (Figure 4.1 A&B) in cells treated for 48 hours with 150nM AZ12253801 treatment. Subsequent experiments therefore, used concentrations of no greater than 100nM of AZ12253801.

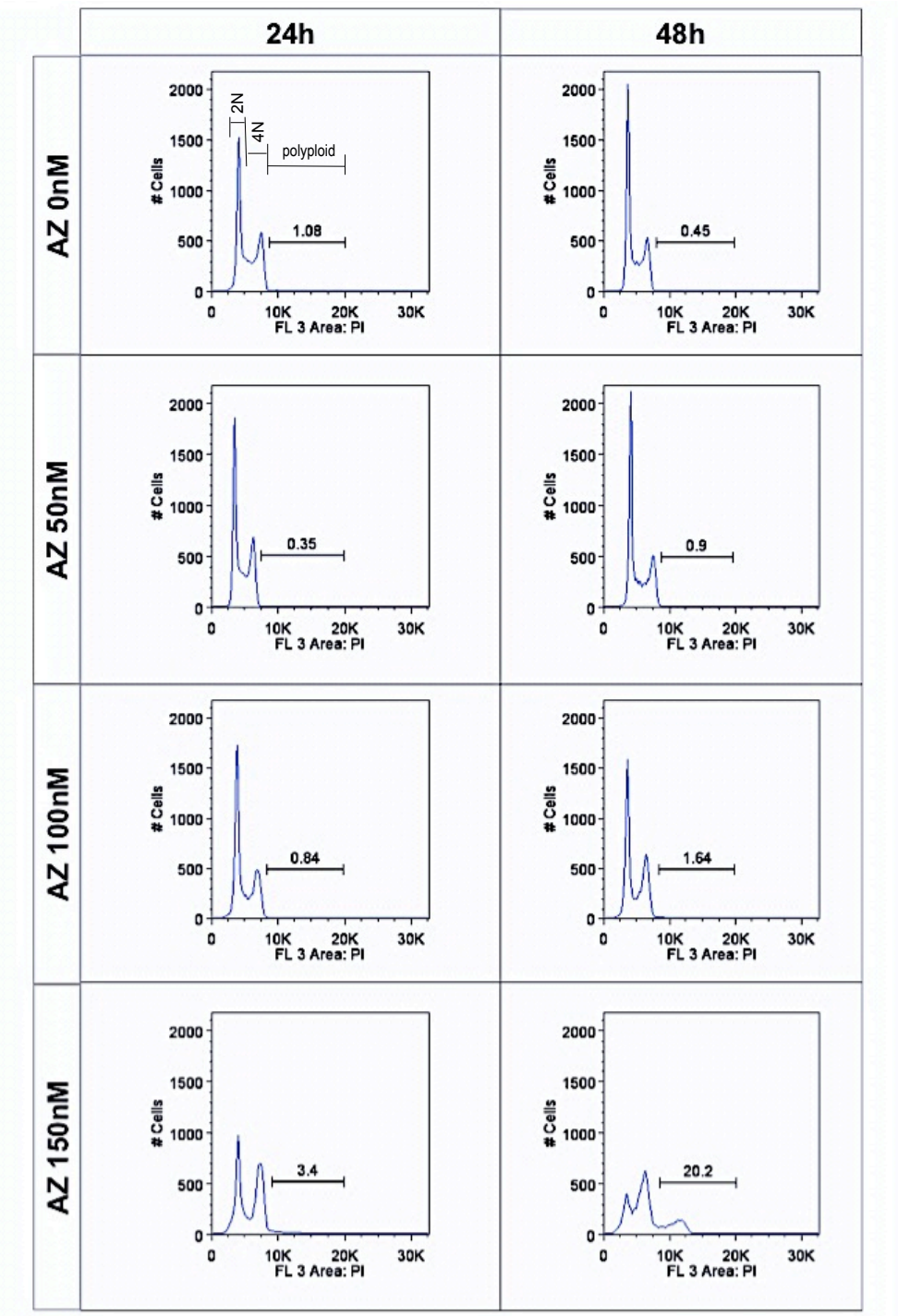


Figure 4.2 Testing AZ12253801 for Induction of polyploidy. CHL-1 cells were treated in complete medium for 48 hours with a dose range of AZ12253801, RNAse A treated and stained with propidium iodide (PI) and analysed by flow cytometry. The proportion (%) polypoid of cells was measured as shown in each histogram plot.

Cell cycle information obtained on PI-stained cells is limited because it is unable to distinguish cells in early S phase from those in G1, and similarly cells in late S phase from those in G2. Therefore, to quantify cell cycle distribution, dual staining with bromodeoxyuridine (BrdU) and PI was used to quantify and differentiate G1, S and G2/M cell populations (Leif et al., 2004).

This BrdU method demonstrated that IGF1R inhibition caused accumulation of cells in G1 after 24 hours (Figure 4.3 A). Treatment with TMZ alone caused a modest increase (approximately 6%) in the G2/M fraction in the first 24 hours. Combining 100nM AZ12253801 with 300μM TMZ for 24 hours resulted in G1 arrest of similar magnitude as in cells treated with AZ12253801 alone, and also caused reduction in both early and late S phase cells compared with either agent alone. There was also greater accumulation of cells in G2/M with the combination treatment, and the proportion of cells in G2/M appeared to remain constant (30%) at both the 24 and 48 hour time points (Figure 4.3 A and B respectively) suggesting that G2/M arrest had occurred.

In order to understand how these changes in cell cycle distribution came about, parallel cultures were lysed and subject to western blotting for cell cycle regulators.

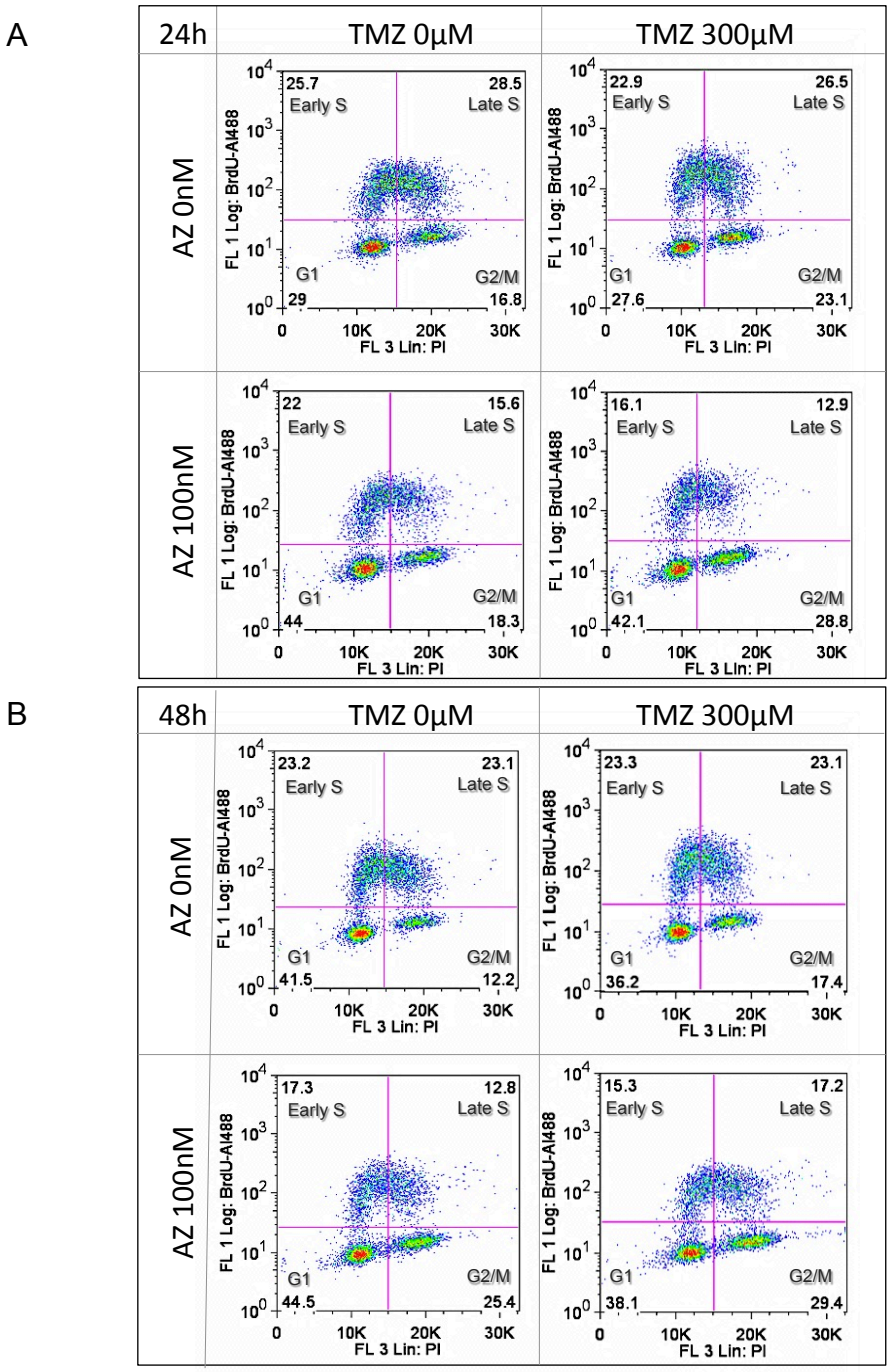


Figure 4.3. The effect of combining IGF1R Inhibition and TMZ on Cell Cycle Distribution by BrdU incorporation. CHL1 cells were treated with AZ12253801(AZ) and TMZ simultaneously for 24 hours (**A**), and 48 hours (**B**), and the BrdU incorporation method of cell cycle analysis by flow cytometry performed. The resulting cell cycle flow cytometry plots used propidium iodide (PI) to stain DNA (x-axis) and Alexa-488 secondary antibody for incorporated BrdU (y-axis). Using FlowJo software, the proportion (%) of cells in each cell cycle phase was measured and are displayed in each respective quadrant above. Similar results were obtained in a second independent experiment.

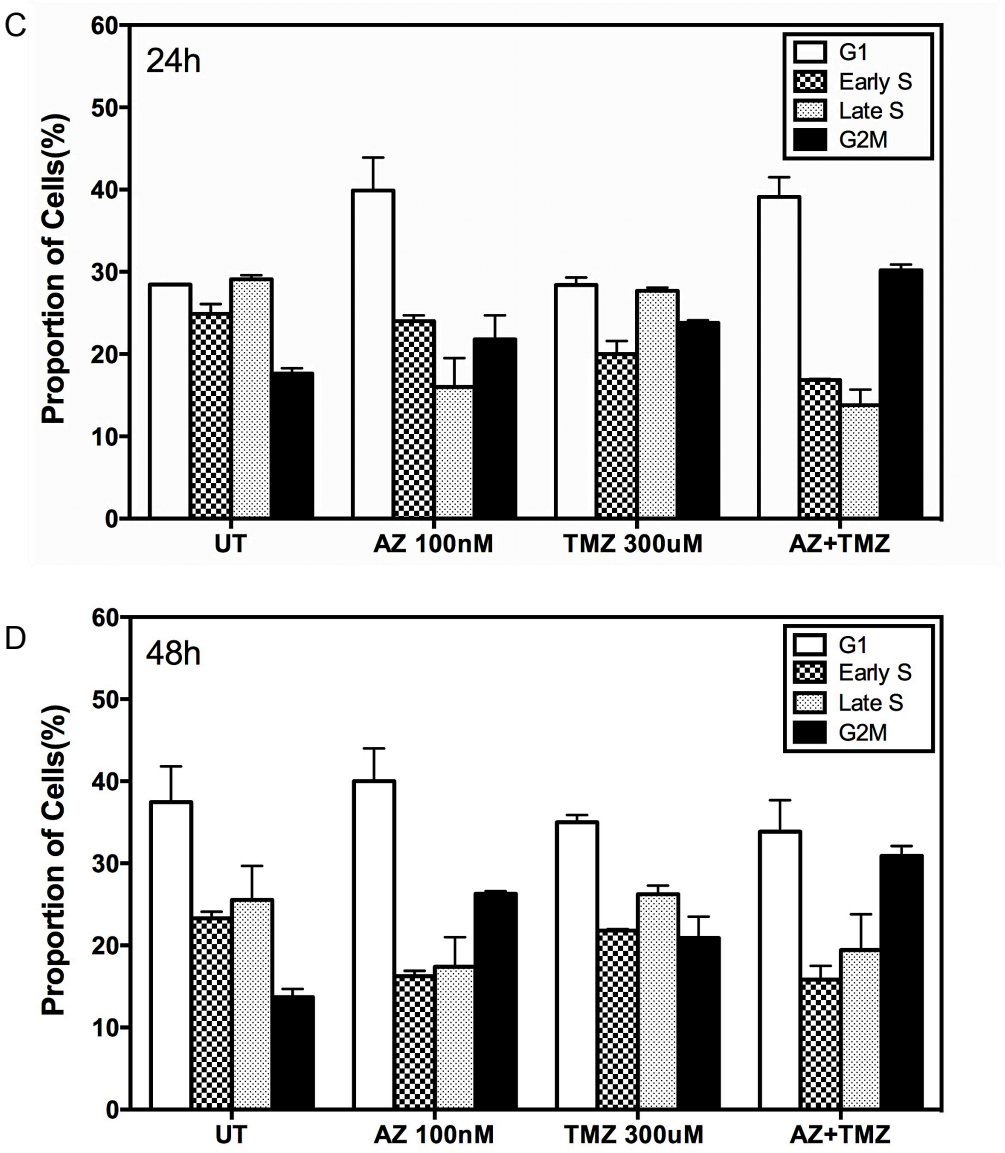


Figure 4.3 (continued). The effect of combining IGF1R inhibition and TMZ on cell cycle progression by BrdU incorporation. (**C**) and **(D)** are bar graph summaries of the cell cycle analysis performed by BrdU incorporation method for Figure 4.3 (A) and (B) respectively, showing the quantification of each phase of the cell cycle for each treatment (bars represent means and error bars are the range of values from two independent experiments).

G2/M transition requires active cdc2-cyclin B1 interaction. Phosphorylation of cdc2 inhibits its interaction with cyclin B1, activating the G2/M checkpoint resulting in G2/M arrest (DiPaola, 2002). By western blot analysis of whole cell lysates, TMZ treatment was seen to cause a modest increase in this inhibitory cdc2 phosphorylation, and also increased cyclin B1 levels (Figure 4.4), perhaps explaining the accumulation of cells in G2/M following TMZ treatment. The addition of AZ12253801, however, did not further increase this effect.

DNA damage is known to activate checkpoint kinases Chk1 and Chk2 by phosphorylation on Serine-345 and Threonine-68 respectively (Ahn et al., 2000; Liu et al., 2000). In contrast, IGF1R signaling activates AKT, which has been shown to cause inhibitory Chk1 phosphorylation on Serine-280 *in vitro* (Liang and Slingerland, 2003). Data in Figure 4.4 indicate that TMZ treatment caused dose dependent Chk1 activation, as shown by increased Ser-345 phosphorylation; however, the addition AZ12253801 appeared to reduce this effect. This is perhaps unexpected given the accompanied greater accumulation of cells in G2/M (Figure 4.3). With respect to the other checkpoint kinase, TMZ treatment alone had little effect on Chk2 phosphorylation, however, in the presence of IGF1R inhibition with AZ12253801, greater Chk2 activation was observed, particularly in combination with 300μM TMZ. This may be consistent with the greater accumulation of cells in G2/M observed in Figure 4.3 (Bartek et al., 2001). In response to DNA damage, Chk2 is phosphorylated by the active, Serine-1981 phosphorylated form of ATM (Bakkenist and Kastan, 2003). TMZ induced phosphorylation of ATM was shown to increase with IGF1R inhibition.

Activation of ATM and Chk2 were not expected following IGF1R inhibition, but could indicate enhanced activation of the DNA damage response, and/or persistent DNA damage, in cells treated with TMZ plus AZ12253801. Hence, subsequent experiments set out to determine whether IGF1R inhibition affected the repair mechanisms utilized in the removal of TMZ-induced DNA damage.

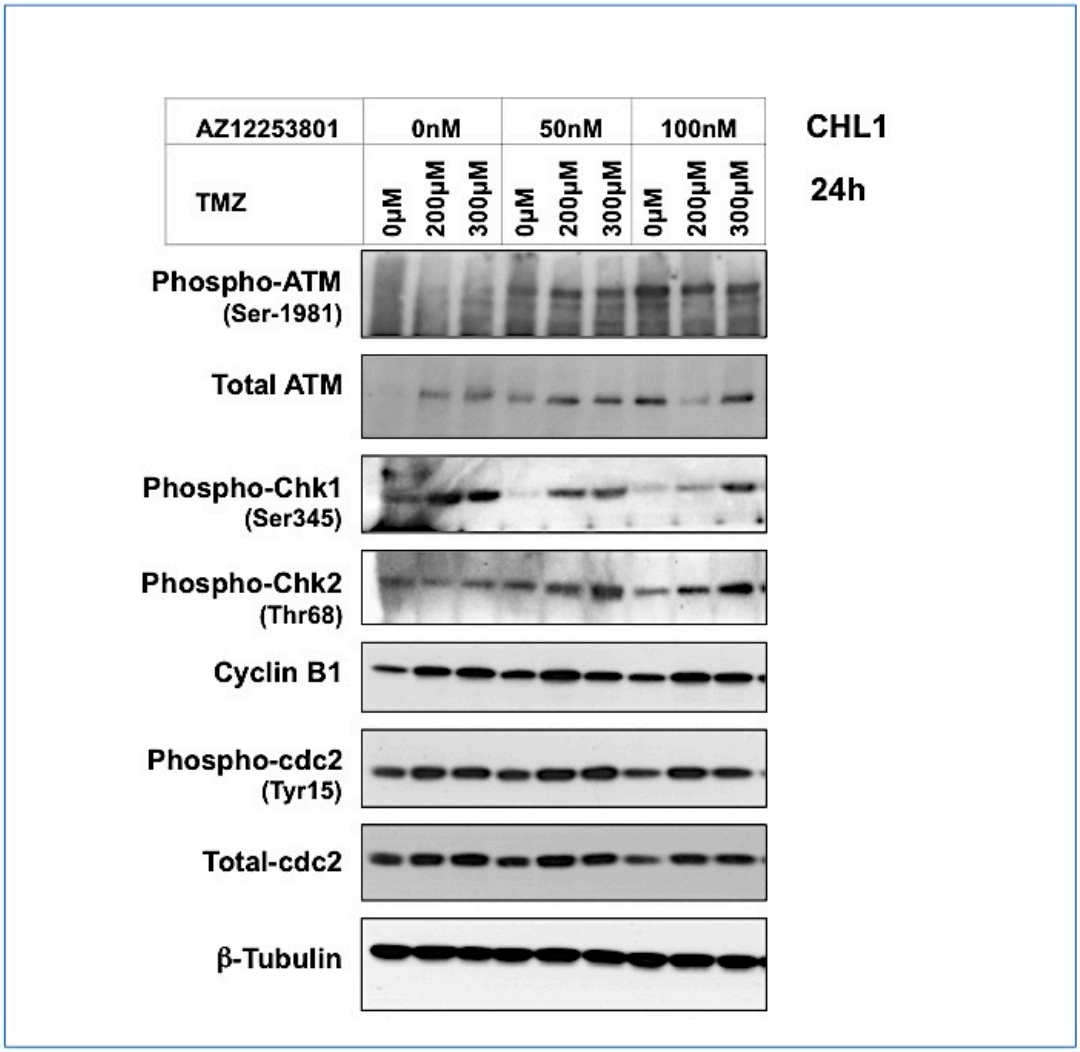


Figure 4.4 The effect of IGF1R inhibition on cell cycle checkpoint mediators induced by TMZ. CHL-1 cells grown in complete medium were treated simultaneously with a combination of TMZ (0, 200 or 300μM) plus AZ12253801 (0, 50 or 100nM) and cells were harvested 24 hours later. Western blot analysis of whole cell lysates was performed, using β-Tubulin as the loading control. Since G2/M arrest was the main effect observed previously in Figure 4.3, G2/M checkpoint mediators Cyclin B1 and phospho-cdc2 (phospho-CDK1) were focused upon in addition to phospho-Chk1 and phospho-Chk2. Similar results were obtained in a second set of independently prepared lysates.

4.3 Investigating Whether IGF1R Signaling Affects Repair of TMZ Induced DNA Damage

A possible link between IGF1R signaling and DNA repair has previously been suggested from previous work in our group and others using radiation-induced damage. Radiosensitisation was achieved in prostate cancer cells by IGF1R depletion (Turney et al., 2012), and in lung cancer using an IGF1R inhibitor (Iwasa et al., 2009). Both these studies found that reduced IGF1R signaling attenuated HR, either in reporter assays (Turney et al., 2012) or by suppression of RAD51 focus formation (Iwasa et al., 2009). IGF1R depletion was shown to induce radiosensitization in a murine melanoma model, and implicated an effect on Atm kinase activity (Macaulay et al., 2001). With this in mind, the present study set out to investigate whether IGF1R inhibition had any effect on TMZ induced DNA damage.

4.3.1 Investigating whether IGF1R Signaling affects repair of alkylated DNA bases

TMZ methylates DNA bases on ring nitrogen atoms and extracyclic oxygen atoms producing over a dozen different alkylated bases or ‘DNA base adducts’ (Kaina et al., 2007). These base lesions vary in toxicity to the cell. Regardless, a number of repair mechanisms of varying complexity are involved in removing these alkylated base lesions. These include direct single

step repair by O^6-methylguanine–DNA methyltransferase (MGMT) which removes O^6-methylguanine (O^6MeG) adducts; and multistep pathways such as mismatch repair (MMR) and Base excision repair (BER) (Fu et al., 2012; Kaina et al., 2007). Failure to deal with alkylated base lesions could result in stalled replication forks, DSB formation and ultimately cell death (Zhang et al., 2012). Therefore the initial experiments determined whether IGF1R signaling affected MGMT expression or repair of alkylated bases.

4.3.1.1 IGF1R Signaling and MGMT

MGMT has been associated with resistance to alkylating agents such as TMZ. *In vitro* MGMT expression is regulated by promoter methylation, and is associated with methylating drug resistance (Esteller and Herman, 2004; Margison et al., 2003; Middleton et al., 1998). The results from the melanoma cell line panel in Figure 3.1 and 3.4 corroborate this.

Interestingly, MGMT was previously identified as a protein up-regulated by IGF1R depletion in breast cancer cells (J Riedemann PhD thesis 2006). To ascertain whether the same effect was induced in melanoma cells, the IGF1R was depleted using siRNA in the CHL-1 human melanoma cell line (Figure 4.5 A), using low concentrations of siRNA (10nM) in a reverse HiPerfect transfection protocol in complete medium. Similar results were also achieved using forward transfection with Oligofectamine (not shown). IGF1R depletion was achieved with a reduction in IGF1R levels to 40-50% of control levels, using two different IGF1R siRNAs. This was accompanied by 1.7 to 2-fold up-

regulation of MGMT (p=0.002 and p=0.005 using IGF1R siRNA 1 and 2 respectively, by one-way ANOVA, Figure 4.5 A and B).

Three further cell lines known to express MGMT (see Figure 3.1) SkMel28, A375 and A375M all showed modest up-regulation of MGMT protein levels with IGF1R depletion. Transfectability amongst cell lines varied, as shown by the differing siRNA concentrations required to achieve IGF1R depletion (Figure 4.5 A, C and D).

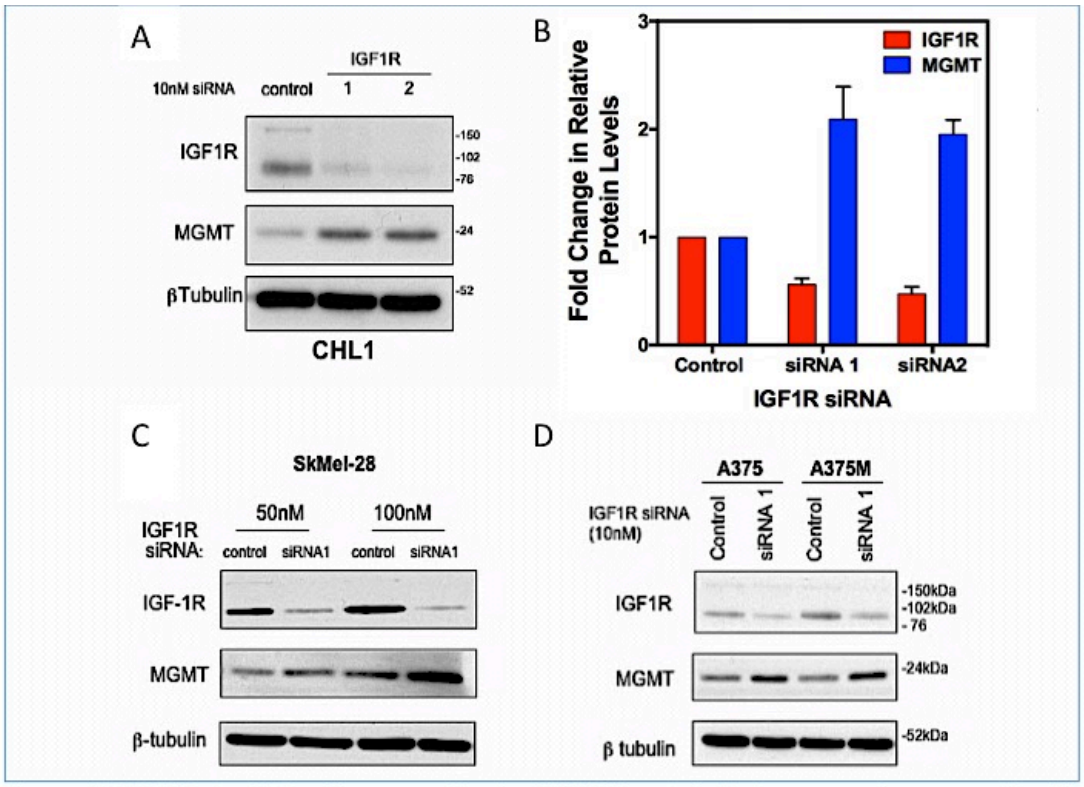


***Figure 4.5* IGF1R Depletion increases level of MGMT protein in human melanoma cells**. (**A**), CHL1 cells were transfected with two different IGF1R siRNAs or non-silencing control siRNA, and harvested after 48h. Western blot of cell lysates is shown. **B** shows quantification of 3 independent replicates of the western blot shown in A using ImageJ software. (**C**) **&** (**D**), IGF1R depletion in SkMel28, A375 and A375M was performed using the method as in A.

To assess the basis for increased MGMT protein levels, CHL-1 cells were harvested 48 hours after IGF1R depletion and RNA extracted for quantitative Real Time PCR (qRT-PCR). IGF1R depletion increased the mRNA expression of MGMT to a similar degree as that observed at the protein level in the parallel western blot (Figure 4.6). It is also noteworthy that siRNA1 increased MGMT levels by a greater amount than siRNA2, despite depleting the IGF1R to a lesser extent compared with siRNA2.

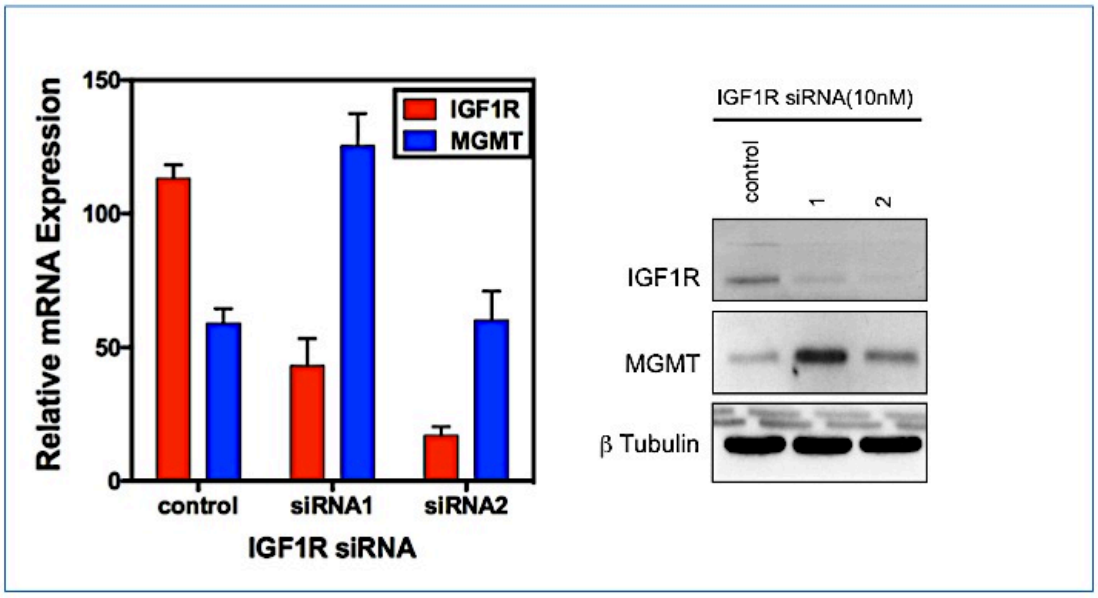


***Figure 4.6* IGF1R Depletion leads to increased MGMT mRNA expression.** CHL1 cells were transfected with two different IGF1R siRNAs or non-silencing control siRNA. Cells were harvested after 48h and the extracted RNA was analyzed by qRT-PCR and expressed relative to GAPDH mRNA expression. These results represent the mean±SEM of triplicate data points obtained from each of 2 independent experiments. Parallel cultures were lysed for western blot shown to the right.

IGF1R signalling is known to be pro-proliferative (Kurmasheva and Houghton, 2006). Increasing cell confluence in human fibroblasts has been related to methylation of the MGMT promotor, which suppresses MGMT expression (Pieper et al., 1999). It may be possible therefore that alteration in MGMT

protein levels may result from the reduction in proliferation induced by IGF1R depletion. However, in CHL-1 cells, increasing cellular confluence resulted in a clear increase in MGMT protein levels (Figure 4.7 A). This suggests that the MGMT up regulation induced by IGF1R depletion was unlikely to be due to changes in cell confluence since IGF1R depleted cells were generally less confluent than controls, as expected from the anti-proliferative effect.

At this point it appeared that IGF1R depletion was inducing upregulation of MGMT at the transcriptional level, although the discrepancy between IGF1R depletion and MGMT upregulation (Figure 4.6) raised concerns that this could be an off-target effect. Two approaches were taken to further assess the link between IGF1R and MGMT expression. Firstly, to assess whether IGF1R activation would result in reciprocal effects on MGMT levels, CHL-1 cells were treated with 50nM IGF-1 ligand. Compared with cells that had been serum starved, IGF-1 induced a reduction in MGMT protein levels over 24 hours. Phospho-AKT was used as an indicator of IGF1R axis stimulation. The reduction of total IGF1R at later time points is not unexpected given that receptor internalisation and degradation occurs following ligand treatment (Figure 4.7 C).

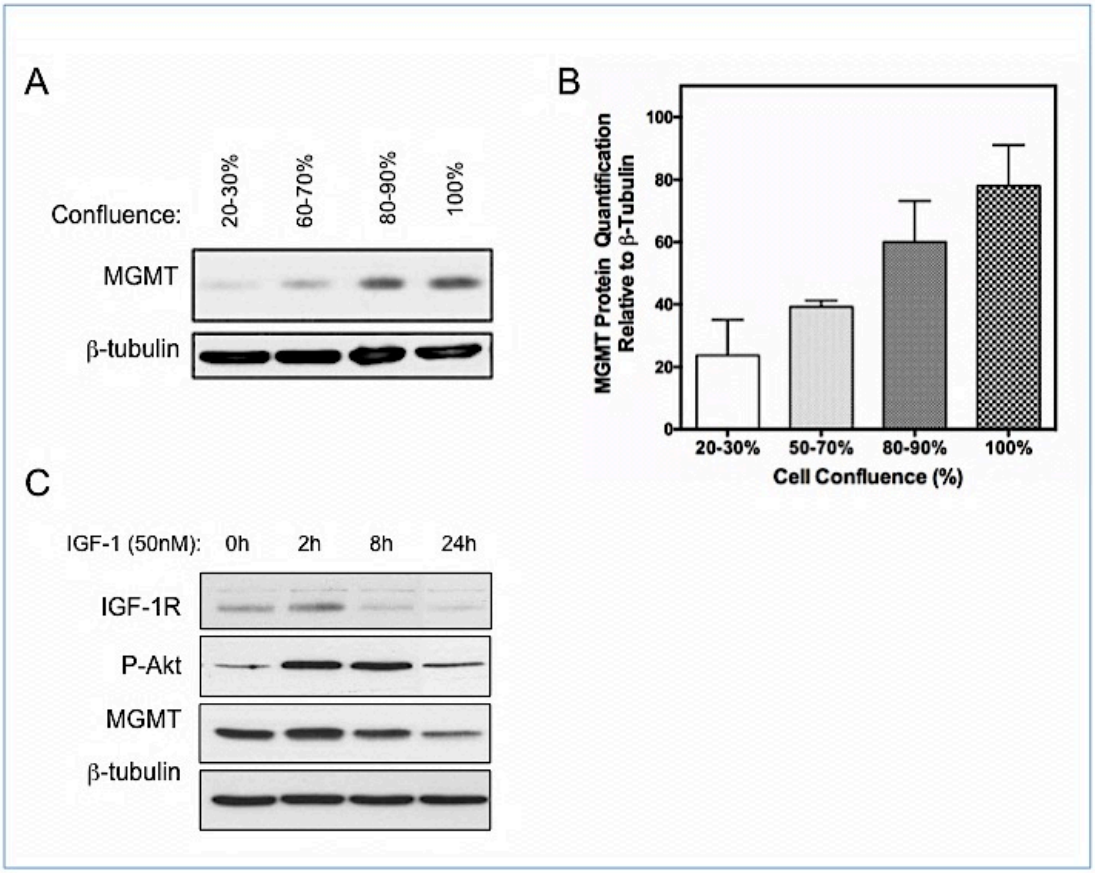


Figure 4.7 **MGMT levels increase with confluence and decrease with IGF-1 stimulation. A,** CHL1 cells were seeded and cultured in complete medium at increasing densities and harvested 48h later. Western blot of the whole cell lysates is shown. **B**, Quantification of 3 independent replicates of the western blot shown in A was performed using ImageJ software. **C**, CHL1 cells were treated with 50nM IGF-1 for 0, 2, 8 and 24h following overnight serum starvation and cell lystes analysed by western blot.

Secondly, in order to assess whether MGMT up-regulation was specifically induced by a reduction in IGF1R signalling, the selective IGF1R inhibitor, AZ12253801, was used. CHL1 cells were treated with AZ12253801 and MGMT levels assessed by western blot. IGF1R inhibition had no effect on MGMT levels (Figure 4.8), in contrast to the previous findings outlined in Figure 4.5 following IGF1R depletion. The IGF1R inhibitor was further assessed under various conditions; including comparison of treatment in

complete medium versus serum-starvation, IGF-1 stimulation and under varying degrees of confluence, but under no conditions could AZ12253801 be shown to influence MGMT levels (not shown).

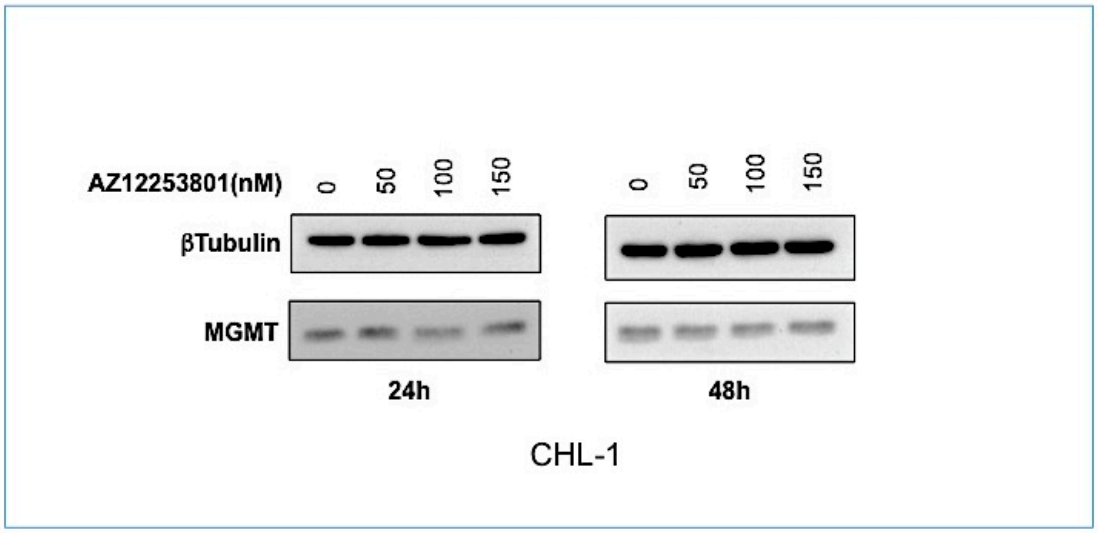


***Figure 4.8* Effect of IGF1R inhibition on MGMT levels**. In complete medium, CHL1 cells were treated with varied doses of AZ12253801 (0, 50, 100, 150nM) for 24 and 48 hours (similar duration to the IGF1R depletion performed in Figure 4.5(A). The western blot of whole cell lysates demonstrates no change in MGMT protein levels with IGF1R inhibition.

Thus, while IGF1R depletion and IGF1R activation had reciprocal effects on MGMT levels, IGF1R inhibition did not appear to influence MGMT levels.

Given the demonstration that IGF1R inhibition (Figure 3.7 B) or depletion (Yeh et al., 2006) improved TMZ induced cytotoxicity and the importance of MGMT as a significant mediator of TMZ resistance, assays were conducted to assess whether IGF1R signaling affected MGMT function.

CHL-1 cells were transfected with IGF1R or control siRNAs or treated with AZ12253801. MGMT activity was quantified by our collaborators, Amanda Watson and Geoff Margison at the Paterson Institute for Cancer Research, Manchester (Morten and Margison, 1988; Watson and Margison, 1999). The results demonstrate that IGF1R depletion (Figure 4.9 A) caused an increase in MGMT activity, which paralleled the effect on protein levels by western blot (Figure 4.5 A and B). IGF1R inhibition had no effect on MGMT activity in CHL-1 cells or in another MGMT expressing cell line, A375M (Figure 4.9 B). The MGMT substrate analogue, O6-Benzylguanine (O6BG) obliterated MGMT activity in both CHL1 and A375M cells, consistent with its known effect as an MGMT inhibitor (Dolan and Pegg, 1997). No MGMT activity was detected in SK-MEL-23 cells, which did not express MGMT on western blot (Figure 3.1). These results using O6BG in MGMT proficient cells, and the lack of activity in MGMT deficient cells support the specificity of the assay.

Our collaborators, Amanda Watson and Geoff Margison at the Paterson Institute for Cancer Research, Manchester, also assayed levels of the base lesion O^6-methylguanine (O^6MeG) that is removed by MGMT, in cells treated with TMZ alone or with AZ12253801 pretreatment (Jackson et al., 2000).

Figure 4.9 C shows that IGF1R inhibition did not significantly increase the accumulation of O^6MeG induced by TMZ treatment in MGMT-expressing CHL-1 cells, or in MGMT deficient SK-MEL-23 cells up to 100μM TMZ. AZ12253801 did seem to increase O^6MeG levels with 200μM TMZ, but this is not an IGF1R mediated effect on MGMT, given that this is an MGMT null cell line. If time had permitted, further repeats of this assay would have been preferred to clarify the significance of this apparent effect.

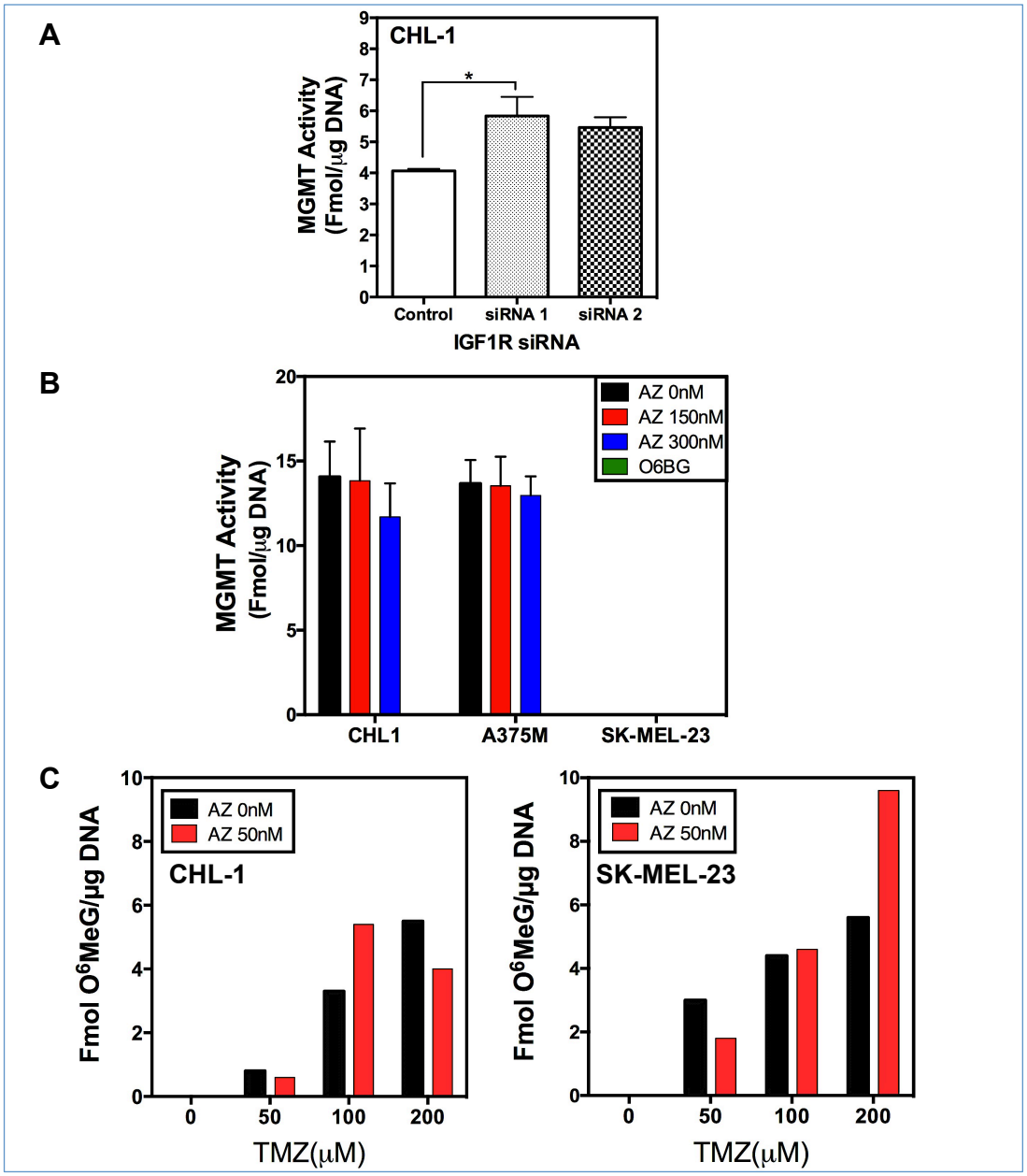


Figure 4.9. **IGF1R depletion or inhibition does not alter MGMT function**. (**A),** CHL-1 cells were transfected with IGF1R siRNA (1 & 2) or control siRNA as described in Figure 4.5(A) and harvested 48h later. (**B)** Three melanoma cell lines (CHL-1, A375M, SK-MEL-23) were each treated for 24 h with AZ12253801 (IGF1R inhibitor 'AZ' 0, 150, 300nM) in complete medium. Each cell line was also treated with MGMT inhibitor (O6BG, 10µM for 2h and washed off with PBS) prior to cell harvest. **(C)** CHL1 (MGMT expressing, left) cells and SK-MEL-23 (MGMT null, right) cells were either pretreated with 50nM of AZ12253801 or solvent (DMSO < 0.1%) for 4 hours. Each cell line was then treated with TMZ (0, 50, 100, 200µM) for 2 hours and cells harvested. Cells harvested were snap frozen and MGMT Activity assay (A and B) or O6MeG base adduct quantification assays (C) were performed by Geoff Margison and Amanda Watson at the PICR, Manchester. Results represent the mean and SEM of 3 independent experiments.

As a final test of the involvement of MGMT in IGF1R mediated TMZ sensitivity, clonogenic assays were performed to test the effects of AZ12253801 in MGMT null SK-MEL-23 cells, and in MGMT-expressing CHL-1 cells following MGMT inhibition.

TMZ treatment was carried out in the MGMT null SK-MEL-23 cell line with and without AZ12253801 in colony formation assay similar to that described in Figure 3.6 B and 3.7. SK-MEL-23 cells were more sensitive to TMZ (SF_{50} value of 28μM) compared with CHL-1 and A375M (SF_{50} values of 240μM Figure 3.7 and SF_{50} 270μM Figure 3.8 respectively), as would be expected from the difference in MGMT expression. SK-MEL-23 cells were also more sensitive to AZ12253801, and so concentrations of 75nM were used in combination with TMZ in this case. Cells treated with TMZ plus AZ12253801 showed significant reduction in colony survival compared with TMZ alone ($p = 0.004$ by one-way ANOVA). This enhanced sensitivity of IGF1R inhibited cells to TMZ cannot be explained by an effect on MGMT, because these cells are MGMT null.

Finally, colony survival assay were used to determine the effect of inhibiting MGMT function on the ability of AZ12253801 to sensitize CHL-1 cells to TMZ. In cells untreated with AZ12253801, O6BG pretreatment increased the effect of TMZ, shifting the SF_{50} from 324 to 228μM. In cells treated with 50 or 100nM AZ12253801, O6BG also enhanced TMZ sensitization, as is evident from the trend observed in the graph in Figure 4.10 B, and table 4.2, which became statistically significant at the highest concentration of TMZ ($p<0.001$ by one-way ANOVA).

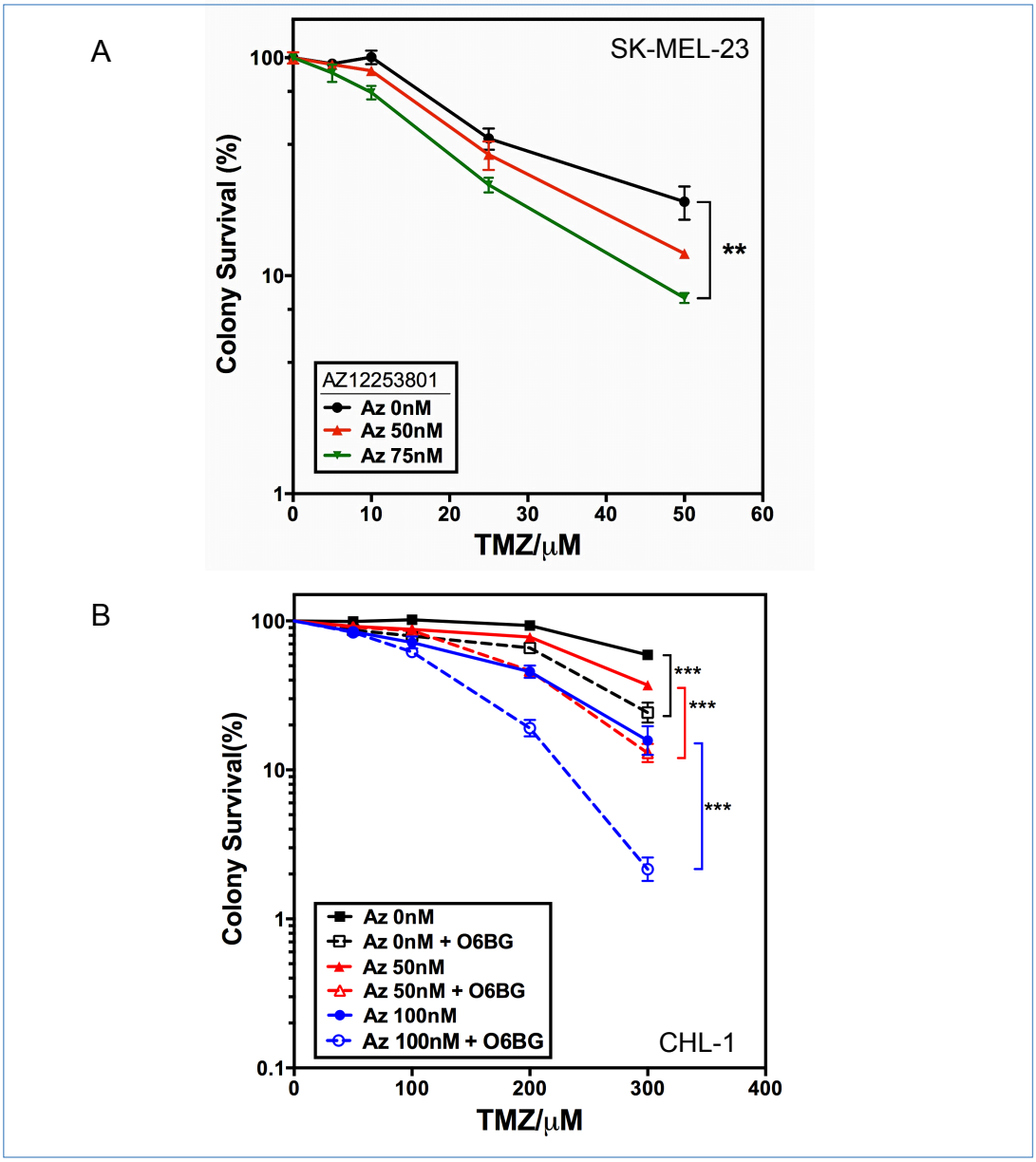


Figure 4.10 IGF1R inhibition is not epistatic with MGMT inhibition. ***A,*** SK-MEL-23 (low MGMT expressing) melanoma cells were seeded in 10cm dishes in complete medium and treated 12 hours later with TMZ (0-300μM) and either solvent (DMSO<0.1%) or AZ12253801 ('Az' 0-75nM) simultaneously. Colonies were fixed and stained 10-14 days later and counted using the Colcount colony counter. Survival fraction is expressed as a percentage of solvent treated dishes. Combination of AZ12253801 with TMZ significantly reduced colony survival compared to TMZ alone ($p = 0.004$ by one-way ANOVA) **B,** CHL-1 (MGMT-expressing) melanoma cells were grown in 10cm dishes and 12 hours later pretreated for 2 hours with 10μM O6BG or solvent (DMSO) prior to simultaneous exposure to TMZ and AZ12253801 ('Az' 0-100nM). Colonies were fixed, stained and counted after 10-14 days as above. O6BG treatment significantly reduced survival in AZ12253801 (50 or 100nM) plus high dose TMZ (300μM) combination treated cells ($p<0.001$ by one-way ANOVA).

Table 4.2 Effect of O6BG on AZ12253801 induced TMZ sensitization

- SF_{50} values derived from curve fit analysis of data in Figure 4.10 B.

AZ12253801 (nM)	O6BG (10μM)	SF_{50} for TMZ (μM)
0	-	324
0	+	228
50	-	272
50	+	194
100	-	179
100	+	124

To sum up this work that investigated a possible relationship between IGF1R signaling and MGMT, the initial observation of a modest increase in MGMT protein in IGF1R depleted breast cancer cells (J Riedemann PhD thesis 2006) was reproduced in four melanoma cell lines using two different IGF1R siRNAs, at relatively low siRNA concentrations in an attempt to minimize off-target effects (Semizarov et al., 2003). Stimulation of the IGF1R axis with IGF-1 ligand produced the opposite effect, suppressing MGMT levels. This initially suggested that IGF1R signaling may influence MGMT, however a number of findings outlined in this section argue against this. Firstly, Figure 4.5 (B) reveals that the degree of IGF1R depletion induced by two siRNAs did not correlate with the change in MGMT levels. Secondly, IGF1R inhibition did not affect MGMT levels or activity, and combining this inhibitor with TMZ did not increase O^6MeG levels. Furthermore, IGF1R inhibition was able to sensitize MGMT null cells to TMZ, and further increased sensitivity to TMZ when MGMT was inhibited in an MGMT expressing cell line. This suggests that in

the context of its effect on TMZ sensitivity, IGF1R inhibition is not in the same pathway as MGMT inhibition. These results provide suggest that the ability of IGF1R inhibition to chemosensitize melanoma cells was not due to the ability of IGF1R to influence MGMT.

4.3.1.2 Investigating the effect IGF1R signaling on Base Excision Repair

In addition to producing the most toxic lesion, O^6MeG, TMZ produces numerous other alkylated base lesions, the most common of which are N^7MeG followed by N^3MeA. N^7MeG on its own is non-toxic, but can undergo spontaneous depurination to form apurinic (AP) sites, which are toxic. The N^3MeA lesion is more cytotoxic than the N7 form since it blocks most DNA polymerases, inhibiting DNA synthesis. The Base Excision Repair (BER) pathway repairs both these lesions (Fu et al., 2012; Kaina et al., 2007).

The initial step in BER is recognition and excision of the altered base by a DNA glycosylase called 3-alkyladeinine DNA glycosylase (AAG) or alkylpurine DNA N-glycosylase. Altered AAG function can significantly impact BER and increase sensitivity to alkylating agents (Fu et al., 2012). Therefore, the initial investigation sought to determine whether IGF1R inhibition with AZ12253801 affected AAG activity. Three melanoma cell lines, CHL-1, A375M and SK-MEL-23, were pretreated for 24 hours with up to 300nM AZ12253801, and for the final 2 hours prior to cell harvest with MGMT inhibitor, O6BG. Frozen samples were kindly assayed for AAG activity by our collaborators, Amanda Watson and Geoff Margison at the Paterson Institute for Cancer Research,

Manchester (Engelward et al., 1997; Samson et al., 1991). The AAG activity assay did not demonstrate any change in AAG activity upon IGF1R inhibition in 3 melanoma cell lines (Figure 4.11 A). O6BG treatment similarly had no significant effect on AAG activity in CHL-1 and SK-MEL-23 (by one-way ANOVA).

TMZ-induced N^7MeG base adducts were also quantified, and were not found to be influenced by pretreatment with AZ12253801 in either MGMT proficient CHL-1 cells or MGMT null SK-MEL-23 cells (Figure 4.11 A). This was consistent with the lack of effect of AZ12253801 in the AAG activity assay (Figure 4.11 B).

Thus, no direct effect of IGF1R signaling on the initial stages of BER was demonstrated with these assays, although these results do not exclude an effect on the later steps of BER, that is, post removal of the alkylated base. Methyl methanesulfonate is another methylating agent, which produces greater quantities of N^7MeG and N^3MeA lesions than TMZ. Resistance to MMS therefore relies more heavily on BER function (Wyatt and Pittman, 2006). Given more time, it would have been interesting to investigate whether IGF1R inhibition affected response to MMS, to further investigate possible involvement of IGF1R signaling on overall BER function.

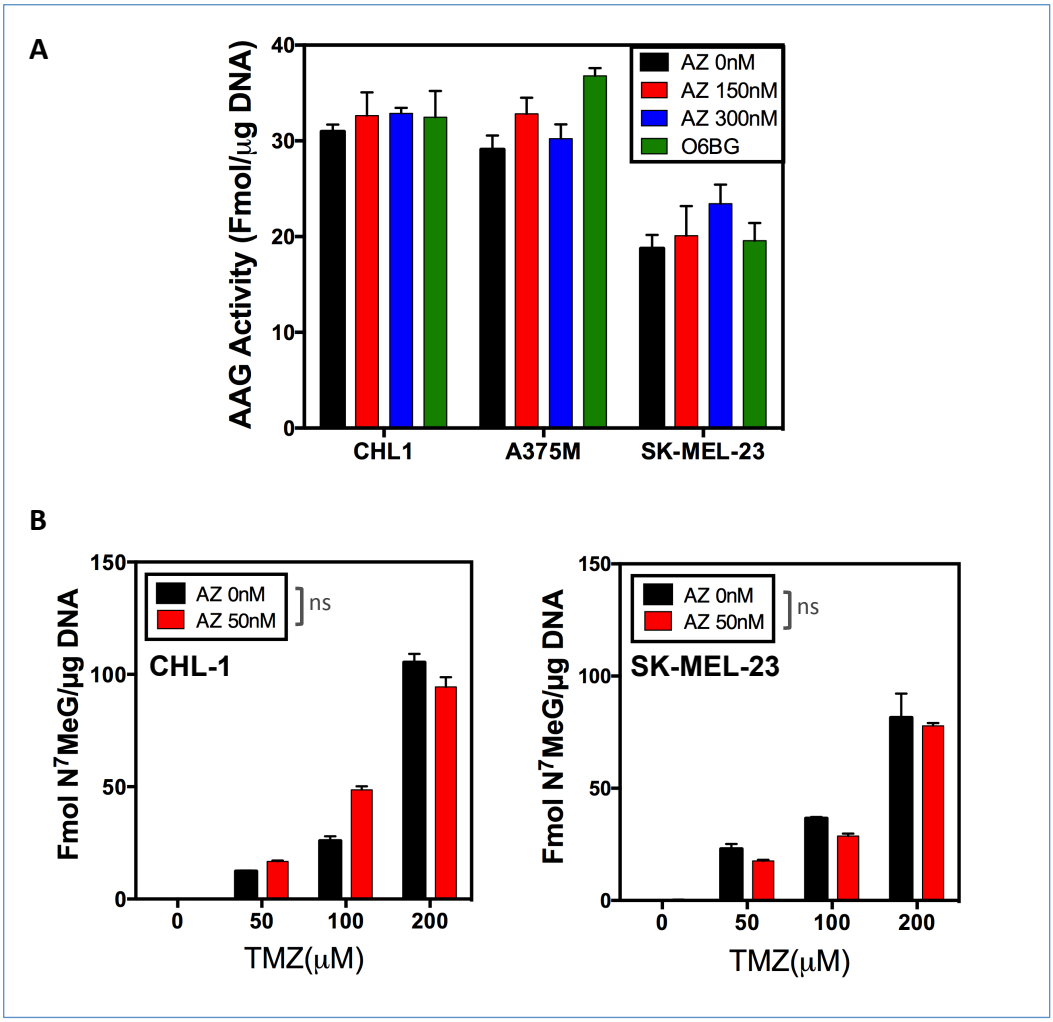


***Figure 4.11 IGF1R inhibition does not affect AAG Activity*. (A)** Three melanoma cell lines (CHL-1, A375M, SK-MEL-23) were each treated for 24 h with 3 doses of AZ12253801 (IGF1R inhibitor 'AZ' 0, 150, 300nM) in complete medium, as described in Figure 4.9(B) . Each cell line was also treated with MGMT inhibitor (O6BG, 10µM for 2h and washed off with PBS prior to cell collection). In **(B)** CHL1 (MGMT expressing, left) cells and SK-MEL-23 (low MGMT expressing, right) cells were either pretreated with 50nM of AZ12253801 or solvent (DMSO) for 4 hours. Each cell line was then treated with TMZ (0, 50, 100, 200µM) for 2 hours and cells harvested. Cells harvested from A and B were snap frozen and AAG Activity assay (A) or N^7MeG base adduct quantification assays (B) kindly performed by Geoff Margison et al at the PICR, Manchester. Results represent the mean and SEM of 3 independent experiments.

4.3.2 Investigating Whether IGF1R inhibition Affects TMZ induced Double Strand Break Formation

The results thus far have indicated that IGF1R signaling does not influence the repair of DNA base adducts. Altered bases themselves or their processing can lead to the formation of replication dependent double strand breaks (DSBs), which are extremely cytotoxic (Hartlerode and Scully, 2009). Examining the induction and repair of this lethal lesion might therefore provide insight into the mechanism of enhanced cytotoxicity encountered when IGF1R inhibition is combined with TMZ.

4.3.2.1 Investigating the effect of IGF1R Inhibition on TMZ induced Gamma-H2AX Focus formation

Within minutes of DSB formation, the histone protein H2AX is phosphorylated at serine-139 by one of three members of the PI3K-like kinase family of proteins, ATM, ATR and DNA-PK to form γ-H2AX. Ser-139 phosphorylation of γ-H2AX continues until a focus of several hundred γ-H2AX molecules forms around each DSB. Such foci can be readily detected by immunofluorescence, and the number of γ-H2AX foci closely correlates with the number of DSBs, and their resolution correlates with DSB repair (Bonner et al., 2008; Svetlova et al., 2010). Therefore evaluation of the induction and resolution of γ-H2AX foci by immunofluorescence may indicate whether IGF1R signaling influences repair of TMZ-induced DSBs.

Figure 4.12 A and B show that γH2AX foci emerged within 12 hours of TMZ treatment, peaked 24 hours post treatment and thereafter, γ-H2AX foci resolved by 48 hours to pre treatment levels, remaining at low levels till the end of the time course at 72 hours. The addition of an IGF1R inhibitor did not appear to alter the induction or resolution of TMZ induced γ-H2AX foci. Dense γH2AX staining has been described in early apoptosis, not necessarily related to DSB formation. The pattern of γ-H2AX staining associated with apoptosis has typically been described as peripheral nuclear or pan-nuclear staining (Bonner et al., 2008; Xie et al., 2007). In order to verify that the dense focal γ-H2AX staining (Figure 4.12 A) was attributed to DSB formation, another mediator downstream of γ-H2AX in the DDR was imaged by immunofluorescence microscopy.

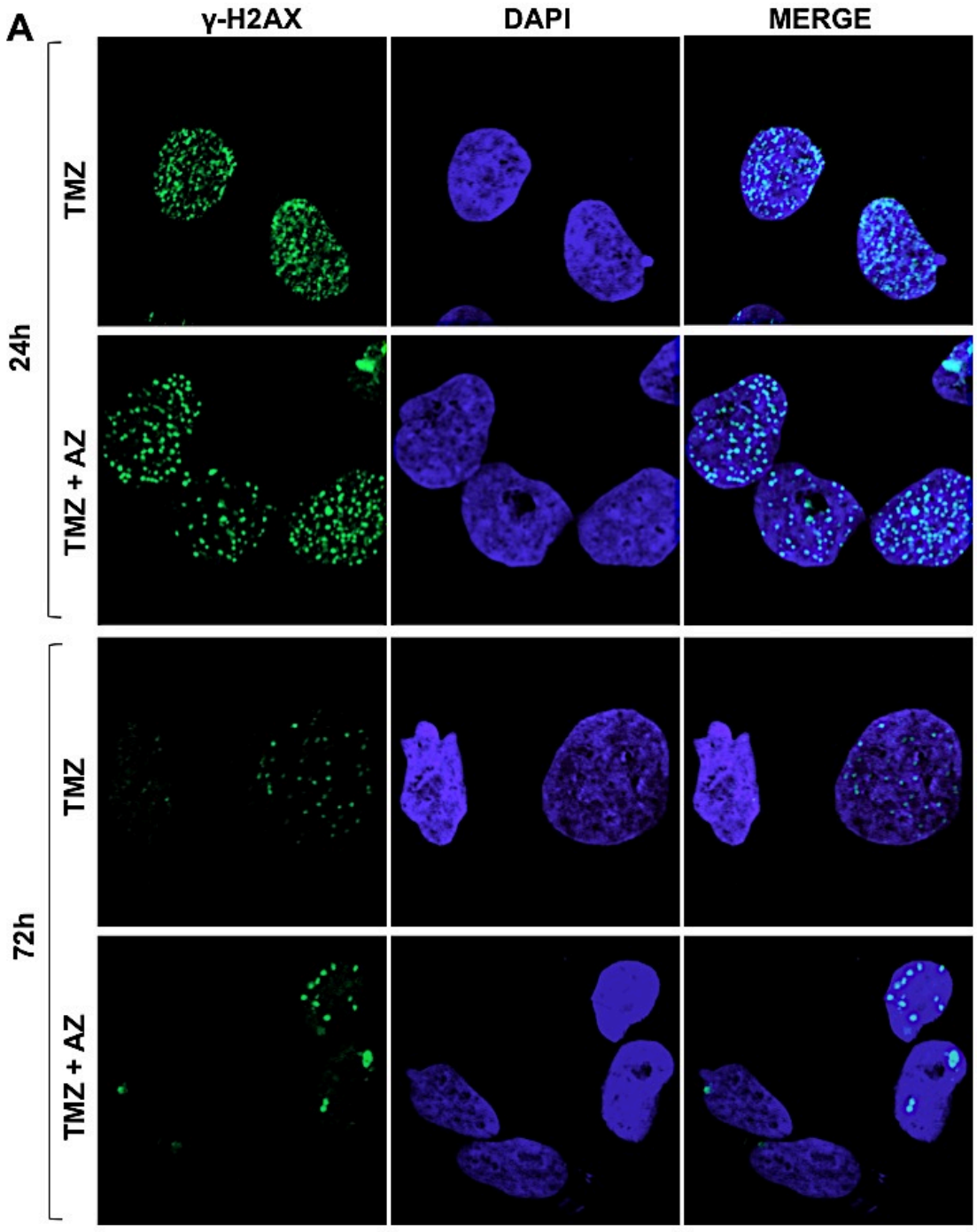


Figure 4.12 (A) Effect of IGF1R inhibition on formation of TMZ induced γ-H2AX foci. CHL1 cells were treated with TMZ, with or without 100nM AZ12253801(AZ) for up to 72 hours and fixed and stained with γ-H2AX antibody (green) and DAPI (blue) to visualize DNA. γ-immunofluorescence staining for 24 and 72 hour treatments are shown demonstrating similar numbers of TMZ induced γ-H2AX foci with or without the addition of AZ12253801.

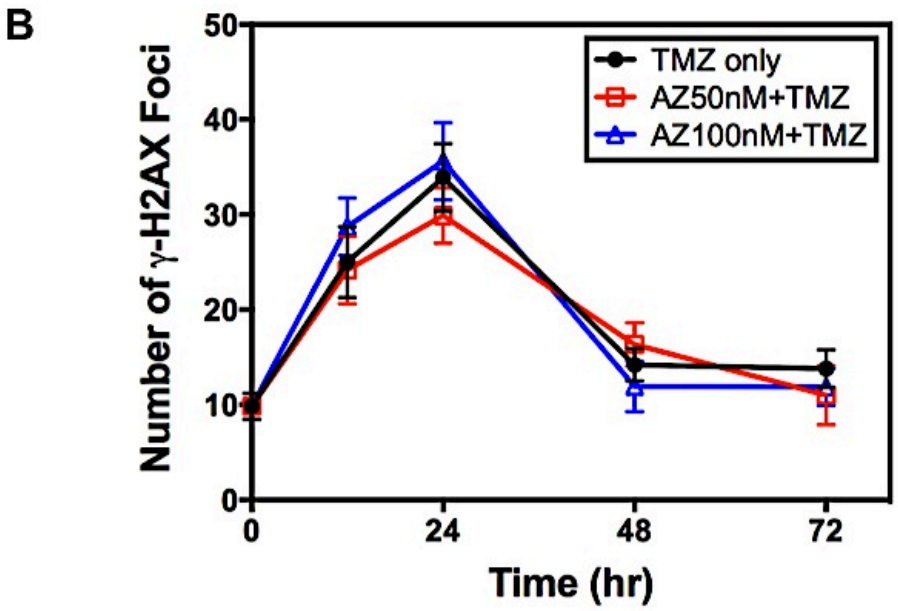


Figure 4.12 (B) Effect of IGF1R inhibition on TMZ induced γ-H2AX foci. CHL1 cells were cultured on cover slips and treated with TMZ (300μM), with or without AZ12253801 (0, 50, 100nM) and fixed after 12h, 24h, 48, and 72h. Staining with anti-γ-H2AX antibody and DAPI to visualize DNA was performed and immunofluorescence microscopy used to obtain images of at least 30 cells per treatment. The γ-H2AX foci were imaged and counted. Graph shows mean and SEM of γ-H2AX foci per cell of two independent experiments.

4.3.2.2 Investigating the effect of IGF1R Inhibition on TMZ induced 53BP1 Focus formation

Immunofluorescent staining for a mediator downstream of γ-H2AX in the DDR was performed to check whether the γ-H2AX immunostaining encountered in Figure 4.12(A) was related to DSB formation and not related to increased apoptosis described in Figure 4.1. MDC1 (mediator of DNA damage checkpoint protein 1) binds to γ-H2AX at DSB sites within minutes of DNA damage and this interaction facilitates the aggregation of other important DNA repair mediators (Stewart et al., 2003; Stucki et al., 2005). MDC1, however, can be cleaved by activated caspase-3 in the apoptotic response, shown to be important for the inactivation of the DNA damage response in apoptosis (Solier and Pommier, 2011). It was thought possible therefore that MDC1 levels could be affected by the pro-apoptotic effect of AZ12253801, in the absence of DNA damage. Instead, immunofluorescent staining of one of the mediators assembled as a result of the γ-H2AX/MDC1 interaction, 53BP1 (Escribano-Diaz et al., 2013; Lottersberger et al., 2013), was preferred to further elucidate whether IGF1R signaling influenced the response to TMZ-induced DSBs.

Figure 4.13 (A&B) shows that TMZ caused accumulation of 53BP1 foci in a pattern similar to that seen with γ-H2AX. Foci were induced within the first 12 hours of treatment, peaking at 24 hours and reducing to pretreatment levels from 48 hours. The effect of AZ12253801 on TMZ induced 53BP1 focus formation however, revealed a slightly different pattern. Though the induction

and resolution of TMZ induced 53BP1 foci was similar in cells treated with AZ12253801, the maximum number such foci appeared to be reduced with increasing IGF1R inhibition. This dose-dependent reduction in TMZ induced 53BP1 focus formation became statistically significant at 24 hours with the addition of 100nM AZ12253801 compared with TMZ treatment alone ($p=0.047$ by one-way ANOVA).

In contrast, Figure 4.12 had shown no difference in γ-H2AX in IGF1R-inhibited cells. This disparity may suggest that not all γ-H2AX foci were due to DSBs, and/or may reflect difference in accumulation of these DDR mediators during the cell cycle.

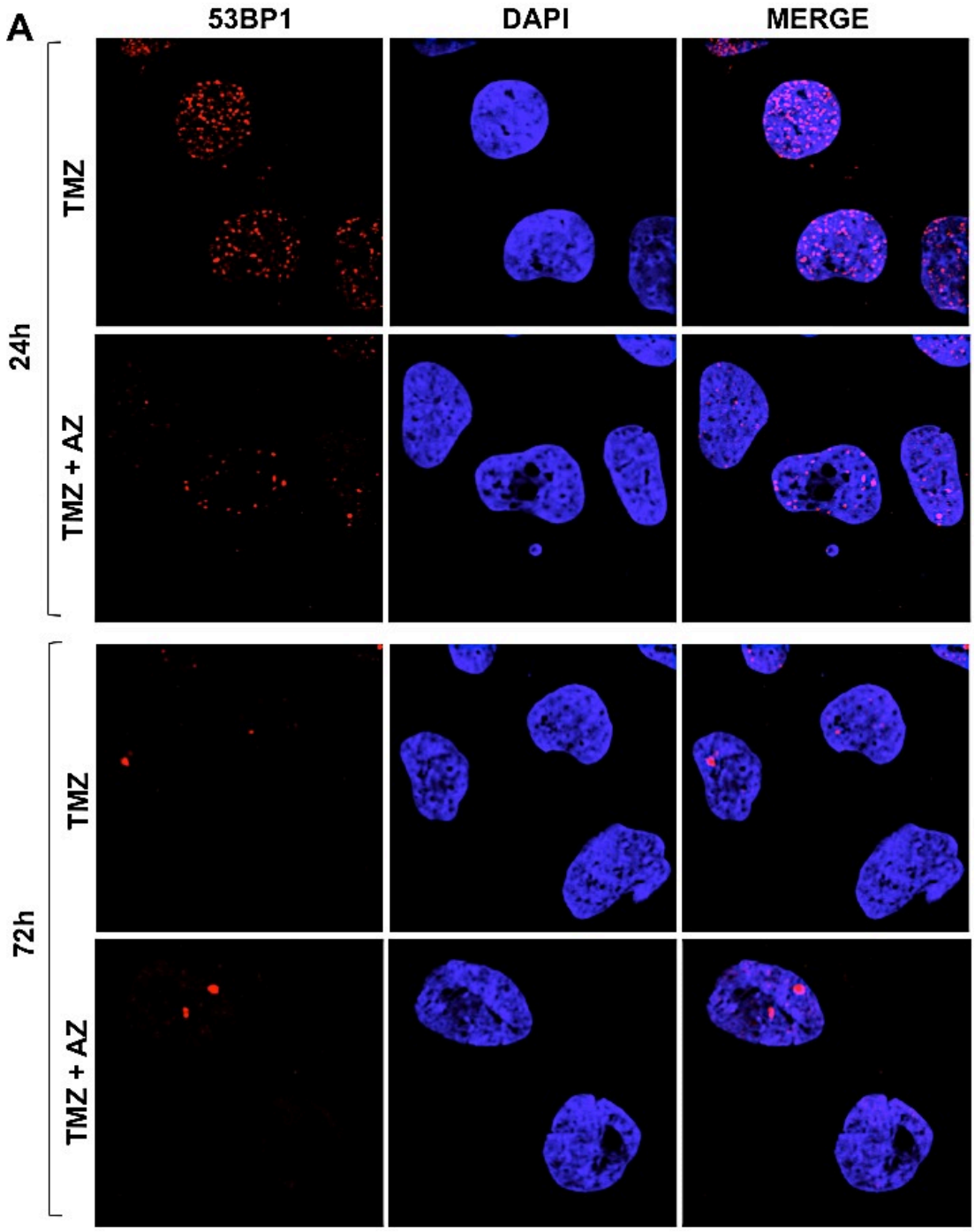


Figure 4.13 (A) Effect of IGF1R inhibition on formation of TMZ induced 53BP1 foci. CHL1 cells were treated with TMZ, with or without 100nM AZ12253801(AZ) for up to 72 hours and fixed and stained with 53BP1 antibody (red) and DAPI (blue) to visualize DNA. 53BP1 immunofluorescence staining for 24 and 72 hour TMZ treatments with and without AZ12253801 are shown here. The quantity of 53BP1 foci appears to be reduced when AZ12253801 is combined with TMZ, compared with that of TMZ alone, for the 24 hour treatment

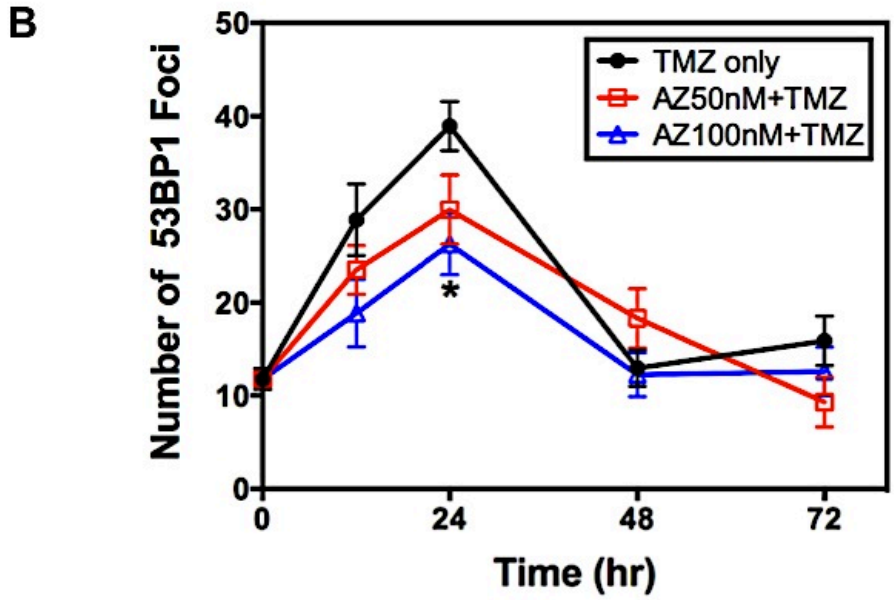


Figure 4.13 (B) Effect of IGF1R inhibition on TMZ induced 53BP1 foci. CHL1 cells were cultured on cover slips and treated with TMZ (300μM), with or without AZ12253801 (0, 50, 100nM), fixed after 12h, 24h, 48, and 72h. Stained with anti-53BP1 antibody and DAPI. Immunofluorescence microscopy was performed to obtain images of at least 30 cells per treatment. 53BP1 foci were counted and analyzed using ImageJ software and statistical analysis performed with GraphPad Prism 6 software. Graph shows mean and SEM of 53BP1 foci per cell of a single experiment. Combining TMZ with 100nM AZ12253801 significantly reduced 53BP1 focus formation compared with TMZ alone at 24 hours ($p = 0.047$ by one-way ANOVA).

While γ-H2AX accumulate at DSBs during any phase of the cell cycle (Banath and Olive, 2003), 53BP1 foci do not assemble in the G2/M phase (Escribano-Diaz et al., 2013; Nakamura et al., 2010).

Consistent with this, Figure 4.3 showed that adding 100nM AZ12253801 to TMZ increased accumulation of cells in G2/M at 24 hours, compared with TMZ alone. DNA damage foci in this phase of the cell cycle may not therefore be identified by immunofluorescent staining for 53BP1. Therefore, the next step was to utilize another marker of DNA damage that shows DNA damage foci in cells in G2 phase.

4.3.2.3 Investigating the effect of IGF1R Inhibition on TMZ induced RPA Focus formation

Since 53BP1 does not accumulate at DSB sites in G2/M, a mediator involved in DNA repair during this phase of the cell cycle was evaluated, focusing on proteins involved in HR. The lack of effect of IGF1R inhibition on TMZ induced γ-H2AX foci (Figure 4.12) suggests that IGF1R signaling may have no overall effect on DSB repair during the 72-hour treatment. Though DSBs are important factors in alkylating agent cytotoxicity, another important and more abundant lesion may be DNA single strand breaks (SSBs). Following alkylating DNA damage, SSBs may arise as normal intermediates of nucleotide excision repair (NER) and base excision repair (BER) (Pascucci et al., 2005). Replication protein A (RPA) has been implicated in both these DNA repair pathways. RPA participates in gap filling during NER and is involved in the later stages of long patch BER (Balajee and Geard, 2004). The earlier assessment of AAG activity showed no effect of IGF1R inhibition (Figure 4.11), but this did not rule out an effect on the later stages of BER. RPA also plays an important role in DSB repair by participating in Homologous Recombination (HR), forming foci predominantly in S, G2 or M (Robison et al., 2007). RPA is therefore an important mediator involved in both SSB and DSB repair (Oakley and Patrick, 2010).

Therefore, the effect of IGF1R inhibition on TMZ induced RPA focus formation was examined by immunofluorescence microscopy (Figure 4.14) using a 72-hour time course of combination treatment of 300μM TMZ or solvent, alone or with AZ12253801 in CHL1 cells. TMZ-treated cells showed a progressive rise

in the number of RPA foci, reaching a maximum at 48 hours. By 72 hours the number of RPA foci reduced by half, almost approaching pretreatment levels (Figure 4.14 B). The addition of IGF1R inhibition resulted in a dose-dependent rise in the number of RPA foci. This was statistically significant in cells treated with 100nM AZ12253801 for the 12h, 24h and 72 hours ($p = 0.0042$, $p = 0.0064$ and $p = 0.047$ respectively by one-way ANOVA). It is also noteworthy that the combination treatment achieved a peak in the number of RPA foci 24 hours earlier than in cells treated with TMZ alone, with a plateau at 48 hours, after which a reduction occurred, although the rate of resolution of RPA foci appeared slower in cells treated with TMZ plus 100nM AZ12253801 (Figure 4.14 B).

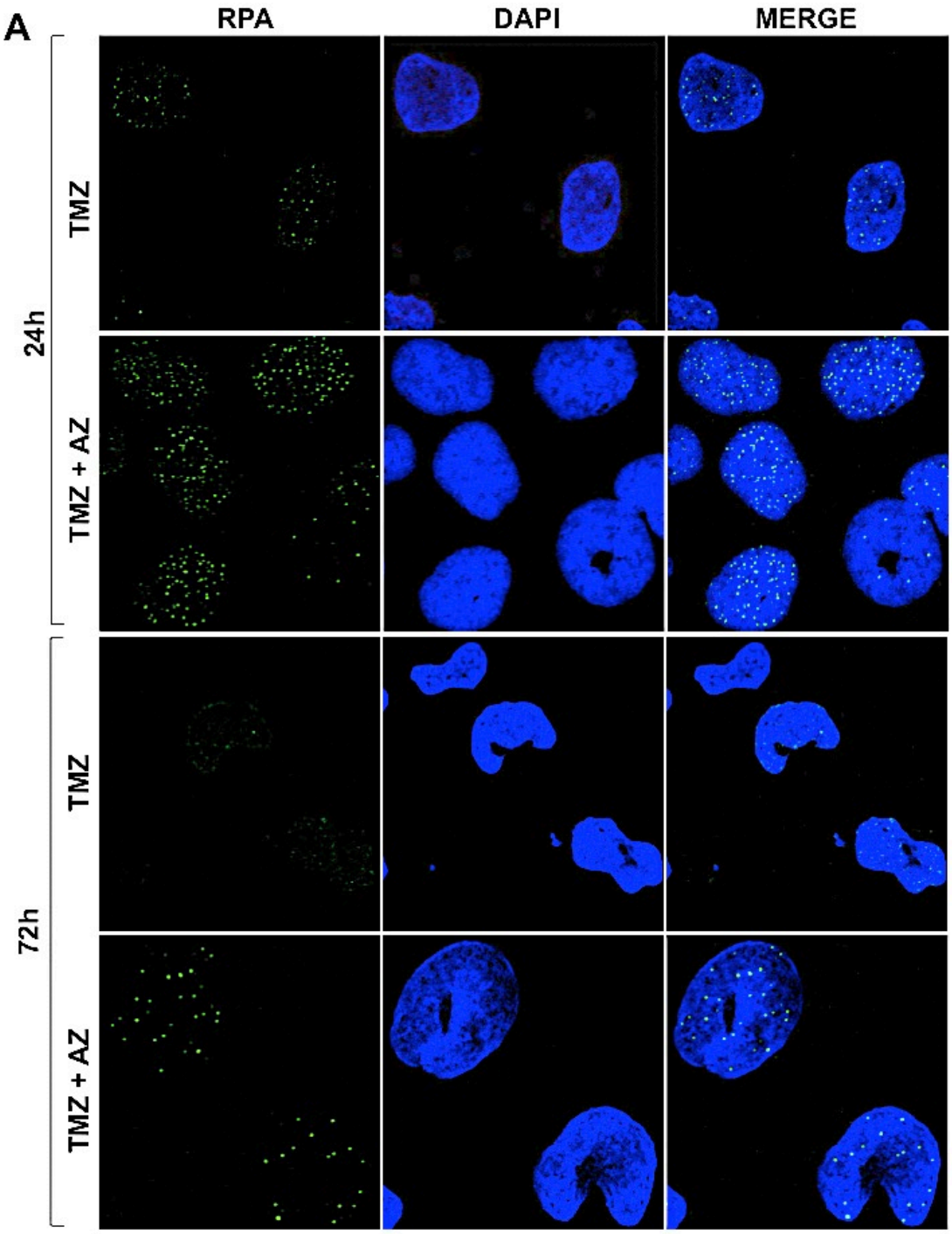


Figure 4.14 (A) IGF1R inhibition increased TMZ induced RPA foci. CHL1 cells were cultured on cover slips and treated with TMZ, with or without 100nM AZ12253801 (AZ) for up to 72 hours and fixed and stained with anti-RPA2 antibody (green) and DAPI to visualize DNA. Immunofluorescence microscopy revealed that AZ12253801 treatment led to an increase in TMZ induced RPA foci (24 and 72 hour time points are shown here).

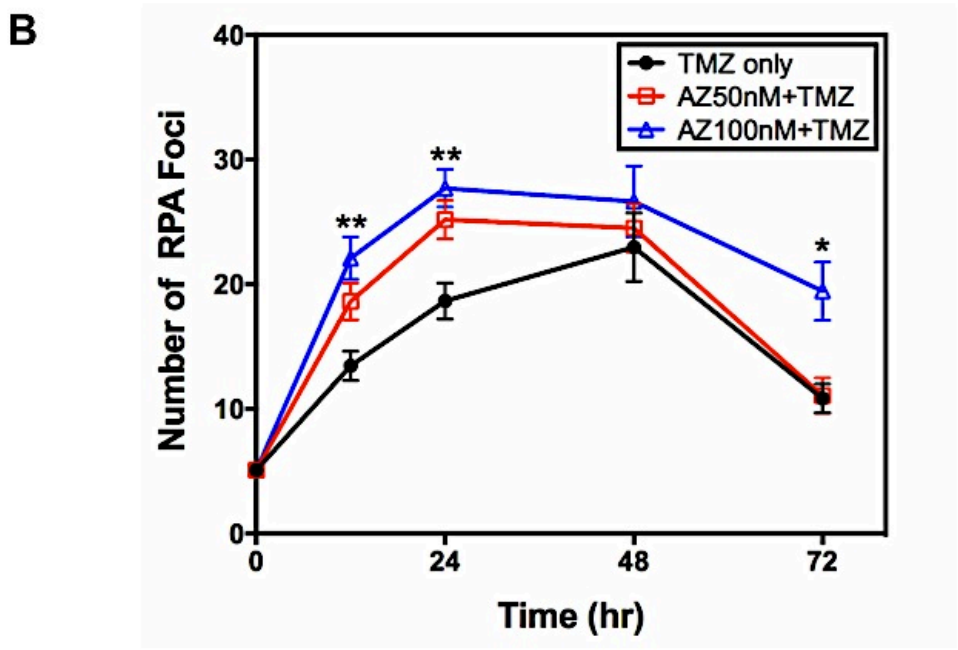


Figure 4.14 (B) IGF1R inhibition increased TMZ induced RPA foci. CHL1 cells were cultured on cover slips and treated with TMZ (300μM), with or without AZ12253801 (0, 50, 100nM) and fixed after 12h, 24h, 48, and 72h. Staining with anti-RPA2 antibody and DAPI to visualize DNA was performed and immunoflourescence microscopy was used to obtain images of at least 50 cells per treatment. RPA foci were counted and analyzed using ImageJ software and statistical analysis performed with GraphPad Prism 6 software. Graph shows mean and SEM of RPA foci per cell of a single experiment. Combining TMZ with 100nM AZ12253801 significantly increased RPA foci formation compared with TMZ alone at 12h, 24h and 72 hours ($p = 0.0042$, $p = 0.0064$ and $p = 0.047$ by one-way ANOVA).

This alteration in RPA focus formation was an interesting finding but is difficult to interpret given the many functions of RPA, which include not only SSB and DSB repair, but also checkpoint activation in response to DNA damage and DNA replication (Oakley and Patrick, 2010; Zou et al., 2006)

If the increase in RPA foci marked an accumulation of stalled replication forks, this would be expected to induce an intra-S checkpoint (Branzei and Foiani, 2005), but in fact cell cycle analysis (Figure 4.3) showed reduction in S phase fraction (Segurado and Tercero, 2009).

If the increase in RPA foci was due to accumulation of unrepaired SSBs, this might also be expected to activate the S phase checkpoint. With no clear evidence that IGF1R inhibition impaired the handling of common TMZ-induced base lesions, SSBs or stalled replication forks, the eventual and most lethal post-replicative outcome of DNA alkylation, would be DSB formation. Since the AZ12253801-TMZ combination was shown to cause G2/M arrest (Figure 4.3) the next experiments measured formation of RAD51, a major mediator of DSB repair when a homologous template is available in G2. This strategy was also chosen since RPA and RAD51 are known to interact at an early stage of homologous recombination DSB repair (Krejci et al., 2012).

4.3.2.4 Investigating the effect of IGF1R Inhibition on TMZ induced RAD51 Focus formation

In addition to repair of DSBs in S and G2 phases of the cell cycle, the homologous recombination repair (HRR) machinery also plays an important role processing collapsed replication forks, which if not repaired would lead to toxic DSBs (Kondo et al., 2010). Since RPA is known to interact with the recombinase, RAD51 (Krejci et al., 2012), the next logical question was therefore whether the dose dependent increase in TMZ induced RPA foci in IGF1R inhibited cells (Figure 4.14) was accompanied by any change in the induction or resolution of RAD51 foci.

Therefore, CHL-1 cells were treated with 300μM TMZ, with or without AZ12253801 (0, 50 or 100nM) for a 72-hour time course. Figure 4.15(A) shows examples of cells exhibiting RAD51 foci after 48 and 72 hour

treatment. The quantification of RAD51 foci for the full time course (0, 12h, 24h, 48h and 72h) is displayed in Figure 4.15(B). Cells treated with TMZ alone showed progressive induction of RAD51 foci after 12 hours of treatment, peaking at 48 hours, followed by a rapid decline to near pre treatment numbers of RAD51 foci at 72 hours. Therefore, the kinetics of RAD51 focus formation after TMZ treatment was different with respect to the appearance of foci and time to achieve peak number of foci, compared with the other DNA damage markers tested. For example, RPA foci began to accumulate within 12 hours of TMZ treatment (Figure 4.14), whereas RAD51 foci did so after 12-24 hours. The possible explanation for this may be related to the need for at least two rounds of replication to cause DSB formation as a consequence of O^6MeG-T mispairing and persistence in MMR proficient cells (Kaina et al., 2007). With a doubling time of approximately 12 hours for CHL-1 cells, this apparent delay in emergence of RAD51 foci may represent the onset of post replicative DSB formation. In addition, early in HRR, DNA strand resection at DSBs produces 3' overhangs of ssDNA, to which RPA binds with much greater affinity than RAD51 (Oakley and Patrick, 2010), and RAD51 cannot bind the overhang until RPA is released (Krejci et al., 2012). This may explain the delay in appearance of RAD51 foci with respect to that of RPA. Similar sequential recruitment of RPA and other HR machinery occurs at stalled replication forks. Shortly after such stalling, the exposed ssDNA at the replication fork is coated by RPA, and there is evidence that RAD51 binds only after the release of RPA (Branzei and Foiani, 2007; Costanzo, 2011).

It was noted that the onset of RAD51 foci (Figure 4.15) did not coincide with that for γ-H2AX or 53BP1 foci (Figures 4.12 and 4.13 respectively) in response to TMZ alone treatment. Also the peak of γ-H2AX and 53BP1 focus formation was at 24 hours, compared with RPA and RAD51, which peaked at 48 hours of TMZ treatment. Therefore it is possible that the emergence of early γ-H2AX and 53BP1 foci may not represent DSBs. Experimental evidence suggests that γ-H2AX aggregates and spreads from stalled replication forks,in response to another DNA damaging agent, hydroxyurea (HU) (Sengupta et al., 2004; Sirbu et al., 2011). Alternatively, others have shown that γ-H2AX and 53BP1 can bind to ssDNA produced as an intermediate during NER, although unlike DSB recognition, 53BP1 binding occurred independently of γ-H2AX (Stiff et al., 2008).

Examining the effect of IGF1R inhibition on TMZ induced RAD51 focus formation (Figure 4.15 B), no significant difference was observed up to 48 hours from the start of treatment. However, beyond 48 hours, IGF1R inhibition caused clear dose-dependent persistence of TMZ induced RAD51 foci. At 72 hours, there were more TMZ-induced RAD51 foci in cells treated with 50 or 100nM AZ12253801 ($p = 0.036$ and $p<0.0001$ respectively compared with controls), and focus numbers were also significantly greater in cells treated with 100nM AZ12253801 than 50nM ($p< 0.0001$ by one-way ANOVA).

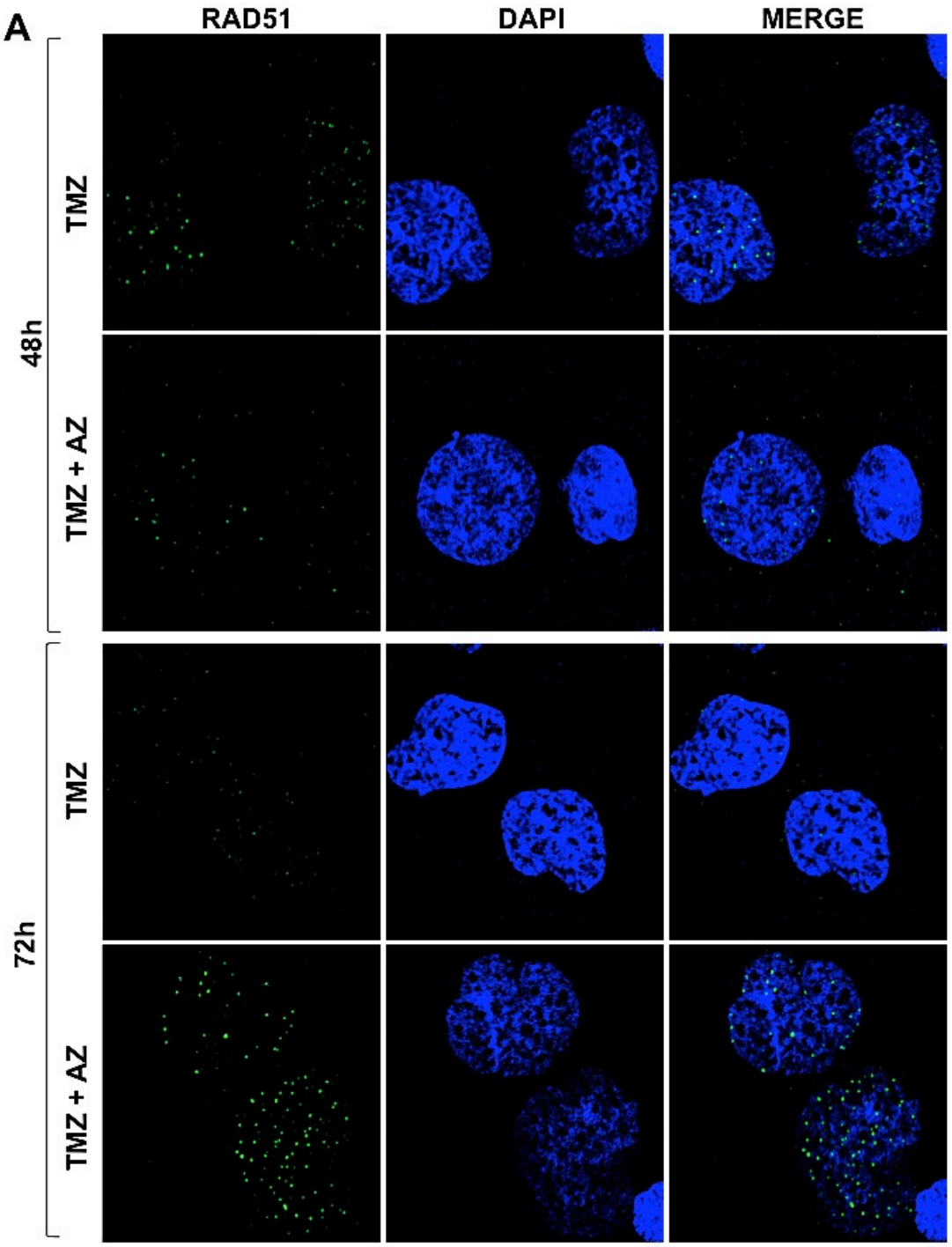


Figure 4.15 (A) IGF1R inhibition causes persistence of TMZ induced RAD51 foci. CHL1 cells were treated with TMZ, with or without 100nM AZ12253801 (AZ) for up to 72 hours and fixed and stained with RAD51 antibody (green) and DAPI to visualize DNA. RAD51 immunofluorescence staining for 48 and 72 hour TMZ treatments with and without AZ12253801 are shown here. This demonstrated that after 72 hours, RAD51 foci were decreasing in the TMZ only group, and persisting or increasing in IGF1R-inhibited cells.

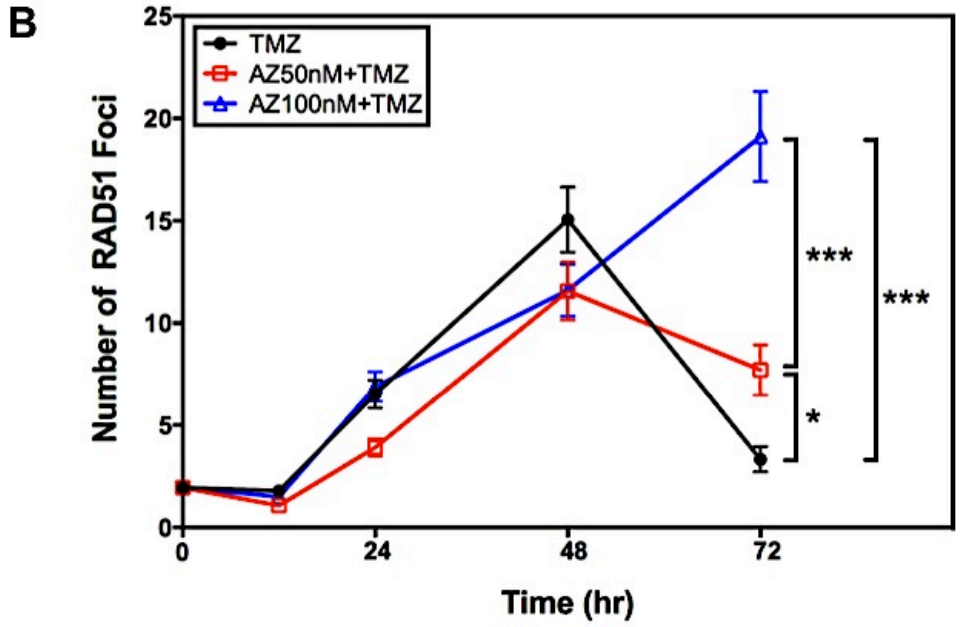


Figure 4.15 (B) IGF1R inhibition causes persistence of TMZ induced RAD51 foci. CHL1 cells were cultured on cover slips and treated with TMZ (300μM) alone or with AZ12253801 (0, 50, 100nM) and fixed after 12h, 24h, 48, and 72h. Staining with anti-RAD51 antibody was performed and immunofluorescence microscopy was used to obtain images of at least 50 cells per treatment. RAD51 foci were counted and analyzed using ImageJ software and statistical analysis performed with GraphPad Prism 6 software. Graph shows mean and SEM of RAD51 foci per cell, with similar results observed in a second experiment. After 72 hours, significantly more RAD51 foci persisted in IGF1R-inhibited cells compared with TMZ only treated cells (TMZ vs AZ50nM+TMZ, p= 0.036; AZ50nM+TMZ vs AZ100nM+TMZ, p <0.0001; TMZ vs AZ100nM+TMZ, p < 0.0001 by one-way ANOVA).

Broadly, there are two possible explanations for the dose-dependent persistence of TMZ induced RAD51 foci in IGF1R inhibited cells. These are: delayed RAD51 loading onto DNA lesions or failure of RAD51 disassembly late in HR.

Examining the overall trend of the plots in Figure 4.15 B, the addition of IGF1R inhibition appeared to reduce the rate of TMZ induced RAD51 focus formation, achieving a similar number of foci after 48 hours in cells treated with 100nM AZ12253801 compared with TMZ alone. Furthermore, there was a trend to reduced numbers of RAD51 foci at 24 to 48 hours in IGF1R inhibited cells (Figure 4.15). As stated above, RAD51 recruitment to either

stalled replication forks or DSBs cannot occur until RPA is released from these lesions.

It is therefore possible that RAD51 loading may be delayed, for example by increased RPA binding affinity. RPA is a heterotrimeric protein comprising subunits RPA1, RPA2 and RPA3. RPA binds to ssDNA with high affinity, and its ssDNA binding affinity can be varied by conformational changes, induced by protein-protein interactions and post-translational modification (Fan and Pavletich, 2012). Evidence suggests that RPA binding to ssDNA stimulates recruitment and binding of ATR-interacting protein ATRIP to the N-terminal domain of RPA1. ATRIP then binds to and activates ATR (Nam and Cortez, 2011), thereby allowing ATR to phosphorylate the N-terminal domain of RPA2. This alters the conformation of the RPA1 subunit to the low affinity mode, reducing ssDNA contact with its DNA binding domain (Oakley and Patrick, 2010). It is possible therefore, that IGF1R inhibition could suppress RPA2 phosphorylation which would cause RPA to remain in its high affinity ssDNA binding state, potentially explaining the delay in RAD51 binding (Figure 4.15). If more time was permitted, this hypothesis would have been tested using antibodies to phosphorylated RPA2.

An alternative explanation for the altered time course of RAD51 foci resolution in IGF1R-inhibited cells (Figure 4.15) is that this may reflect reduced RAD51 filament disassembly. BRCA2 and RAD54 act in concert with RAD51, regulating its function and playing important roles in RAD51 dissociation from DNA lesions. The binding of BRCA2 to the C-terminal domain RAD51 promotes RAD51 binding to ssDNA binding and inhibits RAD51 ATPase, which would otherwise hydrolyse ATP required for RAD51 dissociation. This

binding of RAD51 to the C-terminal domain of BRCA2 is under cell cycle control. Under normal conditions, CDKs are in their active, dephosphorylated form, promoting cell cycle progression. Active CDKs phosphorylate BRCA2 within its C-terminal domain at Ser-3291, thus inhibiting RAD51 binding and preventing HR from occurring. In the presence of DNA damage or replicative stress, ATM or ATR activate Chk1/Chk2, which phosphorylate and inactivate cdc25, a phosphatase that normally keeps CDKs in an active, dephosphorylated state required for normal cell cycle progression. In the presence of ATM/ATR activation, however, CDKs are phosphorylated and inactivated causing cell cycle arrest, and reducing BRCA2 Ser-3291 phosphorylation (Esashi et al., 2005). This allows persistence of the interaction between RAD51 and BRCA2, inhibiting filament disassembly and stabilising replication forks (Holloman, 2011; Lord and Ashworth, 2007). It was notable that combining IGF1R inhibition with TMZ resulted in both G2/M arrest (Figure 4.3) and impaired RAD51 focus resolution (Figure 4.15), which may reflect the close interaction between HR and cell cycle control (Esashi et al., 2005). Given more time, it would have been interesting to test whether IGF1R inhibition affected the interaction of RAD51 with BRCA2.

RAD54 is another important mediator of RAD51 function and filament assembly. The presence of RAD54 facilitates the timely recruitment of RAD51 and BRCA2 to DSBs and the RAD51-RAD54 interaction is said to stabilize the RAD51 filament (Agarwal et al., 2011). RAD51 can remain associated with the dsDNA heteroduplex product of strand exchange until it is displaced by RAD54, thus allowing freed RAD51 to associate with another DSB (Agarwal et al., 2011; Krejci et al., 2012). It is possible that altered RAD51-RAD54

interaction may explain the persistence of RAD51 at the 72-hour time point (Figure 4.15), and this could even occur in the absence of other markers of DSB formation, such as 53BP1 or γH2AX.

4.3.2.5 Investigating the effect of IGF1R Inhibition on Chromatin bound DNA repair mediators

To complement the immunofluorescence data in the previous section, attempts were made to assess the effects of IGF1R inhibition on the binding of DNA repair proteins to chromatin. Initial experiments used western blot analysis of whole cell lysates produced from CHL-1 cells harvested 24 and 48 hours post combination treatment with TMZ (0 to 300μM) and/or AZ12253801 (0 to 100nM) was performed (Figure 4.16). This demonstrated a reduction in MGMT levels following TMZ treatment. This is expected given that after methyl-group removal from O^6MeG, MGMT becomes ubiquitinylated and undergoes proteasomal degradation (Kaina et al., 2007). IGF1R inhibited cells appeared to show less marked TMZ-induced reduction in MGMT but this effect was not consistent. In keeping with the Immunofluorescence findings in Figure 4.12, TMZ induced γ-H2AX levels on western blot analysis of whole cell lysates were not influenced by AZ12253801. In addition, RAD51 levels in these whole cell lysates were unchanged by treatment. This RAD51 antibody detected an additional band of slower electrophoretic mobility (approximately 50kDa in size marked * Figure 4.16) than the expected size of RAD51 at 37kDa. This protein appeared to increase with TMZ treatment, but was unaffected by IGF1R inhibition. This band could be non-specific, or could be RAD51 that has undergone posttranslational modification. RAD51 is known to

undergo phosphorylation (Krejci et al., 2012). Although phosphorylation is unlikely to cause such a large shift in electrophoretic mobility as seen in Figure 4.16. RAD51 also undergoes SUMOylation, which could cause such a change in electrophoretic mobility and inhibition of such SUMOylation impairs RAD51 trafficking (Saitoh et al., 2002). As stated above, this 50kDa band was not affected by the addition of IGF1R inhibition, and would be unlikely to explain the ability of IGF1R to influence the appearance of TMZ induced RAD51 foci (Figure 4.15). Given more time, RAD51 depletion with siRNA could have identified if this 50kDa protein was a product of the *RAD51* gene, or whether this was simply a non-specific band.

This experiment was performed to determine any major changes in total cellular levels of RAD51 in IGF1R-inhibited cells. The next step was to assess levels of RAD51 and other HR components in chromatin fractions.

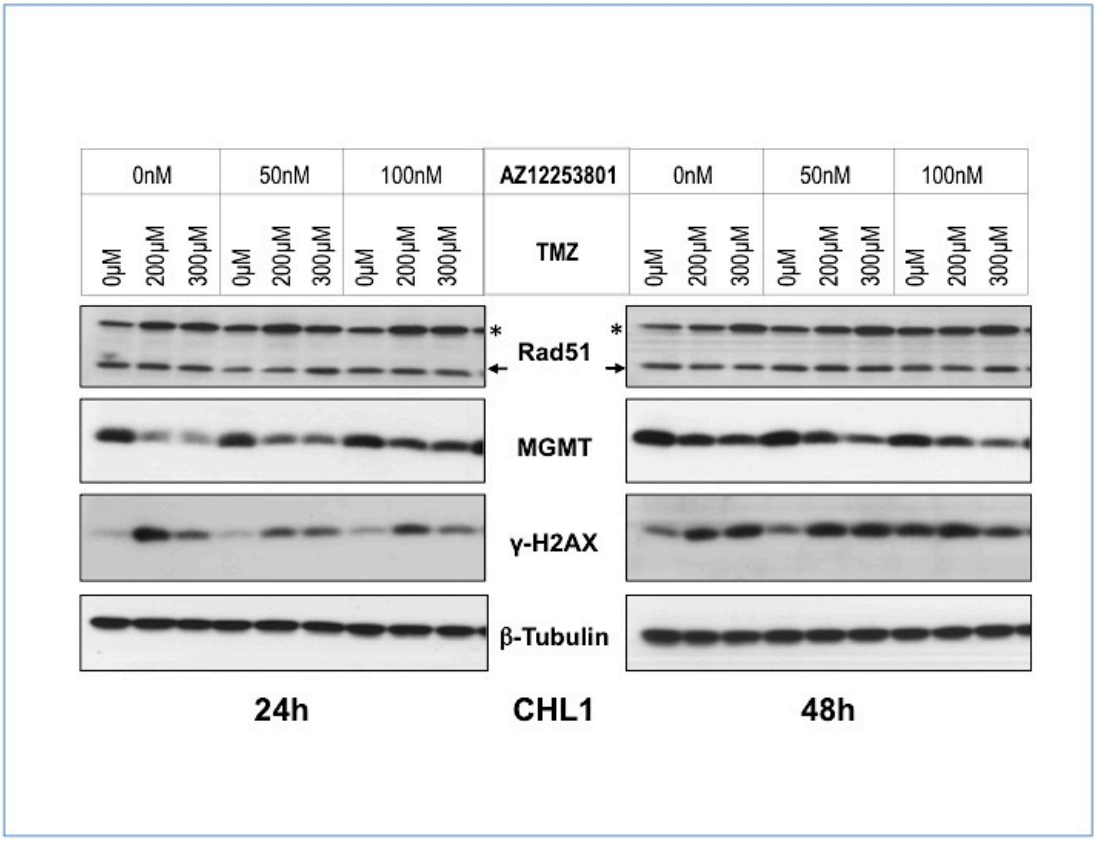


Figure 4.16 The effect of IGF1R inhibition on DNA repair related proteins induced by TMZ. CHL-1 cells grown in complete medium were treated simultaneously with a combination of TMZ (0, 200 or 300μM) plus AZ12253801 (0, 50 or 100nM) and cells were harvested 24 and 48 hours later. Western blot analysis of whole cell lysates was performed, using β-Tubulin as the loading control. The anti-RAD51 antibody detected a 37KDa band corresponding to the molecular weight of Rad51 (labeled arrowhead) and a 50kDa band (labeled asterisk).

In order to verify the effect of IGF1R inhibition on TMZ-induced RAD51 foci and explore the mechanism of this effect (Figures 4.14 and 4.15), another technique was used to assess the binding of repair proteins to chromatin. CHL-1 cells grown in complete medium were treated simultaneously with of TMZ (300μM) and/or AZ12253801 (100nM) and harvested at 24, 48 and 72 hours post treatment. Small-scale biochemical fractionation (Mendez and Stillman, 2000) was performed to isolate chromatin and its bound proteins (labeled 'chromatin lysates' in Figure 4.17). During fractionation, cytosolic

lysates were also produced for each treatment. Figure 4.17 shows the western blot analysis of the chromatin and cytosolic lysates. Blotting for histone H3 and β-tubulin tested the completeness of fractionation. Demonstration of higher histone H3 levels in the chromatin fractions suggested adequate chromatin isolation in CHL-1 cells. There was however, minor chromatin contamination of the cytosolic lysates seen in the longer exposure for histone H3 and probing for β-Tubulin also demonstrated a minor degree of cytosolic contamination of the chromatin fractions (Figure 4.17).

Comparing the cytosolic and chromatin lysates showed evidence that BRCA2, RAD54, RAD52 and Histone H3 were predominantly bound to chromatin, with very little detection in the cytosol. In contrast, 53BP1, RAD51 and RPA were found both in the cytosol and bound to chromatin. It was also noteworthy that, as in the analysis of whole cell extracts (Figure 4.16), the anti-RAD51 antibody detected a 50kDa protein in these chromatin preparations and interestingly, this protein was more abundant in the chromatin fraction, although was unchanged by treatment (Figure 4.17).

These experiments showed no obvious change in the chromatin binding of 53BP1, BRCA2 or RAD52 in any of the conditions, even in the presence of DNA damaging agent, TMZ. In contrast to the immunofluorescence microscopy findings (Figures 4.14 and 4.15) there was no difference in the amount of RPA2 or RAD51 bound to chromatin with TMZ treatment, with or without IGF1 inhibition. It is conceivable that even minor cytosolic contamination might mask subtle changes within the chromatin fractions, if such proteins were abundant in the cytosol. There was however a possible

pattern seen with RAD54, in that TMZ-induced RAD54 binding to chromatin appeared to be reduced in cells treated with AZ12253801 (Figure 4.17).

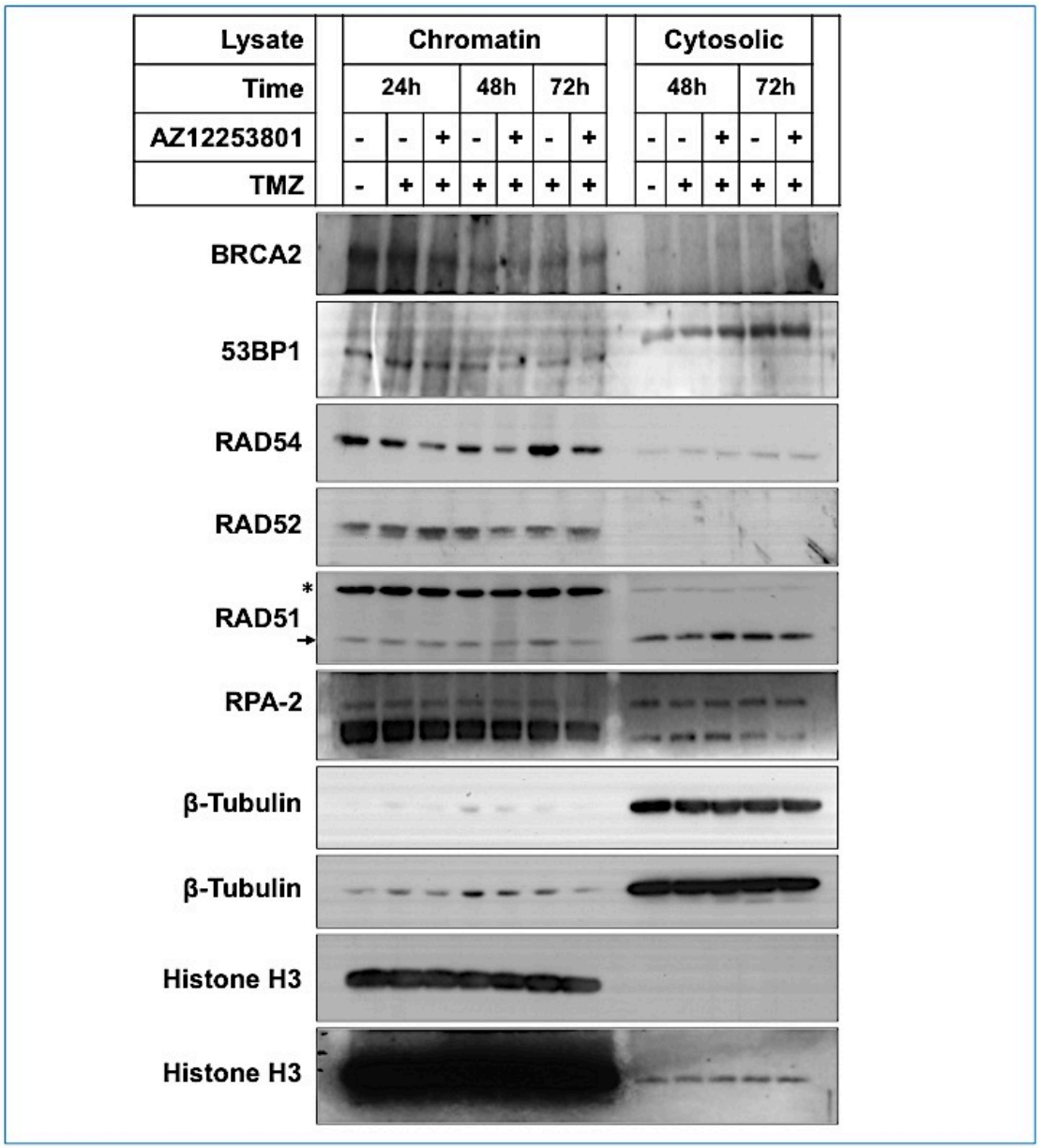


Figure 4.17 The effect of IGF1R inhibition on Chromatin binding of DNA repair mediators induced by TMZ. CHL-1 melanoma cells were treated with TMZ (0 or 300μM) plus AZ12253801 (0 or 100nM) for 24h, 48h and 72h. Chromatin isolation by small-scale biochemical fractionation was performed to generate chromatin and cytosolic fractions. Western blot was performed to detect RAD51, RAD52, RAD54, BRCA2, 53BBP1 and RPA2. Histone H3 and β-Tubulin were used as controls for chromatin and cytosolic lysates respectively. As in Figure 4.16, the anti-RAD51 antibody detected a 37KDa band (labeled arrowhead) and a 50kDa band (labeled asterisk).

The presence of RAD54 is important for RAD51 filament assembly and disassembly as mentioned previously in section 4.3.2.4. In yeast, RAD54 levels are regulated by RAD53, the human equivalent of which is Chk2 (Melo and Toczyski, 2002). RAD53 phosphorylates RAD54 at Thr-132 inhibiting the interaction of RAD54 with RAD51, thereby impairing RAD51 function (Krejci et al., 2012; Niu et al., 2009). IGF1R inhibition was shown to increase Chk2 activation in response to TMZ treatment (Figure 4.4) and it is possible that this may have been accompanied by changes in RAD54 phosphorylation. However, time constraints prevented further investigation of this possibility. In addition, much of the work linking checkpoint control with RAD54 phosphorylation has been performed in yeast models (Melo and Toczyski, 2002) and remains to be investigated in mammalian cells.

The final experiments attempted to assess whether the changes in RAD51 focus formation (Figure 4.15) were functionally significant.

4.3.2.6 Testing the effect of IGF1R Inhibition on Sensitivity to PARP inhibition in Melanoma in vitro

RAD51 is central to homologous recombination. The observation that IGF1R inhibition affected TMZ induced RAD51 foci formation suggested that IGF1R inhibition could influence DSB repair by HR in melanoma cells. Our group and others found that the IGF-1 axis influences HR in prostate cancer cells (Trojanek et al., 2003; Turney et al., 2012) and cells that are deficient in HR are very sensitive to inhibition of Poly (ADP ribose) polymerase 1 or PARP-1 (Bryant et al., 2005; Farmer et al., 2005). Hence, to determine if IGF1R inhibition could sensitize melanoma cells to PARP inhibition, colony survival

assay was performed. AstraZeneca generously provided a PARP inhibitor, Olaparib for these experiements. Figure 4.18 demonstrates that combining IGF1R and PARP inhibition significantly reduced colony survival compared with PARP inhibition alone ($P < 0.0001$, by two-way ANOVA). IGF1R inhibition caused 3.9-fold sensitization to PARP inhibition (Olaparib only SF_{50} = 1400nM; Olaparib + AZ12253801 SF_{50} = 360nM).

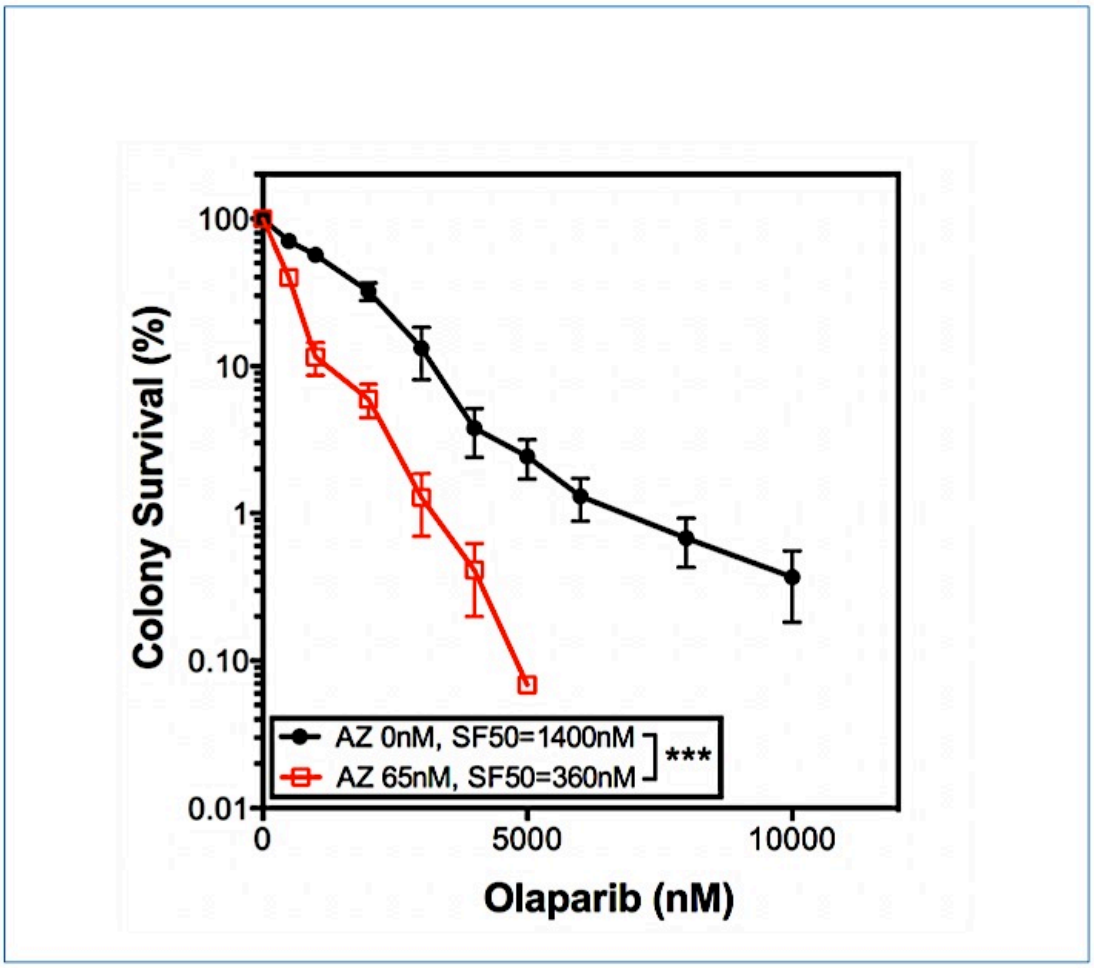


Figure 4.18 IGF1R inhibition enhanced melanoma sensitivity to PARP inhibition. CHL-1 melanoma cells were grown in 10cm dishes in triplicate and 12 hours later pretreated with PARP inhibitor (0-10μM, olaparib) or solvent (DMSO<0.1%) 2 hours prior to treatment with 65nM AZ12253801. Colonies were fixed and stained after 10-14 days. The graph shows mean colony survival and SEM for two independent experiments. Combining IGF1R and PARP inhibition significantly reduced colony survival compared with PARP inhibition alone ($p < 0.0001$, by two-way ANOVA)

This is in accordance with similar findings previously published in an ovarian cancer model using another IGF1R inhibitor (Beauchamp et al., 2009). Taken together with the effect of delayed accumulation of RAD51 foci (Figure 4.15), these data provide further evidence of an effect of IGF1R inhibition on HR.

With evidence that IGF1R inhibition chemosensitizes melanoma cells to TMZ (Figure 3.6B and 3.7) and some initial mechanistic insight into this interaction outlined in this chapter, the next step was to determine the feasibility of using IGF1R inhibition in combination with TMZ in melanoma xenografts.

Chapter 5

Preclinical Testing of the combination of IGF1R inhibition TMZ in melanoma

5.1 Introduction

Type 1 insulin-like growth factor receptor inhibitors are undergoing clinical trials to evaluate their efficacy in cancer therapy. As monotherapy, the only clinical responses have been in sarcomas, whereas the results in more common cancer types have been disappointing (Browne et al., 2011; Buck and Mulvihill, 2011). These early set backs have not discouraged further testing of these agents in cancer. One such therapeutic avenue is the use of IGF1R inhibition to overcome resistance to other agents, and encouragingly, a number of studies have demonstrated benefit in common cancers. For example, IGF1R inhibition was shown to sensitize HER-2 positive breast cancer cell lines to trastuzumab *in vitro*, and another study found that dual IGF1R/IR inhibition, using BMS-754807, combined with hormonal agents could induce tumour regression in an estrogen-dependent breast cancer model *in vivo* (Browne et al., 2011; Hou et al., 2011). With respect to chemotherapy, combining IGF1R inhibition with gemcitabine, has increased

apoptosis in pancreatic cancer cells *in vitro* (Awasthi et al., 2012; Kawanami et al., 2012) and, as mentioned in section 4.2.3, IGF1R inhibition has been shown to overcome resistance to a number DNA damaging agents *in vitro*. In previous work in our group, Yeh et al showed that siRNA-mediated IGF1R depletion sensitized melanoma to TMZ, regardless of BRAF mutation status (Yeh et al., 2006). However, no studies have investigated IGF1R inhibition as a means to overcome chemotherapeutic resistance in melanoma. Thus, based on the results outlined in chapter 3, preclinical studies were initiated to evaluate the effect of IGF1R inhibition in combination with the alkylating agent, TMZ, in melanoma xenografts.

A number of factors influenced the choice of IGF1R inhibitor for the proposed preclinical study. Firstly, only a clinically relevant inhibitor could be taken forward to clinical trial. AZ122253801, the agent used previously (chapters 3 and 4) did not go forward to clinical trials by AstraZeneca, and interpretation of results of its use in a mouse model may potentially be compromised by its propensity for aurora B kinase inhibition, greater in murine than human cells (AstraZeneca in-house data). Additional consideration arose from other studies suggesting that clinically relevant IGF1R inhibiting antibodies may have had limited efficacy due to compensation via the insulin receptor type A (IR-A) (Buck et al., 2010). Therefore, it was decided that a selective ATP-binding competitor of the tyrosine kinase domain of IGF1R and the closely

related insulin receptor, OSI-906 (Buck and Mulvihill, 2011), would be used for the *in vivo* experiments described in this section. This drug was provided by Astellas Pharmaceuticals, has recently completed Phase I trials, and is presently undergoing Phase 2 testing (Carden et al., 2010; Evans et al., 2010; Macaulay et al., 2011).

The initial experiments, therefore, investigated the effectiveness of OSI-906 to inhibit IGF1R signaling and growth of melanoma cells *in vitro*.

5.2 Results and Discussion

5.2.1 Testing the effect of OSI-906 on IGF1R signaling in human melanoma in vitro

To determine the effect of OSI-906 on IGF1R signaling in melanoma, A375M cells were cultured in serum free medium overnight and treated for 1 hour with 0 to 3000nM of OSI-906 (Figure 5.1 A). This demonstrated that OSI-906 treatment reduced phospho-IGF1R levels in a dose dependent manner, with near total abolition of phospho-IGF1R in cells treated with 100nM of OSI-906. A similar dose dependent reduction in phospho-AKT was observed, however elimination of phospho-AKT signal required at least 300nM OSI-906. Phospho-ERK1/2 levels were relatively resistant to OSI-906, remaining unaffected by 3 to 30nM OSI-906, above which there was dose-dependent reduction in phospho-ERK1/2. However, even at the highest concentration of 3000nM OSI-906, residual phospho-ERK1/2 signal was detectable. This effect

is expected given that A375M cells harbour mutant BRAF (Collisson et al., 2003), which causes constitutive ERK1/2 activation.

Having demonstrated that OSI-906 could inhibit IGF1R signaling, the duration of such inhibition was investigated by treating A375M cells with 1000nM OSI-906 and harvesting at 0, 1, 4, 8, 24, 48 and 72 hours, having treated with 50nM IGF-1 in the final 15 minutes of these time points. It was found that phospho-IGF1R levels were undetectable for the entire duration of this time course.

This confirmed that OSI-906 inhibited IGF1R signaling in melanoma cells. The next step was to determine the effect of OSI-906 on the viability of the melanoma cell line panel characterized previously (chapter 3).

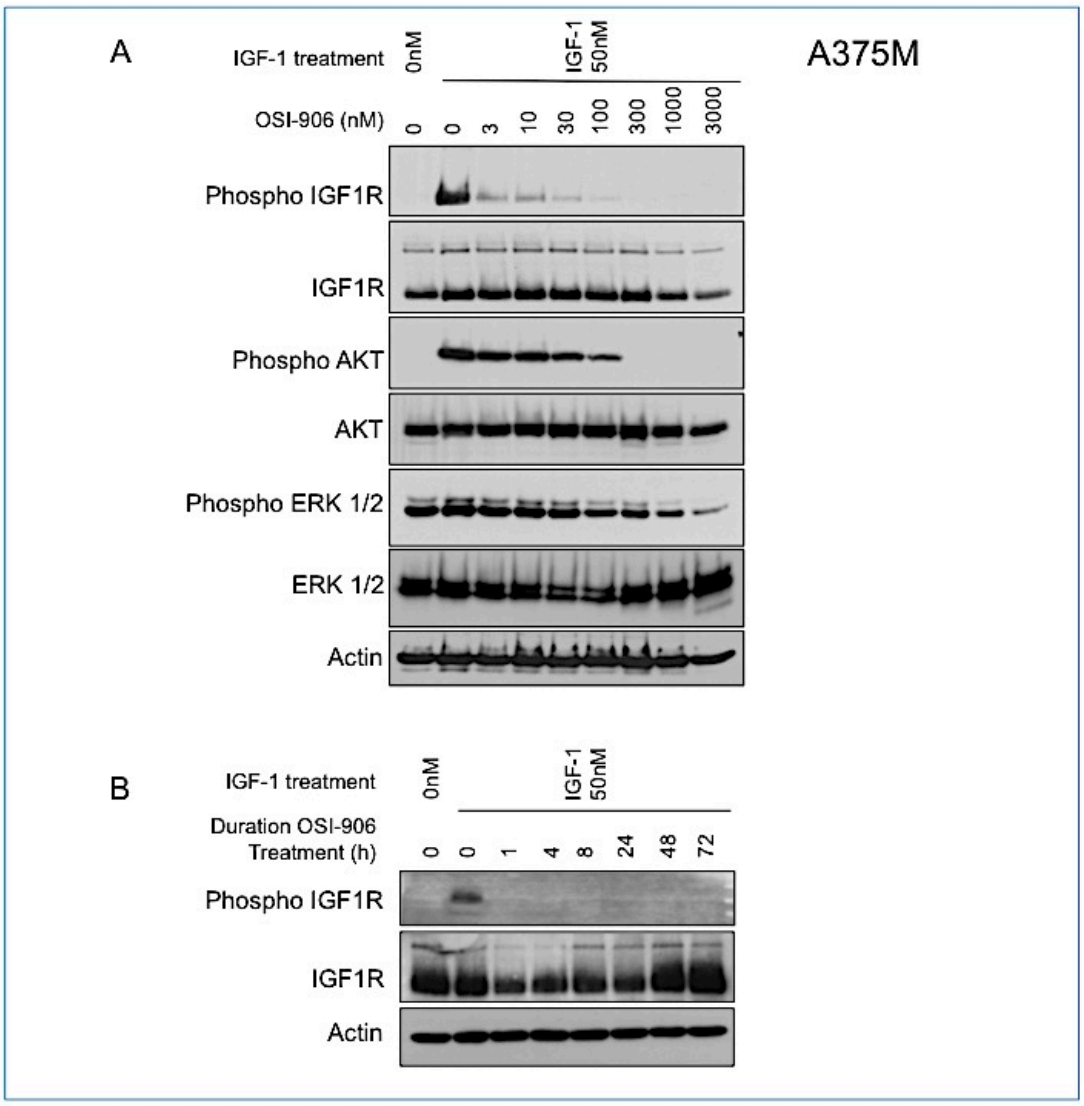


Figure 5.1 OSI-906 inhibited IGF1R receptor activation. (**A**) Serum-starved A375M cells were treated with a dose range of OSI-906 (0 to 3000nM) for 1hr and in the final 15 minutes with 50nM IGF-1. Cells were lysed and western blotted for IGF1R, phospho IGFR, AKT, phospho AKT, ERK 1/2, phospho ERK 1/2 and Actin for loading. (**B**) Serum-starved A375M cells were treated with 1000nM OSI-906 for up to 72 hours, and 50nM IGF-I in the final 15min. Cells were harvested after the stated time points and western blotted for phospho and total IGF1R and Actin.

5.2.2 Testing the effect of OSI-906 on human melanoma cell viability *in vitro*

To determine the effect of OSI-906 on cell viability, the CellTiter-Glo (CTG) assay was used. The COLO858 cell line was not available at the time of this assay, and was not included due to time constraints but assays were completed in the other 9 cell lines.

Cells were seeded at 1000 cells per well in quadruplicate in 96 well plate format. The next day cells were treated with a dose range of OSI-906 (1 to 10,000nM) or solvent (0.6% DMSO) and cell viability measured using the CTG assay. The results demonstrated that OSI-906 could reduce cell viability in a dose dependent manner in melanoma cells, however sensitivity varied among the different cell lines (Figure 5.2), with GI_{50} values ranging from 10nM to greater than 10μM (Table 5.1).

Early phase studies have shown that the clinically achievable concentration of OSI-906 is dependent on the dosing schedule. Pharmacokinetic (PK) studies indicate the continuous dosing of 150mg OSI-906 twice daily produces OSI-906 serum concentrations of 2.4-4.8 μM, whereas intermittent dosing of 600mg resulted in peak concentrations of up 20μM (Carden et al., 2010; Evans et al., 2010). These data suggest that the GI_{50} for most of the cell lines shown in Figure 5.2 were within a clinically achievable range. In two cell lines the GI_{50} values were above the investigated dose range (>10μM). It was therefore unclear whether their GI_{50} values were less than the clinically achievable peak serum concentration of 20μM.

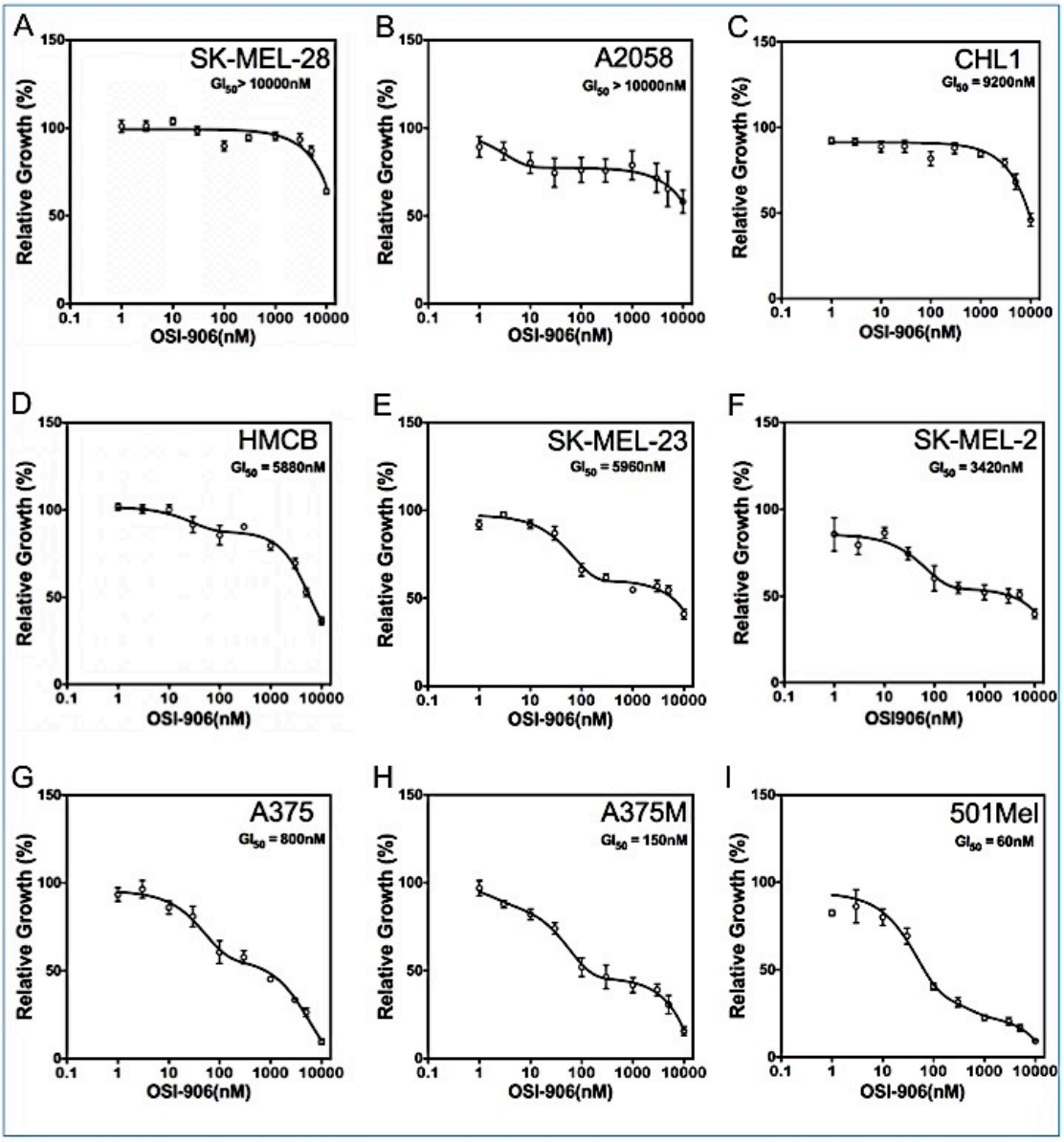


Figure 5.2 The effect of OSI-906 on viability of melanoma cells. (**A**) SK-MEL-28, (**B**) A2058, (**C**) CHL-1, (**D**) HMCB, (**E**) SK-MEL-23, (**F**) SK-MEL-2, (**G**) A375, (**H**) A375M and (**I**) 501Mel melanoma cells were seeded in quadruplicate at 1,000 cells per well in 96 well plate format and the following day treated with solvent (DMSO 0.6%) or OSI-906 (1 to 10000nM). After 5 days, cell viability was quantified using the CTG assay. Graphs show mean viability from 2 independent assays (8 data points) expressed as a percentage of solvent-treated cells, with error bars representing the SEM. The data were curve fitted and GI_{50} values calculated using GraphPad Prism software.

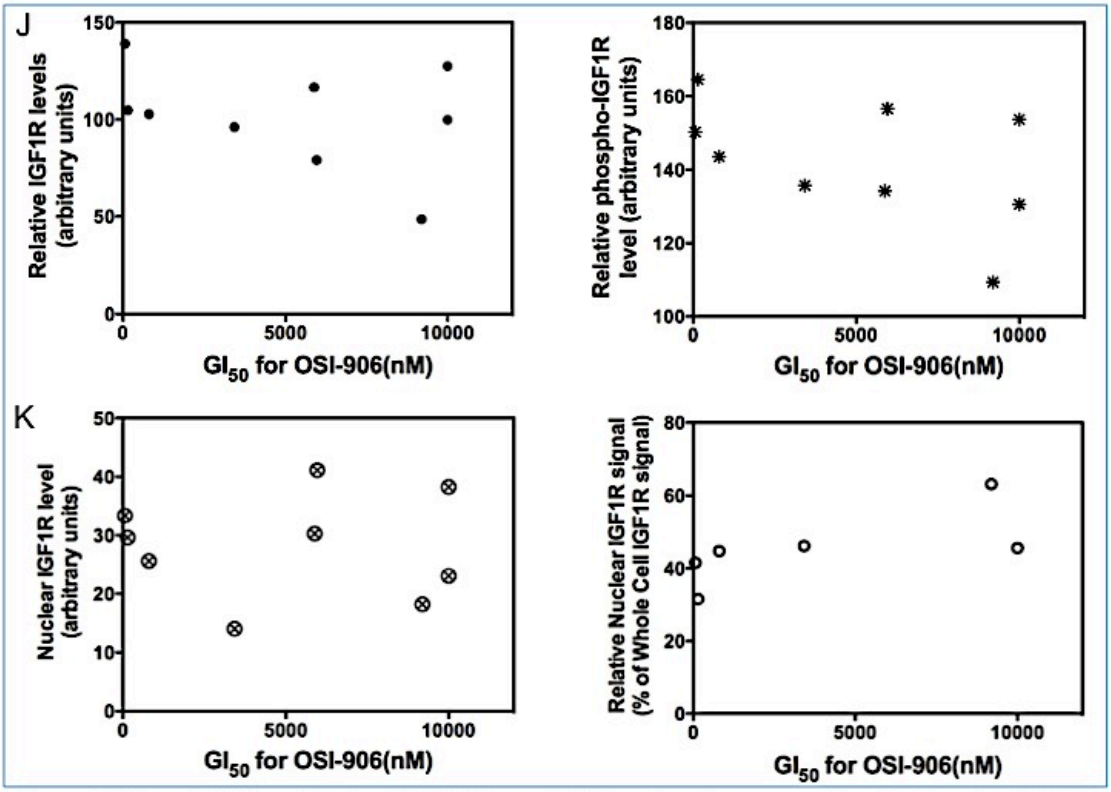


Figure 5.2 (cont'd) The effect of OSI-906 on viability of melanoma cells. (J) Levels of IGF1R (left) and phospho-IGF1R (right) were quantified in the western blot of this cell line panel from Figure 3.1, using ImageJ software. Correlation analysis revealed no significant relationship between GI_{50} for OSI-906 and either IGF1R (left) or phospho-IGF1R (right) (Spearman's rank coefficient, r = -0.35, p=0.33; and r = -0.39, p=0.28 respectively). (K) From the immunofluorescence staining performed in Figure 3.2 & 3.3, ImageJ software was used to quantify nuclear IGF1R levels. Correlation analysis revealed no significant relationship between GI_{50} for OSI-906 and either absolute nuclear IGF1R (left) or relative nuclear IGF1R expression (ie a percentage of whole cell IGF1R expression) (right) (r = -0.008, p=0.94; and r = 0.55, p=0.13 respectively).

CELL LINE	GI_{50} for OSI-906 (nM)	MUTATION STATUS				
		BRAF	NRAS	PTEN	p53	Other
501Mel	60	Mut	WT	WT	Mut	CTNNB1
A375M	150	Mut	WT	WT	WT	CDKN2a
A375	800	Mut	WT	WT	WT	CDKN2a
SK-MEL-2	3420	WT	Mut	WT	Mut	-
HMCB	5880	WT	Mut	WT	WT	-
SK-MEL-23	5960	WT	WT	Del	WT	-
CHL-1	9200	WT	WT	WT	Mut	CDKN2a
A2058	>10000	Mut	WT	Mut	Mut	CDKN2a
SK-MEL-28	>10000	Mut	WT	WT	Mut	EGFR

Table 5.1 Summary of GI_{50} values for OSI-906 and mutation status of melanoma cells (sources: www.sanger.ac.uk/genetics/CGP/CellLines ; http://p53.iarc.fr/CellLineCriteria.aspx; Ducker et al., 2013; Greshock et al., 2010; Lu et al., 2103; McDermott et al., 2007; Tsa0 et al., 2004).

Other groups have tested PQIP, an IGF1R inhibitor with similar structure and activity against IGF1R and IR to OSI-906,

(cis-3-[3-(4-methylpiperazin-l-yl)-cyclobutyl]-1-(2-phe-nyl-quinolin-7-yl)-imidazo[1,5a]pyrazin-8-ylamine). In a large screen of multiple compounds against large cell line panels, PQIP was found to have similar activity in CHL-1, HMCB and SK-MEL-28, with GI_{50} values between 6.9-9.8μM (Greshock et al., 2010), however A375 in their study was less sensitive to PQIP than demonstrated here. Cell line responses to OSI-906 reported in the Genomics of Drug Sensitivity in Cancer data-set suggest that A375 and SK-MEL-2 were more sensitive and A2058, CHL1 and SKmel28 were more resistant in the current study compared with their findings (www.cancerrxgene.org/translation/Drug).

Attempts were made to investigate correlates of the varied sensitivity to OSI-906, using GI_{50} data from Table 5.1 and quantification of IGF axis components from Figure 3.1 (Chapter 3). Correlation analysis showed that melanoma cell line sensitivity to OSI-906, represented by the GI_{50}, did not correlate with total IGF1R levels or basal phospho-IGF1R levels (Figure 5.2 J). This was consistent with previously published data suggesting that IGF1R expression in clinical samples is a poor predictor of response to IGF1R inhibitors (Basu et al., 2011). Similarly, nuclear IGF1R levels determined in (Figure 3.2) did not correlate with OSI-906 sensitivity (Figure 5.2 K).

Table 5.1 also summarises the mutation status of each cell line as well as their GI_{50} values for OSI-906. Commonly encountered mutations in BRAF, PTEN and NRAS genes did not seem to segregate with OSI-906 sensitivity.

It is noteworthy, however, that three out of five mutant BRAF cell lines (A375, A375M and 501Mel) were the most sensitive to OSI-906 treatment, with GI_{50} values in the nanomolar range. Conversely, the cell lines most resistant to OSI-906, with GI_{50} values > 9.2μM, which is almost double the clinically achievable concentration by continuous administration, harboured mutant p53. This suggests that p53 status may influence response to IGF1R inhibition. However, these cell lines were genotypically heterogenous and therefore to test whether p53 status affected OSI-906 sensitivity, a p53-inducible cell line, designated B231 was obtained from Professor Xin Lu (Fogal et al., 2005).

5.2.3 Investigating the effect of p53 status on OSI-906 sensitivity

B231 cells are derived from the parental p53-null H1299 non-small cell lung cancer cell line, by stable expression of WT p53 from a Tet-responsive plasmid (pTRE) (Fogal et al., 2005). To test the effect of p53 status on OSI-906 sensitivity, B231 cells in tetracycline free medium were treated with 2μg/ml Doxycycline or solvent (control) for 18 hours. This was followed by treatment with OSI-906 and 5 days later cell viability was measured with the CTG assay (Figure 5.3). A parallel western blot confirmed that B231 cells did not express p53 in the absence of doxycycline, while doxycycline treatment resulted in induction of p53 expression (Figure 5.3 A). CTG assays revealed that OSI-906 reduced cell viability in a dose dependent manner in B231 cells. In the presence of doxycycline, and therefore induction of WT p53 (DOX +), there was at least an 8-fold sensitisation (GI_{50} = 116nM), compared with p53

null cells (DOX -) that were relatively resistant to OSI-906 (GI_{50}>1000nM). These results suggest that cells harbouring WT p53 are significantly more sensitive to OSI-906 than isogenic p53-null cells. This is perhaps not unexpected given that, there is evidence of cross-talk between p53 and the IGF axis, whereby IGF1R induced Akt activation is known to promote MDM2-mediated p53 degradation. Conversely, p53 regulates IGF1R and IGF binding protein expression (Girnita et al., 2003; Werner et al., 1996). Therefore one might expect that IGF1R inhibition would reduce p53 degradation, thereby enhancing p53 mediated apoptosis, while the presence of p53 mutation may facilitate some degree of evasion from apoptosis induced by IGF1R inhibition. It is noteworthy however that induction of WT p53 expression did not alter IGF1R protein levels in this case (Figure 5.3 A).

The effect of p53 mutation status on IGF1R response is an interesting finding and may impact on the use of OSI-906 clinically, since p53 mutations are common in many cancers. In melanoma however, p53 mutations occur infrequently in clinical samples (Albino et al., 1994). On the other hand, the more clinically prevalent V600E BRAF mutation was present in three of the most sensitive cell lines and, based on this small study, there does not seem to be any evidence to preclude the use of OSI-906 in melanomas harbouring V600E BRAF mutation. The ability of IGF1R blockade to suppress growth in V600E BRAF melanoma is consistent with a previous report from our lab that utilized IGF1R gene silencing (Yeh et al., 2006).

Having confirmed that OSI-906 reduced cell viability in human melanoma cells, the next experiments determined if OSI-906 had any effect on TMZ

sensitivity *in vitro*, to assess whether there was justification for testing this combination in an animal study.

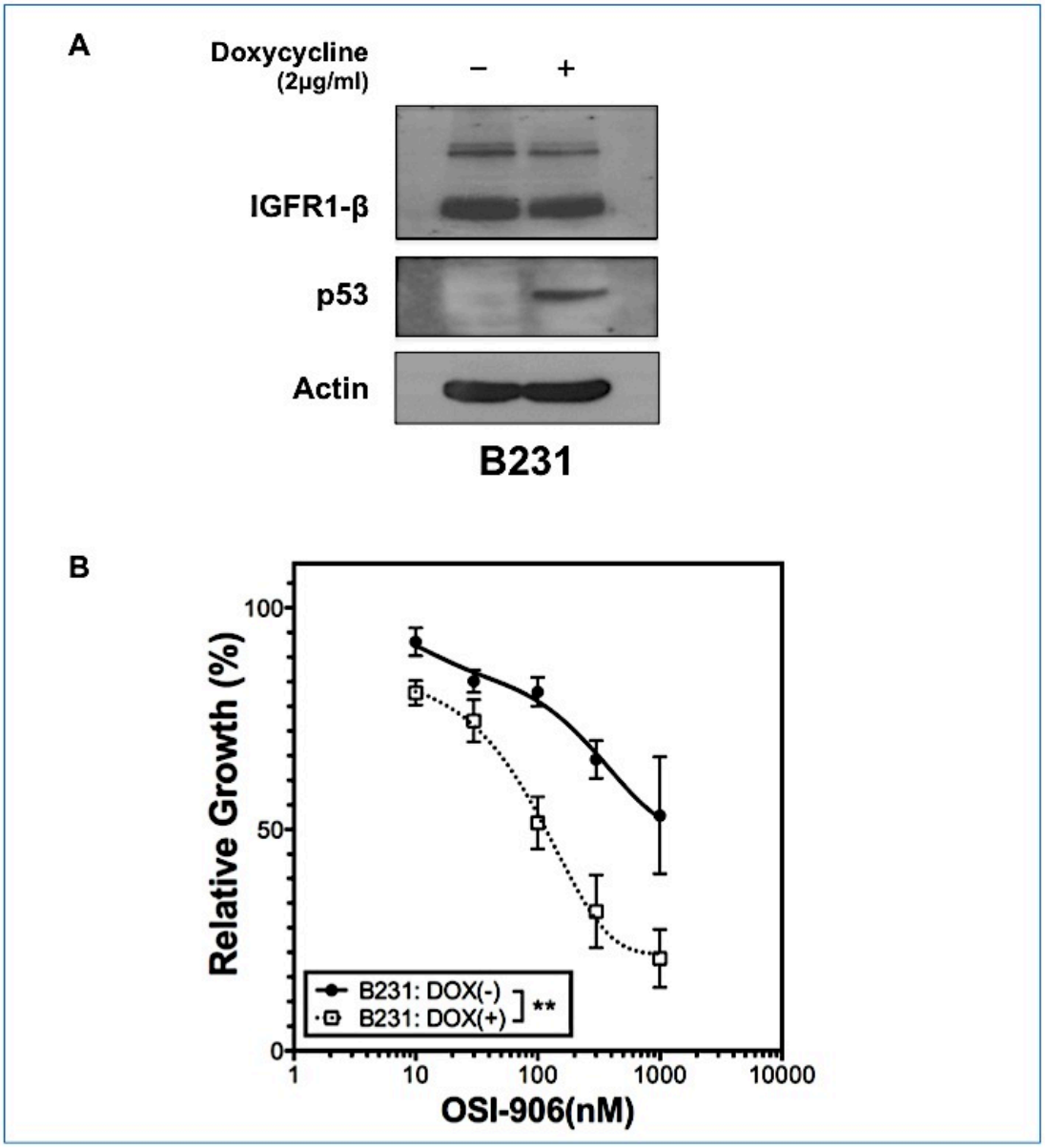
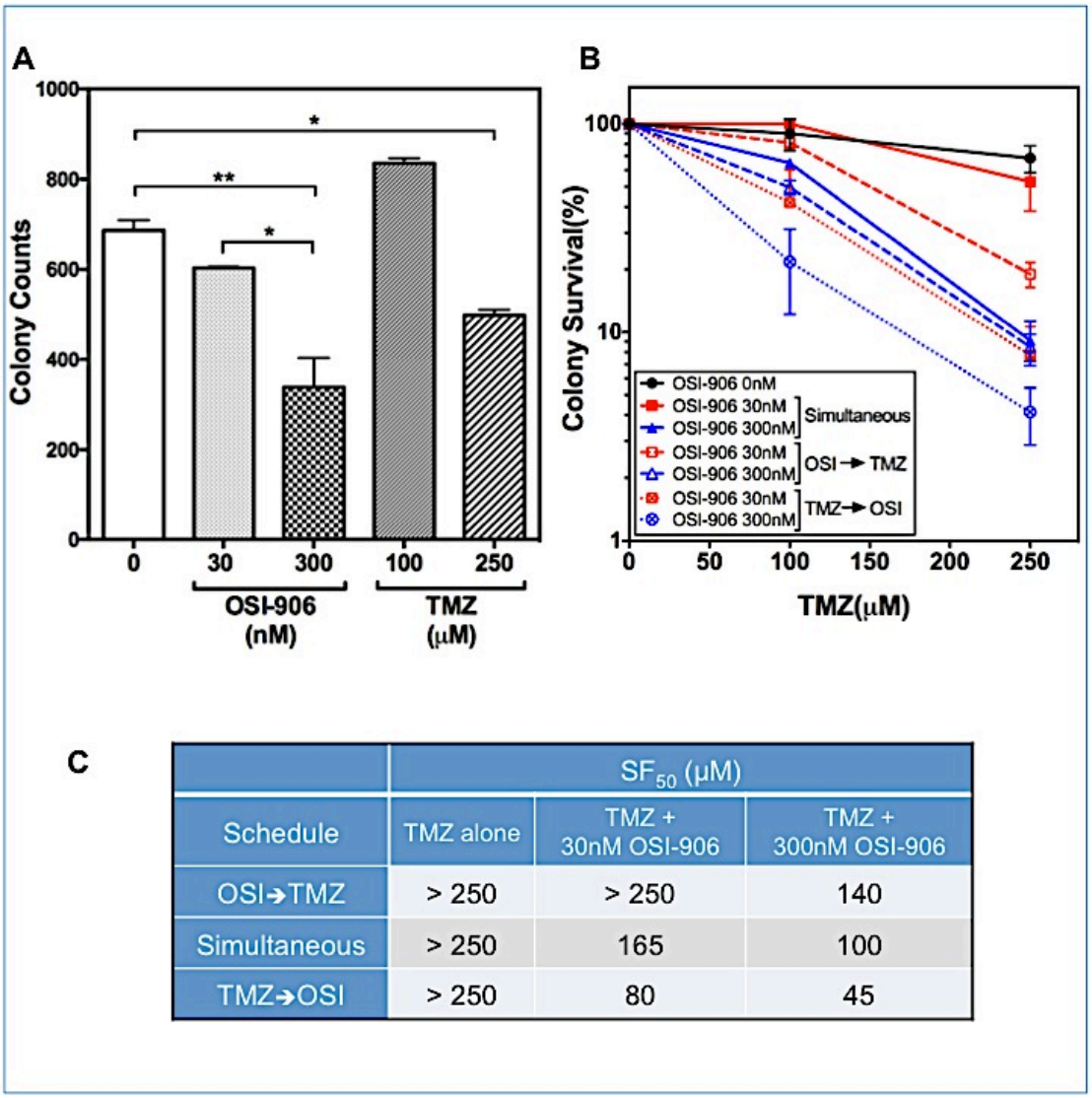


Figure 5.3 Sensitivity to OSI-906 is enhanced by functional p53. (**A**) B231 cells were cultured in Tet-free medium and treated with Doxycycline (2µg/ml) or vehicle (water) for 18 hours. Western blot analysis of the whole cell lysates demonstrated WT-p53 expression induced by doxycycline treatment. (**B**) B231 cells in 96 well plate format were treated with doxycycline or solvent for 18 hours treatment, followed by OSI-906 (0-3000nM) treatment and after 5 days, cell viability was quantified using the CTG assay. Graphs show data from three independent experiments, each with triplicate points, expressed as a fraction of viability in solvent-treated cells. Error bars (SEM). The data were curve fitted and GI_{50} values were calculated using GraphPad Prism software. The sensitivity of B231 cells to OSI-906 was significantly enhanced by induction of WT-p53 expression ($p = 0.0019$, by two-way ANOVA).

5.2.4 Testing the effect of OSI-906 on TMZ sensitivity in melanoma

Work presented in chapter 3 showed that IGF1R inhibition with AZ12253801 sensitized melanoma cells *in vitro* to TMZ (Figure 3.6 and Figure 3.7). As stated above, OSI-906 is a more clinically relevant IGF1R inhibitor; therefore clonogenic assays were performed to test whether OSI-906 affected melanoma cell sensitivity to TMZ. The A375M cell line was chosen for this preclinical study since its genotype, WT p53 and V600E mutant BRAF, is commonly encountered in clinical melanoma samples. Also, previous testing of TMZ in a melanoma xenograft study demonstrated that A375M cells are tumorigenic in mice (Middleton et al., 2000b; Middleton et al., 2000c). Initial assays tested the effect of single drug treatment (OSI-906 or TMZ) on colony survival. This revealed that melanoma survival was inhibited by 250μM TMZ or 300nM OSI-906 (*p = 0.023 and **p = 0.001 respectively by one way ANOVA), but not by 100μM TMZ or 30nM OSI-906 (Figure 5.4 A). Subsequent assays tested these drugs in combination and investigated whether any effect of this drug combination was schedule dependent. Thus, treatment with OSI-906 was applied 24 hours before, simultaneously with, or 24 hours after TMZ treatment. (Figure 5.4 B). In agreement with CTG cell viability assays (Figure 5.2), colony survival assays showed that A375M cells were relatively resistant to TMZ, with SF_{50} values greater that 250μM. There was no evidence of antagonism between these two agents and cells pre-treated with 30nM OSI-906 were no more sensitive than controls. Otherwise, it was evident that OSI-906 treatment resulted in dose-dependent

sensitization of TMZ in A375M cells. Further comparison of the SF_{50} values for each of the three treatment schedules revealed that application of 30 or 300nM OSI-906 24 hours after TMZ treatment resulted in greater reduction in colony survival than either simultaneous or pretreatment with OSI-906 (Figure 5.4 C). In control (OSI-906 untreated) cells, the SF_{50} value for TMZ treatment was >250μM compared with 300nM OSI-906 post-treated cells which was 45μM. This represents greater than 5 fold TMZ sensitization by OSI-906. This is important since this is below the clinically achievable peak of serum concentrations of TMZ, which has been found to be 60-75μM (Middleton et al., 2000a; Sankar et al., 1999).



C

Schedule	SF_{50} (μM)		
	TMZ alone	TMZ + 30nM OSI-906	TMZ + 300nM OSI-906
OSI→TMZ	> 250	> 250	140
Simultaneous	> 250	165	100
TMZ→OSI	> 250	80	45

Figure 5.4 OSI-906 enhances melanoma sensitivity to TMZ in a schedule dependent manner. **(A)** Two thousand A375M cells were seeded in complete medium per 10cm dish in triplicate and 12h later treated with solvent (control), OSI-906 (30, 300nM) or TMZ (100, 250μM). Cell survival was inhibited by 250μM TMZ or 300nM OSI-906 (*p = 0.023 and **p = 0.001 respectively by one way ANOVA). **(B)** A375M cells were seeded for clonogenic assay as in A, and 12 hours later either treated simultaneously with OSI-906 (0, 30 or 300nM) and TMZ (0, 100 or 250μM) or sequentially treated with these two agents. Treatment sequence was therefore OSI-906, followed 24h later by TMZ, or vice versa for the dose ranges above. Survival fraction was expressed as a percentage of solvent treated cultures, where points and error bars represent the mean and SEM respectively of three independent experiments, each with triplicate dishes. GraphPad Prism software was used to perform curve-fit these data in order to interpolate SF_{50} values for TMZ. A tabulated summary of the SF50s is shown in **(C)**.

The results of this assay suggested that there would be merit in preclinical testing of this combination, and were used to guide the treatment schedule in the proposed animal study.

5.2.5 Preclinical Testing of the effect of OSI-906 on TMZ sensitivity in melanoma

Prior to testing the effect of IGF1R inhibition on TMZ sensitivity in an animal study, it was necessary to confirm that the selected human melanoma cell line, A375M, was tumorigenic and also to test the tolerability of each individual drug in the chosen animal model.

5.2.5.1 Tumorigenicity study of A375M cells and TMZ tolerability in athymic nude mice

The A375M cell line was chosen for the xenograft study since its mutation status is commonly encountered clinically, ie WT p53 and V600E mutant BRAF. In addition, previous xenograft studies testing TMZ found A375M to be tumorigenic and TMZ to be tolerable, causing tumour growth delay at 100mg/kg daily for 5 days (Middleton et al., 2000c), comparable to the schedule which is used clinically (Middleton et al., 2000a). The initial investigation sought to confirm that this TMZ regimen was safe and tolerable, prior to commencing a combination study with OSI-906.

A375M cells were mixed with Matrigel and ten million cells inoculated into ten athymic nude mice. Tumour xenografts developed in all ten mice, achieving the required size to begin treatment (100-200mm^3) by 15-17 days post inoculation (Figure 5.5). Mice tolerated intraperitoneal (IP) injections of both TMZ and solvent (200μl of 25% DMSO in 0.9% NaCl), however both these groups displayed 5-10 seconds of 'hunched posturing' immediately following IP injections. Otherwise, mouse welfare was considered to be satisfactory,

with no weight loss greater than 20%. No mice were culled on welfare grounds.

The solvent treated group achieved mean tumour volume of 800mm^3 by day 14-post treatment (31 days post cell inoculation). The TMZ treated group achieved this mean tumour volume on day 30-post treatment (day 47 post cell inoculation). In fact, by day 14 the control group reached maximum tumour volume for this pilot, 800mm^3, while the mean tumour volume of the TMZ treated group was 336mm^3, less than half the volume of the control group. The overall pattern of growth and tumour growth delay observed with TMZ was generally in agreement with previously published data, although Middleton et al (2000), observed slightly faster tumour growth rates in both control and TMZ-treated groups. This may reflect the difference in A375M inoculation method: Middleton et al implanted 1-2mm^3 pieces of A375M xenograft, which previously established growth *in vivo* and would therefore conceivably grow faster than an inoculum of single cell suspension in Matrigel taken directly from *in vitro* culture, as performed in the present study (Figure 5.5). However, given the 100% take rate and uniform growth rates, these results suggested that A375M cells would be suitable for use in a xenograft study in athymic nude mice.

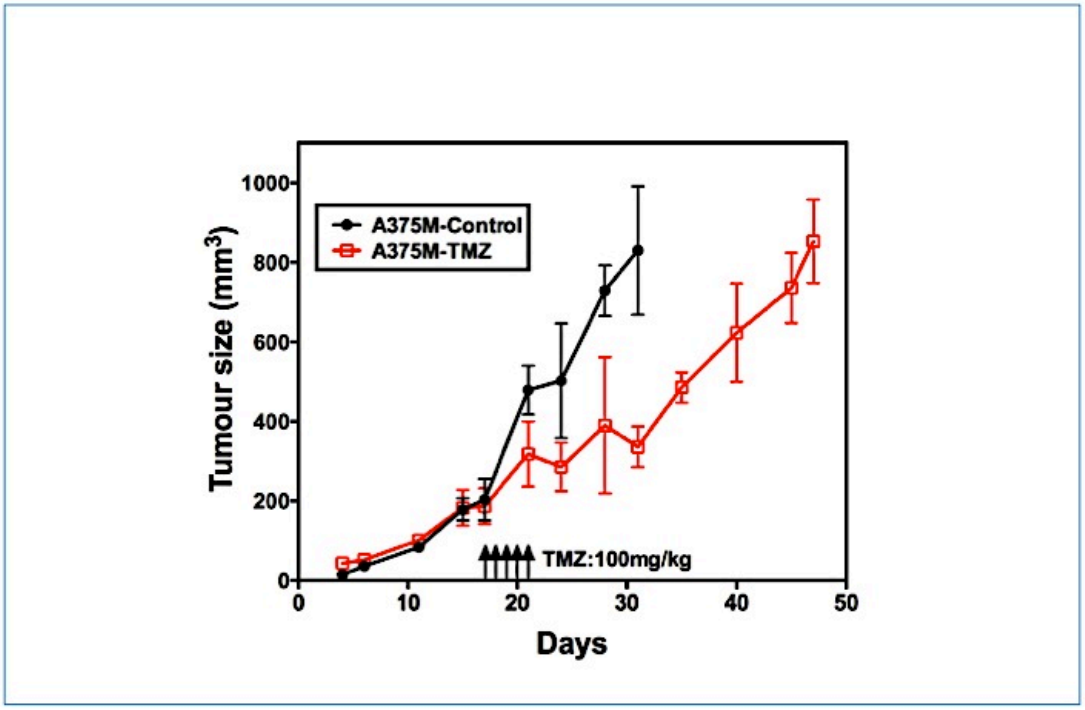


Figure 5.5 A375M cells form xenografts in nude mice and TMZ inhibits xenograft growth. Ten athymic nude mice were injected subcutaneously in the flank with 10^7 A375M cells. When all xenografts were 100-200mm^3, mice were randomized into two matched groups of 5 mice per group. One group was treated with 100mg/kg TMZ once daily by intraperitoneal (IP) injection for 5 days. The second group was treated with solvent (1:3 mix of DMSO and 0.9% NaCl solution) for 5 days by IP injection. General animal health was observed daily and tumour measurements (lxbxhx0.52) recorded 2-3 times weekly. Graph shows mean +/- SEM of tumour volume. A375M cells formed xenografts in all mice. TMZ treatment resulted in tumour growth delay, with controls achieving mean tumour volume of 800mm^3 at 14 days post treatment compared with the TMZ group which required 30 days to achieve this volume (p=0.0058, by two-way ANOVA)

5.2.5.2 Testing the tolerability of OSI-906 in athymic nude mice

Targeted therapy is frequently associated with side effects. The principal rationale for the use of OSI-906 in cancer therapy is to counteract proliferative and anti-apoptotic effects of IGF1R/insulin (IR) receptor signaling, but this can cause side effects, including insulin resistance and glucose intolerance (Carden et al., 2010; Evans et al., 2010; Yee, 2012). It was therefore pertinent to determine whether athymic mice could tolerate any possible side effects associated with OSI-906 therapy. Initial tests of OSI-906 *in vivo* used up to 75mg/kg in another strain of mice for 12 days (Mulvihill et al., 2009) and information from OSI Pharmaceuticals (now Astellas Pharmaceuticals) suggested that doses greater than 50mg/kg might be less tolerable. Other *in vivo* studies used 40mg/kg in athymic nude mice (McKinley et al., 2011). Astellas Pharmaceuticals also suggested that 12-14 day treatments would be most efficacious in their experience (personal communication with Dr E Buck, Astellas Pharmaceuticals). Therefore this study aimed to test the tolerability of 14-day treatment of 40 or 50mg/kg OSI-906. This drug is relatively insoluble in aqueous solution, and on the advice of Astellas, was dissolved in 25mM tartaric acid. However even in this solvent, OSI-906 was relatively insoluble, precipitating out after 30 minutes and was therefore prepared fresh each day immediately prior to administration.

Under similar conditions described previously (Figure 5.5), A375M xenografts were established in 12 mice, which were divided into 3 groups of 4 mice each. The first 2 groups received 40 or 50mg/kg OSI-906 and the final group received treatment with solvent control (25mM tartaric acid; Figure 5.6).

Dosing was carried out by oral gavage, and 4 hours after the final doses on day 14, mice were sacrificed and blood and tumour samples taken for PK analysis. Since OSI-906 can cause hyperglycaemia, polyuria and dehydration, weight loss of 10% or more was managed with IP injection of Ringer's Lactate (RL) solution.

Figure 5.6 (A) shows that even though the overall growth rate of the control group in this case was generally slower than controls in Figure 5.5, the time to attain treatable xenografts (100-200mm^3 tumour volume) was similar in both cases. Comparing all 3 treatment groups in Figure 5.6(A), the mean tumour volumes were not significantly different. Testing effects on tumour growth was not, however, the primary aim of this study, but rather to determine safe and tolerable dosing of OSI-906.

Solvent treated mice maintained weights around basal weight, with a transient decline below this level at the end of the first week of treatment, presumably due to the administration of tartaric acid and the oral gavage process itself, which was performed with minimal trauma by Jordan Tanner (Biomedical Services, John Radcliffe Hospital). OSI-906 was generally well tolerated, although rapid weight loss within 1-2days was observed in both OSI-906 treatment groups, occurring more quickly in the group receiving 50mg/kg OSI-906. Thereafter, mouse weights in these two groups were maintained between 10-15% below the basal weight during which time IP RL solution was administered to minimize the effects of dehydration. Blood glucose levels were measured using a simple mobile glucometer at cardiac puncture on day 14. This did not reveal a statistically significant change in blood glucose, although there was a trend towards OSI-906 causing slightly higher blood glucose

levels than controls, with a trend toward increasing blood glucose with 50 compared with 40mg/kg OSI-906 (Figure 5.6 C: OSI-906 0mg/kg vs 40mg/kg: p=0.63; 0mg/kg vs 50mg/kg, p=0.13; 40mg/kg vs 50mg/kg, p=0.55 by one-way ANOVA).

PK assays performed by Andy Cooke (Astellas Pharmaceuticals, Colorodo), demonstrated that both OSI-906 doses produced similar serum and tumour OSI-906 concentrations, with no detectable OSI-906 in control samples (Figure 5.6 D)

These results suggested that 40mg/kg or 50mg/kg OSI-906 generated circulating OSI-906 levels comparable to clinically achievable values, although neither affected tumour growth. The trend toward higher blood glucose and earlier onset of weight loss suggested 50mg/kg OSI-906 was less well tolerated even though these mice were in no obvious distress compared to the control group or the group dosed with 40mg/kg OSI-906. Following this experiment, it was decided to perform a small trial of the tolerability of the combination of TMZ and 40mg/kg OSI-906 prior to carrying out a larger test of the two treatments in combination.

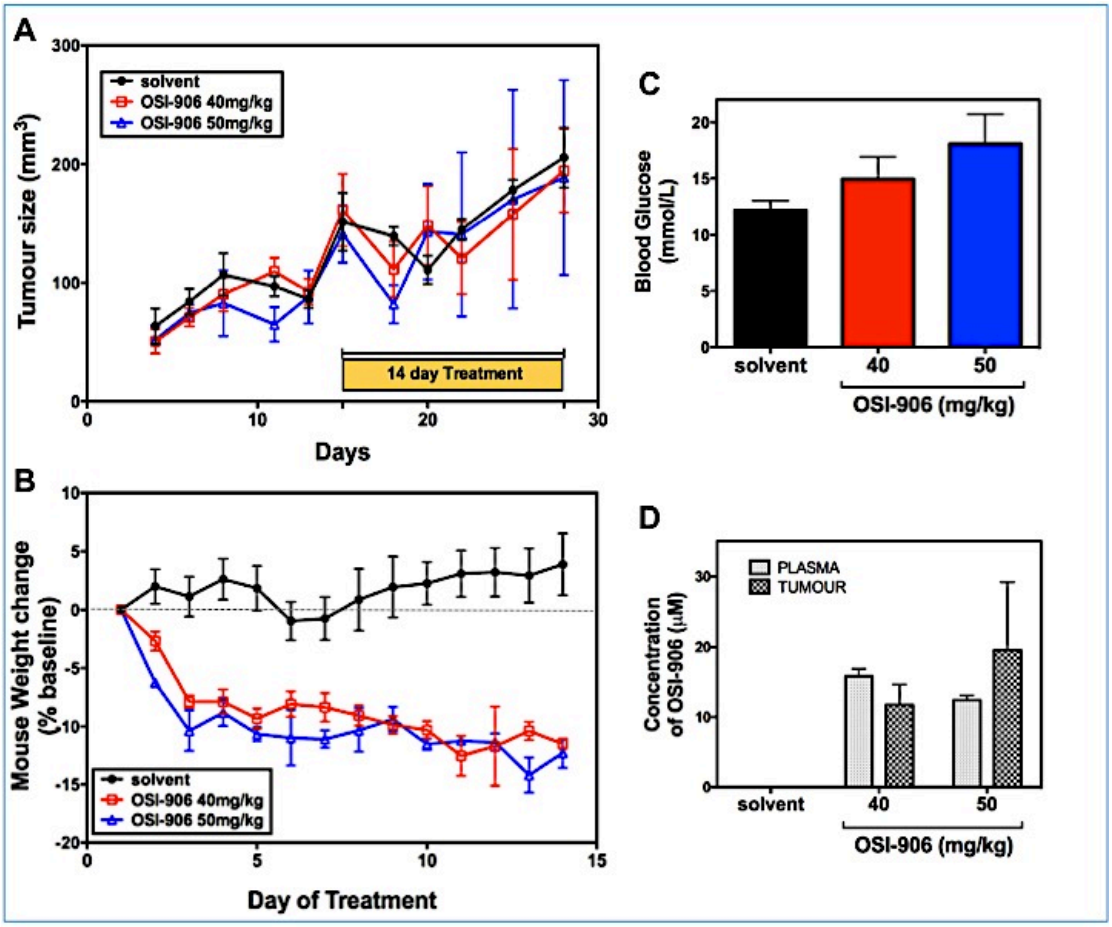


Figure 5.6 OSI-906 was tolerated and bioavailable in athymic nude mice. Three matched groups of 4 mice bearing A375M xenografts were treated with 50mg/kg or 40mg/kg OSI-906 respectively, administered once daily by oral gavage (po) for 14 days, and the third group received solvent (25mM tartaric acid) for the same period. Observations and measurements were carried out as in Figure 5.5. Mice were sacrificed 4 hours after the final treatment on day 14 and blood sampled by cardiac puncture and tumour samples taken for pharmacokinetic assays. **(A)** Graph shows mean +/- SEM tumour volumes, which did not significantly differ between groups for this short experiment (mean tumour volumes per group; error bars SEM). **(B)** Graph shows mean +/- SEM mouse weights expressed as a percentage of the weight on the first day of treatment. Both OSI-906 treated groups sustained weight loss of up to 15% basal weight, with no significant difference between 40mg/kg and 50mg/kg groups. **(C)** At cardiac puncture blood was tested by glucometer (Abbott), the results of which show a trend towards increasing blood glucose levels with higher OSI-906 dosing, although this was not statistically significant (by one-way ANOVA). **(D)** Pharmacokinetic measurements kindly performed by Andy Cooke at Astellas Pharmaceuticals, Colorado, show that 40mg/kg and 50mg/kg dosing of OSI-906 produced similar serum and tumour OSI-906 concentrations, with no detectable OSI-906 in control samples.

5.2.5.3 Initial *in vivo* test of the tolerability of combining OSI-906 with TMZ

In planning this experiment, consideration was given to the potential for increased toxicity using TMZ and OSI-906 in combination. Based on *in vitro* treatment scheduling data (Figure 5.4) four non tumour-bearing mice were first treated with 100mg/kg TMZ by IP injection for 5 days. On the fourth day, mice were divided into 2 groups. Group A started treatment with 40mg/kg OSI-906 once daily by gavage on day 4, 4 hours after TMZ dosing and group B mice received the same 40mg/kg OSI-906 daily dosing starting on day 6, 24hours after the final TMZ dose. However, by 6-7 days, despite IP fluid supplementation, the mice had lost more than 20% of baseline weight and were euthanized on welfare grounds on day 7 (Figure 5.7). This experiment did however provide useful information regarding toxicity issues that required modification of the experimental plan. Group B (ie the non-overlapping combination group) mice lost 15% weight after 5 days of 100mg/kg TMZ alone, suggesting that this dose was not tolerable. In addition, all mice displayed brief hunching, suggesting discomfort, immediately after IP administration of TMZ. Similar behavior was observed in the previous study (Figure 5.5), even in the control group treated with solvent (1:3 DMSO/0.9% NaCl solution). A trial of reducing the DMSO content in this solvent resulted in TMZ precipitating out of solution. Two strategies were adopted to overcome the toxicity problems identified in these two experiments. Firstly, the dose of TMZ needed to be reduced, and secondly, it was important to identify a less toxic solvent and/or route of administration.

Given the possible of toxicity associated with the OSI-906 solvent (25nmM tartaric acid, Figure 5.6) based on slightly reduced feeding observed in this study, the use of an alternative solvent for OSI-906 was also considered.

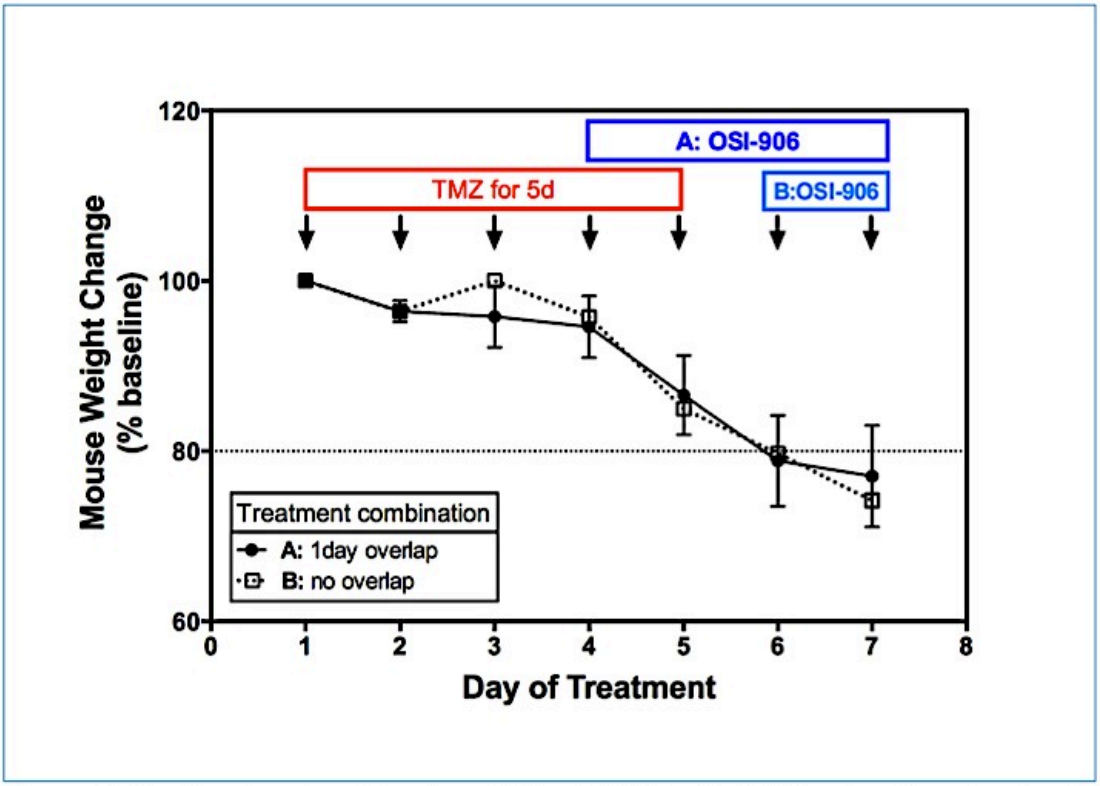


Figure 5.7 Testing the tolerability of combining OSI-906 with TMZ in athymic nude mice by two treatment schedules. Four non tumour-bearing athymic nude mice were first treated with 100mg/kg TMZ by IP injection for 5 days. On the 4th day, mice were randomized into two matched groups each with two mice. Group A received 40mg/kg OSI-906 daily starting on day 4. Group B mice received the same 40mg/kg OSI-906 daily starting on day 6. Graph shows mean +/- range of weights of mice in each group, expressed as percent of baseline weight. All four mice were sacrificed on day 7 and the study prematurely terminated due to toxicity.

5.2.5.4 Second *in vivo* test of the tolerability of combining OSI-906 with TMZ

A second tolerability test was undertaken, using a reduced dose of TMZ, and avoiding the use of IP DMSO that appeared to be irritant. Other groups have successfully used 50mg/kg dosing in a suspension of Ora-Plus (Paddocks Laboratories Inc) in a glioblastoma xenograft model (Kitange et al., 2009; Prasad et al., 2011). Concerns over the use of tartaric acid prompted a comparison of the effects of three different vehicles (tartaric acid, corn oil and Ora-Plus) on tolerance and absorption of OSI-906.

The design of this experiment is shown in Figure 5.8. Control mice (Group A, n=2) received Ora-Plus alone and Group B (n=8) was dosed with 50mg/kg TMZ as a suspension in Ora-Plus by gavage each for 5 days, preparing treatments fresh each day prior to administration. On the sixth day, the TMZ treated group was randomized into four subgroups each with 2 mice. Three of these subgroups received 50mg/kg OSI-906 in tartaric acid (B1), Ora-Plus (B2) or corn oil (B3), while the fourth received Ora-Plus alone (B4). All mice tolerated 50mg/kg TMZ for 5 days followed by OSI-906 for 3 days. Although this small study was not powered to detect differences in tumour growth, TMZ appeared to cause some tumour growth delay (Figure 5.8A). During the subsequent 3 days of OSI-906 dosing, there was little further change in tumour size.

OSI-906 caused greater weight loss than Ora-Plus or TMZ alone treatment (Figure 5.8B). Among the three OSI-906 treated groups, OSI-906 in tartaric acid was associated with the greatest weight loss (12 ± 1.5% below baseline weight) compared with the other OSI-906 treatment groups (weight loss

<10%) although these differences were not significant. Four hours after the final dose of OSI-906, the mice were culled and blood and tumour tissue were assayed for OSI-906 levels (Figure 5.8 C). Oral dosing at 50 mg/kg achieved OSI-906 levels in tumour tissue of 3700 – 5700 ng/ml (8.7 – 13.6 μM), and in plasma of ~4000 - 5600 ng/ml (9.3 – 13.3 μM), corresponding to plasma OSI-906 levels that are achieved clinically (Carden et al., 2010; Evans et al., 2010). Slightly higher and more consistent OSI-906 levels were achieved with OSI-906 administered in Ora-Plus (Figure 5.8C). Hence, this vehicle was chosen to dose both TMZ and OSI-906 in subsequent evaluation of effects of IGF-1R inhibition on melanoma sensitivity to TMZ *in vivo*.

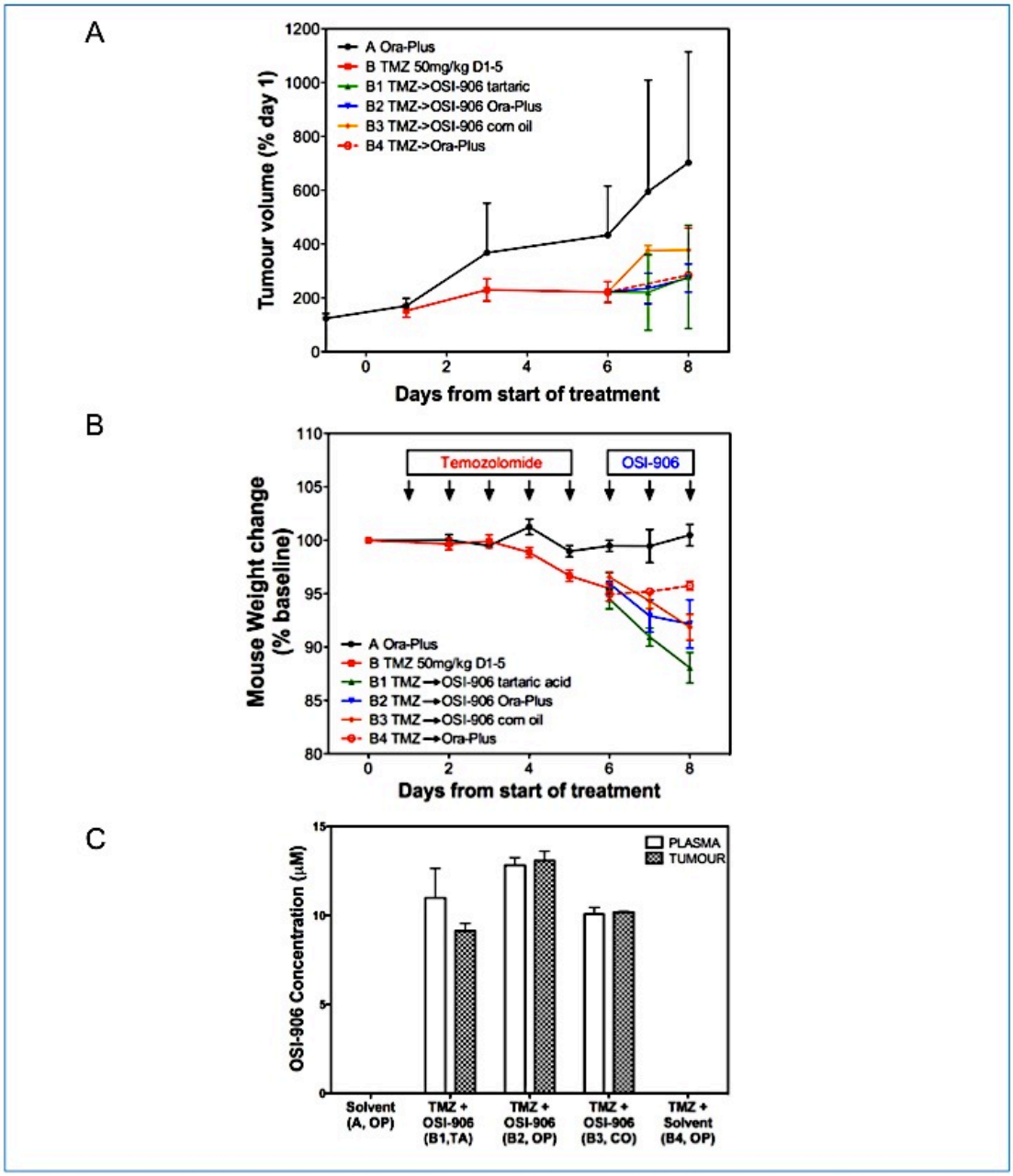


Figure 5.8 Toxicity and pharmacokinetic study of alternative vehicles for TMZ and OSI-906. Mice bearing A375M xenografts, were treated with Ora-Plus (Group A, 2 mice) or 50mg/kg TMZ in Ora-Plus by gavage days 1-5 (Group B. 8 mice). On day 6, mice were randomized into 4 groups of 2, and treated by oral gavage with 50mg/kg OSI-906 in 25mM tartaric acid (TA, B1), Ora-Plus (OP, B2), corn oil (CO, B3) or vehicle (Ora-Plus) alone (B4) on days 6-8. **A**) Tumour volumes and **B**) weights were measured daily. On day 8, 4hr after the final dose of OSI-906, mice were culled and tumour and EDTA plasma were analysed for OSI-906 PK (**C**).

5.2.5.4 Testing the effect of OSI-906 on TMZ sensitivity in human melanoma xenografts

This experiment used twenty-four athymic nude mice, each inoculated with 10^7 A375M cells. When tumours reached ~100-200 mm^3, animals were randomized into four groups, each with 6 mice.

Groups were treated with vehicle (Ora-Plus) alone, 50mg/kg TMZ, 50 mg/kg OSI-906, or both drugs. All treatments were prepared fresh each day. TMZ and OSI-906 were administered in clinically relevant regimens, which for TMZ involved oral dosing on Days 1-5 every 28 days (Middleton et al., 2000a). OSI-906 was dosed on three consecutive days per week, as found to be tolerable in a recent Phase I study (Carden et al., 2010), since it also allowed adherence to the sequence of combination treatment found to be effective *in vitro* in Figure 5.4, ie TMZ followed by OSI-906. Following 3 weeks of OSI-906 treatment, a second cycle of TMZ was administered for 5 days, and three times weekly OSI-906 dosing continued until mice were culled. A third cycle of TMZ treatment would have been due on day 56, however this was not performed since prior to this, all control mice (Ora-Plus alone) achieved the limit for tumour size as guided by the PPL (Geometric Mean Diameter or GMD of 15mm).

Transient weight loss of up to 5% was observed following administration of either TMZ or OSI-906 during the first 3 weeks of treatment, compared with up to 10.5% weight loss with the combination of these drugs during this period (Figure 5.9A). As time progressed, control and OSI-906 only treated groups gained weight above their starting weights (with 10.2% and 12.8% mean weight gain above base weight respectively, at day 40 of treatment). In

contrast, the TMZ only and combination treatment groups fluctuated around the starting weight (with 2.1% weight loss and 1.3% mean weight gain versus base weight respectively, at day 40 of treatment). Mice were not dosed if weight loss was >10% baseline weight, leading to omission of single doses on 2, 2 and 4 occasions in the TMZ, OSI-906 and combination (TMZ plus OSI-906) groups respectively. One animal in each of the TMZ and combination groups experienced weight loss of 20% and was culled on welfare grounds. Otherwise, weight loss was generally <10% of baseline weight and the treatments induced no other apparent toxicity.

Effects on tumour growth are shown in Figure 5.9(B). Untreated control tumours grew rapidly, achieving a volume of 1000 mm^3 in 29 ± 2 days from the start of treatment. TMZ or OSI-906 alone caused only minor growth delay, with time to reach 1000 mm^3 of 36 ± 6 and 39 ± 5 days respectively, not significantly different from controls. In animals receiving combination treatment there was significant growth delay, tumours requiring 79 ± 4 days to attain 1000 mm^3 volume ($p<0.001$ compared with each of the other three groups). Growth delay was also evident when evaluating slopes of the tumour growth curves (Figure 5.9C). Compared with controls, TMZ or OSI-906 separately reduced the gradient of tumour growth by 13% and 25% respectively. If additive, the predicted effect of combination treatment would be 38% reduction in slope. In fact the observed reduction in the group treated with the OSI-906 and TMZ combination was 78%, suggesting supra-additivity. Survival was significantly prolonged in mice receiving combination treatment (median survival of 87.5 days), compared with the other three groups (median

survival of 42, 41 and 50 days in control, OSI-906 only and TMZ only treated groups respectively), as shown in Figure 5D.

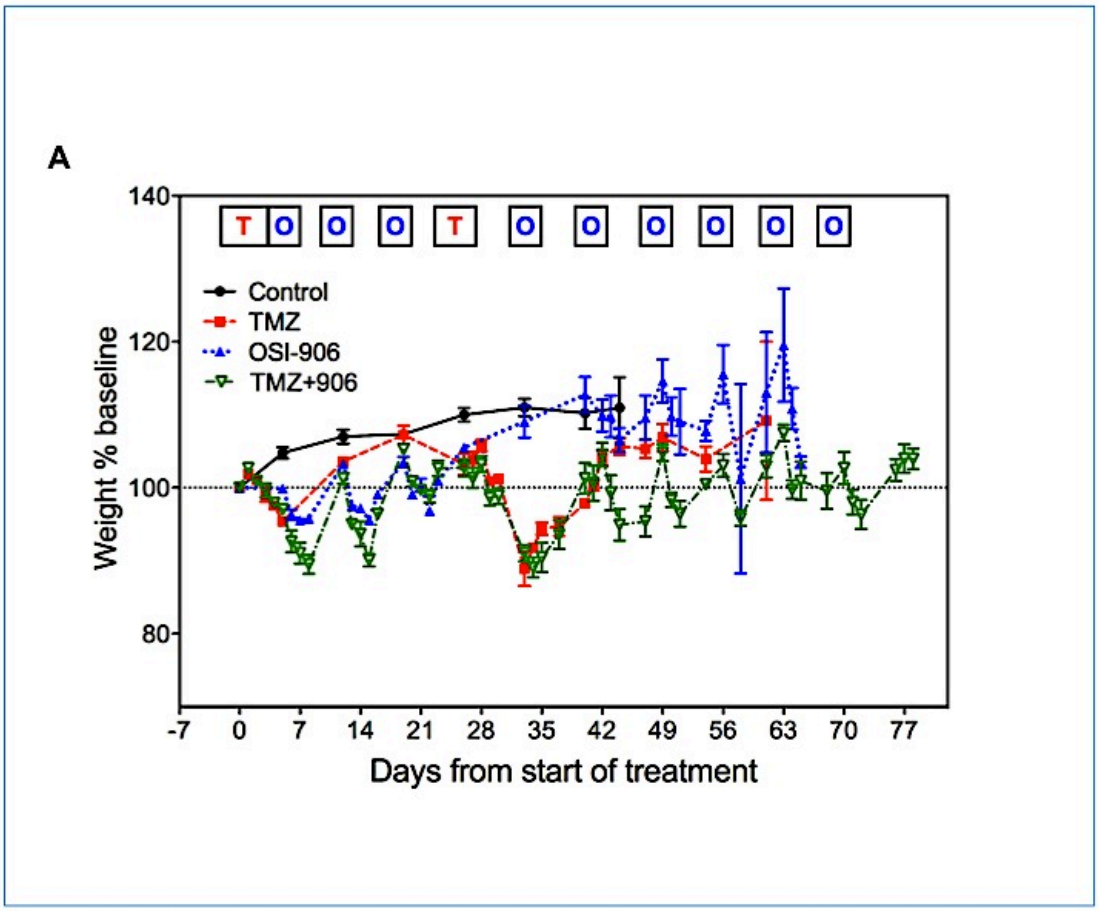


Figure 5.9 OSI-906 enhances the sensitivity of melanoma xenografts to TMZ Groups of 6 mice were inoculated in the subcutaneous tissues of the flank with 10^7 A375M cells in matrigel. When tumours attained 100-200mm^3, animals were treated with Ora-Plus (control), 50mg/kg TMZ (T), 50mg/kg OSI-906 (O) or combination treatment, scheduling OSI-906 to avoid administration immediately before or together with TMZ. **A)** Graph shows sequential weight changes induced by treatment with control, TMZ (T), OSI-906 (O) or combination treatment (TMZ+906).

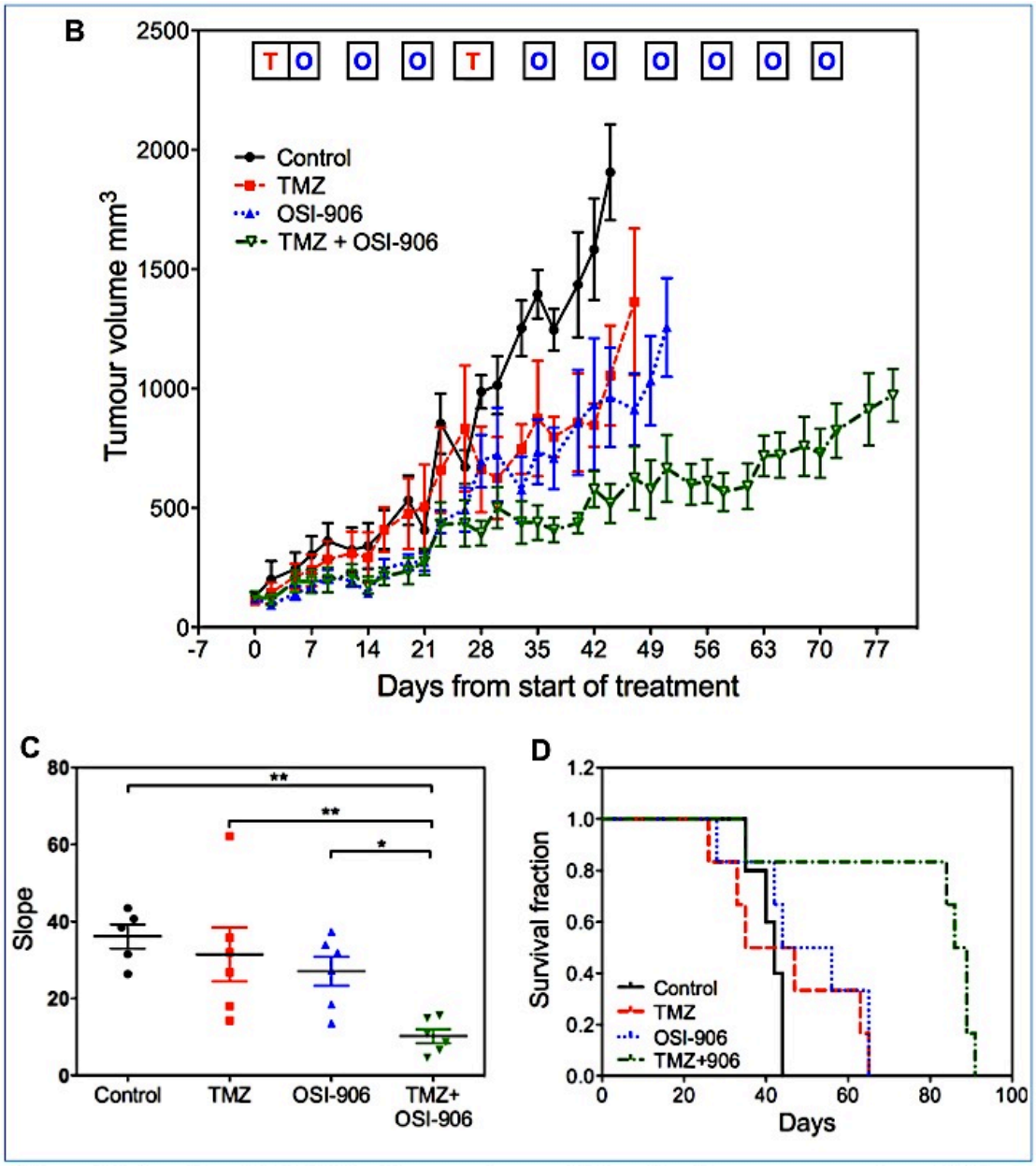


Figure 5.9 (continued) OSI-906 enhances the sensitivity of melanoma xenografts to TMZ
B) Graph shows tumour volumes, mean of 6 mice per group (5 in control group due to failure of tumour take to grow following absorption of matrigel bleb); bars, SEM. **C)** Linear regression analysis of tumour volumes in B was used to calculate slopes of growth of individual tumours. Graph shows individual data points and mean slope of tumour growth; bars, SEM. There were no significant differences between the growth rates of the control, TMZ or OSI-906 –treated tumours, and there was a significant reduction in slope in the combination treatment group compared with each of the other groups (*p<0.05, **p<0.01 by one way ANOVA. **D**) Survival from start of treatment. Survival differences were calculated by log-rank Cox-Mantel test with Bonferroni-correction for multiple comparisons. There were no differences between control, TMZ and OSI-906 -treated groups, while survival in the combination group was significantly longer than control (p<0.01), TMZ-treated (p<0.01) and OSI-906-treated (p<0.01) groups.

Alkylating agents are associated with significant toxicity, of which myelosuppression is the major dose-limiting side effect in clinical use (Trinh et al., 2009). The present preclinical study utilized half the usual TMZ dose used in previous melanoma xenograft studies. The initial test of the combination confirmed that 100mg/kg TMZ was not tolerable alone, and could not be combined with OSI-906 (Figure 5.7), and the subsequent experiments suggested that 50mg/kg TMZ may be tolerable in combination with OSI-906 (Figure 5.8 and 5.9). However, no direct comparison was made between 50 and 100mg/kg TMZ treatment in this animal model. Therefore, it is not clear whether there was any benefit in combining OSI-906 with a lower dose of TMZ, versus the standard 100mg/kg TMZ alone regime. To address this, a comparison of tumour growth curves was made in figure 5.5 and 5.9(B) was made and this is summarized in Table 5.2.

Table 5.2 Comparison of 100mg/kg and 50mg/kg TMZ alone, and in combination with OSI-906.

Initial test of TMZ alone Figure 5.5	**Time to Tumour volume of 800mm^3 (days)**	**Tumour Volume at day 15 (mm^3)**
Control	14	829.8
TMZ 100mg/kg, 5 days	30	336.1
Treatment in Figure 5.9A	Time to Tumour volume of 800mm^3 (days)	Tumour Volume at day 23 (mm^3)
Control	23	853.33
TMZ 50mg/kg, 5 days	34	659.4
TMZ+OSI-906	72	431.7

In Figure 5.5, the control group achieved a mean tumour volume 800mm^3 on day 14 after the start of treatment whereas, by this time, the 100mg/kg TMZ treated group reached 336mm^3, and this group only achieved a tumour size of 800mm^3 by day 30. This represents 2.1-fold delay in tumour growth. This was the maximum tumour size allowed by the project license for this short tolerability/tumorigenicity study. Examining the time taken to achieve a similar tumour size in the larger combination treatment study (Figure 5.9 B), the tumour growth was observed to be slower than in Figure 5.5, with control group mice reaching mean tumour size of 800mm^3 on day 23 of treatment. This may be related to the longer duration of time required to prepare and perform flank injections of A375M cell suspension for the larger combination experiment. The 50mg/kg TMZ alone group took 34 days to achieve this tumour size, while the combination group took 72 days. The latter was 3.1 times longer than control group mice in this study. This indirect comparison suggests that the combination of 50mg/kg of TMZ with OSI-906 may have been more effective than 100mg/kg alone.

These results (Figure 5.9), indicate that OSI-906 can be safely administered in combination with TMZ to xenograft-bearing mice, and suggest that effects on melanoma growth are supra-additive compared with effects of either agent alone.

Targeted therapy has recently provided the prospect of more effective treatment for advanced melanoma. Use of agents targeting mutant BRAF is limited to the 40-60% of patients whose melanomas harbour mutant BRAF (Chapman et al., 2011). The emergence of early resistance is problematic, suggesting that there is room for improvement. Though clinical trials have

demonstrated superiority of BRAF inhibitors over alkylating agents in melanoma (Chapman et al., 2011), none thus far have combined these two agents. IGF1R inhibition has been shown in this project to be effective against melanoma cells *in vitro* regardless of BRAF mutation status, and the demonstration that IGF1R inhibition delays DNA repair (results of this study, chapter 4 and data previously published by our group, (Turney et al., 2012) provides the rationale for combination testing. The results presented in this chapter have shown that combining an alkylating agent together with IGF1R inhibition improves the antitumour effect in melanoma both *in vitro* and *in vivo,* and supports the testing of this combination clinically.

Chapter 6

Conclusions

A panel of melanoma cell lines was assembled in the initial part of this project. Work presented in chapter 3 revealed a significant correlation between basal IGF1R phosphorylation and sensitivity to TMZ in seven MGMT-proficient cell lines. This supported the hypothesis that IGF1R signaling may influence TMZ resistance in melanoma. Quantification of IGF1R expression and phosphorylation in clinical melanoma tissue samples derived from TMZ or DTIC treated patients would be useful to determine if this *in vitro* correlation is clinically relevant. This could be done by immunohistochemical staining of melanoma tissue but may be more quantitatively assessed by an ELISA technique. In addition, melanoma cells with lower levels of MGMT expression correlated with greater TMZ sensitivity. Taken together, these relationships could be used to predict which patients are likely to benefit from TMZ treatment. That is, patients who have low expressing MGMT melanomas may benefit from TMZ treatment. For patients with MGMT-proficient melanomas, higher levels of tumour IGF1R activation could be predicted to be resistant to alkylating monochemotherapy. Careful patient selection guided by such biomarkers could therefore allow more appropriate and effective therapy to be utilized, avoiding unnecessary side effects and valuable time wasted on less effective agents in patients with poor prognosis.

Further work in chapter 3 also showed that IGF1R inhibition using AZ12253801 enhanced TMZ sensitivity in both a WT-BRAF and a mutant V600E BRAF expressing cell line. This was in agreement with previous findings by our group, which demonstrated that IGF1R depletion could also sensitize melanoma cells to TMZ, regardless of BRAF mutation status (Yeh et al., 2006), further supporting a role of IGF1R signaling in TMZ resistance.

Chapter 4 sought to determine how IGF1R inhibition improved the sensitivity melanoma cells to TMZ and found that this was unlikely to be attributable solely to enhanced apoptosis induction within 24-48hr. The sensitization was however accompanied by a modest increase in accumulation of cells in G2/M and Chk2 phosphorylation. These findings were more in keeping with an effect of IGF1R inhibition on DNA repair and the next step examined the effect of IGF1R signaling blockade on the repair of alkylated DNA bases. This demonstrated no effect of either IGF1R inhibition or depletion on MGMT activity or O^6MeG levels. In addition, IGF1R inhibition sensitized MGMT-null SK-MEL-23 cells as well as MGMT-inhibited cells to TMZ. This supported the conclusion that the effect of IGF1R inhibition on TMZ sensitivity was independent of MGMT. Similarly, IGF1R inhibition did not affect AAG activity or N^7MeG levels, suggesting that IGF1R signaling did not affect the early steps of BER (Singer et al., 1992). Methylmethane sulphonate (MMS) is an agent that alkylates DNA bases almost exclusively on the cyclic nitrogen atoms and cells treated with MMS therefore rely functional BER to repair such DNA damage to survive (Sobol et al., 2002). Determination of the effect of IGF1R inhibition on the survival of MMS-treated melanoma cells could be useful in confirming whether IGF1R inhibition affects BER function.

The later sections of chapter 4 showed that IGF1R inhibition increased the formation of TMZ-induced RPA foci and reduced 53BP1 focus formation during the first 24 hours, while not significantly altering TMZ –induced γ-H2AX focus formation. IGF1R inhibition also caused dose dependent persistence of TMZ induced RAD51 foci. The reasons for these phenomena are currently unclear. The RPA coats exposed ssDNA, protecting it from nuclease degradation. Similarly, RPA may aggregate at SSBs and other regions of exposed ssDNA such as following end-resection, which is essential to initiating homologous recombination repair of DSBs. Similarly, 53BP1 promotes NHEJ by opposing DNA end-resection required to initiate HR (Fradet-Turcotte et al., 2013). The reduction in TMZ-induced 53BP1 foci number with IGF1R inhibition presented in chapter 4 may be related to an effect of IGF1R inhibition on end-resection, which remains to be investigated. It may be possible to explore the effect of IGF1R inhibition on end-resection by quantifying TMZ induced Mre11 foci formation by immunofluorescence (Ying et al., 2012).

One possible link between IGF-1 signaling and end-resection could be the reported ability of IGFs to regulate expression of the prolyl isomerase PIN1 (You et al., 2002), which was recently shown to influence DSB repair by suppressing DNA end resection. PIN1 deficient cells exhibited excessive end-resection, associated with reduction in repair by NHEJ (Steger et al., 2013). If IGF1R inhibition affected end-resection, then it would be potentially informative to determine the effect of IGF1R inhibition on PIN1 expression in melanoma cells.

At stalled replication forks, uncoupling of helicases and polymerases results in regions of exposed ssDNA, which become coated with RPA (Costanzo, 2011; Fan and Pavletich, 2012). IGF1R inhibition increased TMZ-induced RPA focus formation but not peak γ-H2AX and 53BP1 foci numbers, which did not coincide with peak RAD51 foci formation. It is possible therefore that the relationship between these DDR mediators may represent their kinetics at stalled replication forks rather than DSBs. Neutral comet assay or pulse-field gel electrophoresis (PFGE) could be used to determine whether IGF1R inhibition is affecting TMZ induced DSB formation, and if performed in parallel with alkaline comet assay could assess whether SSB formation is affected (Bryant, 2012; Collins et al., 2008). DNA fibre analysis would be helpful in assessing if IGF1R inhibition affects TMZ induced DNA replication stress (Frum et al., 2013). Alternatively, isolation of protein on nascent DNA (iPOND) can be used to determine if IGF1R inhibition affects the recruitment or post-translational modification of proteins acting at TMZ induced stalled replication forks (Sirbu et al., 2011).

The results presented in chapter 4 also showed that AZ12253801, impaired the resolution of RAD51 foci in TMZ treated cells. This finding, together with demonstrating that IGF1R inhibition sensitized to PARP inhibition, supports other work from our group which suggested that IGF1R inhibited cells have a reduced ability to repair DSBs by homologous recombination (HR) (Bryant et al., 2005; Chitnis et al., 2013; Farmer et al., 2005; Turney et al., 2012). IGF1R inhibition also appeared to impair RAD54-chromatin binding in TMZ treated cells. RAD54 facilitates RAD51 function (Agarwal et al., 2011) and it is possible that a defect in RAD54 may explain the persistence of TMZ-induced

RAD51 foci in IGF1R inhibited cells. Thus the results shown here may suggest that excessive end-resection may direct IGF-1R inhibited cells towards HR and away from NHEJ, but that cells may be unable to complete HR because of persistence of RAD51 on chromatin. Future work would also include assessment of the effects of IGF1R inhibition on other important mediators of RAD51 function and resolution, such as BRCA1, BRCA2 or RPA phosphorylation (Oakley and Patrick, 2010) (Holloman, 2011; Lord and Ashworth, 2007) (Sorensen et al., 2005; Zhang et al., 2004).

Work presented in Chapter 5 demonstrated that melanoma cells with functional p53 were more sensitive to IGF1R inhibition. This may be important clinically in identifying patients who are likely to benefit from IGF1R inhibitors. Chapter 5 also investigated the feasibility of combining IGF1R inhibition with TMZ treatment in a preclinical study. *In vitro* data showed that IGF1R inhibition following TMZ treatment caused greater reduction in melanoma cell survival than either simultaneous or the reverse combination treatment. *In vivo,* the combination of IGF1R inhibition with TMZ was tolerated and resulted in a significant reduction in tumour growth and prolonged survival compared with control or single agent treatment groups. These results suggest that there may be merit in clinical testing of the tolerability and efficacy of the combination of IGF1R inhibition with TMZ or DTIC in patients with advanced melanoma and that TMZ treatment preceding IGF1R inhibitor treatment may be the most effective treatment schedule.

TMZ penetrates the blood brain barrier and is licensed for use in patients with newly diagnosed GBM (Cohen et al., 2005). In addition, IGF1R inhibition was shown to cause antitumour activity in both *in vitro* and *in vivo* GBM models

(Hagerstrand et al., 2010; Yin et al., 2010). One study demonstrated that simultaneous treatment of TMZ with an anti-IGF1R antibody reduced neuroblastoma cell proliferation and caused significant tumour growth delay *in vivo*. It may therefore be worthwhile testing the combination of linsitinib and TMZ in a GBM model *in vitro* and *in vivo* to determine the feasibility of this combination in patients with GBM.

This thesis provides evidence supporting IGF1R inhibition as a possible therapeutic option in overcoming alkylating drug resistance in malignant melanoma regardless of BRAF mutation status, by a mechanism that appears to affect homologous recombination DNA repair.

Future Directions

1. Determine the applicability of IGF1R expression and activation along with MGMT expression as possible biomarkers of alkylating drug resistance. Clinical melanoma tissue samples derived from TMZ or DTIC treated patients could be assessed by either IHC or ELISA to
2. Assess further the effect of IGF1R inhibition on BER by clonogenic assay in MMS treated melanoma cells.
3. Determine whether IGF1R inhibition is affecting the repair of DSBs using comet assay or PFGE, as well as whether it affects the recovery of stalled replication forks by DNA fibre analysis or iPOND in melanoma cells.

4. Determine the effect of IGF1R inhibition on mediators of RAD51 resolution such as RAD51 paralogues in melanoma.
5. Clinical evaluation of tolerability and effectiveness linsitinib in overcoming alkylating drug resistance in advanced melanoma.
6. Evaluate whether combination of IGF1R inhibition with TMZ is beneficial in other cancer types in which alkylating agent therapy is commonly used, such as GBM.

Bibliography

Adams, T.E., Epa, V.C., Garrett, T.P., and Ward, C.W. (2000). Structure and function of the type 1 insulin-like growth factor receptor. Cellular and molecular life sciences : CMLS *57*, 1050-1093.

Agarwal, S., van Cappellen, W.A., Guenole, A., Eppink, B., Linsen, S.E., Meijering, E., Houtsmuller, A., Kanaar, R., and Essers, J. (2011). ATP-dependent and independent functions of Rad54 in genome maintenance. The Journal of cell biology *192*, 735-750.

Ahn, J.Y., Schwarz, J.K., Piwnica-Worms, H., and Canman, C.E. (2000). Threonine 68 phosphorylation by ataxia telangiectasia mutated is required for efficient activation of Chk2 in response to ionizing radiation. Cancer research *60*, 5934-5936.

Ahnesorg, P., Smith, P., and Jackson, S.P. (2006). XLF interacts with the XRCC4-DNA ligase IV complex to promote DNA nonhomologous end-joining. Cell *124*, 301-313.

Albino, A.P., Vidal, M.J., McNutt, N.S., Shea, C.R., Prieto, V.G., Nanus, D.M., Palmer, J.M., and Hayward, N.K. (1994). Mutation and expression of the p53 gene in human malignant melanoma. Melanoma research *4*, 35-45.

Aleksic, T., Chitnis, M.M., Perestenko, O.V., Gao, S., Thomas, P.H., Turner, G.D., Protheroe, A.S., Howarth, M., and Macaulay, V.M. (2010). Type 1 insulin-like growth factor receptor translocates to the nucleus of human tumor cells. Cancer research *70*, 6412-6419.

Allen, G.W., Saba, C., Armstrong, E.A., Huang, S.M., Benavente, S., Ludwig, D.L., Hicklin, D.J., and Harari, P.M. (2007). Insulin-like growth factor-I receptor signaling blockade combined with radiation. Cancer research *67*, 1155-1162.

Ascierto, P.A., and Kirkwood, J.M. (2008). Adjuvant therapy of melanoma with interferon: lessons of the past decade. Journal of translational medicine *6*, 62.

Ascierto, P.A., Kirkwood, J.M., Grob, J.J., Simeone, E., Grimaldi, A.M., Maio, M., Palmieri, G., Testori, A., Marincola, F.M., and Mozzillo, N. (2012). The role of BRAF V600 mutation in melanoma. Journal of translational medicine *10*, 85.

Atkins, M.B., Lotze, M.T., Dutcher, J.P., Fisher, R.I., Weiss, G., Margolin, K., Abrams, J., Sznol, M., Parkinson, D., Hawkins, M.*, et al.* (1999). High-dose recombinant interleukin 2 therapy for patients with metastatic melanoma: analysis of 270 patients treated between 1985 and 1993. Journal of clinical

oncology : official journal of the American Society of Clinical Oncology *17*, 2105-2116.

Augustine, C.K., Toshimitsu, H., Jung, S.H., Zipfel, P.A., Yoo, J.S., Yoshimoto, Y., Selim, M.A., Burchette, J., Beasley, G.M., McMahon, N.*, et al.* (2010). Sorafenib, a multikinase inhibitor, enhances the response of melanoma to regional chemotherapy. Molecular cancer therapeutics *9*, 2090-2101.

Augustine, C.K., Yoo, J.S., Potti, A., Yoshimoto, Y., Zipfel, P.A., Friedman, H.S., Nevins, J.R., Ali-Osman, F., and Tyler, D.S. (2009). Genomic and molecular profiling predicts response to temozolomide in melanoma. Clinical cancer research : an official journal of the American Association for Cancer Research *15*, 502-510.

Awasthi, N., Zhang, C., Ruan, W., Schwarz, M.A., and Schwarz, R.E. (2012). BMS-754807, a small-molecule inhibitor of insulin-like growth factor-1 receptor/insulin receptor, enhances gemcitabine response in pancreatic cancer. Molecular cancer therapeutics *11*, 2644-2653.

Bagrodia, S., Smeal, T., and Abraham, R.T. (2012). Mechanisms of intrinsic and acquired resistance to kinase-targeted therapies. Pigment cell & melanoma research *25*, 819-831.

Bakkenist, C.J., and Kastan, M.B. (2003). DNA damage activates ATM through intermolecular autophosphorylation and dimer dissociation. Nature *421*, 499-506.

Balajee, A.S., and Geard, C.R. (2004). Replication protein A and gamma-H2AX foci assembly is triggered by cellular response to DNA double-strand breaks. Experimental cell research *300*, 320-334.

Banath, J.P., and Olive, P.L. (2003). Expression of phosphorylated histone H2AX as a surrogate of cell killing by drugs that create DNA double-strand breaks. Cancer research *63*, 4347-4350.

Bartek, J., Falck, J., and Lukas, J. (2001). CHK2 kinase--a busy messenger. Nature reviews Molecular cell biology *2*, 877-886.

Baserga, R., Hongo, A., Rubini, M., Prisco, M., and Valentinis, B. (1997). The IGF-I receptor in cell growth, transformation and apoptosis. Biochimica et biophysica acta *1332*, F105-126.

Basu, B., Olmos, D., and de Bono, J.S. (2011). Targeting IGF-1R: throwing out the baby with the bathwater? British journal of cancer *104*, 1-3.

Beauchamp, M.C., Knafo, A., Yasmeen, A., Carboni, J.M., Gottardis, M.M., Pollak, M.N., and Gotlieb, W.H. (2009). BMS-536924 sensitizes human epithelial ovarian cancer cells to the PARP inhibitor, 3-aminobenzamide. Gynecologic oncology *115*, 193-198.

Bell, R.E., and Levy, C. (2011). The three M's: melanoma, microphthalmia-associated transcription factor and microRNA. Pigment cell & melanoma research *24*, 1088-1106.

Bennett, D.C. (2003). Human melanocyte senescence and melanoma susceptibility genes. Oncogene *22*, 3063-3069.

Bennett, D.C. (2008). How to make a melanoma: what do we know of the primary clonal events? Pigment cell & melanoma research *21*, 27-38.

Bhatia, S., Tykodi, S.S., and Thompson, J.A. (2009). Treatment of metastatic melanoma: an overview. Oncology (Williston Park) *23*, 488-496.

Bis, S., and Tsao, H. (2013). Melanoma genetics: the other side. Clinics in dermatology *31*, 148-155.

Bishop, D.T., Demenais, F., Goldstein, A.M., Bergman, W., Bishop, J.N., Bressac-de Paillerets, B., Chompret, A., Ghiorzo, P., Gruis, N., Hansson, J.*, et al.* (2002). Geographical variation in the penetrance of CDKN2A mutations for melanoma. Journal of the National Cancer Institute *94*, 894-903.

Bodzin, A.S., Wei, Z., Hurtt, R., Gu, T., and Doria, C. (2012). Gefitinib resistance in HCC mahlavu cells: upregulation of CD133 expression, activation of IGF-1R signaling pathway, and enhancement of IGF-1R nuclear translocation. Journal of cellular physiology *227*, 2947-2952.

Boeckmann, L., Nickel, A.C., Kuschal, C., Schaefer, A., Thoms, K.M., Schon, M.P., Thomale, J., and Emmert, S. (2011). Temozolomide chemoresistance heterogeneity in melanoma with different treatment regimens: DNA damage accumulation contribution. Melanoma research *21*, 206-216.

Bonner, W.M., Redon, C.E., Dickey, J.S., Nakamura, A.J., Sedelnikova, O.A., Solier, S., and Pommier, Y. (2008). GammaH2AX and cancer. Nature reviews Cancer *8*, 957-967.

Boutros, R., Lobjois, V., and Ducommun, B. (2007). CDC25 phosphatases in cancer cells: key players? Good targets? Nature reviews Cancer *7*, 495-507.

Branzei, D., and Foiani, M. (2005). The DNA damage response during DNA replication. Current opinion in cell biology *17*, 568-575.

Branzei, D., and Foiani, M. (2007). Interplay of replication checkpoints and repair proteins at stalled replication forks. DNA repair *6*, 994-1003.

Browne, B.C., Crown, J., Venkatesan, N., Duffy, M.J., Clynes, M., Slamon, D., and O'Donovan, N. (2011). Inhibition of IGF1R activity enhances response to trastuzumab in HER-2-positive breast cancer cells. Annals of oncology : official journal of the European Society for Medical Oncology / ESMO *22*, 68-73.

Bryant, H.E. (2012). DNA double-strand break damage and repair assessed by pulsed-field gel electrophoresis. Methods Mol Biol *920*, 315-321.

Bryant, H.E., Schultz, N., Thomas, H.D., Parker, K.M., Flower, D., Lopez, E., Kyle, S., Meuth, M., Curtin, N.J., and Helleday, T. (2005). Specific killing of BRCA2-deficient tumours with inhibitors of poly(ADP-ribose) polymerase. Nature *434*, 913-917.

Buck, E., Gokhale, P.C., Koujak, S., Brown, E., Eyzaguirre, A., Tao, N., Rosenfeld-Franklin, M., Lerner, L., Chiu, M.I., Wild, R.*, et al.* (2010). Compensatory insulin receptor (IR) activation on inhibition of insulin-like growth factor-1 receptor (IGF-1R): rationale for cotargeting IGF-1R and IR in cancer. Molecular cancer therapeutics *9*, 2652-2664.

Buck, E., and Mulvihill, M. (2011). Small molecule inhibitors of the IGF-1R/IR axis for the treatment of cancer. Expert opinion on investigational drugs *20*, 605-621.

Carden, C.P., Kim, E.S., Jones, R.L., Alam, S., Johnson, F., Stephens, A.W., Poondru, S., Gedrich, R., Lippman, S.M., and Kaye, S.B. (2010). Phase I study of intermittent dosing of OSI-906, a dual tyrosine kinase inhibitor of insulin-like growth factor-1 receptor (IGF-1R) and insulin receptor (IR) in patients with advanced solid tumors. Journal of clinical oncology : official journal of the American Society of Clinical Oncology *28: 15s*, suppl; abstr 2530.

Carr, A.M., and Lambert, S. (2013). Replication Stress-Induced Genome Instability: The Dark Side of Replication Maintenance by Homologous Recombination. Journal of molecular biology.

Celebi, J.T., Shendrik, I., Silvers, D.N., and Peacocke, M. (2000). Identification of PTEN mutations in metastatic melanoma specimens. Journal of medical genetics *37*, 653-657.

Chan, J.M., Stampfer, M.J., Giovannucci, E., Ma, J., and Pollak, M. (2000). Insulin-like growth factor I (IGF-I), IGF-binding protein-3 and prostate cancer risk: epidemiological studies. Growth hormone & IGF research : official journal of the Growth Hormone Research Society and the International IGF Research Society *10 Suppl A*, S32-33.

Chandarlapaty, S., Sawai, A., Scaltriti, M., Rodrik-Outmezguine, V., Grbovic-Huezo, O., Serra, V., Majumder, P.K., Baselga, J., and Rosen, N. (2011). AKT inhibition relieves feedback suppression of receptor tyrosine kinase expression and activity. Cancer cell *19*, 58-71.

Chapman, P.B., Einhorn, L.H., Meyers, M.L., Saxman, S., Destro, A.N., Panageas, K.S., Begg, C.B., Agarwala, S.S., Schuchter, L.M., Ernstoff, M.S.*, et al.* (1999). Phase III multicenter randomized trial of the Dartmouth regimen versus dacarbazine in patients with metastatic melanoma. Journal of clinical oncology : official journal of the American Society of Clinical Oncology *17*, 2745-2751.

Chapman, P.B., Hauschild, A., Robert, C., Haanen, J.B., Ascierto, P., Larkin, J., Dummer, R., Garbe, C., Testori, A., Maio, M.*, et al.* (2011). Improved

survival with vemurafenib in melanoma with BRAF V600E mutation. The New England journal of medicine *364*, 2507-2516.

Chartrain, M., Riond, J., Stennevin, A., Vandenberghe, I., Gomes, B., Lamant, L., Meyer, N., Gairin, J.E., Guilbaud, N., and Annereau, J.P. (2012). Melanoma chemotherapy leads to the selection of ABCB5-expressing cells. PloS one *7*, e36762.

Chen, K.G., Valencia, J.C., Gillet, J.P., Hearing, V.J., and Gottesman, M.M. (2009). Involvement of ABC transporters in melanogenesis and the development of multidrug resistance of melanoma. Pigment cell & melanoma research *22*, 740-749.

Chen, Z., Yang, H., and Pavletich, N.P. (2008). Mechanism of homologous recombination from the RecA-ssDNA/dsDNA structures. Nature *453*, 489-484.

Cheng, Y., Zhang, G., and Li, G. (2013). Targeting MAPK pathway in melanoma therapy. Cancer metastasis reviews.

Chipuk, J.E., Moldoveanu, T., Llambi, F., Parsons, M.J., and Green, D.R. (2010). The BCL-2 family reunion. Molecular cell *37*, 299-310.

Chitnis, M.M., Lodhia, K.A., Aleksic, T., Gao, S., Protheroe, A.S., and Macaulay, V.M. (2013). IGF-1R inhibition enhances radiosensitivity and delays double-strand break repair by both non-homologous end-joining and homologous recombination. Oncogene.

Chitnis, M.M., Yuen, J.S., Protheroe, A.S., Pollak, M., and Macaulay, V.M. (2008). The type 1 insulin-like growth factor receptor pathway. Clinical cancer research : an official journal of the American Association for Cancer Research *14*, 6364-6370.

Clemmons, D.R. (2007). Modifying IGF1 activity: an approach to treat endocrine disorders, atherosclerosis and cancer. Nature reviews Drug discovery *6*, 821-833.

Cohen, M.H., Johnson, J.R., and Pazdur, R. (2005). Food and Drug Administration Drug approval summary: temozolomide plus radiation therapy for the treatment of newly diagnosed glioblastoma multiforme. Clinical cancer research : an official journal of the American Association for Cancer Research *11*, 6767-6771.

Coit, D.G., Andtbacka, R., Anker, C.J., Bichakjian, C.K., Carson, W.E., 3rd, Daud, A., Dilawari, R.A., Dimaio, D., Guild, V., Halpern, A.C.*, et al.* (2012). Melanoma. Journal of the National Comprehensive Cancer Network : JNCCN *10*, 366-400.

Collins, A.R., Oscoz, A.A., Brunborg, G., Gaivao, I., Giovannelli, L., Kruszewski, M., Smith, C.C., and Stetina, R. (2008). The comet assay: topical issues. Mutagenesis *23*, 143-151.

Collis, S.J., DeWeese, T.L., Jeggo, P.A., and Parker, A.R. (2005). The life and death of DNA-PK. Oncogene *24*, 949-961.

Collisson, E.A., De, A., Suzuki, H., Gambhir, S.S., and Kolodney, M.S. (2003). Treatment of metastatic melanoma with an orally available inhibitor of the Ras-Raf-MAPK cascade. Cancer research *63*, 5669-5673.

Colombino, M., Capone, M., Lissia, A., Cossu, A., Rubino, C., De Giorgi, V., Massi, D., Fonsatti, E., Staibano, S., Nappi, O.*, et al.* (2012). BRAF/NRAS mutation frequencies among primary tumors and metastases in patients with melanoma. Journal of clinical oncology : official journal of the American Society of Clinical Oncology *30*, 2522-2529.

Coqueret, O. (2002). Linking cyclins to transcriptional control. Gene *299*, 35-55.

Costanzo, V. (2011). Brca2, Rad51 and Mre11: performing balancing acts on replication forks. DNA repair *10*, 1060-1065.

Crews, C.M., Alessandrini, A., and Erikson, R.L. (1992). The primary structure of MEK, a protein kinase that phosphorylates the ERK gene product. Science *258*, 478-480.

Cully, M., You, H., Levine, A.J., and Mak, T.W. (2006). Beyond PTEN mutations: the PI3K pathway as an integrator of multiple inputs during tumorigenesis. Nature reviews Cancer *6*, 184-192.

Datta, S.R., Dudek, H., Tao, X., Masters, S., Fu, H., Gotoh, Y., and Greenberg, M.E. (1997). Akt phosphorylation of BAD couples survival signals to the cell-intrinsic death machinery. Cell *91*, 231-241.

Davies, H., Bignell, G.R., Cox, C., Stephens, P., Edkins, S., Clegg, S., Teague, J., Woffendin, H., Garnett, M.J., Bottomley, W.*, et al.* (2002). Mutations of the BRAF gene in human cancer. Nature *417*, 949-954.

de Murcia, J.M., Niedergang, C., Trucco, C., Ricoul, M., Dutrillaux, B., Mark, M., Oliver, F.J., Masson, M., Dierich, A., LeMeur, M.*, et al.* (1997). Requirement of poly(ADP-ribose) polymerase in recovery from DNA damage in mice and in cells. Proceedings of the National Academy of Sciences of the United States of America *94*, 7303-7307.

Denley, A., Cosgrove, L.J., Booker, G.W., Wallace, J.C., and Forbes, B.E. (2005). Molecular interactions of the IGF system. Cytokine & growth factor reviews *16*, 421-439.

DiPaola, R.S. (2002). To arrest or not to G(2)-M Cell-cycle arrest : commentary re: A. K. Tyagi et al., Silibinin strongly synergizes human prostate carcinoma DU145 cells to doxorubicin-induced growth inhibition, G(2)-M arrest, and apoptosis. Clin. cancer res., 8: 3512-3519, 2002. Clinical cancer research : an official journal of the American Association for Cancer Research *8*, 3311-3314.

Dolan, M.E., and Pegg, A.E. (1997). O6-benzylguanine and its role in chemotherapy. Clinical cancer research : an official journal of the American Association for Cancer Research *3*, 837-847.

Donzelli, M., and Draetta, G.F. (2003). Regulating mammalian checkpoints through Cdc25 inactivation. EMBO reports *4*, 671-677.

Dronca, R.S., Allred, J.B., Perez, D.G., Nevala, W.K., Lieser, E.A., Thompson, M., Maples, W.J., Creagan, E.T., Pockaj, B.A., Kaur, J.S.*, et al.* (2013). Phase II Study of Temozolomide (TMZ) and Everolimus (RAD001) Therapy for Metastatic Melanoma: A North Central Cancer Treatment Group Study, N0675. American journal of clinical oncology.

Ducker, G.S., Atreya, C.E., Simko, J.P., Hom, Y.K., Matli, M.R., Benes, C.H., Hann, B., Nakakura, E.K., Bergsland, E.K., Donner, D.B.*, et al.* (2013). Incomplete inhibition of phosphorylation of 4E-BP1 as a mechanism of primary resistance to ATP-competitive mTOR inhibitors. Oncogene.

Duncan, T., Trewick, S.C., Koivisto, P., Bates, P.A., Lindahl, T., and Sedgwick, B. (2002). Reversal of DNA alkylation damage by two human dioxygenases. Proceedings of the National Academy of Sciences of the United States of America *99*, 16660-16665.

Egan, S.E., Giddings, B.W., Brooks, M.W., Buday, L., Sizeland, A.M., and Weinberg, R.A. (1993). Association of Sos Ras exchange protein with Grb2 is implicated in tyrosine kinase signal transduction and transformation. Nature *363*, 45-51.

Eggermont, A.M., Suciu, S., Santinami, M., Testori, A., Kruit, W.H., Marsden, J., Punt, C.J., Sales, F., Gore, M., Mackie, R.*, et al.* (2008). Adjuvant therapy with pegylated interferon alfa-2b versus observation alone in resected stage III melanoma: final results of EORTC 18991, a randomised phase III trial. Lancet *372*, 117-126.

Elder, D.E. (2006). Pathology of melanoma. Clinical cancer research : an official journal of the American Association for Cancer Research *12*, 2308s-2311s.

Elder, R.H., Jansen, J.G., Weeks, R.J., Willington, M.A., Deans, B., Watson, A.J., Mynett, K.J., Bailey, J.A., Cooper, D.P., Rafferty, J.A.*, et al.* (1998). Alkylpurine-DNA-N-glycosylase knockout mice show increased susceptibility to induction of mutations by methyl methanesulfonate. Molecular and cellular biology *18*, 5828-5837.

Engelman, J.A., Luo, J., and Cantley, L.C. (2006). The evolution of phosphatidylinositol 3-kinases as regulators of growth and metabolism. Nature reviews Genetics *7*, 606-619.

Engelward, B.P., Weeda, G., Wyatt, M.D., Broekhof, J.L., de Wit, J., Donker, I., Allan, J.M., Gold, B., Hoeijmakers, J.H., and Samson, L.D. (1997). Base excision repair deficient mice lacking the Aag alkyladenine DNA glycosylase.

Proceedings of the National Academy of Sciences of the United States of America *94*, 13087-13092.

Esashi, F., Christ, N., Gannon, J., Liu, Y., Hunt, T., Jasin, M., and West, S.C. (2005). CDK-dependent phosphorylation of BRCA2 as a regulatory mechanism for recombinational repair. Nature *434*, 598-604.

Esashi, F., Galkin, V.E., Yu, X., Egelman, E.H., and West, S.C. (2007). Stabilization of RAD51 nucleoprotein filaments by the C-terminal region of BRCA2. Nature structural & molecular biology *14*, 468-474.

Escribano-Diaz, C., Orthwein, A., Fradet-Turcotte, A., Xing, M., Young, J.T., Tkac, J., Cook, M.A., Rosebrock, A.P., Munro, M., Canny, M.D.*, et al.* (2013). A Cell Cycle-Dependent Regulatory Circuit Composed of 53BP1-RIF1 and BRCA1-CtIP Controls DNA Repair Pathway Choice. Molecular cell *49*, 872-883.

Esteller, M., Garcia-Foncillas, J., Andion, E., Goodman, S.N., Hidalgo, O.F., Vanaclocha, V., Baylin, S.B., and Herman, J.G. (2000). Inactivation of the DNA-repair gene MGMT and the clinical response of gliomas to alkylating agents. The New England journal of medicine *343*, 1350-1354.

Esteller, M., and Herman, J.G. (2004). Generating mutations but providing chemosensitivity: the role of O6-methylguanine DNA methyltransferase in human cancer. Oncogene *23*, 1-8.

Evans, T., Lindsay, C.R., Chan, E., Tait, B., Michael, S.A., S. Day, S., Stephens, A.W., Franke, A., Poondru, S., and Puzanov, I. (2010). Phase I dose-escalation study of continuous oral dosing of OSI-906, a dual tyrosine kinase inhibitor of insulin-like growth factor-1 receptor (IGF-1R) and insulin receptor (IR), in patients with advanced solid tumors. Journal of clinical oncology : official journal of the American Society of Clinical Oncology *28: 15s*, suppl; abstr 2531.

Fan, J., and Pavletich, N.P. (2012). Structure and conformational change of a replication protein A heterotrimer bound to ssDNA. Genes & development *26*, 2337-2347.

Farmer, H., McCabe, N., Lord, C.J., Tutt, A.N., Johnson, D.A., Richardson, T.B., Santarosa, M., Dillon, K.J., Hickson, I., Knights, C.*, et al.* (2005). Targeting the DNA repair defect in BRCA mutant cells as a therapeutic strategy. Nature *434*, 917-921.

Feldser, D., Agani, F., Iyer, N.V., Pak, B., Ferreira, G., and Semenza, G.L. (1999). Reciprocal positive regulation of hypoxia-inducible factor 1alpha and insulin-like growth factor 2. Cancer research *59*, 3915-3918.

Flaherty, K.T., Lee, S.J., Zhao, F., Schuchter, L.M., Flaherty, L., Kefford, R., Atkins, M.B., Leming, P., and Kirkwood, J.M. (2013). Phase III trial of carboplatin and paclitaxel with or without sorafenib in metastatic melanoma.

Journal of clinical oncology : official journal of the American Society of Clinical Oncology *31*, 373-379.

Flaherty, K.T., Robert, C., Hersey, P., Nathan, P., Garbe, C., Milhem, M., Demidov, L.V., Hassel, J.C., Rutkowski, P., Mohr, P.*, et al.* (2012). Improved survival with MEK inhibition in BRAF-mutated melanoma. The New England journal of medicine *367*, 107-114.

Fogal, V., Hsieh, J.K., Royer, C., Zhong, S., and Lu, X. (2005). Cell cycle-dependent nuclear retention of p53 by E2F1 requires phosphorylation of p53 at Ser315. The EMBO journal *24*, 2768-2782.

Fradet-Turcotte, A., Canny, M.D., Escribano-Diaz, C., Orthwein, A., Leung, C.C., Huang, H., Landry, M.C., Kitevski-LeBlanc, J., Noordermeer, S.M., Sicheri, F.*, et al.* (2013). 53BP1 is a reader of the DNA-damage-induced H2A Lys 15 ubiquitin mark. Nature *499*, 50-54.

Frank, N.Y., Margaryan, A., Huang, Y., Schatton, T., Waaga-Gasser, A.M., Gasser, M., Sayegh, M.H., Sadee, W., and Frank, M.H. (2005). ABCB5-mediated doxorubicin transport and chemoresistance in human malignant melanoma. Cancer research *65*, 4320-4333.

Franke, T.F., Hornik, C.P., Segev, L., Shostak, G.A., and Sugimoto, C. (2003). PI3K/Akt and apoptosis: size matters. Oncogene *22*, 8983-8998.

Franken, N.A., Rodermond, H.M., Stap, J., Haveman, J., and van Bree, C. (2006). Clonogenic assay of cells in vitro. Nature protocols *1*, 2315-2319.

Frum, R.A., Deb, S., and Deb, S.P. (2013). Use of the DNA fiber spreading technique to detect the effects of mutant p53 on DNA replication. Methods Mol Biol *962*, 147-155.

Fu, D., Calvo, J.A., and Samson, L.D. (2012). Balancing repair and tolerance of DNA damage caused by alkylating agents. Nature reviews Cancer *12*, 104-120.

Furlanetto, R.W., Harwell, S.E., and Baggs, R.B. (1993). Effects of insulin-like growth factor receptor inhibition on human melanomas in culture and in athymic mice. Cancer research *53*, 2522-2526.

Gandini, S., Sera, F., Cattaruzza, M.S., Pasquini, P., Abeni, D., Boyle, P., and Melchi, C.F. (2005a). Meta-analysis of risk factors for cutaneous melanoma: I. Common and atypical naevi. Eur J Cancer *41*, 28-44.

Gandini, S., Sera, F., Cattaruzza, M.S., Pasquini, P., Picconi, O., Boyle, P., and Melchi, C.F. (2005b). Meta-analysis of risk factors for cutaneous melanoma: II. Sun exposure. Eur J Cancer *41*, 45-60.

Gandini, S., Sera, F., Cattaruzza, M.S., Pasquini, P., Zanetti, R., Masini, C., Boyle, P., and Melchi, C.F. (2005c). Meta-analysis of risk factors for cutaneous melanoma: III. Family history, actinic damage and phenotypic factors. Eur J Cancer *41*, 2040-2059.

Gao, J., Chang, Y.S., Jallal, B., and Viner, J. (2012). Targeting the insulin-like growth factor axis for the development of novel therapeutics in oncology. Cancer research *72*, 3-12.

Garraway, L.A., Widlund, H.R., Rubin, M.A., Getz, G., Berger, A.J., Ramaswamy, S., Beroukhim, R., Milner, D.A., Granter, S.R., Du, J.*, et al.* (2005). Integrative genomic analyses identify MITF as a lineage survival oncogene amplified in malignant melanoma. Nature *436*, 117-122.

Geoerger, B., Brasme, J.F., Daudigeos-Dubus, E., Opolon, P., Venot, C., Debussche, L., Vrignaud, P., and Vassal, G. (2010). Anti-insulin-like growth factor 1 receptor antibody EM164 (murine AVE1642) exhibits anti-tumour activity alone and in combination with temozolomide against neuroblastoma. Eur J Cancer *46*, 3251-3262.

Ghosh, P., Dahms, N.M., and Kornfeld, S. (2003). Mannose 6-phosphate receptors: new twists in the tale. Nature reviews Molecular cell biology *4*, 202-212.

Girnita, L., Girnita, A., and Larsson, O. (2003). Mdm2-dependent ubiquitination and degradation of the insulin-like growth factor 1 receptor. Proceedings of the National Academy of Sciences of the United States of America *100*, 8247-8252.

Gluckman, P.D., and Pinal, C.S. (2003). Regulation of fetal growth by the somatotrophic axis. The Journal of nutrition *133*, 1741S-1746S.

Goh, A.M., Coffill, C.R., and Lane, D.P. (2011). The role of mutant p53 in human cancer. The Journal of pathology *223*, 116-126.

Goodarzi, A.A., Yu, Y., Riballo, E., Douglas, P., Walker, S.A., Ye, R., Harer, C., Marchetti, C., Morrice, N., Jeggo, P.A.*, et al.* (2006). DNA-PK autophosphorylation facilitates Artemis endonuclease activity. The EMBO journal *25*, 3880-3889.

Gorlia, T., van den Bent, M.J., Hegi, M.E., Mirimanoff, R.O., Weller, M., Cairncross, J.G., Eisenhauer, E., Belanger, K., Brandes, A.A., Allgeier, A.*, et al.* (2008). Nomograms for predicting survival of patients with newly diagnosed glioblastoma: prognostic factor analysis of EORTC and NCIC trial 26981-22981/CE.3. The lancet oncology *9*, 29-38.

Gottlieb, T.M., and Jackson, S.P. (1993). The DNA-dependent protein kinase: requirement for DNA ends and association with Ku antigen. Cell *72*, 131-142.

Gray-Schopfer, V., Wellbrock, C., and Marais, R. (2007). Melanoma biology and new targeted therapy. Nature *445*, 851-857.

Greshock, J., Bachman, K.E., Degenhardt, Y.Y., Jing, J., Wen, Y.H., Eastman, S., McNeil, E., Moy, C., Wegrzyn, R., Auger, K.*, et al.* (2010). Molecular target class is predictive of in vitro response profile. Cancer research *70*, 3677-3686.

Ha, L., Merlino, G., and Sviderskaya, E.V. (2008). Melanomagenesis: overcoming the barrier of melanocyte senescence. Cell Cycle *7*, 1944-1948.

Hagerstrand, D., Lindh, M.B., Pena, C., Garcia-Echeverria, C., Nister, M., Hofmann, F., and Ostman, A. (2010). PI3K/PTEN/Akt pathway status affects the sensitivity of high-grade glioma cell cultures to the insulin-like growth factor-1 receptor inhibitor NVP-AEW541. Neuro-oncology *12*, 967-975.

Hankinson, S.E., Willett, W.C., Colditz, G.A., Hunter, D.J., Michaud, D.S., Deroo, B., Rosner, B., Speizer, F.E., and Pollak, M. (1998). Circulating concentrations of insulin-like growth factor-I and risk of breast cancer. Lancet *351*, 1393-1396.

Harrison, K.L., Wood, M., Lees, N.P., Hall, C.N., Margison, G.P., and Povey, A.C. (2001). Development and application of a sensitive and rapid immunoassay for the quantitation of N7-methyldeoxyguanosine in DNA samples. Chem Res Toxicol *14*, 295-301.

Hartlerode, A.J., and Scully, R. (2009). Mechanisms of double-strand break repair in somatic mammalian cells. The Biochemical journal *423*, 157-168.

Hegi, M.E., Diserens, A.C., Gorlia, T., Hamou, M.F., de Tribolet, N., Weller, M., Kros, J.M., Hainfellner, J.A., Mason, W., Mariani, L.*, et al.* (2005). MGMT gene silencing and benefit from temozolomide in glioblastoma. The New England journal of medicine *352*, 997-1003.

Hellawell, G.O., Turner, G.D., Davies, D.R., Poulsom, R., Brewster, S.F., and Macaulay, V.M. (2002). Expression of the type 1 insulin-like growth factor receptor is up-regulated in primary prostate cancer and commonly persists in metastatic disease. Cancer research *62*, 2942-2950.

Helleday, T., Lo, J., van Gent, D.C., and Engelward, B.P. (2007). DNA double-strand break repair: from mechanistic understanding to cancer treatment. DNA repair *6*, 923-935.

Hocker, T., and Tsao, H. (2007). Ultraviolet radiation and melanoma: a systematic review and analysis of reported sequence variants. Human mutation *28*, 578-588.

Hodi, F.S., O'Day, S.J., McDermott, D.F., Weber, R.W., Sosman, J.A., Haanen, J.B., Gonzalez, R., Robert, C., Schadendorf, D., Hassel, J.C.*, et al.* (2010). Improved survival with ipilimumab in patients with metastatic melanoma. The New England journal of medicine *363*, 711-723.

Hoek, K.S., and Goding, C.R. (2010). Cancer stem cells versus phenotype-switching in melanoma. Pigment cell & melanoma research *23*, 746-759.

Holloman, W.K. (2011). Unraveling the mechanism of BRCA2 in homologous recombination. Nature structural & molecular biology *18*, 748-754.

Homet, B., and Ribas, A. (2013). New Drug Targets in Metastatic Melanoma. The Journal of pathology.

Hou, X., Huang, F., Macedo, L.F., Harrington, S.C., Reeves, K.A., Greer, A., Finckenstein, F.G., Brodie, A., Gottardis, M.M., Carboni, J.M.*, et al.* (2011). Dual IGF-1R/InsR inhibitor BMS-754807 synergizes with hormonal agents in treatment of estrogen-dependent breast cancer. Cancer research *71*, 7597-7607.

Hwa, V., Oh, Y., and Rosenfeld, R.G. (1999). The insulin-like growth factor-binding protein (IGFBP) superfamily. Endocrine reviews *20*, 761-787.

Ibrahim, N., and Haluska, F.G. (2009). Molecular pathogenesis of cutaneous melanocytic neoplasms. Annual review of pathology *4*, 551-579.

Iliakis, G., Wang, Y., Guan, J., and Wang, H. (2003). DNA damage checkpoint control in cells exposed to ionizing radiation. Oncogene *22*, 5834-5847.

Inamdar, G.S., Madhunapantula, S.V., and Robertson, G.P. (2010). Targeting the MAPK pathway in melanoma: why some approaches succeed and other fail. Biochemical pharmacology *80*, 624-637.

Iwasa, T., Okamoto, I., Suzuki, M., Hatashita, E., Yamada, Y., Fukuoka, M., Ono, K., and Nakagawa, K. (2009). Inhibition of insulin-like growth factor 1 receptor by CP-751,871 radiosensitizes non-small cell lung cancer cells. Clinical cancer research : an official journal of the American Association for Cancer Research *15*, 5117-5125.

Jackson, P.E., Cooper, D.P., Meyer, T.A., Wood, M., Povey, A.C., and Margison, G.P. (2000). Formation and persistence of O(6)-methylguanine in the mouse colon following treatment with 1,2-dimethylhydrazine as measured by an O(6)-alkylguanine-DNA alkyltransferase inactivation assay. Toxicology letters *115*, 205-212.

Jansen, B., Wacheck, V., Heere-Ress, E., Schlagbauer-Wadl, H., Hoeller, C., Lucas, T., Hoermann, M., Hollenstein, U., Wolff, K., and Pehamberger, H. (2000). Chemosensitisation of malignant melanoma by BCL2 antisense therapy. Lancet *356*, 1728-1733.

Jelezcova, E., Trivedi, R.N., Wang, X.H., Tang, J.B., Brown, A.R., Goellner, E.M., Schamus, S., Fornsaglio, J.L., and Sobol, R.W. (2010). Parp1 activation in mouse embryonic fibroblasts promotes Pol beta-dependent cellular hypersensitivity to alkylation damage. Mutation research *686*, 57-67.

Jiricny, J. (2006). The multifaceted mismatch-repair system. Nature reviews Molecular cell biology *7*, 335-346.

Jones, R.M., and Petermann, E. (2012). Replication fork dynamics and the DNA damage response. The Biochemical journal *443*, 13-26.

Kaidi, A., Weinert, B.T., Choudhary, C., and Jackson, S.P. (2010). Human SIRT6 promotes DNA end resection through CtIP deacetylation. Science *329*, 1348-1353.

Kaina, B., Christmann, M., Naumann, S., and Roos, W.P. (2007). MGMT: key node in the battle against genotoxicity, carcinogenicity and apoptosis induced by alkylating agents. DNA repair *6*, 1079-1099.

Kaina, B., Fritz, G., Mitra, S., and Coquerelle, T. (1991). Transfection and expression of human O6-methylguanine-DNA methyltransferase (MGMT) cDNA in Chinese hamster cells: the role of MGMT in protection against the genotoxic effects of alkylating agents. Carcinogenesis *12*, 1857-1867.

Kanter-Lewensohn, L., Dricu, A., Girnita, L., Wejde, J., and Larsson, O. (2000). Expression of insulin-like growth factor-1 receptor (IGF-1R) and p27Kip1 in melanocytic tumors: a potential regulatory role of IGF-1 pathway in distribution of p27Kip1 between different cyclins. Growth Factors *17*, 193-202.

Karasic, T.B., Hei, T.K., and Ivanov, V.N. (2010). Disruption of IGF-1R signaling increases TRAIL-induced apoptosis: a new potential therapy for the treatment of melanoma. Experimental cell research *316*, 1994-2007.

Kauffmann, A., Rosselli, F., Lazar, V., Winnepenninckx, V., Mansuet-Lupo, A., Dessen, P., van den Oord, J.J., Spatz, A., and Sarasin, A. (2008). High expression of DNA repair pathways is associated with metastasis in melanoma patients. Oncogene *27*, 565-573.

Kawanami, T., Takiguchi, S., Ikeda, N., and Funakoshi, A. (2012). A humanized anti-IGF-1R monoclonal antibody (R1507) and/or metformin enhance gemcitabine-induced apoptosis in pancreatic cancer cells. Oncology reports *27*, 867-872.

Kawate, H., Itoh, R., Sakumi, K., Nakabeppu, Y., Tsuzuki, T., Ide, F., Ishikawa, T., Noda, T., Nawata, H., and Sekiguchi, M. (2000). A defect in a single allele of the Mlh1 gene causes dissociation of the killing and tumorigenic actions of an alkylating carcinogen in methyltransferase-deficient mice. Carcinogenesis *21*, 301-305.

Kim, J.G., Kang, M.J., Yoon, Y.K., Kim, H.P., Park, J., Song, S.H., Han, S.W., Park, J.W., Kang, G.H., Kang, K.W.*, et al.* (2012). Heterodimerization of glycosylated insulin-like growth factor-1 receptors and insulin receptors in cancer cells sensitive to anti-IGF1R antibody. PloS one *7*, e33322.

Kirkwood, J.M., Ibrahim, J.G., Sondak, V.K., Richards, J., Flaherty, L.E., Ernstoff, M.S., Smith, T.J., Rao, U., Steele, M., and Blum, R.H. (2000). High- and low-dose interferon alfa-2b in high-risk melanoma: first analysis of intergroup trial E1690/S9111/C9190. Journal of clinical oncology : official journal of the American Society of Clinical Oncology *18*, 2444-2458.

Kirkwood, J.M., Strawderman, M.H., Ernstoff, M.S., Smith, T.J., Borden, E.C., and Blum, R.H. (1996). Interferon alfa-2b adjuvant therapy of high-risk resected cutaneous melanoma: the Eastern Cooperative Oncology Group Trial EST 1684. Journal of clinical oncology : official journal of the American Society of Clinical Oncology *14*, 7-17.

Kitange, G.J., Carlson, B.L., Schroeder, M.A., Grogan, P.T., Lamont, J.D., Decker, P.A., Wu, W., James, C.D., and Sarkaria, J.N. (2009). Induction of MGMT expression is associated with temozolomide resistance in glioblastoma xenografts. Neuro-oncology *11*, 281-291.

Klapacz, J., Meira, L.B., Luchetti, D.G., Calvo, J.A., Bronson, R.T., Edelmann, W., and Samson, L.D. (2009). O6-methylguanine-induced cell death involves exonuclease 1 as well as DNA mismatch recognition in vivo. Proceedings of the National Academy of Sciences of the United States of America *106*, 576-581.

Kohn, A.D., Summers, S.A., Birnbaum, M.J., and Roth, R.A. (1996). Expression of a constitutively active Akt Ser/Thr kinase in 3T3-L1 adipocytes stimulates glucose uptake and glucose transporter 4 translocation. The Journal of biological chemistry *271*, 31372-31378.

Kondo, N., Takahashi, A., Ono, K., and Ohnishi, T. (2010). DNA damage induced by alkylating agents and repair pathways. Journal of nucleic acids *2010*, 543531.

Kozlowski, J.M., Hart, I.R., Fidler, I.J., and Hanna, N. (1984). A human melanoma line heterogeneous with respect to metastatic capacity in athymic nude mice. Journal of the National Cancer Institute *72*, 913-917.

Krejci, L., Altmannova, V., Spirek, M., and Zhao, X. (2012). Homologous recombination and its regulation. Nucleic acids research *40*, 5795-5818.

Kubota, Y., Nash, R.A., Klungland, A., Schar, P., Barnes, D.E., and Lindahl, T. (1996). Reconstitution of DNA base excision-repair with purified human proteins: interaction between DNA polymerase beta and the XRCC1 protein. The EMBO journal *15*, 6662-6670.

Kurmasheva, R.T., and Houghton, P.J. (2006). IGF-I mediated survival pathways in normal and malignant cells. Biochimica et biophysica acta *1766*, 1-22.

Kushnir, I., and Merimsky, O. (2013). The evolution in melanoma treatment as a reflection of precision-oriented medicine. Oncology letters *5*, 424-426.

Laron, Z., Klinger, B., Erster, B., and Silbergeld, A. (1989). Serum GH binding protein activities identifies the heterozygous carriers for Laron type dwarfism. Acta endocrinologica *121*, 603-608.

Larsson, O., Girnita, A., and Girnita, L. (2005). Role of insulin-like growth factor 1 receptor signalling in cancer. British journal of cancer *92*, 2097-2101.

Lavin, M.F., Delia, D., and Chessa, L. (2006). ATM and the DNA damage response. Workshop on ataxia-telangiectasia and related syndromes. EMBO reports *7*, 154-160.

Lee, C., Collichio, F., Ollila, D., and Moschos, S. (2013). Historical review of melanoma treatment and outcomes. Clinics in dermatology *31*, 141-147.

Lee, S.M., Thatcher, N., and Margison, G.P. (1991). O6-alkylguanine-DNA alkyltransferase depletion and regeneration in human peripheral lymphocytes following dacarbazine and fotemustine. Cancer research *51*, 619-623.

Leif, R.C., Stein, J.H., and Zucker, R.M. (2004). A short history of the initial application of anti-5-BrdU to the detection and measurement of S phase. Cytometry Part A : the journal of the International Society for Analytical Cytology *58*, 45-52.

Lens, M.B., and Dawes, M. (2003). Isolated limb perfusion with melphalan in the treatment of malignant melanoma of the extremities: a systematic review of randomised controlled trials. The lancet oncology *4*, 359-364.

Liang, J., and Slingerland, J.M. (2003). Multiple roles of the PI3K/PKB (Akt) pathway in cell cycle progression. Cell Cycle *2*, 339-345.

Liu, J., Xu, L., Sandler, S.J., and Marians, K.J. (1999). Replication fork assembly at recombination intermediates is required for bacterial growth. Proceedings of the National Academy of Sciences of the United States of America *96*, 3552-3555.

Liu, J.P., Baker, J., Perkins, A.S., Robertson, E.J., and Efstratiadis, A. (1993). Mice carrying null mutations of the genes encoding insulin-like growth factor I (Igf-1) and type 1 IGF receptor (Igf1r). Cell *75*, 59-72.

Liu, Q., Guntuku, S., Cui, X.S., Matsuoka, S., Cortez, D., Tamai, K., Luo, G., Carattini-Rivera, S., DeMayo, F., Bradley, A.*, et al.* (2000). Chk1 is an essential kinase that is regulated by Atr and required for the G(2)/M DNA damage checkpoint. Genes & development *14*, 1448-1459.

Long, G.V., Menzies, A.M., Nagrial, A.M., Haydu, L.E., Hamilton, A.L., Mann, G.J., Hughes, T.M., Thompson, J.F., Scolyer, R.A., and Kefford, R.F. (2011). Prognostic and clinicopathologic associations of oncogenic BRAF in metastatic melanoma. Journal of clinical oncology : official journal of the American Society of Clinical Oncology *29*, 1239-1246.

Long, X., Lin, Y., Ortiz-Vega, S., Yonezawa, K., and Avruch, J. (2005). Rheb binds and regulates the mTOR kinase. Current biology : CB *15*, 702-713.

Lord, C.J., and Ashworth, A. (2007). RAD51, BRCA2 and DNA repair: a partial resolution. Nature structural & molecular biology *14*, 461-462.

Lottersberger, F., Bothmer, A., Robbiani, D.F., Nussenzweig, M.C., and de Lange, T. (2013). Role of 53BP1 oligomerization in regulating double-strand break repair. Proceedings of the National Academy of Sciences of the United States of America *110*, 2146-2151.

Lu, M., Breyssens, H., Salter, V., Zhong, S., Hu, Y., Baer, C., Ratnayaka, I., Sullivan, A., Brown, N.R., Endicott, J.*, et al.* (2013). Restoring p53 function in human melanoma cells by inhibiting MDM2 and cyclin B1/CDK1-phosphorylated nuclear iASPP. Cancer cell *23*, 618-633.

Ma, S., Egyhazi, S., Ueno, T., Lindholm, C., Kreklau, E.L., Stierner, U., Ringborg, U., and Hansson, J. (2003). O6-methylguanine-DNA-methyltransferase expression and gene polymorphisms in relation to chemotherapeutic response in metastatic melanoma. British journal of cancer *89*, 1517-1523.

Ma, X.M., and Blenis, J. (2009). Molecular mechanisms of mTOR-mediated translational control. Nature reviews Molecular cell biology *10*, 307-318.

Ma, Y., Pannicke, U., Schwarz, K., and Lieber, M.R. (2002). Hairpin opening and overhang processing by an Artemis/DNA-dependent protein kinase complex in nonhomologous end joining and V(D)J recombination. Cell *108*, 781-794.

Macaulay, V.M., Middleton, M.R., Eckhardt, S.G., Juergens, R.A., Rudin, C.A., Manukyants, A., Gogov, S., Poondru, S., Gedrich, R., and Gadgeel, S.M. (2011). Phase I study of OSI-906, dual tyrosine kinase inhibitor of insulin-like growth factor-1 receptor (IGF-1R) and insulin receptor (IR) in combination with erlotinib (E) in patients with advanced solid tumors. Journal of clinical oncology : official journal of the American Society of Clinical Oncology *29*, suppl; abstr 3098.

Macaulay, V.M., Salisbury, A.J., Bohula, E.A., Playford, M.P., Smorodinsky, N.I., and Shiloh, Y. (2001). Downregulation of the type 1 insulin-like growth factor receptor in mouse melanoma cells is associated with enhanced radiosensitivity and impaired activation of Atm kinase. Oncogene *20*, 4029-4040.

Maio, M., Di Giacomo, A.M., Robert, C., and Eggermont, A.M. (2013). Update on the role of ipilimumab in melanoma and first data on new combination therapies. Current opinion in oncology *25*, 166-172.

Manning, B.D., and Cantley, L.C. (2007). AKT/PKB signaling: navigating downstream. Cell *129*, 1261-1274.

Margison, G.P., Povey, A.C., Kaina, B., and Santibanez Koref, M.F. (2003). Variability and regulation of O6-alkylguanine-DNA alkyltransferase. Carcinogenesis *24*, 625-635.

Marsden, J.R., Newton-Bishop, J.A., Burrows, L., Cook, M., Corrie, P.G., Cox, N.H., Gore, M.E., Lorigan, P., MacKie, R., Nathan, P.*, et al.* (2010a). Revised U.K. guidelines for the management of cutaneous melanoma 2010. The British journal of dermatology *163*, 238-256.

Marsden, J.R., Newton-Bishop, J.A., Burrows, L., Cook, M., Corrie, P.G., Cox, N.H., Gore, M.E., Lorigan, P., Mackie, R., Nathan, P.*, et al.* (2010b). Revised UK guidelines for the management of cutaneous melanoma 2010. Journal of plastic, reconstructive & aesthetic surgery : JPRAS *63*, 1401-1419.

Massoner, P., Ladurner-Rennau, M., Eder, I.E., and Klocker, H. (2010). Insulin-like growth factors and insulin control a multifunctional signalling

network of significant importance in cancer. British journal of cancer *103*, 1479-1484.

Matsumoto, Y., and Kim, K. (1995). Excision of deoxyribose phosphate residues by DNA polymerase beta during DNA repair. Science *269*, 699-702.

Mayo, L.D., Turchi, J.J., and Berberich, S.J. (1997). Mdm-2 phosphorylation by DNA-dependent protein kinase prevents interaction with p53. Cancer research *57*, 5013-5016.

McDermott, D.F., Sosman, J.A., Gonzalez, R., Hodi, F.S., Linette, G.P., Richards, J., Jakub, J.W., Beeram, M., Tarantolo, S., Agarwala, S.*, et al.* (2008). Double-blind randomized phase II study of the combination of sorafenib and dacarbazine in patients with advanced melanoma: a report from the 11715 Study Group. Journal of clinical oncology : official journal of the American Society of Clinical Oncology *26*, 2178-2185.

McDermott, U., Sharma, S.V., Dowell, L., Greninger, P., Montagut, C., Lamb, J., Archibald, H., Raudales, R., Tam, A., Lee, D.*, et al.* (2007). Identification of genotype-correlated sensitivity to selective kinase inhibitors by using high-throughput tumor cell line profiling. Proceedings of the National Academy of Sciences of the United States of America *104*, 19936-19941.

McGill, G.G., Horstmann, M., Widlund, H.R., Du, J., Motyckova, G., Nishimura, E.K., Lin, Y.L., Ramaswamy, S., Avery, W., Ding, H.F.*, et al.* (2002). Bcl2 regulation by the melanocyte master regulator Mitf modulates lineage survival and melanoma cell viability. Cell *109*, 707-718.

McKinley, E.T., Bugaj, J.E., Zhao, P., Guleryuz, S., Mantis, C., Gokhale, P.C., Wild, R., and Manning, H.C. (2011). 18FDG-PET predicts pharmacodynamic response to OSI-906, a dual IGF-1R/IR inhibitor, in preclinical mouse models of lung cancer. Clinical cancer research : an official journal of the American Association for Cancer Research *17*, 3332-3340.

Medema, R.H., Kops, G.J., Bos, J.L., and Burgering, B.M. (2000). AFX-like Forkhead transcription factors mediate cell-cycle regulation by Ras and PKB through p27kip1. Nature *404*, 782-787.

Meek, D.W. (2009). Tumour suppression by p53: a role for the DNA damage response? Nature reviews Cancer *9*, 714-723.

Melo, J., and Toczyski, D. (2002). A unified view of the DNA-damage checkpoint. Current opinion in cell biology *14*, 237-245.

Mendez, J., and Stillman, B. (2000). Chromatin association of human origin recognition complex, cdc6, and minichromosome maintenance proteins during the cell cycle: assembly of prereplication complexes in late mitosis. Molecular and cellular biology *20*, 8602-8612.

Menzies, A.M., and Long, G.V. (2013). New combinations and immunotherapies for melanoma: latest evidence and clinical utility. Therapeutic advances in medical oncology *5*, 278-285.

Middleton, M.R., Grob, J.J., Aaronson, N., Fierlbeck, G., Tilgen, W., Seiter, S., Gore, M., Aamdal, S., Cebon, J., Coates, A.*, et al.* (2000a). Randomized phase III study of temozolomide versus dacarbazine in the treatment of patients with advanced metastatic malignant melanoma. Journal of clinical oncology : official journal of the American Society of Clinical Oncology *18*, 158-166.

Middleton, M.R., Kelly, J., Goodger, S., Thatcher, N., and Margison, G.P. (2000b). Four-hourly scheduling of temozolomide improves tumour growth delay but not therapeutic index in A375M melanoma xenografts. Cancer chemotherapy and pharmacology *45*, 15-20.

Middleton, M.R., Kelly, J., Thatcher, N., Donnelly, D.J., McElhinney, R.S., McMurry, T.B., McCormick, J.E., and Margison, G.P. (2000c). O(6)-(4-bromothenyl)guanine improves the therapeutic index of temozolomide against A375M melanoma xenografts. International journal of cancer Journal international du cancer *85*, 248-252.

Middleton, M.R., Lunn, J.M., Morris, C., Rustin, G., Wedge, S.R., Brampton, M.H., Lind, M.J., Lee, S.M., Newell, D.R., Bleehen, N.M.*, et al.* (1998). O6-methylguanine-DNA methyltransferase in pretreatment tumour biopsies as a predictor of response to temozolomide in melanoma. British journal of cancer *78*, 1199-1202.

Miknyoczki, S.J., Jones-Bolin, S., Pritchard, S., Hunter, K., Zhao, H., Wan, W., Ator, M., Bihovsky, R., Hudkins, R., Chatterjee, S.*, et al.* (2003). Chemopotentiation of temozolomide, irinotecan, and cisplatin activity by CEP-6800, a poly(ADP-ribose) polymerase inhibitor. Molecular cancer therapeutics *2*, 371-382.

Miller, A.J., and Mihm, M.C., Jr. (2006). Melanoma. The New England journal of medicine *355*, 51-65.

Molhoek, K.R., Shada, A.L., Smolkin, M., Chowbina, S., Papin, J., Brautigan, D.L., and Slingluff, C.L., Jr. (2011). Comprehensive analysis of receptor tyrosine kinase activation in human melanomas reveals autocrine signaling through IGF-1R. Melanoma research *21*, 274-284.

Morten, J.E., and Margison, G.P. (1988). Increased O6-alkylguanine alkyltransferase activity in Chinese hamster V79 cells following selection with chloroethylating agents. Carcinogenesis *9*, 45-49.

Morton, D.L. (2012). Overview and update of the phase III Multicenter Selective Lymphadenectomy Trials (MSLT-I and MSLT-II) in melanoma. Clinical & experimental metastasis *29*, 699-706.

Moynahan, M.E., Chiu, J.W., Koller, B.H., and Jasin, M. (1999). Brca1 controls homology-directed DNA repair. Molecular cell *4*, 511-518.

Mulvihill, M.J., Cooke, A., Rosenfeld-Franklin, M., Buck, E., Foreman, K., Landfair, D., O'Connor, M., Pirritt, C., Sun, Y., Yao, Y.*, et al.* (2009).

Discovery of OSI-906: a selective and orally efficacious dual inhibitor of the IGF-1 receptor and insulin receptor. Future medicinal chemistry *1*, 1153-1171.

Munshi, A., Hobbs, M., and Meyn, R.E. (2005). Clonogenic cell survival assay. Methods in molecular medicine *110*, 21-28.

Murray-Zmijewski, F., Slee, E.A., and Lu, X. (2008). A complex barcode underlies the heterogeneous response of p53 to stress. Nature reviews Molecular cell biology *9*, 702-712.

Nahor, I., Abramovitch, S., Engeland, K., and Werner, H. (2005). The p53-family members p63 and p73 inhibit insulin-like growth factor-I receptor gene expression in colon cancer cells. Growth hormone & IGF research : official journal of the Growth Hormone Research Society and the International IGF Research Society *15*, 388-396.

Nakagawa, M., Uramoto, H., Oka, S., Chikaishi, Y., Iwanami, T., Shimokawa, H., So, T., Hanagiri, T., and Tanaka, F. (2012). Clinical significance of IGF1R expression in non-small-cell lung cancer. Clinical lung cancer *13*, 136-142.

Nakamura, A.J., Rao, V.A., Pommier, Y., and Bonner, W.M. (2010). The complexity of phosphorylated H2AX foci formation and DNA repair assembly at DNA double-strand breaks. Cell Cycle *9*, 389-397.

Nam, E.A., and Cortez, D. (2011). ATR signalling: more than meeting at the fork. The Biochemical journal *436*, 527-536.

Nazarian, R., Shi, H., Wang, Q., Kong, X., Koya, R.C., Lee, H., Chen, Z., Lee, M.K., Attar, N., Sazegar, H.*, et al.* (2010). Melanomas acquire resistance to B-RAF(V600E) inhibition by RTK or N-RAS upregulation. Nature *468*, 973-977.

Neudauer, C.L., and McCarthy, J.B. (2003). Insulin-like growth factor I-stimulated melanoma cell migration requires phosphoinositide 3-kinase but not extracellular-regulated kinase activation. Experimental cell research *286*, 128-137.

Nicholson, D.W., Ali, A., Thornberry, N.A., Vaillancourt, J.P., Ding, C.K., Gallant, M., Gareau, Y., Griffin, P.R., Labelle, M., Lazebnik, Y.A.*, et al.* (1995). Identification and inhibition of the ICE/CED-3 protease necessary for mammalian apoptosis. Nature *376*, 37-43.

Niu, H., Wan, L., Busygina, V., Kwon, Y., Allen, J.A., Li, X., Kunz, R.C., Kubota, K., Wang, B., Sung, P.*, et al.* (2009). Regulation of meiotic recombination via Mek1-mediated Rad54 phosphorylation. Molecular cell *36*, 393-404.

O'Connor, R., Kauffmann-Zeh, A., Liu, Y., Lehar, S., Evan, G.I., Baserga, R., and Blattler, W.A. (1997). Identification of domains of the insulin-like growth factor I receptor that are required for protection from apoptosis. Molecular and cellular biology *17*, 427-435.

Oakley, G.G., and Patrick, S.M. (2010). Replication protein A: directing traffic at the intersection of replication and repair. Frontiers in bioscience : a journal and virtual library *15*, 883-900.

Ochs, K., and Kaina, B. (2000). Apoptosis induced by DNA damage O6-methylguanine is Bcl-2 and caspase-9/3 regulated and Fas/caspase-8 independent. Cancer research *60*, 5815-5824.

Ogawa, T., Yu, X., Shinohara, A., and Egelman, E.H. (1993). Similarity of the yeast RAD51 filament to the bacterial RecA filament. Science *259*, 1896-1899.

Okazaki, T., and Honjo, T. (2007). PD-1 and PD-1 ligands: from discovery to clinical application. International immunology *19*, 813-824.

Okuyama, S., Gonzalez, R., and Lewis, K.D. (2010). Pegylated interferon alpha-2b as adjuvant treatment of Stage III malignant melanoma: an evidence-based review. Core evidence *5*, 39-48.

Park, E.J., Chan, D.W., Park, J.H., Oettinger, M.A., and Kwon, J. (2003). DNA-PK is activated by nucleosomes and phosphorylates H2AX within the nucleosomes in an acetylation-dependent manner. Nucleic acids research *31*, 6819-6827.

Parker, A.S., Cheville, J.C., Janney, C.A., and Cerhan, J.R. (2002). High expression levels of insulin-like growth factor-I receptor predict poor survival among women with clear-cell renal cell carcinomas. Human pathology *33*, 801-805.

Pascucci, B., Russo, M.T., Crescenzi, M., Bignami, M., and Dogliotti, E. (2005). The accumulation of MMS-induced single strand breaks in G1 phase is recombinogenic in DNA polymerase beta defective mammalian cells. Nucleic acids research *33*, 280-288.

Patel, P.M., Suciu, S., Mortier, L., Kruit, W.H., Robert, C., Schadendorf, D., Trefzer, U., Punt, C.J., Dummer, R., Davidson, N.*, et al.* (2011). Extended schedule, escalated dose temozolomide versus dacarbazine in stage IV melanoma: final results of a randomised phase III study (EORTC 18032). Eur J Cancer *47*, 1476-1483.

Patton, E.E., Widlund, H.R., Kutok, J.L., Kopani, K.R., Amatruda, J.F., Murphey, R.D., Berghmans, S., Mayhall, E.A., Traver, D., Fletcher, C.D.*, et al.* (2005). BRAF mutations are sufficient to promote nevi formation and cooperate with p53 in the genesis of melanoma. Current biology : CB *15*, 249-254.

Pegg, A.E. (2000). Repair of O(6)-alkylguanine by alkyltransferases. Mutation research *462*, 83-100.

Peruzzi, F., Prisco, M., Dews, M., Salomoni, P., Grassilli, E., Romano, G., Calabretta, B., and Baserga, R. (1999). Multiple signaling pathways of the

insulin-like growth factor 1 receptor in protection from apoptosis. Molecular and cellular biology *19*, 7203-7215.

Pieper, R.O., Lester, K.A., and Fanton, C.P. (1999). Confluence-induced alterations in CpG island methylation in cultured normal human fibroblasts. Nucleic acids research *27*, 3229-3235.

Pitts, T.M., Tan, A.C., Kulikowski, G.N., Tentler, J.J., Brown, A.M., Flanigan, S.A., Leong, S., Coldren, C.D., Hirsch, F.R., Varella-Garcia, M.*, et al.* (2010). Development of an integrated genomic classifier for a novel agent in colorectal cancer: approach to individualized therapy in early development. Clinical cancer research : an official journal of the American Association for Cancer Research *16*, 3193-3204.

Pollak, M. (2008). Insulin and insulin-like growth factor signalling in neoplasia. Nature reviews Cancer *8*, 915-928.

Pollock, P.M., Harper, U.L., Hansen, K.S., Yudt, L.M., Stark, M., Robbins, C.M., Moses, T.Y., Hostetter, G., Wagner, U., Kakareka, J.*, et al.* (2003). High frequency of BRAF mutations in nevi. Nature genetics *33*, 19-20.

Pollock, P.M., Walker, G.J., Glendening, J.M., Que Noy, T., Bloch, N.C., Fountain, J.W., and Hayward, N.K. (2002). PTEN inactivation is rare in melanoma tumours but occurs frequently in melanoma cell lines. Melanoma research *12*, 565-575.

Polo, S.E., and Jackson, S.P. (2011). Dynamics of DNA damage response proteins at DNA breaks: a focus on protein modifications. Genes & development *25*, 409-433.

Posnick, L.M., and Samson, L.D. (1999). Imbalanced base excision repair increases spontaneous mutation and alkylation sensitivity in Escherichia coli. Journal of bacteriology *181*, 6763-6771.

Prasad, G., Sottero, T., Yang, X., Mueller, S., James, C.D., Weiss, W.A., Polley, M.Y., Ozawa, T., Berger, M.S., Aftab, D.T.*, et al.* (2011). Inhibition of PI3K/mTOR pathways in glioblastoma and implications for combination therapy with temozolomide. Neuro-oncology *13*, 384-392.

Renehan, A.G., Zwahlen, M., Minder, C., O'Dwyer, S.T., Shalet, S.M., and Egger, M. (2004). Insulin-like growth factor (IGF)-I, IGF binding protein-3, and cancer risk: systematic review and meta-regression analysis. Lancet *363*, 1346-1353.

Resnicoff, M., Coppola, D., Sell, C., Rubin, R., Ferrone, S., and Baserga, R. (1994). Growth inhibition of human melanoma cells in nude mice by antisense strategies to the type 1 insulin-like growth factor receptor. Cancer research *54*, 4848-4850.

Ringvoll, J., Nordstrand, L.M., Vagbo, C.B., Talstad, V., Reite, K., Aas, P.A., Lauritzen, K.H., Liabakk, N.B., Bjork, A., Doughty, R.W.*, et al.* (2006). Repair

deficient mice reveal mABH2 as the primary oxidative demethylase for repairing 1meA and 3meC lesions in DNA. The EMBO journal *25*, 2189-2198.

Robertson, A.B., Klungland, A., Rognes, T., and Leiros, I. (2009). DNA repair in mammalian cells: Base excision repair: the long and short of it. Cellular and molecular life sciences : CMLS *66*, 981-993.

Robison, J.G., Dixon, K., and Bissler, J.J. (2007). Cell cycle-and proteasome-dependent formation of etoposide-induced replication protein A (RPA) or Mre11/Rad50/Nbs1 (MRN) complex repair foci. Cell Cycle *6*, 2399-2407.

Rochester, M.A., Riedemann, J., Hellawell, G.O., Brewster, S.F., and Macaulay, V.M. (2005). Silencing of the IGF1R gene enhances sensitivity to DNA-damaging agents in both PTEN wild-type and mutant human prostate cancer. Cancer gene therapy *12*, 90-100.

Roesch, A., Fukunaga-Kalabis, M., Schmidt, E.C., Zabierowski, S.E., Brafford, P.A., Vultur, A., Basu, D., Gimotty, P., Vogt, T., and Herlyn, M. (2010). A temporarily distinct subpopulation of slow-cycling melanoma cells is required for continuous tumor growth. Cell *141*, 583-594.

Roth, R.B., and Samson, L.D. (2002). 3-Methyladenine DNA glycosylase-deficient Aag null mice display unexpected bone marrow alkylation resistance. Cancer research *62*, 656-660.

Rudolph, P., Schubert, C., Tamm, S., Heidorn, K., Hauschild, A., Michalska, I., Majewski, S., Krupp, G., Jablonska, S., and Parwaresch, R. (2000). Telomerase activity in melanocytic lesions: A potential marker of tumor biology. The American journal of pathology *156*, 1425-1432.

Rughani, M.G., Gupta, A., and Middleton, M.R. (2013). New treatment approaches in melanoma: current research and clinical prospects. Therapeutic advances in medical oncology *5*, 73-80.

Sachdev, D., and Yee, D. (2001). The IGF system and breast cancer. Endocrine-related cancer *8*, 197-209.

Saikali, Z., Setya, H., Singh, G., and Persad, S. (2008). Role of IGF-1/IGF-1R in regulation of invasion in DU145 prostate cancer cells. Cancer cell international *8*, 10.

Saitoh, H., Pizzi, M.D., and Wang, J. (2002). Perturbation of SUMOlation enzyme Ubc9 by distinct domain within nucleoporin RanBP2/Nup358. The Journal of biological chemistry *277*, 4755-4763.

Salama, A.K. (2013). Evolving pharmacotherapies for the treatment of metastatic melanoma. Clinical Medicine Insights Oncology *7*, 137-149.

Samson, L., Derfler, B., Boosalis, M., and Call, K. (1991). Cloning and characterization of a 3-methyladenine DNA glycosylase cDNA from human cells whose gene maps to chromosome 16. Proceedings of the National Academy of Sciences of the United States of America *88*, 9127-9131.

San Filippo, J., Sung, P., and Klein, H. (2008). Mechanism of eukaryotic homologous recombination. Annual review of biochemistry *77*, 229-257.

Sankar, A., Thomas, D.G., and Darling, J.L. (1999). Sensitivity of short-term cultures derived from human malignant glioma to the anti-cancer drug temozolomide. Anti-cancer drugs *10*, 179-185.

Schatton, T., and Frank, M.H. (2008). Cancer stem cells and human malignant melanoma. Pigment cell & melanoma research *21*, 39-55.

Schwartzentruber, D.J., Lawson, D.H., Richards, J.M., Conry, R.M., Miller, D.M., Treisman, J., Gailani, F., Riley, L., Conlon, K., Pockaj, B.*, et al.* (2011). gp100 peptide vaccine and interleukin-2 in patients with advanced melanoma. The New England journal of medicine *364*, 2119-2127.

Segurado, M., and Tercero, J.A. (2009). The S-phase checkpoint: targeting the replication fork. Biology of the cell / under the auspices of the European Cell Biology Organization *101*, 617-627.

Sehat, B., Tofigh, A., Lin, Y., Trocme, E., Liljedahl, U., Lagergren, J., and Larsson, O. (2010). SUMOylation mediates the nuclear translocation and signaling of the IGF-1 receptor. Science signaling *3*, ra10.

Sekulic, A., Haluska, P., Jr., Miller, A.J., Genebriera De Lamo, J., Ejadi, S., Pulido, J.S., Salomao, D.R., Thorland, E.C., Vile, R.G., Swanson, D.L.*, et al.* (2008). Malignant melanoma in the 21st century: the emerging molecular landscape. Mayo Clinic proceedings Mayo Clinic *83*, 825-846.

Sell, C., Dumenil, G., Deveaud, C., Miura, M., Coppola, D., DeAngelis, T., Rubin, R., Efstratiadis, A., and Baserga, R. (1994). Effect of a null mutation of the insulin-like growth factor I receptor gene on growth and transformation of mouse embryo fibroblasts. Molecular and cellular biology *14*, 3604-3612.

Semenza, G.L. (2007). Hypoxia-inducible factor 1 (HIF-1) pathway. Science's STKE : signal transduction knowledge environment *2007*, cm8.

Semizarov, D., Frost, L., Sarthy, A., Kroeger, P., Halbert, D.N., and Fesik, S.W. (2003). Specificity of short interfering RNA determined through gene expression signatures. Proceedings of the National Academy of Sciences of the United States of America *100*, 6347-6352.

Sengupta, S., Robles, A.I., Linke, S.P., Sinogeeva, N.I., Zhang, R., Pedeux, R., Ward, I.M., Celeste, A., Nussenzweig, A., Chen, J.*, et al.* (2004). Functional interaction between BLM helicase and 53BP1 in a Chk1-mediated pathway during S-phase arrest. The Journal of cell biology *166*, 801-813.

Sharma, S.V., Lee, D.Y., Li, B., Quinlan, M.P., Takahashi, F., Maheswaran, S., McDermott, U., Azizian, N., Zou, L., Fischbach, M.A.*, et al.* (2010). A chromatin-mediated reversible drug-tolerant state in cancer cell subpopulations. Cell *141*, 69-80.

Shaw, R.J., and Cantley, L.C. (2006). Ras, PI(3)K and mTOR signalling controls tumour cell growth. Nature *441*, 424-430.

Shrivastav, N., Li, D., and Essigmann, J.M. (2010). Chemical biology of mutagenesis and DNA repair: cellular responses to DNA alkylation. Carcinogenesis *31*, 59-70.

Singer, B., Antoccia, A., Basu, A.K., Dosanjh, M.K., Fraenkel-Conrat, H., Gallagher, P.E., Kusmierek, J.T., Qiu, Z.H., and Rydberg, B. (1992). Both purified human 1,N6-ethenoadenine-binding protein and purified human 3-methyladenine-DNA glycosylase act on 1,N6-ethenoadenine and 3-methyladenine. Proceedings of the National Academy of Sciences of the United States of America *89*, 9386-9390.

Sirbu, B.M., Couch, F.B., Feigerle, J.T., Bhaskara, S., Hiebert, S.W., and Cortez, D. (2011). Analysis of protein dynamics at active, stalled, and collapsed replication forks. Genes & development *25*, 1320-1327.

Sobol, R.W., Watson, D.E., Nakamura, J., Yakes, F.M., Hou, E., Horton, J.K., Ladapo, J., Van Houten, B., Swenberg, J.A., Tindall, K.R.*, et al.* (2002). Mutations associated with base excision repair deficiency and methylation-induced genotoxic stress. Proceedings of the National Academy of Sciences of the United States of America *99*, 6860-6865.

Soengas, M.S., and Lowe, S.W. (2003). Apoptosis and melanoma chemoresistance. Oncogene *22*, 3138-3151.

Solier, S., and Pommier, Y. (2011). MDC1 cleavage by caspase-3: a novel mechanism for inactivating the DNA damage response during apoptosis. Cancer research *71*, 906-913.

Solit, D.B., and Rosen, N. (2011). Resistance to BRAF inhibition in melanomas. The New England journal of medicine *364*, 772-774.

Somasundaram, R., Villanueva, J., and Herlyn, M. (2012). Intratumoral heterogeneity as a therapy resistance mechanism: role of melanoma subpopulations. Adv Pharmacol *65*, 335-359.

Sorensen, C.S., Hansen, L.T., Dziegielewski, J., Syljuasen, R.G., Lundin, C., Bartek, J., and Helleday, T. (2005). The cell-cycle checkpoint kinase Chk1 is required for mammalian homologous recombination repair. Nature cell biology *7*, 195-201.

Soufir, N., Avril, M.F., Chompret, A., Demenais, F., Bombled, J., Spatz, A., Stoppa-Lyonnet, D., Benard, J., and Bressac-de Paillerets, B. (1998). Prevalence of p16 and CDK4 germline mutations in 48 melanoma-prone families in France. The French Familial Melanoma Study Group. Human molecular genetics *7*, 209-216.

Stambolic, V., Suzuki, A., de la Pompa, J.L., Brothers, G.M., Mirtsos, C., Sasaki, T., Ruland, J., Penninger, J.M., Siderovski, D.P., and Mak, T.W.

(1998). Negative regulation of PKB/Akt-dependent cell survival by the tumor suppressor PTEN. Cell *95*, 29-39.

Steger, M., Murina, O., Huhn, D., Ferretti, L.P., Walser, R., Hanggi, K., Lafranchi, L., Neugebauer, C., Paliwal, S., Janscak, P.*, et al.* (2013). Prolyl isomerase PIN1 regulates DNA double-strand break repair by counteracting DNA end resection. Molecular cell *50*, 333-343.

Steuerman, R., Shevah, O., and Laron, Z. (2011). Congenital IGF1 deficiency tends to confer protection against post-natal development of malignancies. European journal of endocrinology / European Federation of Endocrine Societies *164*, 485-489.

Stevens, M.F., Hickman, J.A., Langdon, S.P., Chubb, D., Vickers, L., Stone, R., Baig, G., Goddard, C., Gibson, N.W., Slack, J.A.*, et al.* (1987). Antitumor activity and pharmacokinetics in mice of 8-carbamoyl-3-methyl-imidazo[5,1-d]-1,2,3,5-tetrazin-4(3H)-one (CCRG 81045; M & B 39831), a novel drug with potential as an alternative to dacarbazine. Cancer research *47*, 5846-5852.

Stewart, G.S., Wang, B., Bignell, C.R., Taylor, A.M., and Elledge, S.J. (2003). MDC1 is a mediator of the mammalian DNA damage checkpoint. Nature *421*, 961-966.

Stiff, T., Cerosaletti, K., Concannon, P., O'Driscoll, M., and Jeggo, P.A. (2008). Replication independent ATR signalling leads to G2/M arrest requiring Nbs1, 53BP1 and MDC1. Human molecular genetics *17*, 3247-3253.

Stratikopoulos, E., Szabolcs, M., Dragatsis, I., Klinakis, A., and Efstratiadis, A. (2008). The hormonal action of IGF1 in postnatal mouse growth. Proceedings of the National Academy of Sciences of the United States of America *105*, 19378-19383.

Stucki, M., Clapperton, J.A., Mohammad, D., Yaffe, M.B., Smerdon, S.J., and Jackson, S.P. (2005). MDC1 directly binds phosphorylated histone H2AX to regulate cellular responses to DNA double-strand breaks. Cell *123*, 1213-1226.

Sung, P., and Klein, H. (2006). Mechanism of homologous recombination: mediators and helicases take on regulatory functions. Nature reviews Molecular cell biology *7*, 739-750.

Svetlova, M.P., Solovjeva, L.V., and Tomilin, N.V. (2010). Mechanism of elimination of phosphorylated histone H2AX from chromatin after repair of DNA double-strand breaks. Mutation research *685*, 54-60.

Tas, F., Keskin, S., Karadeniz, A., Dagoglu, N., Sen, F., Kilic, L., and Yildiz, I. (2011). Noncutaneous melanoma have distinct features from each other and cutaneous melanoma. Oncology *81*, 353-358.

Thallinger, C., Poeppl, W., Pratscher, B., Mayerhofer, M., Valent, P., Tappeiner, G., and Joukhadar, C. (2007). CCI-779 plus cisplatin is highly

effective against human melanoma in a SCID mouse xenotranplantation model. Pharmacology *79*, 207-213.

Topalian, S.L., Hodi, F.S., Brahmer, J.R., Gettinger, S.N., Smith, D.C., McDermott, D.F., Powderly, J.D., Carvajal, R.D., Sosman, J.A., Atkins, M.B.*, et al.* (2012). Safety, activity, and immune correlates of anti-PD-1 antibody in cancer. The New England journal of medicine *366*, 2443-2454.

Tran, H., Brunet, A., Griffith, E.C., and Greenberg, M.E. (2003). The many forks in FOXO's road. Science's STKE : signal transduction knowledge environment *2003*, RE5.

Trinh, V.A., Patel, S.P., and Hwu, W.J. (2009). The safety of temozolomide in the treatment of malignancies. Expert opinion on drug safety *8*, 493-499.

Trojanek, J., Ho, T., Del Valle, L., Nowicki, M., Wang, J.Y., Lassak, A., Peruzzi, F., Khalili, K., Skorski, T., and Reiss, K. (2003). Role of the insulin-like growth factor I/insulin receptor substrate 1 axis in Rad51 trafficking and DNA repair by homologous recombination. Molecular and cellular biology *23*, 7510-7524.

Tsao, H., Atkins, M.B., and Sober, A.J. (2004a). Management of cutaneous melanoma. The New England journal of medicine *351*, 998-1012.

Tsao, H., Chin, L., Garraway, L.A., and Fisher, D.E. (2012). Melanoma: from mutations to medicine. Genes & development *26*, 1131-1155.

Tsao, H., Goel, V., Wu, H., Yang, G., and Haluska, F.G. (2004b). Genetic interaction between NRAS and BRAF mutations and PTEN/MMAC1 inactivation in melanoma. The Journal of investigative dermatology *122*, 337-341.

Tsaryk, R., Fabian, K., Thacker, J., and Kaina, B. (2006). Xrcc2 deficiency sensitizes cells to apoptosis by MNNG and the alkylating anticancer drugs temozolomide, fotemustine and mafosfamide. Cancer letters *239*, 305-313.

Turner, B.C., Haffty, B.G., Narayanan, L., Yuan, J., Havre, P.A., Gumbs, A.A., Kaplan, L., Burgaud, J.L., Carter, D., Baserga, R.*, et al.* (1997). Insulin-like growth factor-I receptor overexpression mediates cellular radioresistance and local breast cancer recurrence after lumpectomy and radiation. Cancer research *57*, 3079-3083.

Turney, B.W., Kerr, M., Chitnis, M.M., Lodhia, K., Wang, Y., Riedemann, J., Rochester, M., Protheroe, A.S., Brewster, S.F., and Macaulay, V.M. (2012). Depletion of the type 1 IGF receptor delays repair of radiation-induced DNA double strand breaks. Radiotherapy and oncology : journal of the European Society for Therapeutic Radiology and Oncology *103*, 402-409.

Turney, B.W., Turner, G.D., Brewster, S.F., and Macaulay, V.M. (2011). Serial analysis of resected prostate cancer suggests up-regulation of type 1 IGF receptor with disease progression. BJU international *107*, 1488-1499.

Tworkoski, K., Singhal, G., Szpakowski, S., Zito, C.I., Bacchiocchi, A., Muthusamy, V., Bosenberg, M., Krauthammer, M., Halaban, R., and Stern, D.F. (2011). Phosphoproteomic screen identifies potential therapeutic targets in melanoma. Molecular cancer research : MCR *9*, 801-812.

Ullrich, A., Gray, A., Tam, A.W., Yang-Feng, T., Tsubokawa, M., Collins, C., Henzel, W., Le Bon, T., Kathuria, S., Chen, E.*, et al.* (1986). Insulin-like growth factor I receptor primary structure: comparison with insulin receptor suggests structural determinants that define functional specificity. The EMBO journal *5*, 2503-2512.

Uribe, P., Wistuba, II, and Gonzalez, S. (2003). BRAF mutation: a frequent event in benign, atypical, and malignant melanocytic lesions of the skin. The American Journal of dermatopathology *25*, 365-370.

Vanhaesebroeck, B., and Alessi, D.R. (2000). The PI3K-PDK1 connection: more than just a road to PKB. The Biochemical journal *346 Pt 3*, 561-576.

Vecchione, A., Marchese, A., Henry, P., Rotin, D., and Morrione, A. (2003). The Grb10/Nedd4 complex regulates ligand-induced ubiquitination and stability of the insulin-like growth factor I receptor. Molecular and cellular biology *23*, 3363-3372.

Villanueva, J., Vultur, A., Lee, J.T., Somasundaram, R., Fukunaga-Kalabis, M., Cipolla, A.K., Wubbenhorst, B., Xu, X., Gimotty, P.A., Kee, D.*, et al.* (2010). Acquired resistance to BRAF inhibitors mediated by a RAF kinase switch in melanoma can be overcome by cotargeting MEK and IGF-1R/PI3K. Cancer cell *18*, 683-695.

Wacheck, V., Losert, D., Gunsberg, P., Vornlocher, H.P., Hadwiger, P., Geick, A., Pehamberger, H., Muller, M., and Jansen, B. (2003). Small interfering RNA targeting bcl-2 sensitizes malignant melanoma. Oligonucleotides *13*, 393-400.

Wang, Y., Ji, P., Liu, J., Broaddus, R.R., Xue, F., and Zhang, W. (2009). Centrosome-associated regulators of the G(2)/M checkpoint as targets for cancer therapy. Molecular cancer *8*, 8.

Watson, A.J., and Margison, G.P. (1999). O (6)-Alkylguanine-DNA Alkyltransferase Assay. Methods in molecular medicine *28*, 167-178.

Werner, H. (2012). Tumor suppressors govern insulin-like growth factor signaling pathways: implications in metabolism and cancer. Oncogene *31*, 2703-2714.

Werner, H., Karnieli, E., Rauscher, F.J., and LeRoith, D. (1996). Wild-type and mutant p53 differentially regulate transcription of the insulin-like growth factor I receptor gene. Proceedings of the National Academy of Sciences of the United States of America *93*, 8318-8323.

Weston, R., Peeters, H., and Ahel, D. (2012). ZRANB3 is a structure-specific ATP-dependent endonuclease involved in replication stress response. Genes & development *26*, 1558-1572.

Wisdom, R., Johnson, R.S., and Moore, C. (1999). c-Jun regulates cell cycle progression and apoptosis by distinct mechanisms. The EMBO journal *18*, 188-197.

Wu, C.P., Sim, H.M., Huang, Y.H., Liu, Y.C., Hsiao, S.H., Cheng, H.W., Li, Y.Q., Ambudkar, S.V., and Hsu, S.C. (2013). Overexpression of ATP-binding cassette transporter ABCG2 as a potential mechanism of acquired resistance to vemurafenib in BRAF(V600E) mutant cancer cells. Biochemical pharmacology *85*, 325-334.

Wu, S., and Singh, R.K. (2011). Resistance to chemotherapy and molecularly targeted therapies: rationale for combination therapy in malignant melanoma. Current molecular medicine *11*, 553-563.

Wyatt, M.D., and Pittman, D.L. (2006). Methylating agents and DNA repair responses: Methylated bases and sources of strand breaks. Chem Res Toxicol *19*, 1580-1594.

Wylie, A.A., Pulford, D.J., McVie-Wylie, A.J., Waterland, R.A., Evans, H.K., Chen, Y.T., Nolan, C.M., Orton, T.C., and Jirtle, R.L. (2003). Tissue-specific inactivation of murine M6P/IGF2R. The American journal of pathology *162*, 321-328.

Xie, A., Hartlerode, A., Stucki, M., Odate, S., Puget, N., Kwok, A., Nagaraju, G., Yan, C., Alt, F.W., Chen, J.*, et al.* (2007). Distinct roles of chromatin-associated proteins MDC1 and 53BP1 in mammalian double-strand break repair. Molecular cell *28*, 1045-1057.

Yata, K., and Esashi, F. (2009). Dual role of CDKs in DNA repair: to be, or not to be. DNA repair *8*, 6-18.

Yee, D. (2012). Insulin-like growth factor receptor inhibitors: baby or the bathwater? Journal of the National Cancer Institute *104*, 975-981.

Yeh, A.H., Bohula, E.A., and Macaulay, V.M. (2006). Human melanoma cells expressing V600E B-RAF are susceptible to IGF1R targeting by small interfering RNAs. Oncogene *25*, 6574-6581.

Yin, S., Girnita, A., Stromberg, T., Khan, Z., Andersson, S., Zheng, H., Ericsson, C., Axelson, M., Nister, M., Larsson, O.*, et al.* (2010). Targeting the insulin-like growth factor-1 receptor by picropodophyllin as a treatment option for glioblastoma. Neuro-oncology *12*, 19-27.

Ying, S., Hamdy, F.C., and Helleday, T. (2012). Mre11-dependent degradation of stalled DNA replication forks is prevented by BRCA2 and PARP1. Cancer research *72*, 2814-2821.

You, H., Zheng, H., Murray, S.A., Yu, Q., Uchida, T., Fan, D., and Xiao, Z.X. (2002). IGF-1 induces Pin1 expression in promoting cell cycle S-phase entry. Journal of cellular biochemistry *84*, 211-216.

Yu, H., Mistry, J., Nicar, M.J., Khosravi, M.J., Diamandis, A., van Doorn, J., and Juul, A. (1999). Insulin-like growth factors (IGF-I, free IGF-I and IGF-II) and insulin-like growth factor binding proteins (IGFBP-2, IGFBP-3, IGFBP-6, and ALS) in blood circulation. Journal of clinical laboratory analysis *13*, 166-172.

Zelzer, E., Levy, Y., Kahana, C., Shilo, B.Z., Rubinstein, M., and Cohen, B. (1998). Insulin induces transcription of target genes through the hypoxia-inducible factor HIF-1alpha/ARNT. The EMBO journal *17*, 5085-5094.

Zha, J., and Lackner, M.R. (2010). Targeting the insulin-like growth factor receptor-1R pathway for cancer therapy. Clinical cancer research : an official journal of the American Association for Cancer Research *16*, 2512-2517.

Zhang, D., and Brodt, P. (2003). Type 1 insulin-like growth factor regulates MT1-MMP synthesis and tumor invasion via PI 3-kinase/Akt signaling. Oncogene *22*, 974-982.

Zhang, D., Samani, A.A., and Brodt, P. (2003). The role of the IGF-I receptor in the regulation of matrix metalloproteinases, tumor invasion and metastasis. Horm Metab Res *35*, 802-808.

Zhang, J., Stevens, M.F., and Bradshaw, T.D. (2012). Temozolomide: mechanisms of action, repair and resistance. Current molecular pharmacology *5*, 102-114.

Zhang, J., Willers, H., Feng, Z., Ghosh, J.C., Kim, S., Weaver, D.T., Chung, J.H., Powell, S.N., and Xia, F. (2004). Chk2 phosphorylation of BRCA1 regulates DNA double-strand break repair. Molecular and cellular biology *24*, 708-718.

Zhao, H., Dupont, J., Yakar, S., Karas, M., and LeRoith, D. (2004). PTEN inhibits cell proliferation and induces apoptosis by downregulating cell surface IGF-IR expression in prostate cancer cells. Oncogene *23*, 786-794.

Zou, Y., Liu, Y., Wu, X., and Shell, S.M. (2006). Functions of human replication protein A (RPA): from DNA replication to DNA damage and stress responses. Journal of cellular physiology *208*, 267-273.